Unimolecular Micelles and their Application Possibilities *via* the Passerini Three-Component Reaction

Zur Erlangung des akademischen Grades eines

DOKTORS DER NATURWISSENSCHAFTEN

(Dr. rer. nat.)

Fakultät für Chemie und Biowissenschaften

Karlsruher Institut für Technologie (KIT)

genehmigte

DISSERTATION

von

M.Sc. Stefan Oelmann

aus

Karlsruhe

Dekan: Prof. Dr. R. Fischer

Referent: Prof. Dr. M. A. R. Meier

Korreferent: Prof. Dr. P. Theato

Tag der mündlichen Prüfung: 18.07.2018

“Alle Wissenschaftler versuchen, an der

Pyramide menschlichen Wissens weiter zu bauen.

Ich hoffe, dass ich einen kleinen Stein dazutun konnte.”

Stephen W. Hawking

Die vorliegende Arbeit wurde von Januar 2015 bis Juli 2018 unter Anleitung von Prof. Dr. Michael A. R. Meier am Karlsruher Institut für Technologie angefertigt.

Hiermit erkläre ich wahrheitsgemäß, dass ich die vorliegende Arbeit selbstständig angefertigt und keine anderen als die angegebenen Quellen und Hilfsmittel benutzt sowie die wörtlich oder inhaltlich übernommenen Stellen als solche kenntlich gemacht und die Satzung des Karlsruher Instituts für Technologie (KIT) zur Sicherung guter wissenschaftlicher Praxis in der jeweils gültigen Fassung beachtet habe. Des Weiteren erkläre ich, dass ich mich derzeit in keinem laufenden Promotionsverfahren befinde, und auch keine vorausgegangenen Promotionsversuche unternommen habe.

---------- ----------

Ort, Datum Unterschrift

VORWORT

Zuallererst möchte ich mich bei Mike bedanken, der mir seit meiner Bachelorarbeit sein Vertrauen in mich und meine Arbeit schenkte und mir dadurch die Entscheidung sehr vereinfachte auch meine Promotion in dieser einzigartigen Gruppe durchzuführen. Aufgrund seiner freundschaftlichen und loyalen Persönlichkeit war er nicht nur bei jeglichen Fragen und Problemen für einen da, sondern schaffte es auch, zusammen mit seinem kleinen Sohn Tim, mir während einer langen und schweren Zeit im Krankenhaus ein Lächeln ins Gesicht zu zaubern. Auch die gemeinsamen Zeiten auf diversen Konferenzen und Ausflügen gepaart mit dem ein oder anderen Kaltgetränk werden mir immer in guter Erinnerung bleiben.😉 Ich wünsche dir und deiner Familie alles erdenklich Gute und hoffe, dass wir auch in Zukunft den Kontakt pflegen werden.

Weiterhin danke ich dem gesamten Arbeitskreis, sowohl allen Alumni als auch den aktuellen Arbeitskollegen für die stets hilfsbereite und freundliche Arbeitsatmosphäre. Ein großer Dank gebührt auch Pinar und Beccy, welche beide immer dafür sorgten, dass in unserer Gruppe alles glatt läuft und uns einen großen Teil der Arbeit abgenommen haben. Weiterhin hervorzuheben ist Olli, der mich durch seine hervorragende Betreuung während der Bachelorarbeit in die Gruppe und in die Welt der Polymerchemie einführte. Ganz besonders danken möchte ich Pia, Yasmin und Katharina für das gründliche Korrigieren dieser Arbeit, sowie Beccy und Dennis, welche mich synthetisch in größtem Maße unterstützten und Susanne die mit ihrer Idee den Weg für diese Arbeit ebnete.

Vielen Dank auch an die Analytik-Abteilung des Instituts für Organische Chemie, an die Masseabteilung des AK Barner-Kowollik, an Tobias Bantle vom AK Bräse für die HPLC-Messungen sowie an Sebastian Jung vom AK Podlech für die Einführung und die Hilfe bei den UV-VIS Messungen.

Moreover, I would like to thank Cameron and his group for the opportunity to do this cooperation in Nottingham, for the great working atmosphere and for the amazing time, which completed this work. “È stato un piacere.”😉

Un ringraziamento speciale va ad Alessandra per l'aiuto, per la sua amicizia, per il suo essere che ha reso questo tempo indimenticabile e per la sua straordinaria abilità di lavorare in team.

Unvergessen sind natürlich auch zahlreiche „Kaffee"-Pausen, meistens ohne Kaffee für mich, mit Katharina Yasmin und Maike und dem damit verbundenen Gossip sowie den unzähligen Gesprächen über kleine flugunfähige Seevögel der Südhalbkugel.😉

Größter Dank gebührt meiner Familie und vor allem meiner Schwester und meiner Mutter, welche mir die Chemie quasi in die Wiege legte. Nur durch eure Unterstützung und unseren großartigen Zusammenhalt war es mir möglich so weit zu kommen. Deshalb möchte ich euch diese Arbeit widmen.

Das Beste kommt natürlich auch hier zum Schluss: Kennengelernt durch eine Schnapswanderung, lieben gelernt durch gemeinsame Arbeiten im Labor und verbunden durch gemeinsame Ziele. Alles hat in diesem Arbeitskreis angefangen und es wird uns darüber hinaus fester zusammenschweißen als es unsere gemeinsam entwickelten, nachwachsenden Haftklebstoffe jemals hätten machen können. Der wichtigste Dank geht an meine Wiebke, welche mich von Anfang an in allem bestärkte und in jeder Lebenslage für mich da war.

ZUSAMMENFASSUNG

Unimolekulare Mizellen zeigen aufgrund ihrer vielseitigen Materialeigenschaften interessante Anwendungsmöglichkeiten, welche auf ihre kovalent verknüpften Kern-Schale-Architekturen zurückzuführen sind. Sie können unter anderem als Drug-Delivery-Systeme verwendet werden. Diese kovalent verknüpften Strukturen begünstigen eine erhöhte Stabilität in Lösung im Vergleich zu klassischen Mizellen, welche durch Selbstassemblierung von niedermolekularen amphiphilen Molekülen gebildet werden. Aufgrund des kovalenten Charakters der unimolekularen Mizellen liegt kein dynamisches Gleichgewicht zwischen Mizelle und den amphiphilen Molekülen vor. Die chemischen Strukturen solcher Kern-Schale-Architekturen basieren insbesondere auf Dendrimeren, hyperverzweigten Polymeren oder amphiphilen, sternförmigen Blockcopolymeren.

In der vorliegenden Arbeit wurde eine neue Stufenwachstumspolymerisation auf Basis einer Passerini-Dreikomponentenreaktion (Passerini-3KR) entwickelt, um gezielt solche sternförmigen Blockcopolymere herzustellen. Die Passerini-3KR ist aufgrund der hohen Ausbeuten und Atomökonomie, der einfach umsetzbaren Reaktionsführung, der hundertprozentigen Endgruppentreue und vor allem der großen strukturellen Vielfalt der Produkte ein beliebtes Synthesetool in der organischen und Polymerchemie. Von großer Wichtigkeit für diese Arbeit war auch, dass bei dieser Reaktion die Wahl der Seitengruppen nahezu frei ist, was wiederum die Einstellung der Eigenschaften, wie Polarität und Funktionalität im Kern der amphiphilen, unimolekularen Mizellen ermöglichte. Zusammen mit der in dieser Arbeit beschriebenen Molekulargewichtskontrolle bietet die Passerini-3KR ein einfaches und vielfältiges makromolekulares Design.

Die Molekulargewichtskontrolle konnte durch die Einführung eines monofunktionellen irreversiblen Kettentransferreagenzes (ICTA) in den Polymerisationsprozess realisiert werden. Durch das Verhältnis von ICTA zu Monomer konnte das Molekulargewicht gezielt eingestellt werden (analog zu dem Initiator zu Monomer Verhältnis bei lebenden/kontrollierten Polymerisationen, aber mechanistisch vollkommen unterschiedlich). Durch die Verwendung eines tri- und tetrafunktionalen ICTA konnten mittels der Passerini-3KR auch drei- und vierarmige Sternpolymere hergestellt werden. Die daraus erhaltenen Sternpolymere wurden anschließend mit einer wasserlöslichen

Polyethylenglycol (PEG)-basierten Schale funktionalisiert, um amphiphile Sternblockcopolymere mit unimolekularem, mizellarem Verhalten zu generieren. Hierfür wurden die vorhandenen Carbonsäure-Endgruppen der Sternpolymere mit einem PEG-Aldehyd und einem Isocyanid bzw. PEG-Isocyanid in einer weiteren Passerini-3KR umgesetzt, um so eine wasserlösliche Schale mit und ohne Verzweigung am Verknüpfungspunkt der Polymerblöcke zu erhalten. Des Weiteren wurde der Einfluss des Molekulargewichtes der PEG-Reste auf das Aggregationsverhalten der Sternblockcopolymere in wässriger Lösung untersucht. Durch die Anzahl an Wiederholeinheiten im Kern und durch die Wahl unterschiedlicher Isocyanide als Seitenketten, sowie durch die Oxidation der Thioether-Funktionen zu Sulfonen im Polymerrückgrad, konnte die Polarität und die Mikroumgebung im Kern gezielt eingestellt und an die Einkapselung von gewünschten Gastmolekülen angepasst werden. Das Aggregationsverhalten in wässriger Lösung, sowie das Einschlussverhalten und der Transport verschiedener Farbstoffe wurde sowohl visuell oder mittels Dynamischer Lichtstreuung (DLS), als auch mit UV/VIS Spektroskopie und Hochleistungsflüssigkeitschromatographie (HPLC) untersucht. In letztgenannten Untersuchungen konnte zudem gezeigt werden, dass diese Polymere biokompatibel sind und sich für Anwendungen als Drug-Delivery-Systeme eignen, was Zelluntersuchungen, sowie die Einkapselung als auch die Freilassung eines Wirkstoffes (Azithromycin) bestätigten.

ABSTRACT

Due to their versatile material properties based on the covalently linked core-shell architectures, unimolecular micelles show interesting applications in drug delivery and other applications. These covalently linked structures facilitate the increased stability in solution compared to classical micelles, which are formed by self-assembly of low molecular weight amphiphilic molecules. Due to the covalent nature of unimolecular micelles, there is no dynamic equilibrium between the micelle and the amphiphilic molecules. The chemical structure of such unimolecular core-shell architectures is based on dendrimers, hyperbranched polymers or amphiphilic star-shaped block copolymers.

In this thesis, a new step-growth polymerization, based on the Passerini three-component reaction (Passerini-3CR) was developed to produce star-shaped block copolymers, is introduced. Due to high yields and atom economy, easy synthesis protocols, 100% end-group fidelity and large structural diversity, the Passerini-3CR reaction is a popular synthesis tool in organic chemistry as well as in polymer chemistry. The almost free choice of side groups within this reaction was of great importance for this work, since it enabled the tuning of properties such as polarity and functionality in the core of the amphiphilic unimolecular micelles. Together with the molecular weight control described in this work, the Passerini-3CR offers a simple and versatile macromolecular design.

Molecular weight control could be realized by introducing a monofunctional irreversible chain transfer agent (ICTA) to the polymerization process. The molecular weight could then be adjusted through the ratio of ICTA to monomer (similar to the initiator to monomer ratio in living/controlled polymerizations, but *via* a completely different mechanism). By using a tri- and tetrafunctional ICTA, three- and four-armed star-shaped polymers could be prepared *via* the Passerini-3CR. Afterwards, the resulting star-shaped polymers were functionalized with a water-soluble polyethylene glycol (PEG)-based shell to obtain amphiphilic star-shaped block copolymers with unimolecular micellar behavior. For this purpose, the carboxylic acid end groups of the star-shaped polymers were functionalized with a PEG-aldehyde and an isocyanide or PEG-isocyanide using another Passerini-3CR to obtain a water-soluble shell with and without branching point between the polymer blocks. Furthermore, the influence of the molecular weight of the PEG residues on the aggregation behavior of the star-shaped

block copolymers in aqueous solution was investigated. By the number of repeating units in the core, the choice of different isocyanides as side groups, as well as the oxidation of the thioether functions to sulfones in the polymer backbone, the polarity and microenvironment in the core could be adjusted. Aggregation behavior, encapsulation behavior and transport of various dyes were investigated visually or by dynamic light scattering (DLS), UV/VIS spectroscopy and high-performance liquid chromatography (HPLC). In addition, recent studies have shown that these polymers are biocompatible and suitable for drug delivery applications, impressively confirmed by cell examinations and the encapsulation and release of an antibiotic (Azithromycin).

TABLE OF CONTENT

1. INTRODUCTION

How does one design a medical drug to make an impact at the right location in the body? Customarily, dosage forms such as tablets, capsules or creams affect the release of contained drug. In today's dosage forms, only a small portion of the administered drug reaches the desired site of activity. The remaining part is nonspecifically distributed in the entire body and can occasionally cause side-effects, for instance during chemotherapy of cancer tumors. On this account, it should be an important aim of pharmaceutical research to develop transport systems that deliver the drug to the desired site of activity, more precisely to the disease.[1] A promising approach is the covalent or physically drug binding to nanostructured carrier systems. The size of these carrier systems is only a few nanometers and thus much smaller (100 to 200 times) than the cells of a human body.[2, 3] After injection into the bloodstream, nanoparticles are rapidly removed from the blood circulation and accumulated in the cells of the mononuclear phagocyte system (MPS).[4] This defense system against foreign invaders, such as bacteria, is involved in a variety of cells of the liver, spleen, lung, lymph nodes and the bone marrow. Therefore, nanoparticles, treated as bacteria due to their small size, are in principle suitable for drug transportation specifically into all MPS cells, to release them in a controlled manner.[5, 6] These nanostructured carrier systems include, among others, liposomes or micelles.

A particularly interesting subgroup of classical micelles are unimolecular micelles. The possibility of determining the architecture and the dimension in a targeted manner and adapt it to specific conditions make this type of micelle so special. There are various polymer architectures that can act as unimolecular micelles, discussed in detail in the following sections.[7] Referring to this, mainly amphiphilic star-shaped block copolymers are investigated in this work. Since the number and length of the arms can be tuned and freely chosen, this architecture type is best suited for the use as unimolecular micelle.

The synthesis of these amphiphilic star-shaped block copolymers will be realized *via* the Passerini three-component reaction (Passerini-3CR). The named reaction is a part of the large research field of multicomponent reactions (MCRs). Commonly, MCRs are characterized by high yields, simple reaction conditions and high atom economy including more than two starting materials.[8] Another important advantage of MCRs is

the molecular and modular diversity, which can be reached by the variance of the readily available components.[9, 10] In recent years, MCRs have been introduced to the field of polymer chemistry. This led to the opportunity of designing defined and highly complex macromolecular architectures in a straightforward fashion. Especially the Passerini-3CR is a useful tool for the design of such architectures, due to the readily available starting materials and easy reaction protocols. With this reaction, macromolecules containing a substituted ester- and/or amide backbone can be obtained, showing interesting properties for drug delivery systems. All these advantages make MCRs and especially the Passerini-3CR to a versatile, highly attractive and efficient synthesis tool for drug delivery systems.

2. THEORETICAL BACKGROUND

2.1 Multicomponent reactions

The field of multicomponent reactions (MCRs) is a rapidly developing and modern research topic in organic and polymer chemistry with a high potential for future applications. This type of one-pot reaction uses three or more starting materials to form highly complex and defined molecules, containing all or the majority of atoms of the reactants.[11, 12] The advantage of these high atom-efficient reactions is the reduction of reaction steps and the prevention of intermediates, which have to be purified. The group of Wright postulated MCRs as being “ideal” reactions due to their high yields, simple reaction conditions, environmentally friendly and readily available compounds, as well as the already mentioned high atom-efficiency.[13] These features, combined with their modular nature and the simple variation of the components, make MCRs a versatile tool for combinatorial chemistry and drug discovery.[14, 15] In general, MCRs can be distinguished in three basic reaction mechanisms, due to the reversibility of the individual reaction steps, having a major impact on the yield of each MCRs type (Figure 1). Type I MCRs have to deal with low yields, due to the individual equilibrium constants of each reversible step. Within type II MCRs, only the last step is irreversible, leading to a shift of the equilibrium towards the product and consequently to higher yields. The highest yields can be obtained by type III MCRs including exclusively irreversible steps.[12]

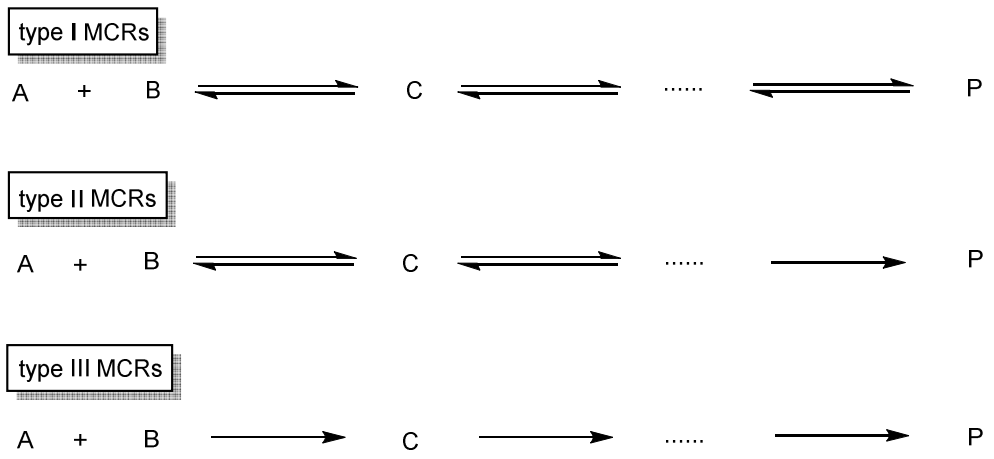

Figure 1: The three basic types of MCRs.[12]

Moreover, MCRs can be divided into three categories: non-isocyanide-based MCRs, isocyanide based MCRs (IMCRs) and metal-catalyzed MCRs.[16] The first in literature described non-isocyanide-based MCR is known as the Strecker three-component reaction (S-3CR) from 1850, comprising an aldehyde, ammonia and hydrogen cyanide to form an *α*-amino nitrile (Scheme 1).[17] A subsequent acidic hydrolysis leads to a racemic mixture of the corresponding amino acids. Afterwards, several variants were developed to obtain enantiopure amino acids.[18, 19] In 1882, Arthur Hantzsch described a four-component reaction (H-4CR) to obtain pyridines. Therefore, ammonia, two equivalents of a *β*-ketoester and an aldehyde were reacted to form dihydropyrimidines, leading to the corresponding pyridines *via* a simple oxidation (Scheme 1).[20] Eight years later, in 1890, the related pyrrole synthesis was reported by Hantzsch (H-3CR), using a *β*-ketoester, ammonia and *α*-haloketones (Scheme 1).[21] In 1891, the aza-analogon of the Hantzsch dihydropyridine synthesis was discovered by Biginelli (B-3CR). The latter reaction is an acid-catalyzed condensation of an aldehyde component with urea, to obtain an imine, subsequently reacting with a *β*-ketoester. A following intramolecular condensation using the second urea-amine, leads to dihydropyrimidinones (Scheme 1).[22] Another literature-known three-component reaction was investigated by Mannich (M-3CR) in 1920. He describes the reaction of a formaldehyde, an amine and an aldehyde or ketone under acidic conditions, to end up with a *β*-aminocarbonyl. Here, the amine and formaldehyde build the corresponding iminium-ion, which is subsequently attacked by the aldehyde- or ketone-component (Scheme 1).[23] In 1934, the Bucherer-Bergs reaction was reported, describing the reaction of an aldehyde, carboxylic acid, ammonia and hydrogen cyanide to end up with hydantoins (Scheme 1).[24, 25] The Kabachnik-Fields reaction, based on the formation of aminophosphonates using an amine, an oxo-component (aldehyde or ketone) and a dialkylphosphate was discovered in 1952 (Scheme 1).[26] A few years later, in 1956, Asinger described the reaction of two equivalents of a ketone, ammonia and elemental sulfur to obtain thiazolines (Scheme 1).[27]

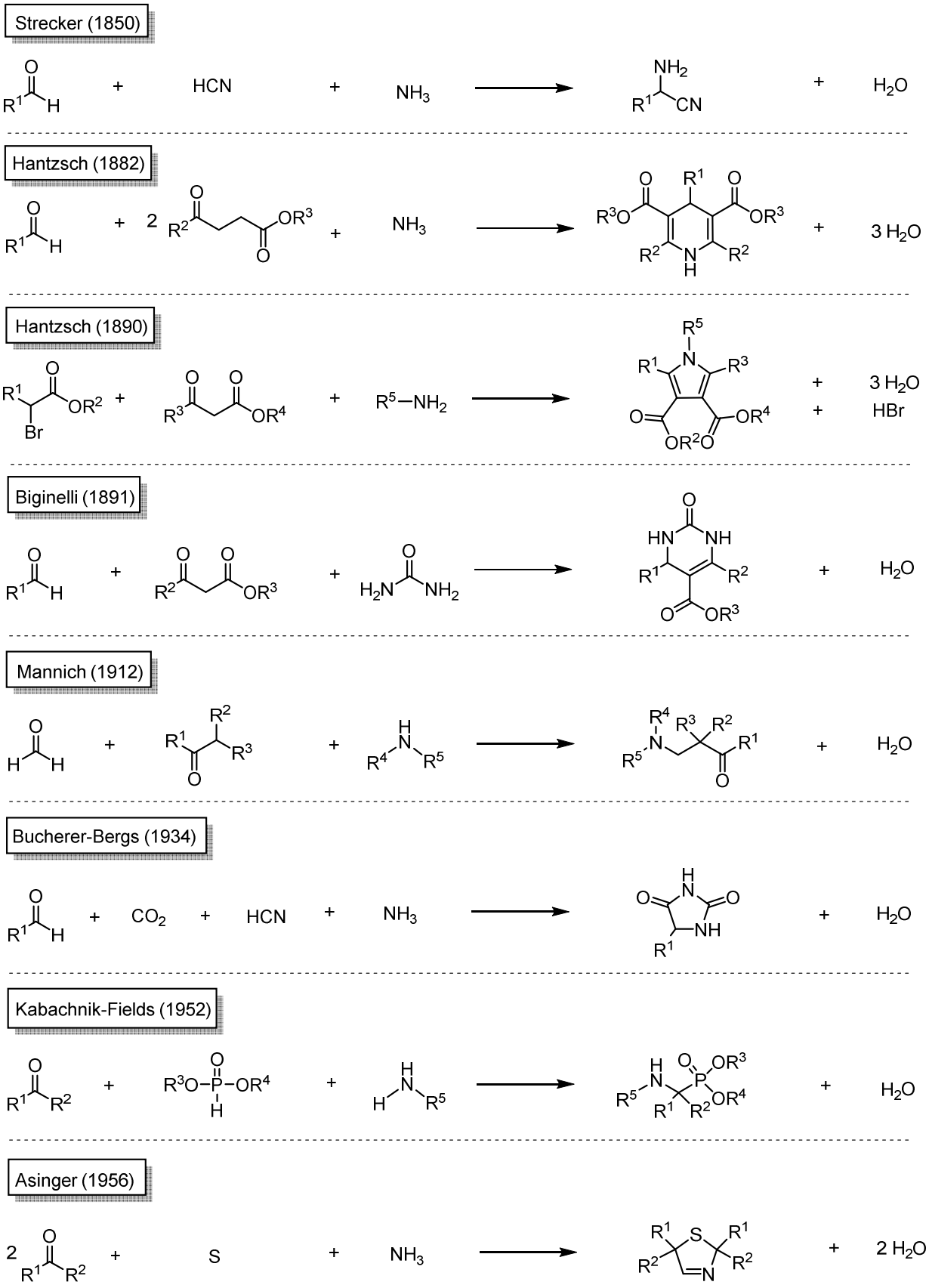

Scheme 1: A selection of historically ordered important non-isocyanide-based MCRs.[17-27]

In line with the industry standard, the CO-containing metal-catalyzed MCRs are especially relevant. One of them was developed by Roelen in 1938, who described the hydroformylation of alkenes.[28] One year later, in 1939, Reppe investigated the metal-catalyzed hydrocarboxylation of alkynes.[29] A recent and valuable carbon monoxide containing and metal-catalyzed synthesis in organic chemistry was developed by Pauson and Khand in 1971.[30] This [2+2+1]-cycloaddition of an alkyne, an alkene and carbon monoxide leads to substituted cyclopentenones. In the following years, many catalytic alternatives to the Pauson-Khand reaction were reported.[31, 32]

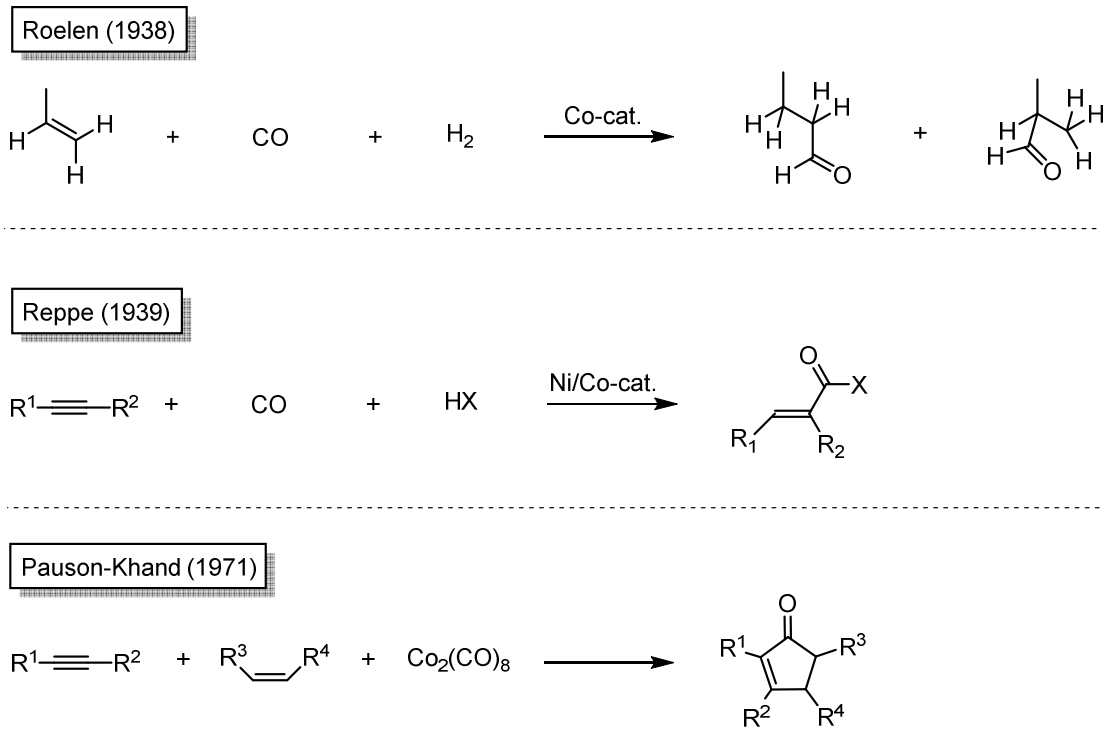

Scheme 2: A selection of historically ordered important metal-catalyzed MCRs.[28-32]

2.2 Isocyanide-based multicomponent reactions

Isocyanide-based MCRs are a very important class of MCRs. The most famous representatives cover the Passerini three-component reaction (Passerini-3CR) and the Ugi four-component reaction (Ugi-4CR), which will be explained in detail in the following chapters. But prior to this, the reactivity, the synthesis and the properties of isocyanides will be discussed.

2.2.1 Isocyanides

The extraordinary reactivity of isocyanides is based on their two resonance structures (Scheme 3). For one of the resonance structures, the stable, formally divalent carbon atom can lead to a similar reactivity like it is known from carbenes. The other resonance structure exhibits a negatively charged carbon, which is able to react as a nucleophile. After the nucleophilic attack, it becomes an electrophile and can therefore be nucleophilically attacked. The latter process is called *α*-addition and is the key step in the following described Passerini-3CR and Ugi-4CR. The positively charged nitrogen atom in the same resonance structure results in *α*-acidity, which can be additionally increased by electron withdrawing substituents in *α*-position.[11]

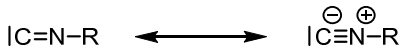

Scheme 3: Two different resonance structures of isocyanides.[11]

Under acidic conditions, isocyanides can hydrolyze and form the corresponding formamide, whereas in basic media they show outstanding stability.[33] In general, isocyanides are used in heterocycle synthesis of imidazoles or oxazoles.[34 - 36] Furthermore, by initiation with Brønstedt or Lewis acids and by decomposition of metallo-isocyanide-complexes, isocyanides can be polymerized. Naturally occurring isocyanides are derived from amino acids (terrestrial-derived) or are based on terpenes (marine-derived, e.g. in sponges).[37, 38]

In 1859, isocyanides were accidently discovered by Lieke (Scheme 4).[39] Reacting allyl iodide with silver cyanide did not lead as expected to allyl nitrile, but to the corresponding allyl isocyanide, which was proven by Gautier ten years later, in 1869. By hydrolysis, he showed that the corresponding formamide was obtained. In case of the nitrile, he would have received the corresponding carboxylic acid.[40] In 1867, Hofmann postulated the reaction of a primary amine, chloroform and potassium hydroxide to synthesize isocyanides in another approach (Scheme 4).[41] First, chloroform and potassium hydroxide form a reactive dichlorocarbene, which is attacked by the primary amine leading to an ionic intermediate. After the elimination of potassium chloride and water, the isocyanide was obtained. These reaction conditions revealed only moderate yields. Therefore, more than 100 years later, Ugi *et al.* used a

biphasic system in the presence of a phase-transfer catalyst to improve the yields.[42] The synthesis route, which is nowadays the method of choice, was discovered by Ugi in 1958 (Scheme 4).[43] The dehydration of *N*-formamides, using phosgene as dehydration agent and a base, leads to the required isocyanide. For economic reasons, the highly toxic phosgene is still used in industry as dehydration agent, whereas in laboratory scale, mainly the less toxic phosphorous(V)oxychloride is used.[44-46] The isocyanide synthesis of Ugi was the breakthrough and the reason for the rapid development of IMCRs. Recently, in 2015, the group of Dömling introduced the Leuckart-Wallach reaction for the synthesis of isocyanides.[47] This reaction, starting from an aldehyde or ketone, leads to *N*-formamides, which were transferred to isocyanides *via* an *in-situ*-dehydration, using triphosgene (Scheme 4).[48]

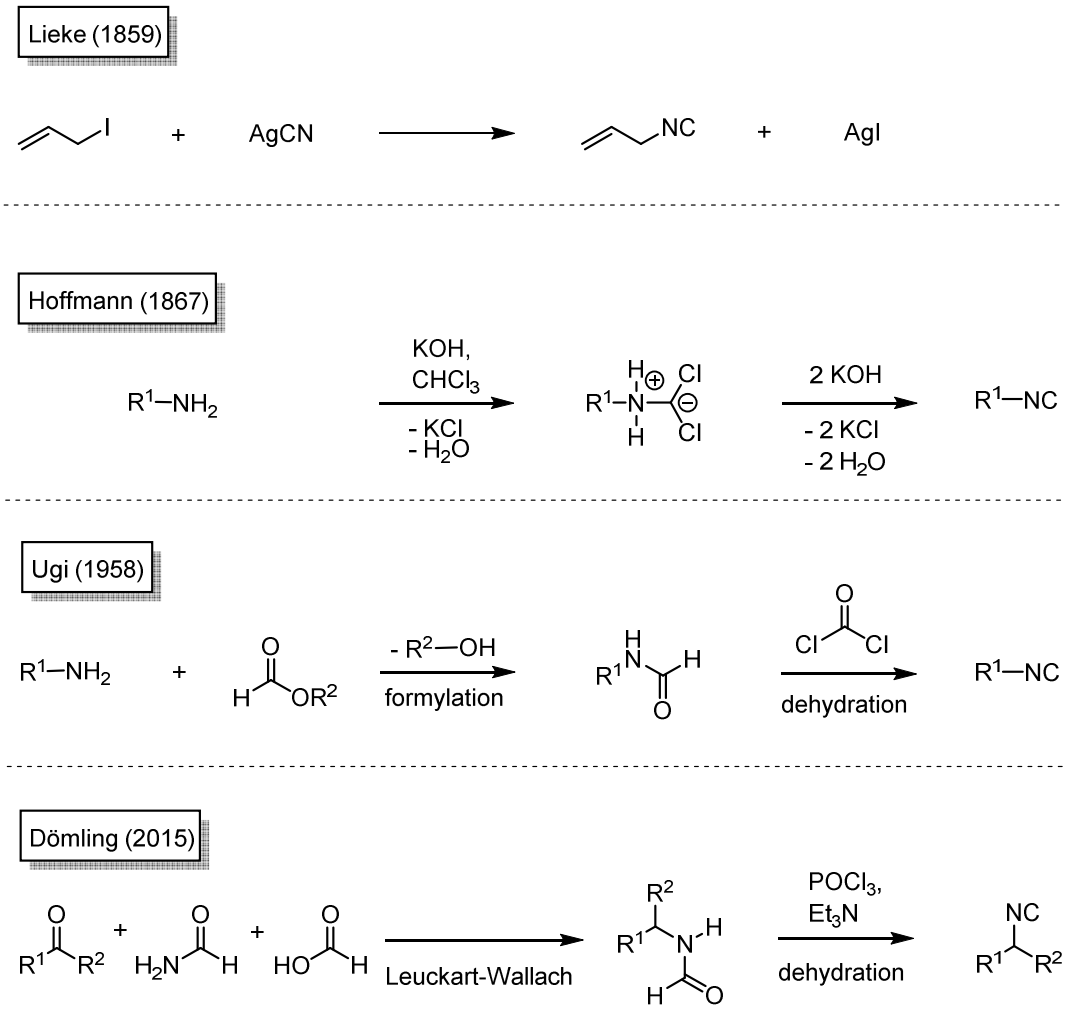

Scheme 4: A selection of historically ordered important isocyanide syntheses.[39-47]

2.2.2 Passerini three-component reaction (Passerini-3CR)

In 1921, Mario Passerini discovered the Passerini-three-component reaction (Passerini-3CR), which combines a carboxylic acid, an oxo component (aldehyde or ketone) and an isocyanide to synthesize an *α*-acyloxycarboxamide.[49] The commonly accepted mechanism starts with the activation of the carbonyl component *via* the formation of a hydrogen bonded adduct with the carboxylic acid. In the following key step of the mechanism, the *α*-addition, the oxo-component is nucleophilically attacked by the carbon atom of the isocyanide. This carbon atom simultaneously reacts as an electrophile with the carboxylic acid. A subsequent intramolecular rearrangement with acyl transfer provides the Passerini product (Scheme 5).

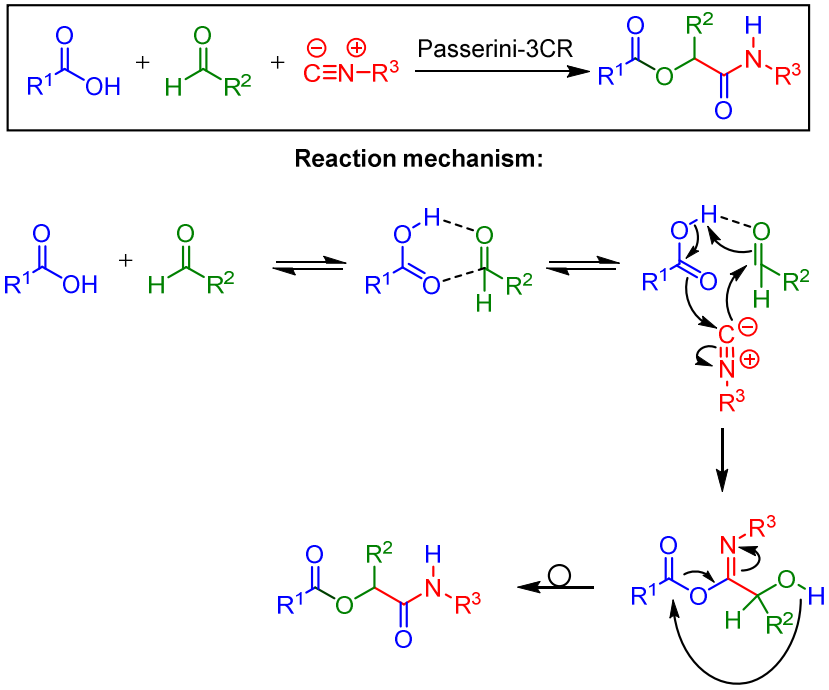

Scheme 5: Mechanism of the Passerini-3CR using a carboxylic acid, an oxo-component (aldehyde) and an isocyanide.[50, 51]

The commonly accepted mechanism was proposed by Passerini and later confirmed by kinetic investigations of Baker and Ugi in 1951 and 1961.[50, 51] Four years later, in 1965, Eholzer and his group proposed another mechanism including a protonation of the isocyanide by the carboxylic acid as first step.[52] This suggestion was disproved and the mechanism proposed by Passerini was confirmed again, but by using a second carboxylic acid involved in the mechanism after the *α*-addition (Scheme 6).[53, 54] Due

to these results, obtained by quantum chemical calculations in the gas phase, the Passerini-3CR would be seen as a four-component reaction mechanistically or as an organo-catalyzed reaction. In general, however, the mechanism is not finally clarified.

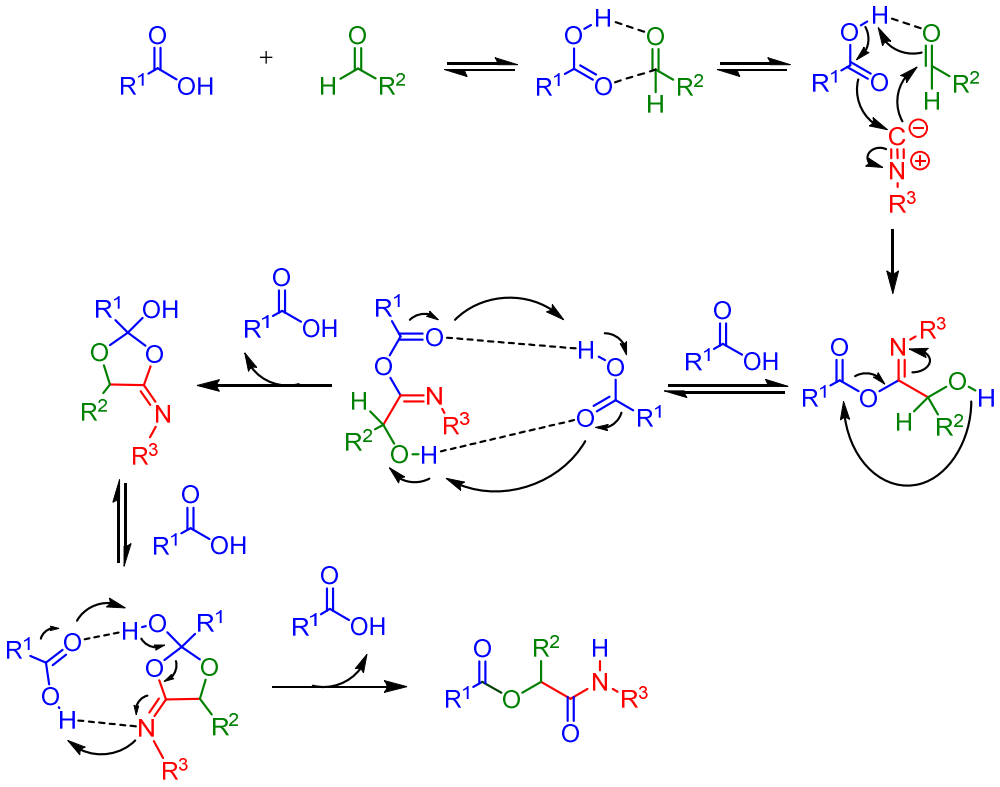

Scheme 6: Recently proposed mechanism of the Passerini-3CR involving two carboxylic acids.[53, 54]

Furthermore, many variations of the Passerini-3CR were reported, replacing carboxylic acids with hydrazoic acid, which gives an easy access of substituted tetrazoles (Scheme 7, a)).[55, 56] Additionally, carboxylic acids can be substituted byalcohols, leading to *α*-alkoxy amide derivatives (Scheme 7, b))[57-61] and due to the *in-situ* oxidation to the corresponding aldehydes, alcohols can be used as alternatives to aldehydes, which is handy due to the difficult synthesis, low availability and limited shelf-life of aldehydes.[62] Here, 2-iodoxybenzoic acid (IBX) was used as oxidizing agent. Other variations comprise the substitution of the oxo-component with acyl isocyanates (Scheme 7, c)) or ketenes (Scheme 7, d)), leading to *N*,*N*-diacyloxamides or *α*,*γ*-diketo-carboxamides.[63, 64]

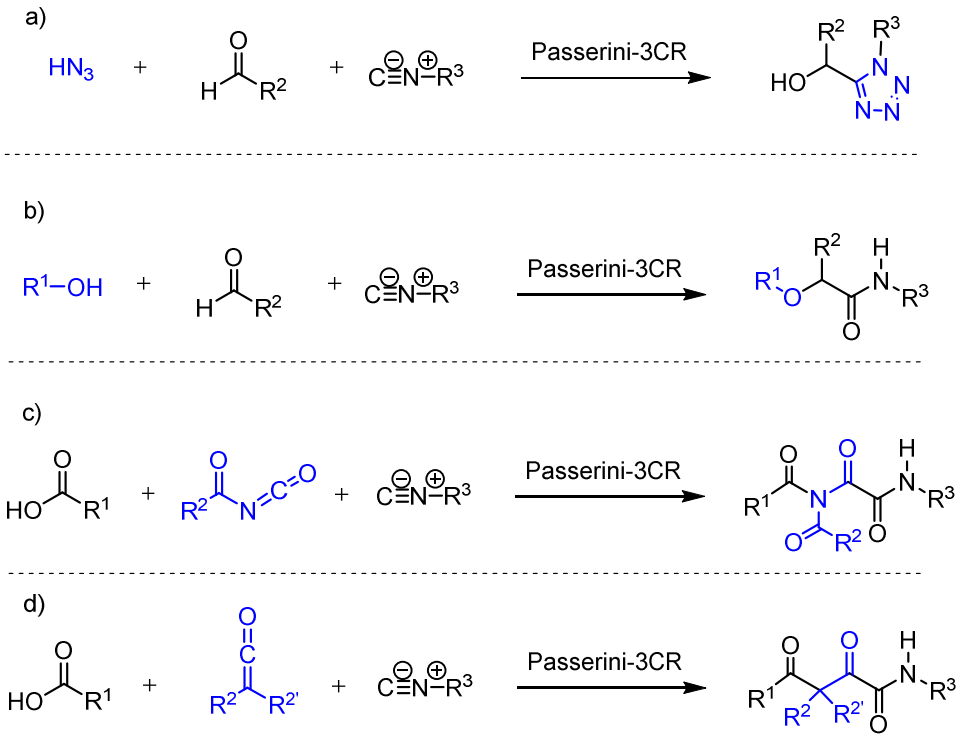

Scheme 7: Variations of the Passerini-3CR using hydrazoic acid a) or alcohols b) instead of carboxylic acids and using acyl isocyanates c) or ketenes d) instead of aldehydes.[55-64]

The simplest approach of using multicomponent reactions in polymer chemistry is for monomer synthesis. On this account, the Passerini-3CR has been described in the synthetic route to lactides, for the synthesis of ADMET (acyclic diene metathesis) monomers, [65-67] as well as for the synthesis of several acrylates, with a diverse substitution pattern.[68] Due to the simple structural variation of the monomers, some of the properties of the obtained polymers could be selectively adjusted, which has been shown for the upper critical solution temperature (UCST) of polyacrylates.[68] Li *et al.* were able to show the Passerini-3CRs´ suitability for the functionalization of polymer chains.[69] Therewith, a polyethylene glycol (PEG) aldehyde was functionalized simultaneously with an alkyne and an ATRP initiator, which were directly bound to an isocyanide and to an acid component. The obtained functionalized PEGs were excellent candidates for synthesizing miktoarm star-shaped polymers.

Of particular interest is the purpose of the Passerini-3CR in step growth polymerizations. In principle, the use of monomers owing two functional groups (for example AA + BB, or AB-type monomers) within a Passerini-3CR led to the formation of macrocycles or polymers, analogously to a "classical" polycondensation.[70] For

polymer synthesis, there are three potential combinations of two bifunctional and one monofunctional components known: a) the combination of a dicarboxylic acid with a dialdehyde and an isocyanide,[65] b) the combination of a dicarboxylic acid with a diisocyanide and an aldehyde[71] and c) the combination of a dialdehyde with a diisocyanide and a carboxylic acid.[72] Depending on the type of above combinations, polyesters or polyamides with functional side chains can be obtained (Scheme 8).

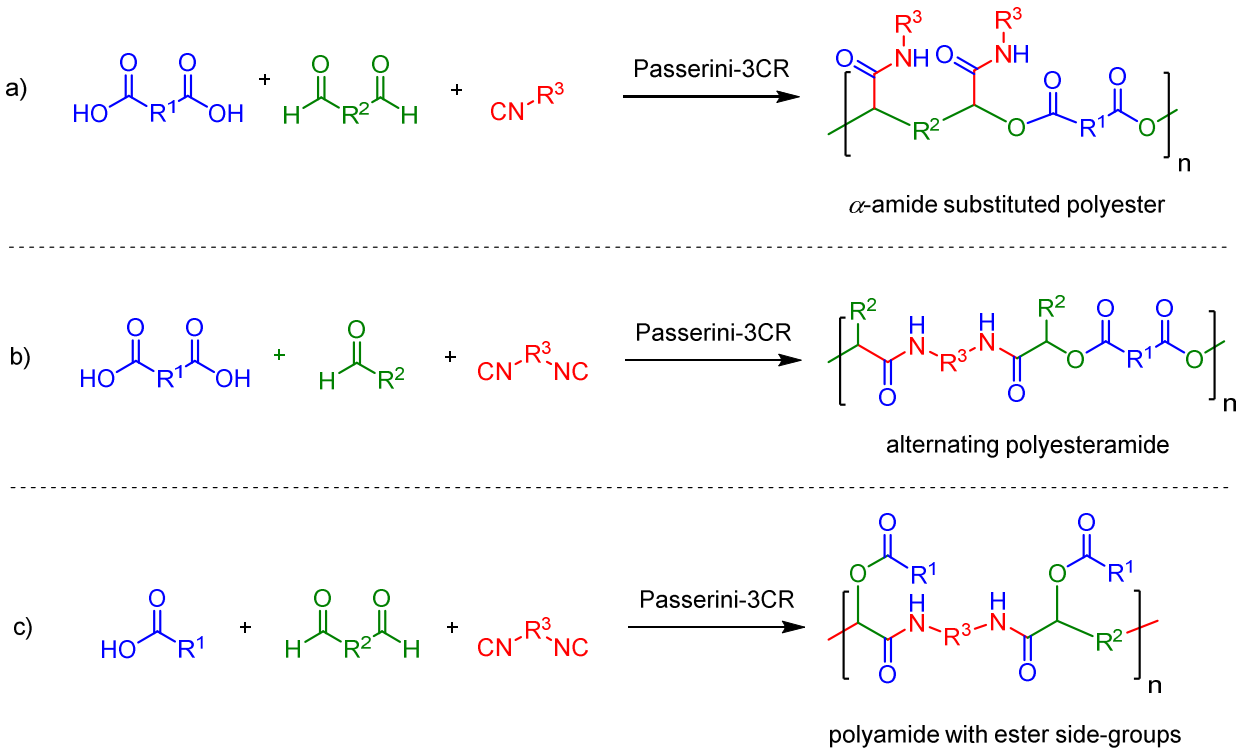

Scheme 8: Potential combinations of two bifunctional and one monofunctional components, for the synthesis of functional polymers *via* the Passerini-3CR.[63, 71, 72]

The first described example of a Passerini three-component polymerization (Passerini-3CP) was developed in 2011 by Meier *et al.*[65] Long-chain dicarboxylic acids and dialdehydes were reacted with different isocyanides to end up with substituted polyesters (Scheme 8, a)), reaching high molecular weights (M_n > 50,000 g/mol). Herein, the thermal properties of the polymers could be varied by the choice of the isocyanides. In 2012, Li *et al.* described the Passerini-3CR of dicarboxylic acids and diisocyanides with aldehydes (Scheme 8, b)).[71] In addition to kinetic studies, supporting the step-growth mechanism and reaction optimization, the authors described the use of 10-undecenal as aldehyde component, leading to polyesters owing double bonds in the side chains, disposed for further modification. Making use

of alcohols instead of aldehydes in an oxidative Passerini reaction, as it is known from organic synthesis, seemed to be ineffective due to the low molecular weights achieved.[72, 73] The third potential combination (Scheme 8, c)), investigated by the group of Li again, showed that only by the excess of the monofunctional component (here the acid component) higher molecular weights could be reached.[72]

In addition to the above-mentioned examples, it is also possible to use AB-type monomers in a Passerini-3CP, leading to a simpler and more efficient (only two component) polymerization process. In principle, there are also three possibilities for AB-type monomers, whereas isocyanides show a low acid stability, which excludes its combination. The combination of an acid and an aldehyde function in an AB-type monomer thus seems to be the best choice, since the synthesis of isocyanides requires several steps. The one-step synthesis of such an AB-type monomer and its polymerization with different isocyanides was intensely investigated by the group of Meier (Scheme 9, a)). Interestingly, the thermal properties of those polymers were controlled not only by the choice of the isocyanide, but also by the oxidation of the sulfide to sulfone in the polymer backbone, which increased the glass transition by about 30 °C.[74] Li *et al.* investigated 4-oxobutyric acid as analogous AB-type monomer (Scheme 9, b)).[75] However, mainly ring closing to the *γ*-butyrolactone was observed. The original polymer structure targets were only obtained by using *α*, *β*-unsaturated 4-oxobutyric acid as AB-type monomer and subsequent hydrogenation, in moderate molecular weights (< 10,000 g/mol).

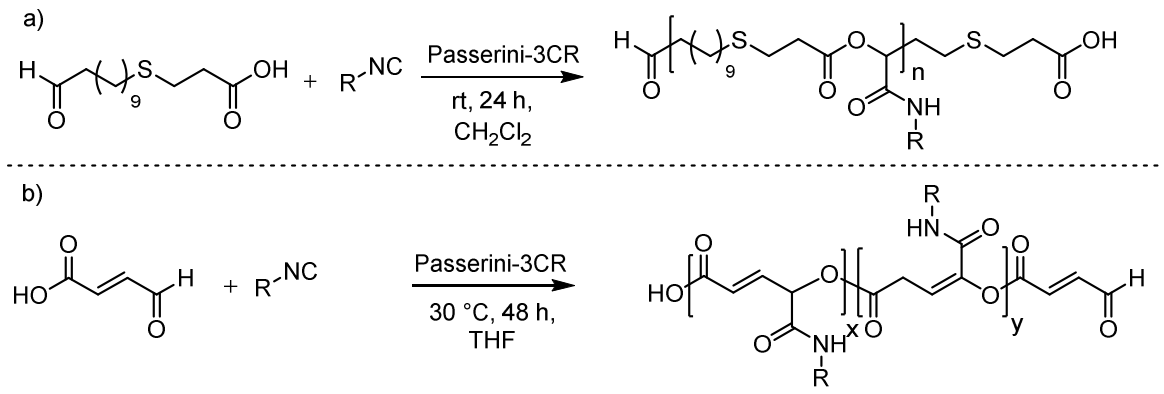

Scheme 9: Passerini-3CR using an AB-type monomer and an isocyanide.[74, 75]

Recently, Li and his group investigated a Passerini-3CR of 6-oxohexanoic acid using different isocyanides leading to functional poly(caprolactone)s (Scheme 10).[76] The

obtained functional polymers beared tunable amide-linked side groups at the *ε*-position. Furthermore, the copolymerization using the same AB-type monomer was successfully demonstrated. Therefore, a mixture of two isocyanides was used in different molar ratios. Afterwards, a thiol-ene addition reaction using a thiol-glucose on the homopolymer containing alkenyl groups was demonstrated to modify the polymer itself. In order to test their compatibility for biomedical applications, their degradation and cytotoxicity was investigated.

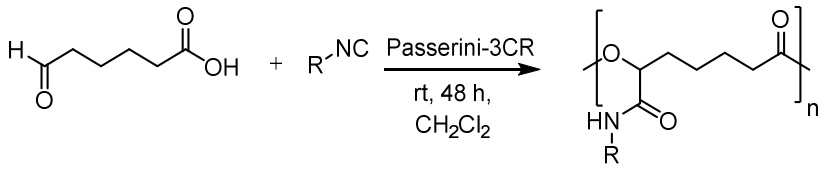

Scheme 10: Synthesis of functional poly(caprolactone)s *via* the Passerini-3CR of 6-oxohexanoic using different isocyanides.[76]

Xie and coworkers studied the synthesis of reduction-sensitive amphiphilic copolymers *via* the Passerini-3CR for biomedical applications (Scheme 11).[77] The polymerization was performed by using 1,6-diisocyanohexane, 3,3'-dithiodipropionic acid and 4-(methoxytriethyleneoxy)-carboxybenzaldehyde. Afterwards, the polymer backbone was functionalized by introducing hydrophilic ethylene glycol to the side chains. The amphiphilic character of the polymer enables the formation of micelles by self-assembly. Under reductive conditions, involved disulfide bonds were broken and the following disassembly of the micelles led to a rearrangement of the hydrophobic fragments. Furthermore, these amphiphilic micelles were tested as drug delivery systems. Therefore, curcumin, an effective anticancer agent, was encapsulated to demonstrate the outstanding encapsulation efficiency and the fast intracellular release. Additionally, the micelles showed an excellent biocompatibility, which indicates the suitability for drug delivery in anti-cancer therapy of these polymers synthesized by Passerini-3CR.

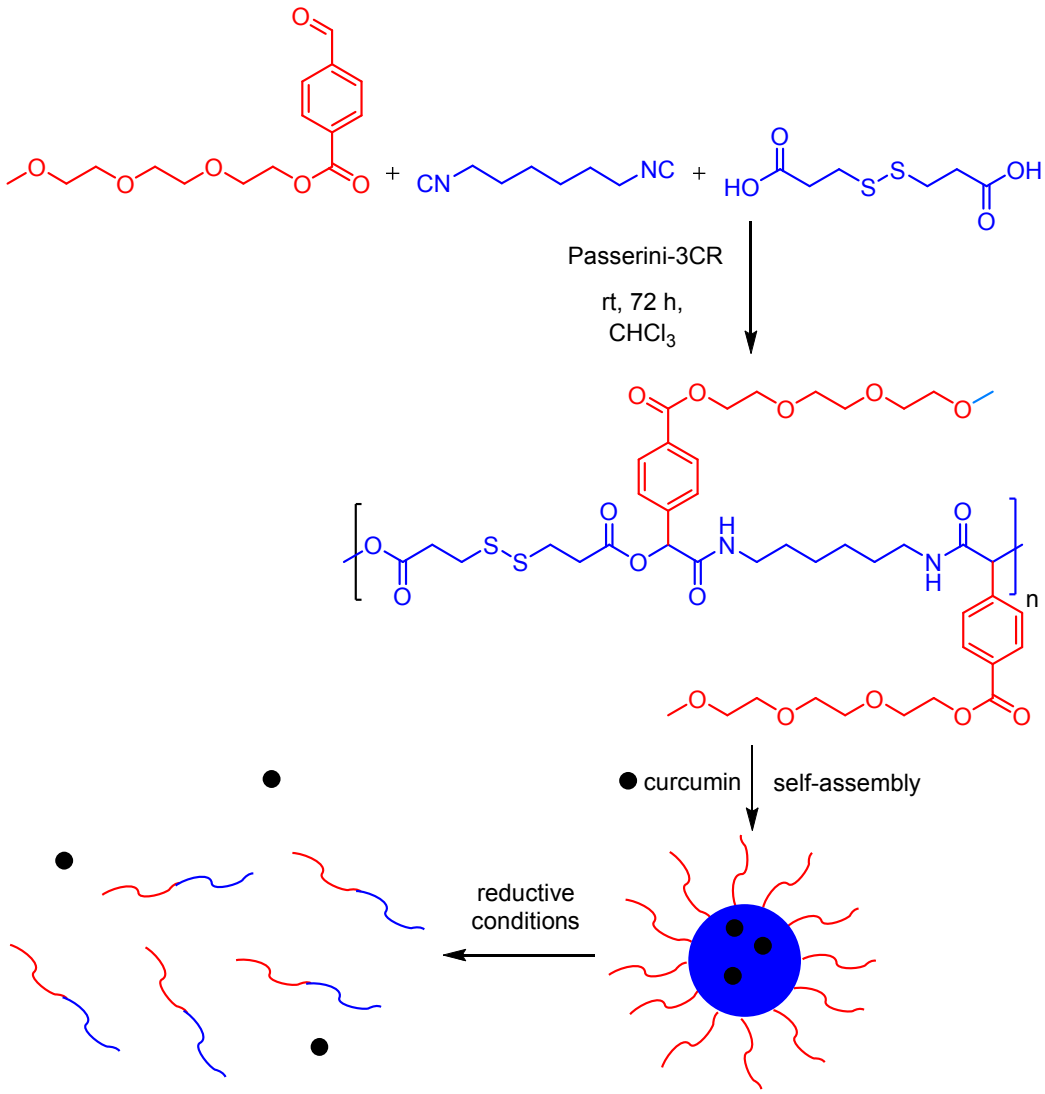

Scheme 11: Synthesis of amphiphilic micelles *via* Passerini-3CR of 1,6-diisocyanohexane, 3,3'-dithiodipropionic acid and 4-(methoxytriethyleneoxy)-carboxybenzaldehyde and following encapsulation and release tests of curcumin.[77]

Moreover, polyfunctional monomers have also been used in Passerini-3CRs to obtain hyperbranched polymers,[78] as well as crosslinked hydrogels.[79] Besides the combination of Passerini reactions with photochemistry, e.g. to design photo-degradable polymers[80], the Passerini reaction was also used for the design of different macromolecular architectures. Of particular interest are new approaches focusing on dendrimer synthesis[81] (see chapter 2.3) and the design of monodisperse, sequence-defined macromolecules[82] through Passerini-3CR.

2.2.3 Ugi four-component reaction (Ugi-4CR)

Parts of this chapter were published previously:

A. Llevot, A. C. Boukis, S. Oelmann, K. Wetzel and M. A. R. Meier, *Top. Curr. Chem.*, **2017**, *375*, 66. Copyright © 2017, with kind permission from Springer Nature.

The Ugi four-component reaction (Ugi-4CR), discovered by Ivar Karl Ugi in 1959, involves the reaction of a carboxylic acid, a ketone or aldehyde, an isocyanide and a primary amine as fourth component to generate an *α*-aminoacylamide under the release of water (Scheme 12).[83] The commonly accepted mechanism is initiated by the Schiff-base formation of the aldehyde with the amine, which is subsequently protonated by the carboxylic acid to form an iminium ion. Then, the lone pair of the nucleophilic carbon of the isocyanide attacks the electrophilic center of the iminium ion, while concertedly acting as electrophile and reacting with the carboxylic acid (*α*-addition). The subsequent intramolecular Mumm rearrangement finally leads to the *α*-aminoacylamide.[84]

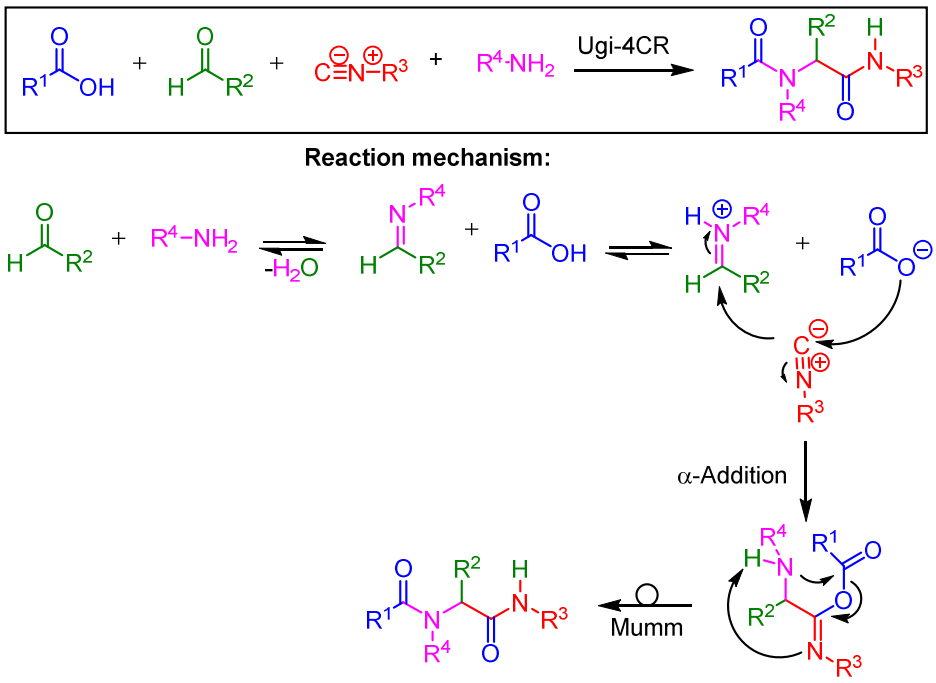

Scheme 12: Overall reaction and mechanism of the Ugi-4CR involving carboxylic acid, aldehyde, an isocyanide and a primary amine.[83, 84]

The introduction of a fourth component to the Ugi-4CR increases the structural diversity and the thermal stability (by the creation of two amide bonds instead of one ester and one amide bond) of the final products, in comparison to the Passerini-3CR.

For the *α*-addition, there are two possible pathways: An ionic and a non-ionic pathway (Scheme 13). The non-ionic pathway describes the reaction of the protonated imine with the carboxylic acid anion leading to the hemiaminal and followed by the insertion of the isocyanide. In the ionic mechanism of this step, the protonated imine is nucleophilically attacked by the isocyanide to form the corresponding nitrilium ion, followed by the addition of the carboxylic acid anion. In 2012, the group of Fleurat-Lessard investigated both pathways and found out, that the ionic mechanism occurs only in protic solvents like methanol, due to the imine protonation and the non-ionic pathway was only found in the aprotic solvent toluene.[85]

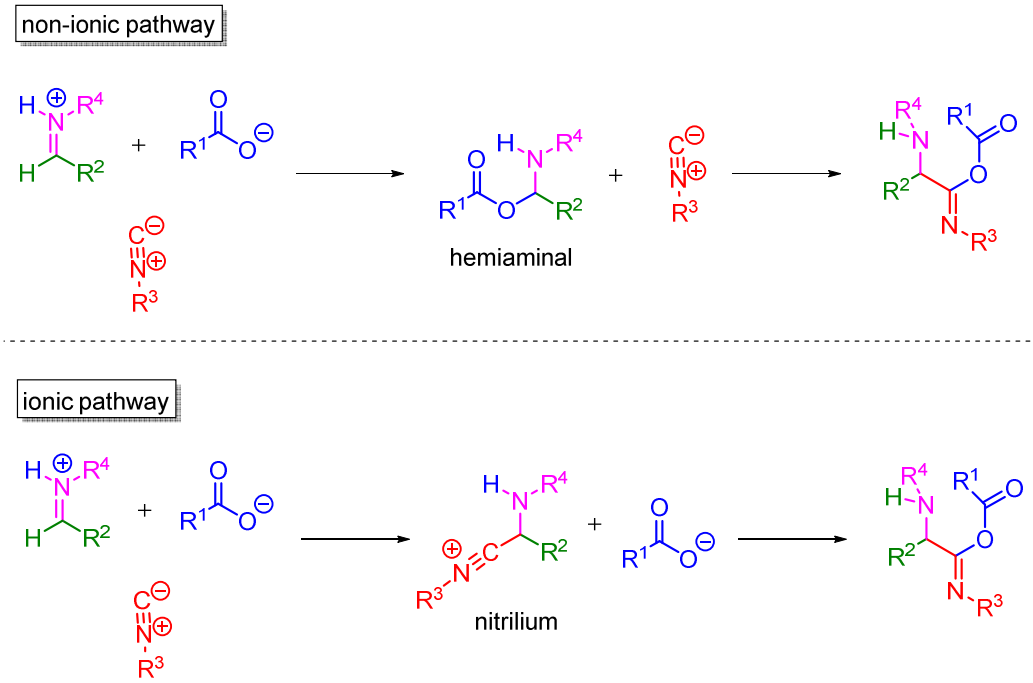

Scheme 13: Non-ionic and ionic pathway of the *α*-addition during the Ugi-4CR.[85]

In the Ugi-4CR, primary amines can be substituted by secondary amines and the carboxylic acid component can be replaced by a variety of other components, like hydrogen cyanate, thiocarboxylic acids, hydrazoic acid, electron-deficient phenols, alcohols and carbon dioxide, which leads to an immense structural diversity.[86-91] One of the most known variants of the Ugi reaction is the Ugi-5CR[89] using alcohols and

carbon dioxide instead of carboxylic acids to synthesize carbamates (Scheme 14). It was published in 1961 by Ugi *et al.* Another interesting modification of the Ugi reaction is the Ugi-Smiles[91] reaction using electron-deficient phenols like nitrophenols or quinoline and pyridine derivatives instead of carboxylic acids.[92] The special thing about this variant is, that in the last step a Smiles-rearrangement occurs instead of a Mumm-rearrangement. The Smiles rearrangement is an intramolecular nucleophilic aromatic substitution of an aromatic sulfone, sulfide, ether or other aromatic compounds containing electron-withdrawing groups (EWG).[93] In this way, aryl sulfones can be converted to their corresponding sulfonic acids, for example.

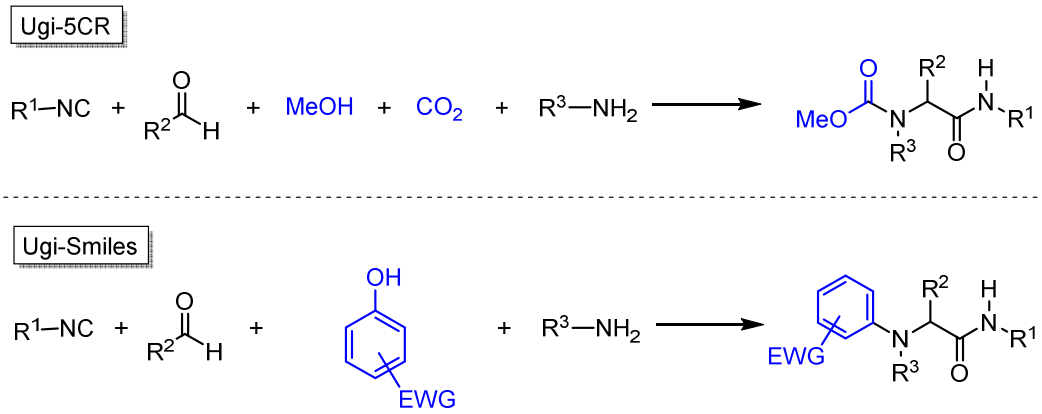

Scheme 14: Ugi-5CR using methanol and carbon dioxide instead of carboxylic acid to synthesize carbamates and Ugi-Smiles reaction using electron-deficient phenols instead of carboxylic acid.[87, 89]

The Ugi-4CR was also used in polymer chemistry by synthesizing monomers with polymerizable end groups, as direct polymerization method or as post-polymerization modification method. In the following part, the focus is on the direct polymerization using the Ugi-4CR. Therefore, it is necessary to use two bifunctional and two monofunctional components. In recent years, diversely substituted polyamides were produced by the Ugi four-component polycondensation process in this way. *Via* this versatile methodology, the possibility to combine different mono- and bi-functional components of different nature enables tuning the macromolecular structure of the obtained polymers.

Meier and coworkers investigated the optimal polymerization conditions for the combination of two bifunctional and two monofunctional components. This approach enables six possible combinations to generate diversely substituted polyamides *via* the

Ugi-4CR (diisocyanide + dialdehyde, diamine + diisocyanide, dialdehyde + diamine, diamine + carboxylic diacid, dialdehyde + carboxylic diacid and diisocyanide + carboxylic diacid) (Scheme 15).[94] The design of the side groups, as well as the repeating units could be tuned by variation of the starting components. The reaction conditions were optimized in order to obtain high molar mass polymers. All reactions were performed at room temperature for at least 36 h without catalyst. Although Ugi-4CRs are usually carried out in methanol, the use of different mixtures of tetrahydrofuran (THF)/methanol was required in order to prevent the precipitation of the polymers during reaction. The concentration also plays an important role in this process. Indeed, high dilution led to ring formation, whereas high concentration favored polymer formation, as can be expected for a step-growth polymerization. However, too high concentration resulted in high viscosity of the reaction mixture, which resulted in a decrease of the molar mass of the polymer. Considering all these parameters, Meier and coworkers investigated the best THF/methanol mixture and the optimal concentration for each of the mentioned combinations. After optimization, polymers with a molar mass above 10,000 g/mol were obtained after precipitation for all six combinations. Depending on their structure, the polymers showed glass transitions ranging from 1 to 65 °C. Furthermore, the mild conditions and tolerance of the Ugi-4CR towards many functional groups enabled the reaction with an alkyne-containing component. The resulting polyamide, bearing terminal alkynes in its side chains, offered the opportunity of post-polymerization modifications. The successful coupling *via* azide-alkyne cycloaddition demonstrated possible efficient grafting-onto reactions.

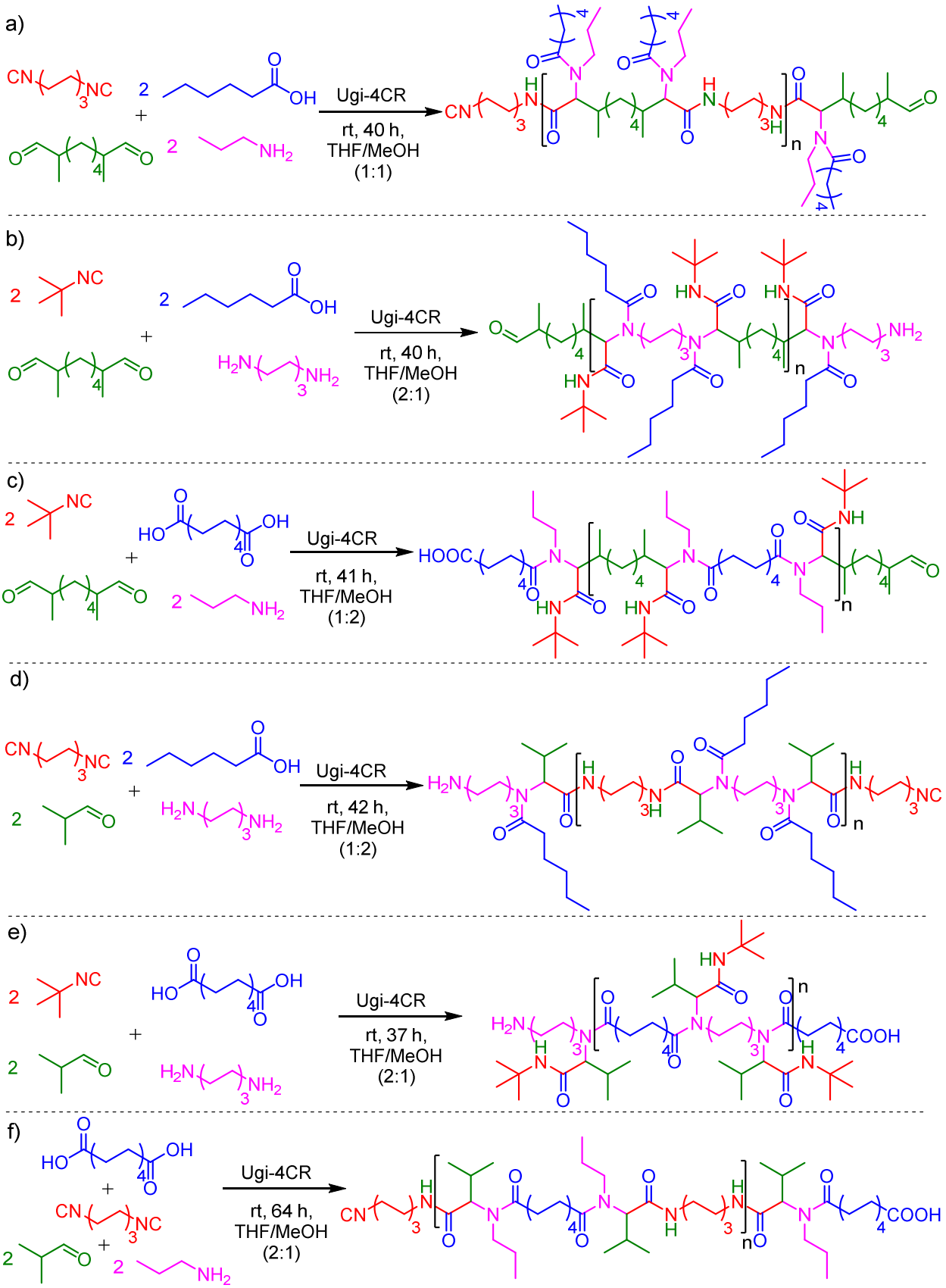

Scheme 15: Six possible combinations *via* the Ugi-4CR using two bifunctional and two monofunctional monomers (diisocyanide + dialdehyde (a), dialdehyde + diamine (b), dialdehyde + carboxylic diacid (c), diamine + diisocyanide (d), diamine + carboxylic diacid (e), and diisocyanide + carboxylic diacid (f)).[94]

In addition, Meier and coworkers reported the incorporation of carbon dioxide into polymers *via* the Ugi five component condensation (Ugi-5CC).[95] This reaction is a modified version of the Ugi-4CR, with the use of an alcohol (mostly methanol), a primary amine, an oxo-component (ketone or aldehyde), an isocyanide and carbon dioxide. The Ugi-5CC was employed as direct polymerization method using two bifunctional components (1,12-diaminododecane and 1,6-diisocyanohexane), an aldehyde, methanol and carbon dioxide to produce polyamides containing methyl carbamate side chains (Scheme 16). They could then be further converted into the corresponding polyhydantoins using an aqueous potassium hydroxide solution. A decrease of glass transition temperature from 37 °C to 0 °C was observed upon formation of the polyhydantoin. The molar masses of the synthesized polymers reached 20,000 g/mol. Thus, the Ugi-5CC is a novel route to synthesize polyurethanes, polycarbonates and polyhydantoins in a straightforward fashion and, moreover, catalyst-free way, avoiding the handling of toxic isocyanate or phosgene, commonly used in such synthesis.

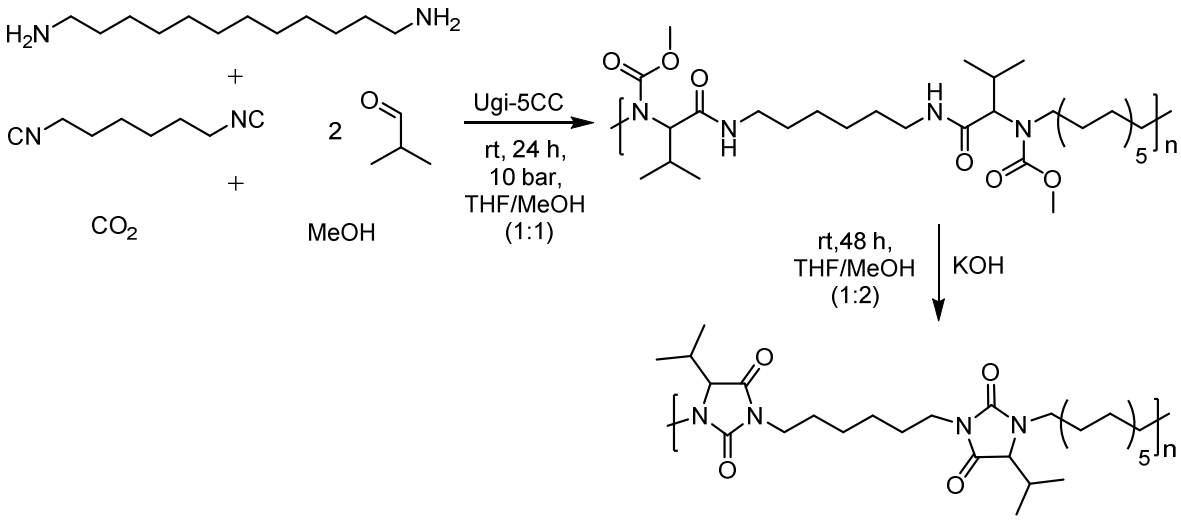

Scheme 16: Polymerization of 1,12-diaminododecane, carbon dioxide, 1,6-diisocyanohexane and methanol *via* Ugi-5CC and subsequent treatment with potassium hydroxide yielding the corresponding polyhydantoin.[95]

Luxenhofer and coworkers also investigated the six above-mentioned possible combinations of components of the Ugi-4CR for the synthesis of polymers bearing aromatic moieties in the backbone and side chain (Scheme 17).[96] After screening the reaction conditions, most of the combinations led to the formation of oligomers.

However, polymers with higher molar masses (between 28,000 g/mol and 44,000 g/mol) could be prepared for the diisocyanide + dialdehyde combination by reacting benzoic acid, hexadecan-1-amine, 1,6-diisocyanohexane and phthalaldehyde for five days at room temperature, using *N*-methyl-2-pyrrolidone (NMP) as solvent under argon atmosphere. For the described combination, the polymer backbone is formed before the Mumm rearrangement starts, whereas in all other combinations the polymer backbone is formed during the Mumm rearrangement, which might be an explanation for the better polymerization results.

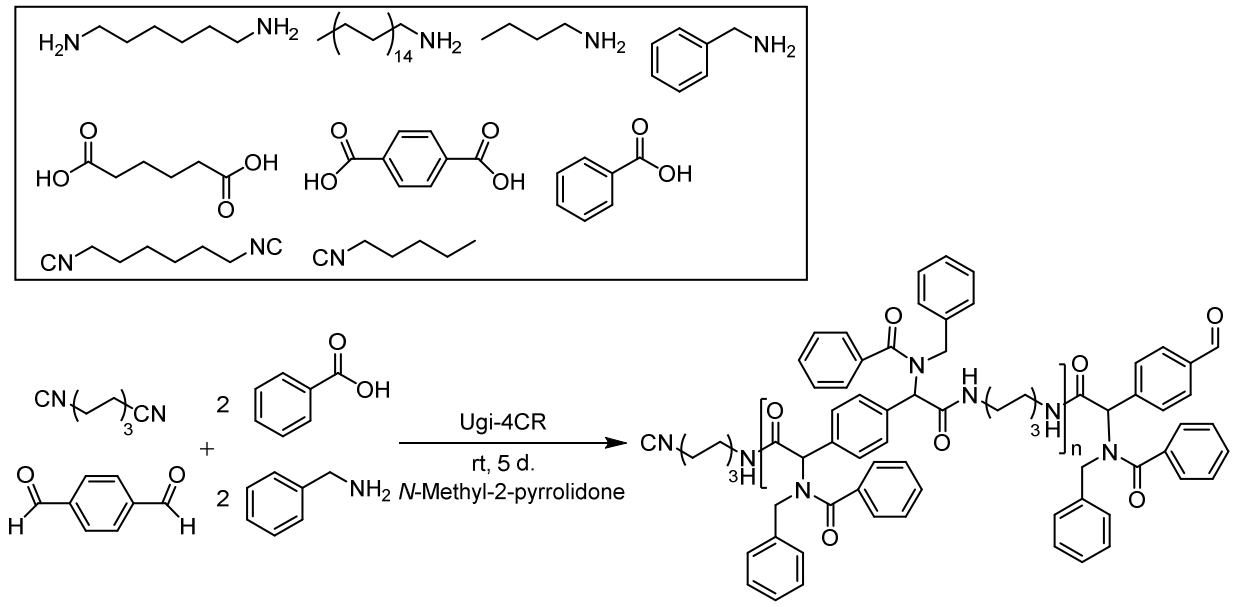

Scheme 17: Polymerization of benzoic acid, hexadecan-1-amine, phtalaldehyde and 1,6-diisocyanohexane *via* Ugi-4CR.[96]

Despite its bifunctionality, levulinic acid has to be modified chemically before its polymerization. The only example of its direct polymerization was reported by Becer and coworkers, who used it in the Ugi-4CR for the synthesis of polyamides (Scheme 18).[97] By bearing carboxylic acid and ketone moieties in its structure, levulinic acid acts as an AB-type monomer in an Ugi-4CR. Two equivalents of levulinic acid were reacted with one equivalent of diisocyanide and one equivalent of diamine in a microwave reactor at 100 °C in methanol for 30 minutes. 1,6-Diisocyanocyclohexane was chosen as diisocyanide and varying diamines have been tested. The use of ethylenediamine led to polymers with a molar mass of 8,000 g/mol, and the use of longer chain diamines, such as hexamethylenediamine or 1,12-diaminododecane

yielded polymers with molar masses up to 12,000 g/mol. A secondary amine (spermine) could also be used as a building block in the modified Ugi-4CR. The polymerization with a triamine (*tris*(2-aminoethyl)amine) resulted in a crosslinked spongy material and the use of an aromatic diamine (*p*-phenylenediamine) mainly yielded oligomers or macrocycles. Depending on the length of the employed amine, the levulinic acid derived polymers exhibited a T_g ranging from 52 to 120 °C.

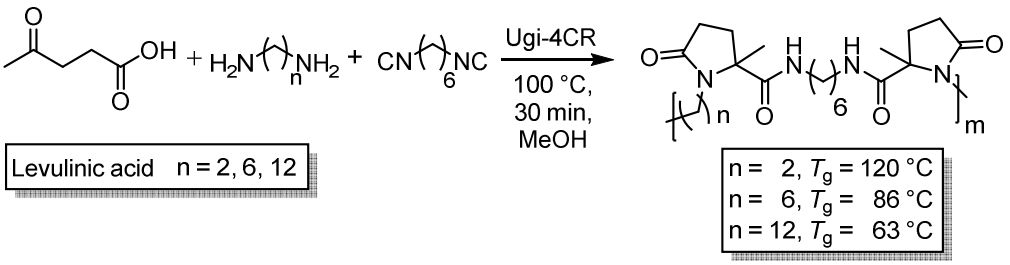

Scheme 18: Polymerization of levulinic acid, 1,6-diisocyclohexane and various diamines *via* Ugi-4CR.[97]

In a similar strategy, Tao, Wang and coworkers evaluated for the first time the use of natural amino acids in the Ugi-4CR for the synthesis of structurally diverse polypeptoids.[98] Amino acids, containing both carboxylic acid and amino groups in their structures, are prominent to be used as AB-type monomers for Ugi-4CR (Scheme 19). The combination with additional aldehydes and isocyanides results in polypeptoid structures with polyamide and substitution on the amide nitrogen. Although the polymerization of *α*-amino acids, such as glycine or alanine, was unsuccessful due to the formation of a six-membered ring as intermediate, lysine, which contains two amino groups including an *ε*-amino group at a higher “distance” to the *α*-carboxyl group, enabled the polymerization. After the protection of the *α*-amino group with *tert*-butyloxycarbonyl (Boc) protecting group, the AB-type monomer reacted with benzaldehyde and *tert*-butyl isocyanide at room temperature for 96 hours in methanol. Subsequently, the Boc protecting groups were cleaved to obtain the deprotected polypeptoids, reaching molar masses up to 11,000 g/mol. The obtained polymer displays an amphiphilic character and can therefore be self-assembled into nanoparticles in an aqueous environment in order to be investigated as carrier for drug delivery. In this context, the polymer proved to be biocompatible and to exhibit antibacterial properties. In similar procedures, *L*-glutamic acid methyl ester and N_α-

Boc-*L*-ornithine reacted with benzaldehyde and *tert*-butyl isocyanide to prepare poly(*γ*-peptoid)s and poly(*δ*-peptoid)s. Additionally, this strategy gave the opportunity to introduce functional groups into polypeptoids, such as alkenes or fluorescent moieties by variation the aldehyde structure.

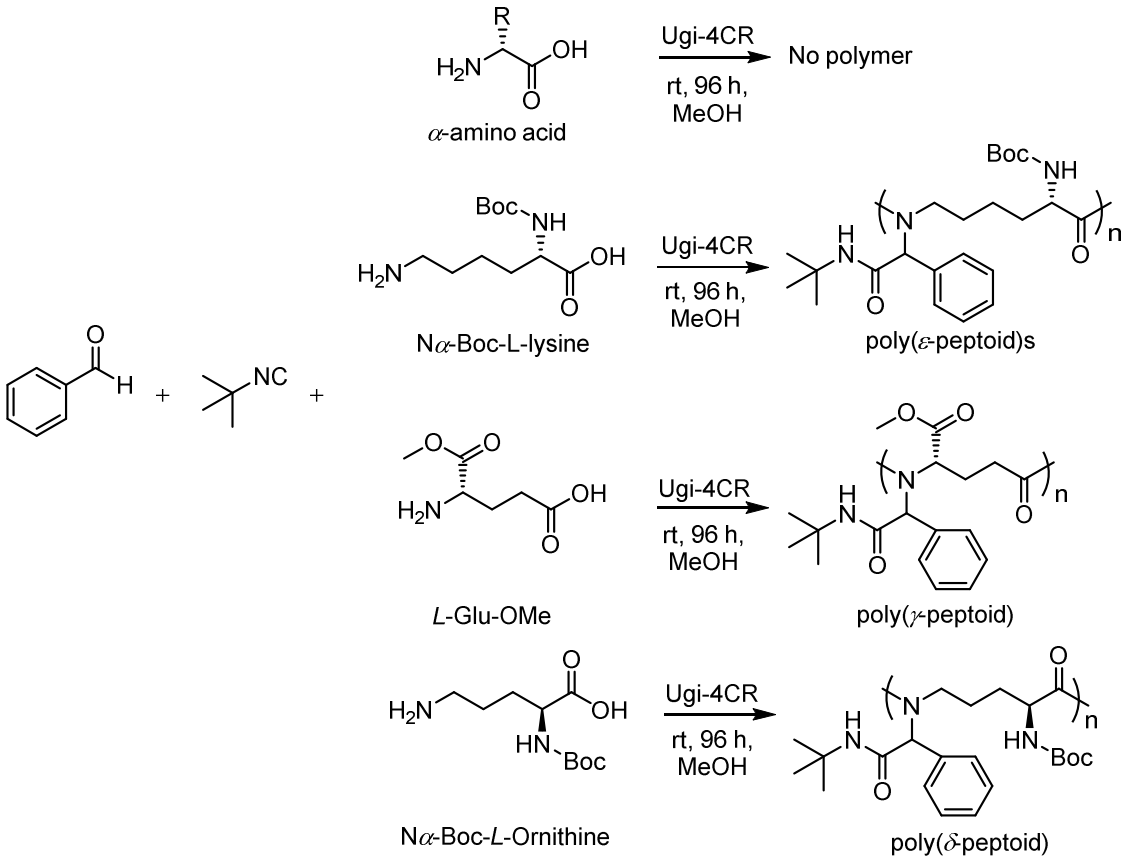

Scheme 19: Polymerization of amino acids with benzaldehyde and *tert*-butyl isocyanide *via* Ugi-4CR.[98]

2.3 Architecture control *via* multicomponent reactions

Parts of this chapter were published previously:

A. Llevot, A. C. Boukis, S. Oelmann, K. Wetzel and M. A. R. Meier, *Top. Curr. Chem.*, **2017**, *375*, 66. Copyright © 2017, with kind permission from Springer Nature.

The synthesis of well-defined polymer architectures is a topic of high interest. Multicomponent reactions revealed to be a powerful tool for the synthesis of such

architectures, due to their modular nature, efficiency and the relatively simple reaction conditions.[99]

For instance, dendrimers are an important class of highly-defined macromolecules, benefiting from their monodispersity and high functionality. Their synthesis can be performed by two main approaches: the divergent and the convergent pathway. The divergent synthesis of dendrimers consists in using a multifunctional core, in which each functional group reacts with one novel unit. The added groups display new functionalities available for further addition of a new unit. This sequence is repeated until the dendrimer reaches the desired size.

Wessjohann *et al.* described a divergent synthesis by using the Passerini-3CR of monoprotected bifunctional isocyanides, aldehydes and carboxylic acids to obtain a three-armed core unit with terminal benzyl esters.[100, 101] After cleaving the protecting groups *via* hydrogenation to the corresponding carboxylic acid and repeating these two steps (Passerini-3CR and hydrogenation), dendrimers of the third generation were received. This concept was extended using more building blocks *via* the Ugi-4CR.[100, 101] The same idea of using monoprotected bifunctional components led to a core unit with four methyl ester protected branches. The use of a large range of building blocks and different protecting groups offered the opportunity of selectively functionalized branches. Furthermore, the degree of branching was controlled by using monofunctional building blocks.

In another divergent approach, castor oil-derived chemicals (10-undecenal, 10-undecenoic acid and 10-isocyanodec-1-ene) containing a terminal double bond were used in a Passerini-3CR to form a core unit (Scheme 20).[102] Afterwards, the three terminal olefins were reacted in a cross-metathesis reaction with *tert*-butyl acrylate. Hydrogenation of the newly formed double bonds and formation of the introduced *tert*-butyl esters to carboxylic acid groups allowed further Passerini-3CRs. Repeating this protocol led to the formation of a third-generation dendrimer. The group of Li replaced the olefin cross-metathesis reaction with a thiol-yne reaction to introduce terminal alkynes, which resulted in additional branching.[103] This simple change led to a higher structural diversity within the dendrimers.

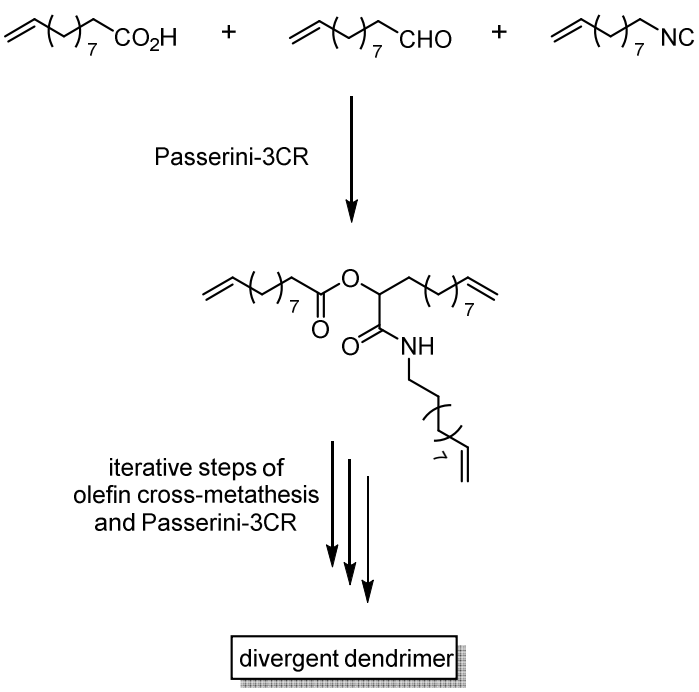

Scheme 20: Synthesis of divergent dendrimers from castor oil-derived chemicals.[102]

In a convergent synthesis, different precursors (dendrons), often built from small molecules, react to form the core of the dendrimer (Scheme 21).

In 2012, Rudick and coworkers described, for the first time, the convergent synthesis of dendrimers using Passerini-3CR.[104] They synthesized second generation dendrons with an alcohol end group at the center, which was used as platform for the synthesis of the three Passerini precursors (aldehyde, carboxylic acid, isocyanide). The three resulting dendrons were then coupled into one dendrimer *via* Passerini-3CR (Scheme 21). However, this approach suffered from long reaction times and from the lack of reactivity of the dendrons. In order to solve this issue, the authors further investigated this reaction by introducing an unbranched linker in order to increase the distance between the reactive groups and the branching point, thus decreasing the steric interactions between the reagents.[105] As expected, the use of dendrons with poly(alkyl ether) spacers exhibited a very short reaction time in the Passerini-3CR. However, the authors demonstrated that the reason for the observed increased reactivity does not lie in the decrease of the steric hindrance but in an unexpected electronic effect. Indeed, the increase of the aldehyde electrophilicity through the presence of strong electron-withdrawing substituents, revealed to be the key factor of the accelerating effect. Under these conditions, the reaction time could be reduced from 65 or 72 hours for not activated components to 24 hours employing the activated aldehyde (for the

second generation dendrons). Moreover, the authors showed that the reaction time of the Passerini-3CR increased with increasing generation.

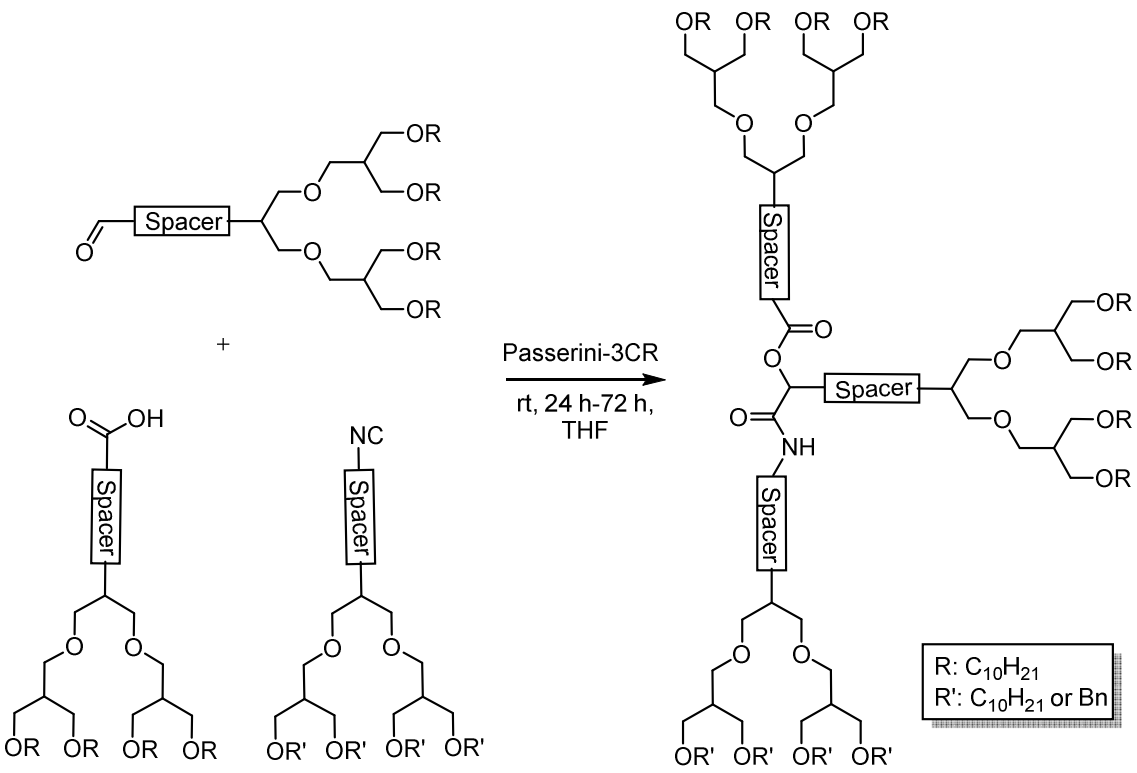

Scheme 21: Convergent synthesis of dendrimers using Passerini-3CR.[104, 105]

The synthesis of copolymers with defined architecture is also an important field of macromolecular engineering. For this purpose, both Passerini-3CR and Ugi-4CR have already been investigated.

The synthesis of Passerini-derived graft copolymers was investigated by the group of Li.[106] Therefore, adipaldehyde, 1,6-diisocyanohexane and 2-bromoisobutyric acid reacted in a Passerini-3CR to a polymer containing a polyamide backbone with pending hydroxyl groups or atom-transfer radical polymerization (ATRP) initiators. A subsequent ring-opening polymerization of *ε*-caprolactone or ATRP of methyl methacrylate and *N*-isopropylacrylamide led to copolymers. The authors also reported on the functionalization of PEG with an ATRP initiator and an alkynyl group by Passerini-3CR as precursors for miktoarm terpolymers (Scheme 22).[107]

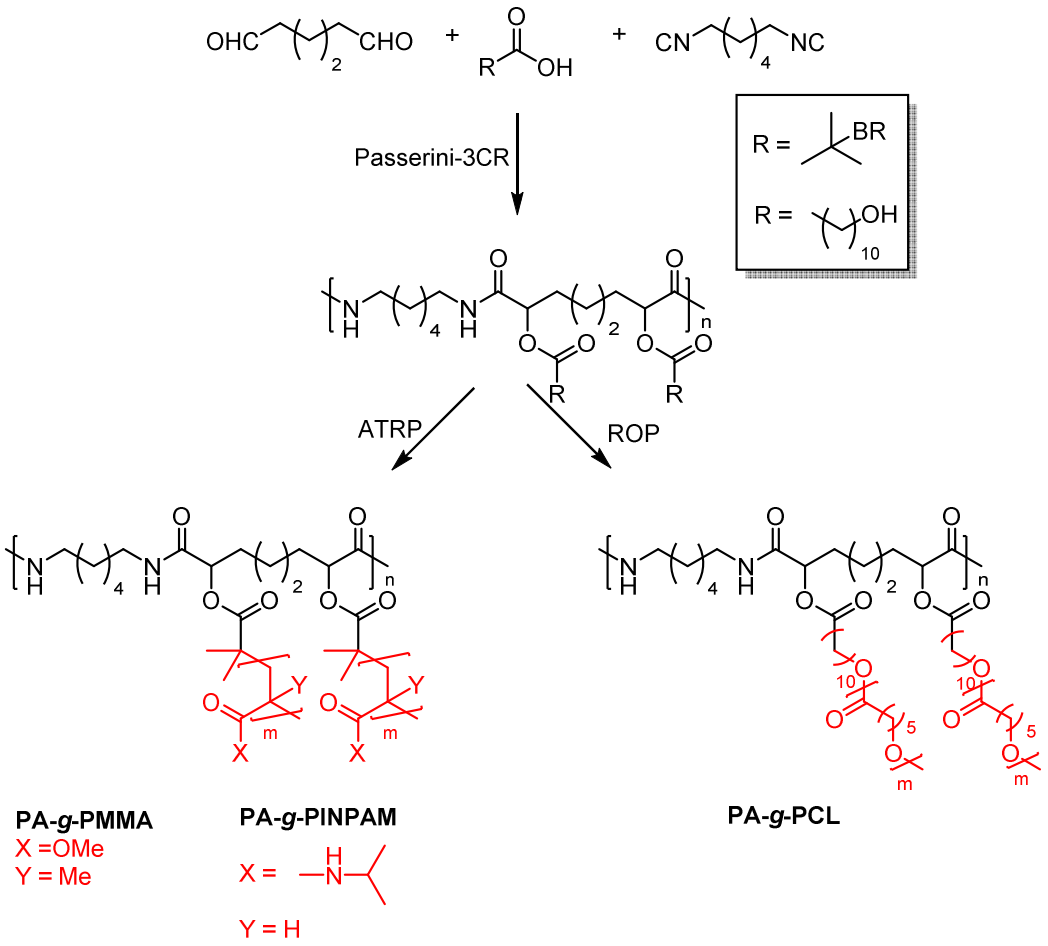

Scheme 22: Synthesis of graft copolymers *via* Passerini-3CR followed by ring-opening polymerization (ROP) or atom-transfer radical polymerization (ATRP).[106, 107]

Tao and coworkers investigated a conjugation method *via* the Ugi-4CR of benzaldehyde-terminated PMMA and aniline-terminated PEG, using an excess of functional isocyanides and carboxylic acids to obtain a mid-vinyl PMMA-*b*-PEG polymer.[108] Furthermore, they transformed this linear copolymer into a miktoarm star-shaped copolymer by introducing a RAFT agent for grafting-from with *N*-isopropylacrylamide (NIPAM).[109] Afterwards, a protein reactive functionality was introduced in the polymer backbone in the same manner to PEGylate a protein, which led to an improve of pharmacological and biologic activity.[110, 111] The incorporation of fluorescent molecules using the Ugi-4CR was also tested.

2.4 Unimolecular micelles

Unimolecular micelles possess interesting material properties due to their architecture and the ability to determine the dimension of the micelle, resulting in a multitude of possible applications. They can be used, for example, as catalysts or as hosts for organic low molecular weight guest molecules. [112] In addition, they are often able to stabilize metal nanoparticles. Characteristic of unimolecular micelles is, that the amphiphilic molecular parts of the aggregate are covalently linked together by a central molecule. This covalently linked core-shell architecture with a defined, adjustable microenvironment in the core, that is different from the adjustable microenvironment of the shell, may allow targeted encapsulation of guest molecules based on supramolecular interactions. [113] This leads to new applications in the field of encapsulation and transport of guest molecules, as templates for the synthesis of catalytically active metal nanoparticles or as interesting materials for the development of sensors.[114] However, most commonly these polymers are used in targeted pharmacotherapy (targeted drug delivery).[115] Compared to classic micelles, which are based on the association of low molecular weight amphiphilic molecules, unimolecular micelles are characterized by increased stability towards temperature, pH, solvents and other physical and chemical influences due to the covalent linkages. Due to this linkage in unimolecular micelles, there is no dynamic equilibrium between the individual amphiphilic molecules and the micelle. Individual parts of the molecule cannot leave the union of the unimolecular micelle, which makes them independent of the complex self-aggregation processes of classical micelles.[116, 117]

These core-shell structures of unimolecular micelles can be constructed from different polymer architectures (Figure 2).

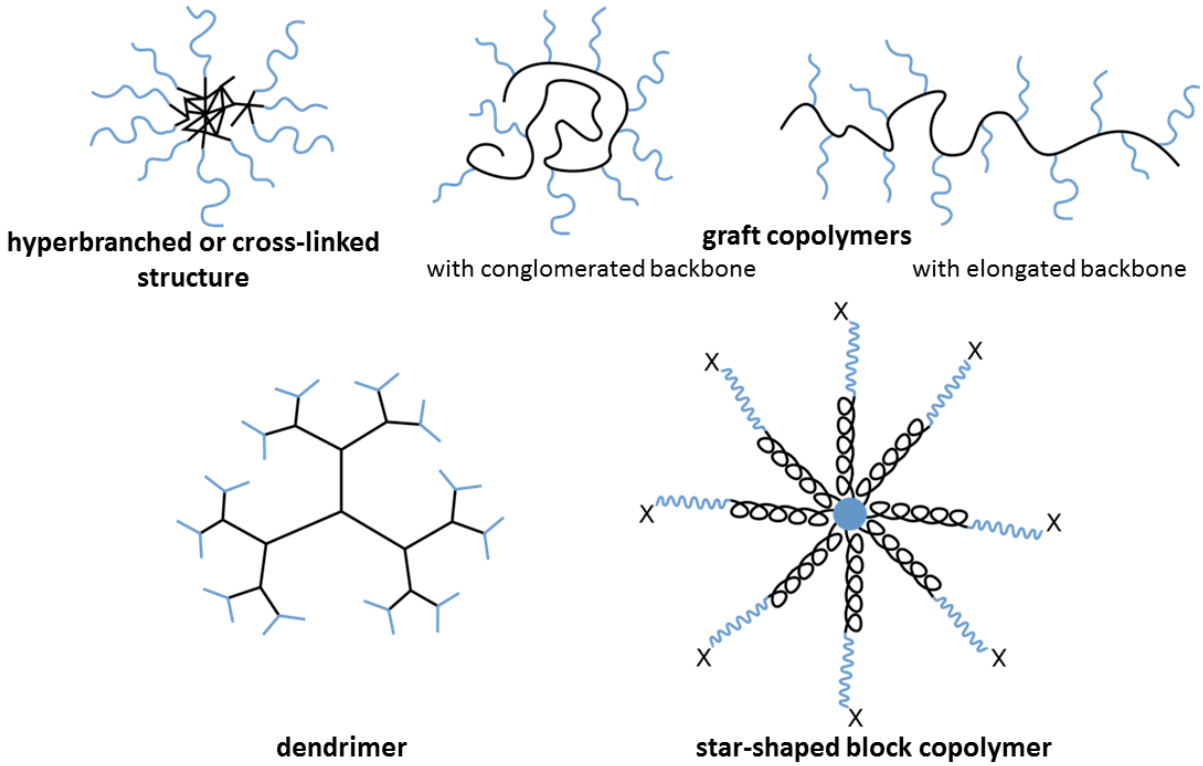

Figure 2: Various polymer architectures which can act as unimolecular micelles with hydrophobic chains (black) and hydrophilic chains (blue).[118]

Polymers with hyperbranched or cross-linked hydrophobic chains attached to hydrophilic chains show amphiphilic properties and behave like unimolecular micelles.[119-121] For the construction of such architectures, a linear hydrophilic polymer is first synthesized. Subsequently, a di- or multifunctional and hydrophobic monomer (e.g. a divinyl compound) is added to form a crosslinked core. The control over this reaction is usually difficult, whereby the core dimensions are difficult to adjust and usually inconsistent. Moreover, it is impossible to predict the exact number of hydrophilic arms on the core. As a consequence, polydisperse particles are often formed.[122]

Furthermore, graft copolymers with a hydrophobic backbone, which carries hydrophilic side chains can also adopt a core-shell conformation. An advantage of this type of macromolecule is, that different micellar shapes can be achieved, depending on the chain stiffness of the backbone. For example, a chain-rigid polymer backbone can form cylindrical micellar shapes, while flexible backbones are expected to form spherical micelles.[123]

Dendrimers bearing polar groups can also form unimolecular micelles.[124, 125] They are very well-defined in their dendritic structure, but require multistep organic syntheses.[126-130]

The best control over the dimension of the unimolecular micelle is achieved through the synthesis of star-shaped block copolymers with their covalently linked and hydrophobic core bound to a hydrophilic shell.[131, 132] They often show similar properties and applications, but are much easier to synthesize. The advantage of such star-shaped block copolymers is, that the number of arms can be precisely adjusted by the number of initiation groups. In addition, the lengths of the hydrophobic and hydrophilic blocks can also be precisely adjusted by the concentration ratio between monomer and initiator. This allows the adjustment of the solution properties and the dimensions of the micelle. The synthesis of such star-shaped block copolymers has been realized in a variety of ways and it has been shown, that their properties and applications often resemble those of dendrimers or hyperbranched polymers.[133, 134]

Recently, polypeptide PEG miktoarm star-shaped polymers with a fluorescently labeled core molecule have been prepared by RAFT (reversible addition-fragmentation chain transfer) and click chemistry.[135] In addition to a low cytotoxicity, these polymers could complex and transport siRNA (small interfering ribonucleic acid). Furthermore, ABC miktoarm star-shaped polymers with poly(3-hexylthiophene), polystyrene and poly(2-vinylpyridine) segments and low dispersities (Đ < 1.05) were prepared by an efficient combination of polymer conjugation and living anionic polymerization.[136] Whittaker *et al.* also reported a simple and highly efficient method based on iterative Cu(0)-mediated controlled radical polymerization for the synthesis of highly-defined multiblock star-shaped copolymers.[137] Thus, 5-armed star-shaped polymers with up to five different polymer blocks in each arm could be obtained. Sequential ATRP has also been used to synthesize 21-arm star-shaped polymers based on initiator-functionalized cyclodextrin.[138] The arms were made of poly(*tert*-butyl acrylate)-b-polystyrene. After hydrolysis of the *tert*-butyl esters, amphiphilic polymers were obtained and their unimolecular micellar behavior was confirmed by DLS (Dynamic light scattering), TEM (Transmission electron microscopy) and AFM (Atomic force microscopy).

2.5 Drug delivery systems

Drug delivery systems have become of great interest in recent years. The efficient transport of a drug not only improves its efficiency, but also its patient tolerance. This is especially the case when an active ingredient does not reach its target tissue, or only to a small extent. Many drugs also require frequent use and often have side effects of varying degrees. In addition, drug delivery also simplifies the handling of a drug and an improved compliance with the dosing rules can be achieved. As many highly potent drugs already exist, the interest has focused on optimizing drug effects *via* new drug delivery systems.[139]

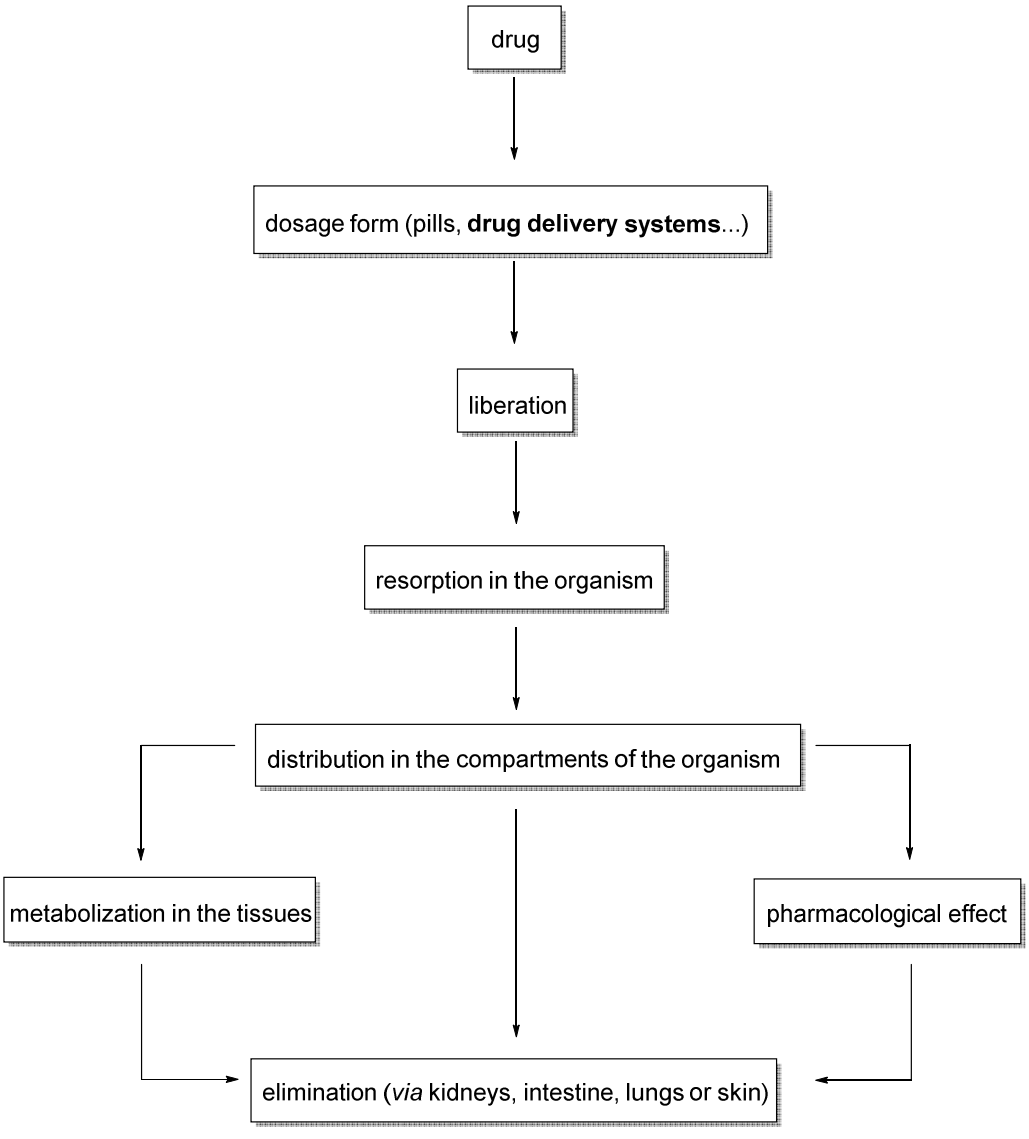

Figure 3: The route of the drug from its dosage form to its elimination from the organism.[140]

Before discussing the possible drug delivery systems, the route of the drug from its dosage form to its elimination from the organism will be explained (Figure 3).

A drug is a substance, which is responsible for the pharmacological effect. This substance is converted to its dosage form and consists the active pharmaceutical ingredient as well as additives and excipients, which should not show any pharmacological effects of their own (for example pills or drug delivery systems). The subsequent liberation of the drug from the dosage form is characterized by solubility and dissolution rate and is influenced by local temperature and blood flow. This is followed by the absorption of the drug from the body surface or from inside the body to the bloodstream or lymphatic system. The resorption of the drug is a requirement for its effect. The drug has to overcome the skin, the mucous membrane or other barriers. The amount of drug, which is resorbed from the dosage form per time, is called bioavailability. The following distribution is the way in which a drug is distributed to the body tissue or organs. The most important requirement for the distribution of a drug in the organism is a corresponding blood supply. Drugs can also be effective in the blood itself. The final elimination describes all processes that stop the effect of the drug. This can be done by a chemical transformation of the drug or by elimination through various organs (metabolism). Most drugs are eliminated *via* the kidneys, the intestine, the lungs or the skin.[140]

The drug delivery system should, in the best case, deliver the drug at a constant rate. This continuous resorption makes it possible to equalize the liberation of the drug to its elimination, which should create an equilibrium. In comparison to conventional dosage forms, significantly lower amounts of substance are required. These reduced amounts result in a reduction of undesired side effects and an increased safety of the medication therapy. Conventional dosage forms show a short effective duration, which leads to a relatively high application frequency and a fluctuation of the concentrations in the blood and in the tissue. High concentrations alternate with low concentrations, so that an optimal therapeutic concentration is achieved only for a limited time. These concentration variations and the limited effective duration of conventional dosage forms have led to the concept and realization of (controlled) drug delivery systems. The majority of newly developed drug delivery systems include polymers, which have to demonstrate the following requirements:[141]

- simple application
- low price and easy synthesis
- low polydispersity
- good solubility
- biocompatibility
- biodegradability
- reproducible and constant liberation rate
- safety against overdoses
- less side effects due to lower dosage

By using polymeric drug delivery systems, not only the effect of the drug, but also the effect of the dosage form on the recipient tissue must be considered. In addition, it must be ensured, that the properties of the polymers do not change adversely during exposure in the biological environment. For degradable polymers, the degradation products should not be toxic or carcinogenic. Furthermore, they should be excreted as quickly as possible with the least possible accumulation in the tissue. There are several drug delivery systems, which have advantages and disadvantages depending on the application.

2.5.1 Membrane systems

In membrane systems, the drug, encapsulated in one or more membranes, is applied to the body and passes through the membranes into the organism *via* diffusion or osmosis. The membranes are usually semipermeable. Microporous membranes allow, depending on pore size, diffusion of higher molecular weight drugs. In microporous, degradable membranes, the operational removal of the membrane system after consumption of the drug is not necessary. Such systems degrade in the body by hydrolytic or enzymatic degradation.[142] When the membrane system comes in contact with the body fluid, water diffuses through the solid membrane into the system. As a result, the hydrostatic pressure increases within the membrane, which allows the constant release of the drugs. The diffusion characteristics of polymers can be influenced by several factors, which is of great importance for membrane systems which exhibit diffusion-controlled drug release (Table 1).[143] For polymers having

relatively stiff backbones, such as polystyrene, diffusion decreased due to the increased mobility of the chain segments compared to polymers having flexible backbones, such as polyethylene. For membrane systems polysiloxanes, hydrogels and polyvinyl acetate are frequently used. These polymers are relatively inert to drugs and only degrade slowly in the body.[144]

Table 1: Influencing factors on the diffusion coefficient of polymers.[143]

influencing factors of the polymer		influence on diffusion coefficient
molecular weight	↑	↓
degree of cross-linking	↑	↓
stiffness of the backbone	↑	↓
interaction between molecules	↑	↓
degree of crystallization	↑	↓
plasticizer content	↑	↑
filler content	↑	↑

2.5.2 Matrix systems

In matrix systems, the drug is dissolved or dispersed in the polymer matrix. For such drug delivery systems, microporous or biodegradable matrix systems are used. In degradable therapeutic systems, where the drug is distributed or chemically bound in the degradable polymer matrix, the rate of release depends on the rate of degradation of the polymer. Depending on the material, the degradation occurs hydrolytically or enzymatically. For such systems, water-soluble polymers and hydrolytically or enzymatically degradable polymers are used. Examples of these are polylactides, polyglycolides, poly (*ε*-caprolactone) or poly (*β*-hydroxybutyric acid). In the degradable systems, mixtures of the polymer and the drug are processed simultaneously. At high processing temperatures, such as in the extrusion process, the drug should not show thermally induced chemical changes. With limited temperature stability of the drug, an alternative processing method (processing from the solution) must be chosen.[144]

2.5.3 Carrier systems

In drug carrier systems, the drug is chemically bound to the side chains of a degradable or biologically inert backbone.[145] Advantages of those systems are a higher specificity due to a higher availability of the drug, a longer effective duration and increased therapeutic effect. In addition, carrier systems generally have a very high drug content of up to 80 weight percent.[146] The polymer carrier must be hydrophilic to ensure solubility in water and should have the necessary functional groups for covalent attachment of the drug. The concept of covalent attachment of a biodegradable spacer, which can be cleaved by specific enzymatic or hydrolytic reaction, has been proposed to make the drug effective at a specific release rate at a specific location.[147] In order to allow a specific localization, it has also been proposed, that in addition a specific functional group (targeting residue) is bound to the polymer in order to achieve a cell-specific uptake (Figure 4). Among the polymers investigated so far, dextran, polyethylene glycol, *N*-(2-hydroxypropyl)methacrylamide (HPMA)-copolymers and polyaspartic acid have been established as non-toxic polymers for the use as carrier materials.[148]

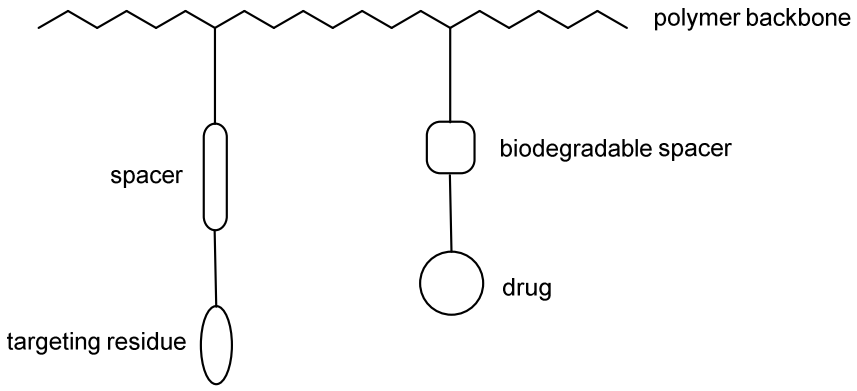

Figure 4: Structure of a water-soluble polymeric carrier material for drug delivery systems.[147, 148]

2.5.4 Micelles and liposomes

Classical micelles in aqueous solutions formed by self-assembly of amphiphilic block copolymers (5-50 nm) or unimolecular micelles (see chapter 2.4) became very important in the field of drug delivery applications. The drugs are physically

encapsulated in the core of the micelles and transported using concentrations, which would normally not be possible due to the limited water solubility of some drugs. Due to the hydrophilic shells, the micelles can form hydrogen bonds with the aqueous environment to protect itself against hydrolysis and enzymatic degradation. The fact, that the molecular weight and block length and in the case of unimolecular micelles the number of arms can be easily changed, allows control of the morphology and size of the micelles. This allows the setting of certain properties for the desired drug. Furthermore, block copolymers can be functionalized with cross linkable molecules to increase the stability of the classical micelles.[149, 150]

Liposomes have a membrane shell of a bilayer of molecules that have both a non-polar and a polar part. Therefore, water-soluble drugs were encapsulated inside the aggregation of the hydrophobic ends and fat-soluble drugs were encapsulated into the hydrophilic layer. Synthetic liposomes are mostly stable in the organism and show a low toxicity.[150-153]

In both cases the micelles or the liposomes are affiliated from phagocytic cells and degraded to release the drug.[150]

3. AIM

The aim of this work was the establishment of a straightforward and scalable synthesis of unimolecular micelles based on amphiphilic star-shaped block copolymers with adjustable microenvironment in the core and a water-soluble shell. For this purpose, the Passerini-3CR reaction, using an AB-type monomer and multifunctional core molecules acting as ICTA, should be used, to obtain water-soluble core-shell architectures with different numbers of arms and adjustable degree of polymerization. A synthesized library of amphiphilic star-shaped block copolymers with selective structural variation, polarity of the core, shell architecture and degree of polymerization should be investigated for their unimolecular micellar behavior and their encapsulation and transport behavior for a better understanding of structure-property relationships and thus the design of new host-guest polymers. Furthermore, the biocompatibility and the potential application as drug delivery systems of these polymers should be confirmed.

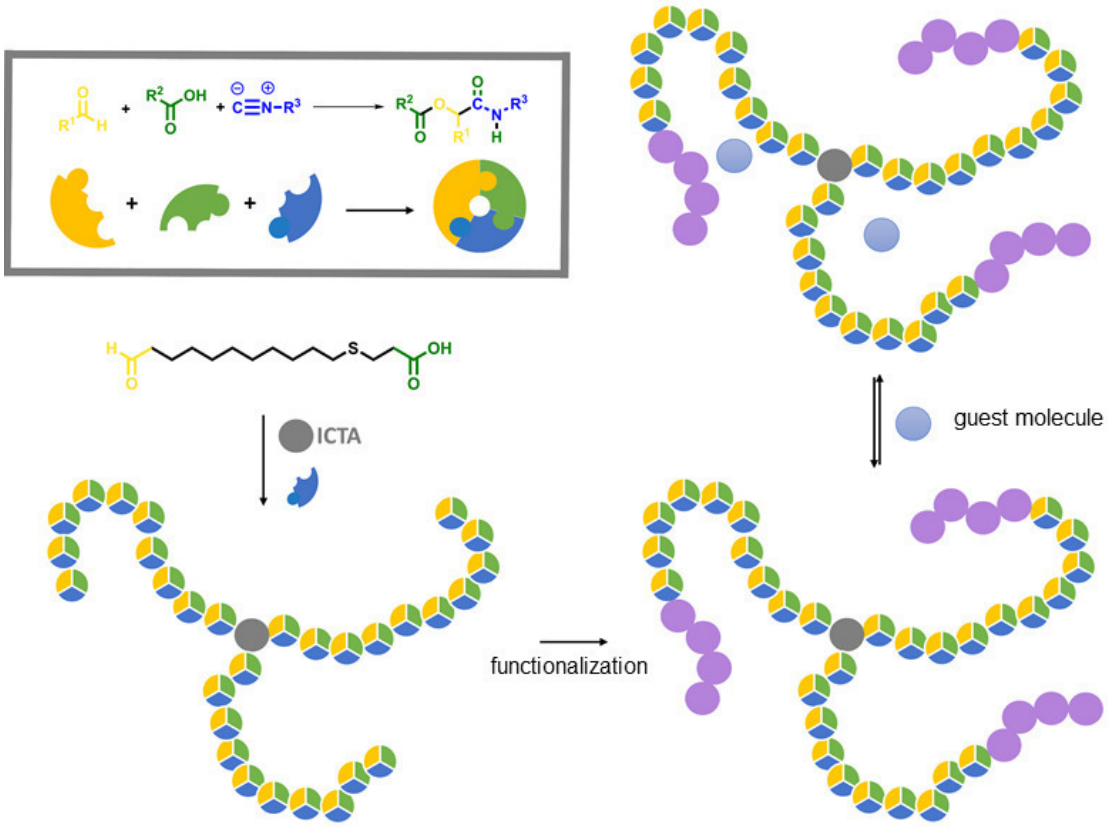

4. RESULTS AND DISCUSSION

4.1 Controlling molecular weight and polymer architecture *via* the Passerini-3CR

This chapter and the associated sections in the Experimental Part were published previously:

S. Oelmann, S. C. Solleder, and M. A. R. Meier, *Polym. Chem.,* **2016**, *7*, 1857. Copyright © 2016, permission from the Royal Society of Chemistry.

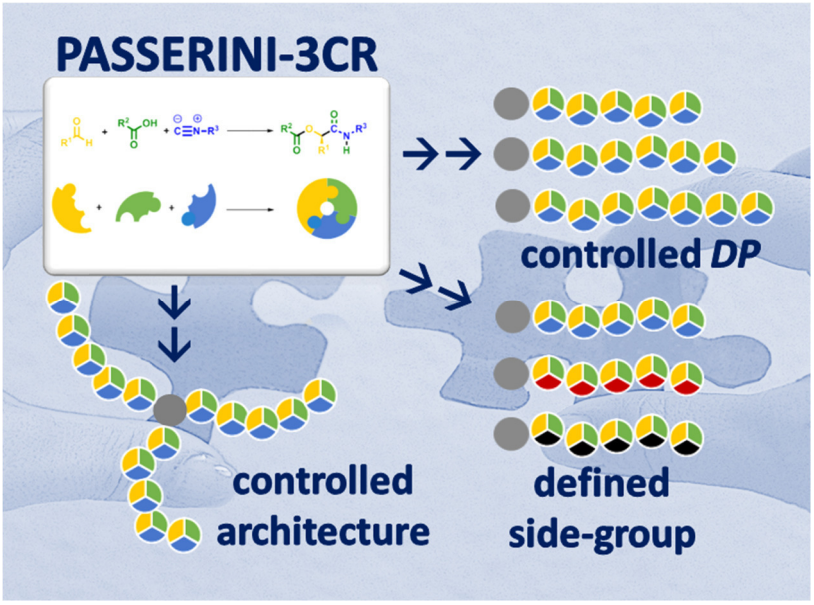

Abstract

A new approach to control the molecular weight and polymer architecture using the Passerini three-component step-growth polymerization is described. Starting from an AB-type monomer, linear homopolymers, diblock copolymers, as well as star-shaped polymers were synthesized in an efficient manner. By varying the ratio of the AB-type monomer and a suitable ICTA, different polymer architectures with specific molecular weights and high end-group fidelity were obtained.

Introduction

In order to obtain better control over the material properties of polymers, it is essential to synthesize polymers with well-defined structures.[154] Usually, living/controlled polymerization techniques, such as reversible addition-fragmentation chain transfer (RAFT) or atom transfer radical polymerization (ATRP), which are the most extensively studied controlled radical polymerization techniques, or anionic polymerization are used to prepare various well-defined macromolecular architectures.[155] However, well-defined polymers were also synthesized *via* polycondensation reactions by using monomers, which react selectively with the polymer chain ends.[156-158] For instance, our group synthesized defined macromolecular architectures using head-to-tail acyclic diene metathesis (ADMET) polymerization.[159, 160] This synthesis procedure was accomplished by taking advantage of the different reactivities of terminal double bonds and acrylates in olefin metathesis reactions.[161]

Recently, multicomponent reactions (MCRs) have been introduced to the field of polymer science as straightforward polymerization technique with a step-growth character.[162] This type of reaction is performed with more than two starting materials in one-pot and leads to functional materials in a straightforward fashion. In polymer chemistry, isocyanide-based multicomponent reactions (IMCRs), such as the Passerini-3CR, are often used.[163, 164] For instance, by using bifunctional components, a polymerization process is induced and substituted polyesters, polyamides and poly(ester amide)s are obtained.[165 - 167] Furthermore, with AB-type bifunctional monomers, it is possible to perform the reaction with only two components, which leads to an easier and more efficient polymerization process.[168, 169] It is also possible to synthesize multi-block copolymers with sequence-ordered side groups.[170] Moreover, several applications of metal-catalyzed MCRs are described in polymer chemistry.[171, 172]

4.1.1 Synthesis of linear homo- and block copolymers

This section focusses on the synthesis of well-defined polymer architectures employing the Passerini-3CR as polymerization technique. The approach relies on the use of a monocarboxylic acid as an ICTA in combination with bifunctional monomer **3** and an isocyanide to achieve control over the molecular weight. The thus resulting carboxylic

acid end-group subsequently allows the synthesis of block copolymers. Moreover, the use of a tricarboxylic acid as core unit should result in the formation of star-shaped homo- and copolymers. Thus, an AB-type monomer **3**, containing a carboxylic acid and an aldehyde unit was prepared by a thiol-ene reaction of 10-undecenal **1** and 3-mercaptopropionic acid **2** (Scheme 23).[168]

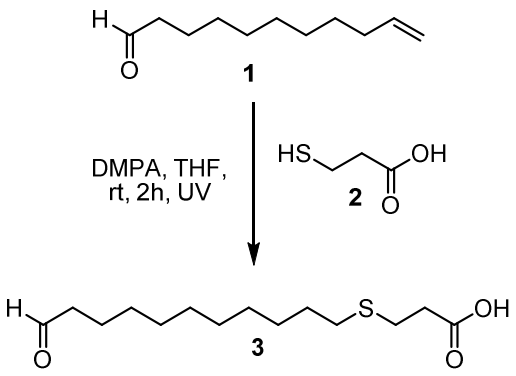

Scheme 23: Synthesis of AB-type monomer **3** *via* thiol-ene reaction.

The Passerini polymerization of monomer **3** was then performed in dichloromethane (DCM) at room temperature using four different isocyanides **5**-**8** with a ratio of monomer **3** : isocyanide **5-8** : 10-undecenoic acid **4** of 20:100:1. 10-Undecenoic acid **4** served as ICTA (Scheme 24).

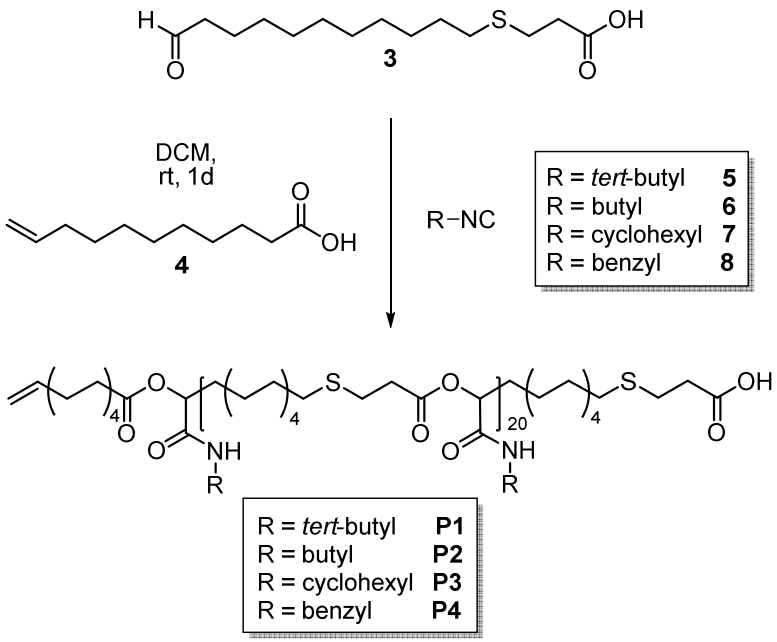

Scheme 24: Passerini-3CR using different isocyanides **5**-**8**.

4. Results and Discussion

Molecular weights of the obtained polymers were measured by SEC and additionally calculated from ^{1}H NMR data (see associated sections in the Experimental Part). If this process proceeds as anticipated, monomer **3** as well as the formed oligomers of **3** and the respective isocyanide would add irreversibly to **4** (and later on growing polymer chains) until all monomer is consumed and the molecular weight would be predetermined by the ratio of [**3**]:[**4**], comparable to the monomer : initiator ratio in controlled/living polymerizations. The calculated molecular weights were calculated with following formula:

$$M_n = M_n(\text{Monomer } \mathbf{3} + \text{Isocyanide}) * \text{n} + M_n(\text{ITCA } \mathbf{4})$$

Representative example with **P1**:

$$M_n = \left(274.42\,\frac{\text{g}}{\text{mol}} + 83.13\,\frac{\text{g}}{\text{mol}}\right) * 20 + 184{,}27\,\frac{\text{g}}{\text{mol}} = 7{,}335\,\frac{\text{g}}{\text{mol}}$$

Indeed, for all investigated isocyanides **5-8**, the expected molecular weights corresponded well to the actual values determined by ^{1}H NMR integration of the end group signal and the signals of the repeating units (Table 2).

Table 2: Molecular weights of polyesters **P1**-**P4** synthesized with different isocyanides **5**-**8** (ratio monomer **3** : isocyanide **5**-**8** : 10-undecenoic acid **4** of 20:100:1).

polymer	M_n calc. [g/mol]	M_n NMR [g/mol]	M_n SEC [g/mol]	Đ M_w/M_n	T_g [°C]
P1	7,335	7,377	12,000	1.51	5
P2	7,616	7,950	11,800	1.51	-11
P3	7,856	8,884	12,000	1.67	3
P4	8,016	7,052	11,000	1.46	1

SEC analysis revealed higher molecular weights than expected, which is due to the different hydrodynamic volumes compared to the linear PMMA calibration standards. The thermal properties of the polyesters were determined by DSC, which revealed an amorphous behavior with glass transitions (T_g) ranging from -11 °C to 5 °C, depending on the isocyanide.

Delighted by these results, the polymerization behavior was further investigated by a step-wise addition of monomer **3** in portions of five equivalents. After each batch addition of fresh monomer, the reaction was allowed to proceed until there was no more change in molecular weight by SEC (Figure 5) and longer times to reach a constant molecular weight were required after each addition.

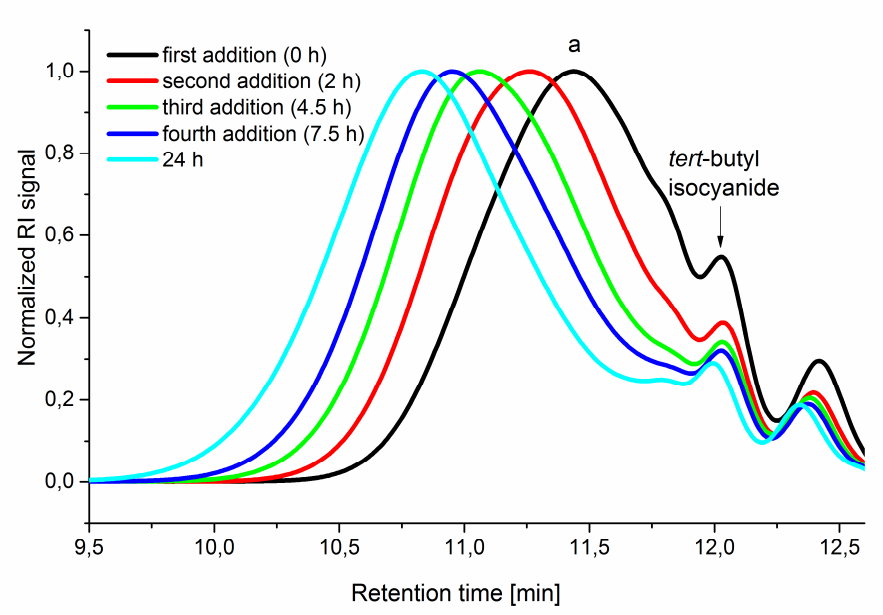

Figure 5: SEC chromatogram showing the growth of polyester **P1** during the addition of **5** equivalents of monomer **3** after specific time periods measured from reaction mixture; (a = first (0 h), b = second (2 h), c = third (4.5 h), d = fourth addition (7.5h), e = 24 h).

Most importantly, it was clearly shown by this experiment, that the polymer chain grows until all monomer is consumed and that the polymerization can be continued, i.e. the chain extended, by simply adding additional amounts of monomer **3**. After two hours a ^{1}H NMR spectra of the crude reaction mixture was measured to see if there was a full conversion of AB-type monomer **3**. Figure 6 confirmed this assumption, since no aldehyde signal could be observed.

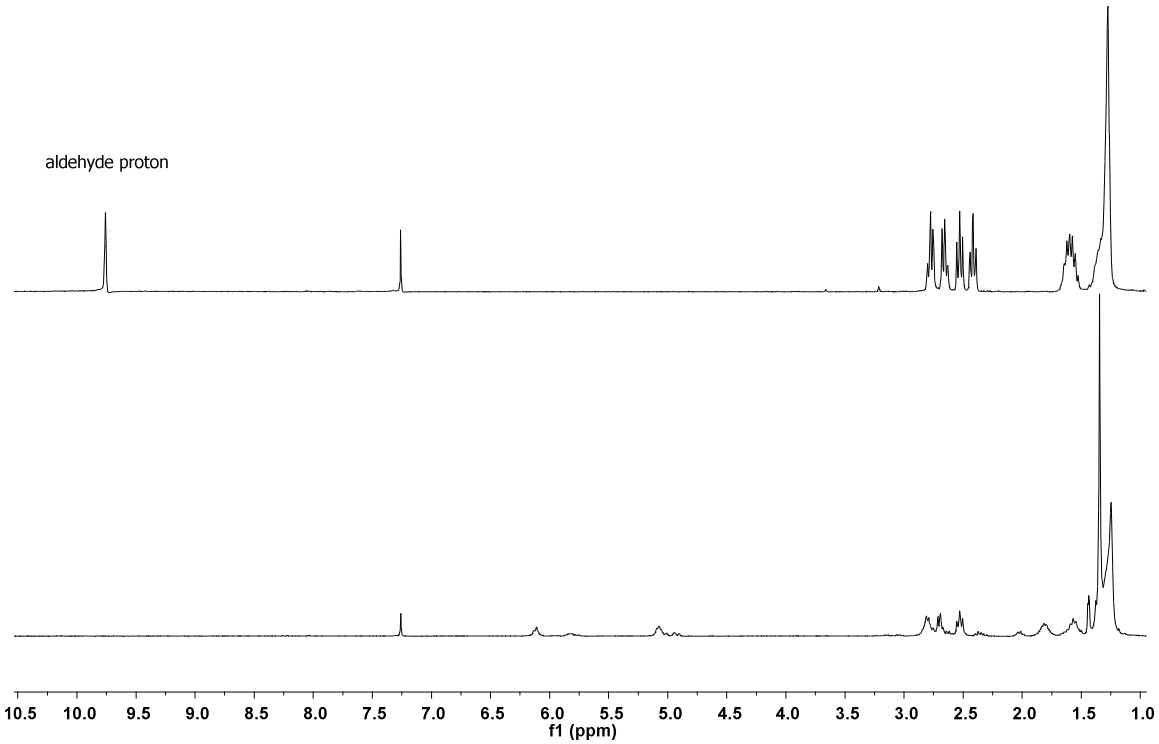

Figure 6: Comparison of ^{1}H NMR spectra of AB-type monomer **3** (above) and **P1** (below) after 2 hours with 5.00 equivalents of monomer **3** and without precipitation.

To further demonstrate the control over the molecular weight using this method, different ratios of AB-type monomer **3** and ICTA **4** (10:1 to 40:1) were investigated (Scheme 25).

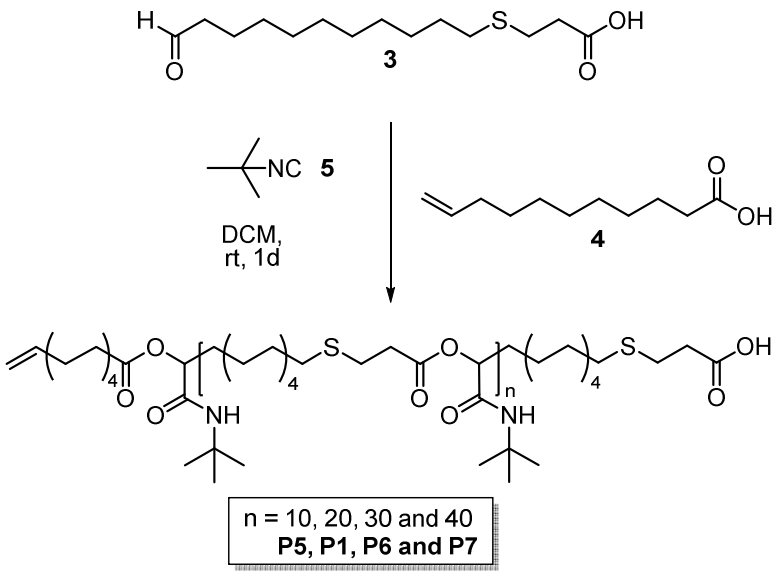

Scheme 25: Passerini-3CR using different ratios of AB-type monomer **3** and ICTA **4** (10:1 to 40:1).

It could be shown that the molecular weights of the resulting polymers calculated from ^{1}H NMR data were in good agreement with the expected molecular weights (Table 3). Furthermore, the SEC results show an increase of the molecular weight using higher ratios of AB-type monomer **3** and ICTA **4** by a shift of the curve to lower retention times (Figure 7).

Table 3: Molecular weights of polyesters **P1** and **P5**-**P7** obtained by using different ratios of monomer **3** and ICTA **4** (determined by ^{1}H NMR and SEC).

polymer	ratio [**3**]:[**4**]	M_n calc. [g/mol]	M_n NMR [g/mol]	M_n SEC [g/mol]	Đ M_w/M_n
P5	10:1	3,760	4,146	9,100	1.60
P1	20:1	7,335	7,377	12,000	1.51
P6	30:1	10,911	10,997	14,200	1.40
P7	40:1	14,486	14,515	15,700	1.37

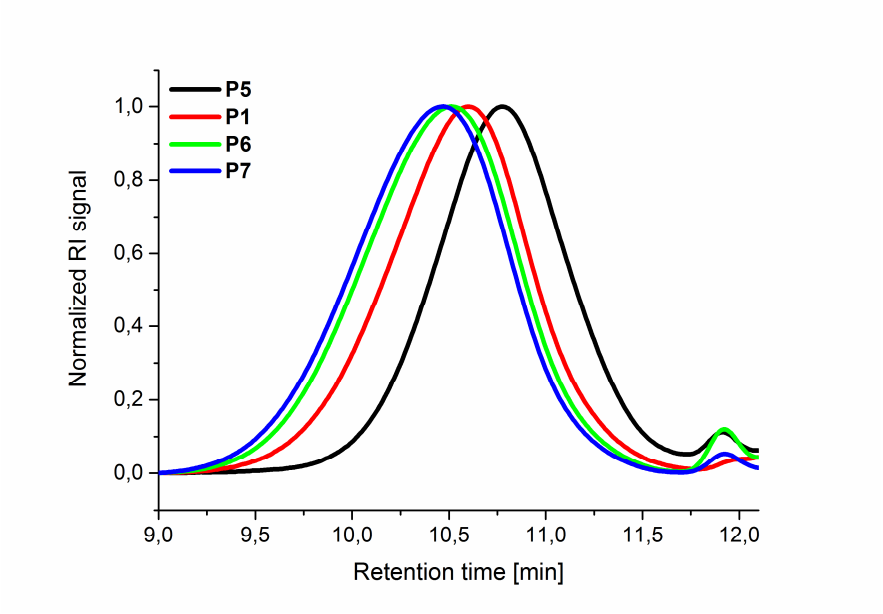

Figure 7: SEC results of polymerizations with varying ratios of AB-type monomer **3** and 10-undecenoic acid **4** (**P5** = 10:1, **P1** = 20:1, **P6** = 30:1, **P7** = 40:1).

Using a ratio of [**3**]:[**4**] of 40:1, a further addition of isocyanide **5** after 24 hours was necessary to obtain full conversion. A reason could be the increasing viscosity of the reaction mixture upon reaching higher molecular weights. By diluting the mixture with additional isocyanide **5**, viscosity decreased while reactivity increased, leading to full

conversion. Each linear homopolymer **P1-P7** was additionally characterized *via* mass spectroscopy (see associated sections in the Experimental Part). Figure 8 is showing the representative mass spectra of **P1** with the expected number of repeating units n as well as the expected theoretical masses, respectively. Unfortunately, proper ionization of **P4** was not possible.

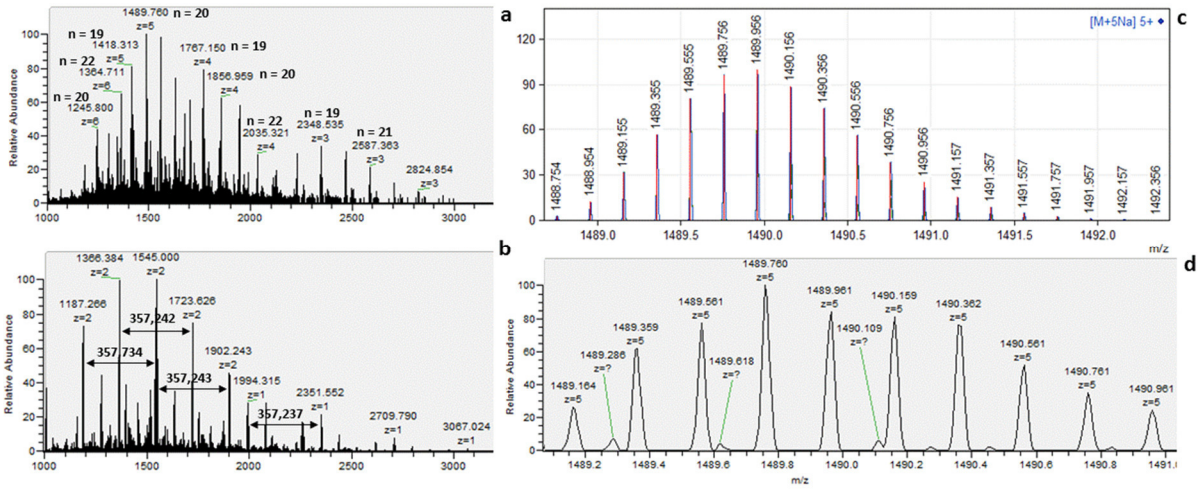

Figure 8: Mass spectra of homopolymer **P1** with n repeating units and a calculated mass of 357.234 g/mol per repeating unit (a = retention time of 13.14 min, b = retention time of 11.84-14.05 min, c = calculated isotope pattern, d = experimental isotope pattern at a retention time of 13.14 min).

Starting from homopolymer **P1**, which reacts as macro ICTA, a chain extension by a second Passerini polymerization was performed with benzyl isocyanide **8** under the same reaction conditions yielding diblock copolymers **P8** and **P9** by the use of different ratios (monomer **3** : homopolymer **P1,** 20:1 (**P8**) and 10:1 (**P9**)) (Scheme 26).

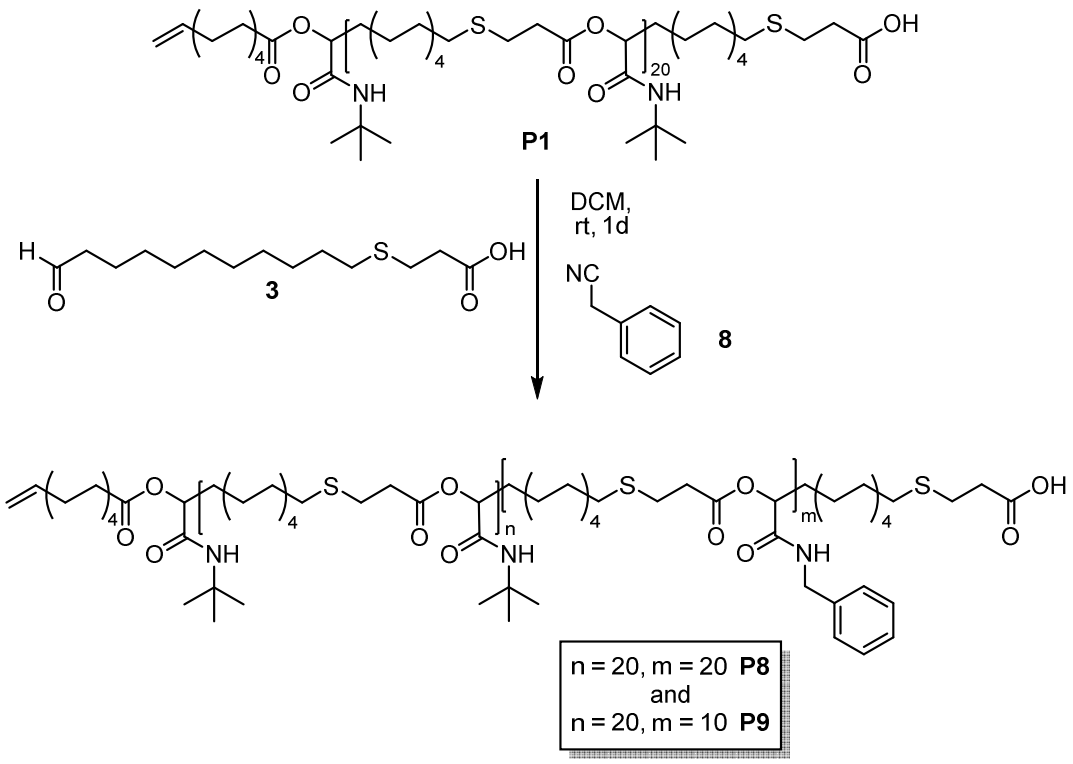

Scheme 26: Passerini-3CR to form block copolymers **P8** and **P9** using different ratios of AB-type monomer **3** and macro ICTA **P1** for the second block containing benzyl side groups.

^{1}H NMR analysis of the resulting polymers **P8** and **P9** showed an excellent correlation of the double bond end group signals and the signals of the two different blocks. Symmetric molecular weight distribution, showing the presence of a unique block copolymer and full monomer conversion were observed by SEC analysis (Figure 9). The molecular weights calculated from ^{1}H NMR data fit to the expected molecular weights of **P8** (15,300 g/mol) and **P9** (11,300 g/mol), respectively.

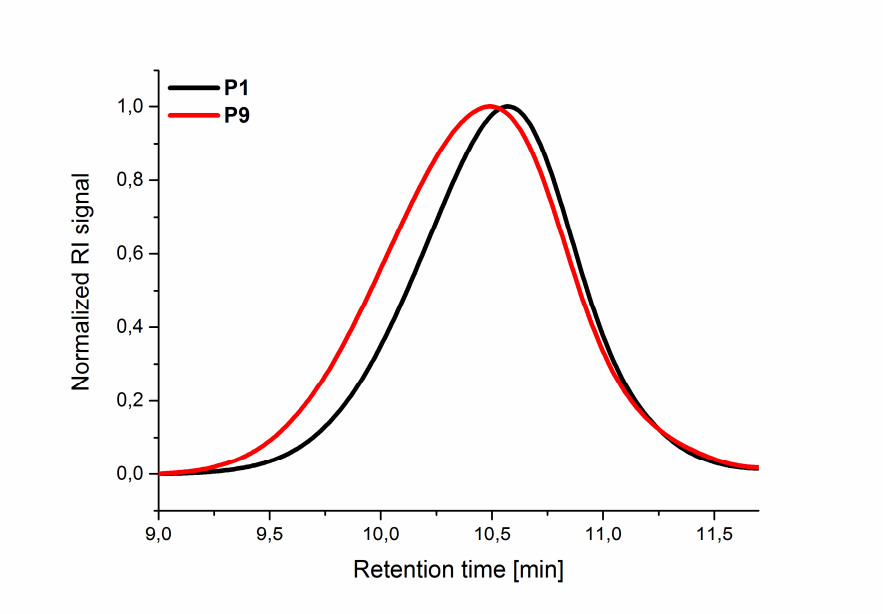

Figure 9: SEC results of diblock copolymer **P9** synthesized from homopolymer **P1** in ratios of the two different blocks of 20:10 (*tert*-butyl side group : benzyl side group).

4.1.2 Synthesis of three-armed star-shaped homo- and block copolymers

To extend this study, ICTA **4** was replaced by a trifunctional core unit **9**, which should result in the formation of a star-shaped homopolymer and subsequently in a star-shaped copolymer. The Passerini polymerization was performed with *tert*-butyl isocyanide **5** and AB-type monomer **3** with a ratio of monomer **3** : isocyanide **5** : trimesic acid **9** of 60:300:1 (Scheme 27).

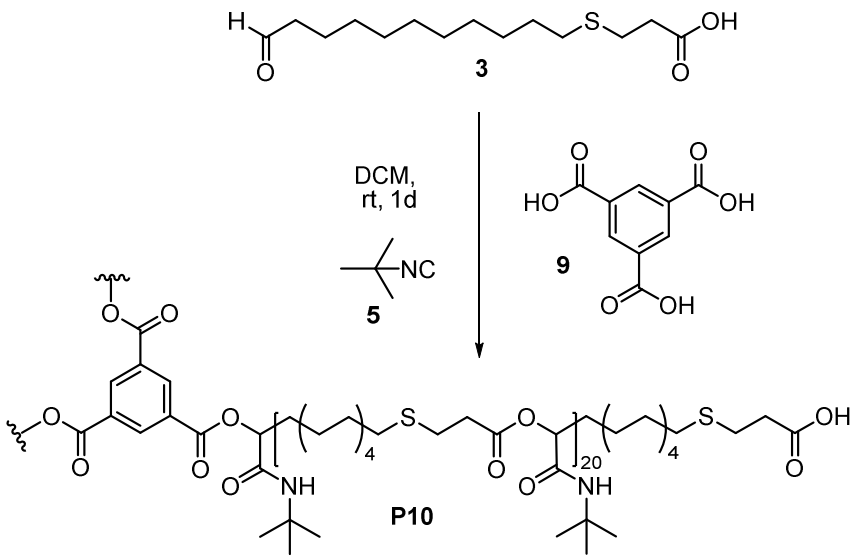

Scheme 27: Synthesis of star-shaped homopolymer **P10** using a trifunctional ICTA **9**.

Subsequent SEC analysis revealed lower molecular weights than the theoretical calculation, which is typical for star-shaped polymers. ^{1}H NMR analysis of star-shaped homopolymer **P10** indicated complete conversion of the ICTA by a slight shift of the aromatic protons **a** of the core unit compared to the protons of trimesic acid **9** (see associated sections in the Experimental Part)**.** With a ratio of 60:1 (AB-type monomer **3** : core **9**), full monomer conversion was detected by ^{1}H NMR. The ratio of the protons **a** of the core, to the protons **b** and **c** of the arms, confirmed this assumption. The resulting star-shaped polyester **P10** was chain-extended by a further Passerini reaction with benzyl isocyanide **8** under the same reaction conditions, leading to star-shaped block-copolymer **P11** (Scheme 28).

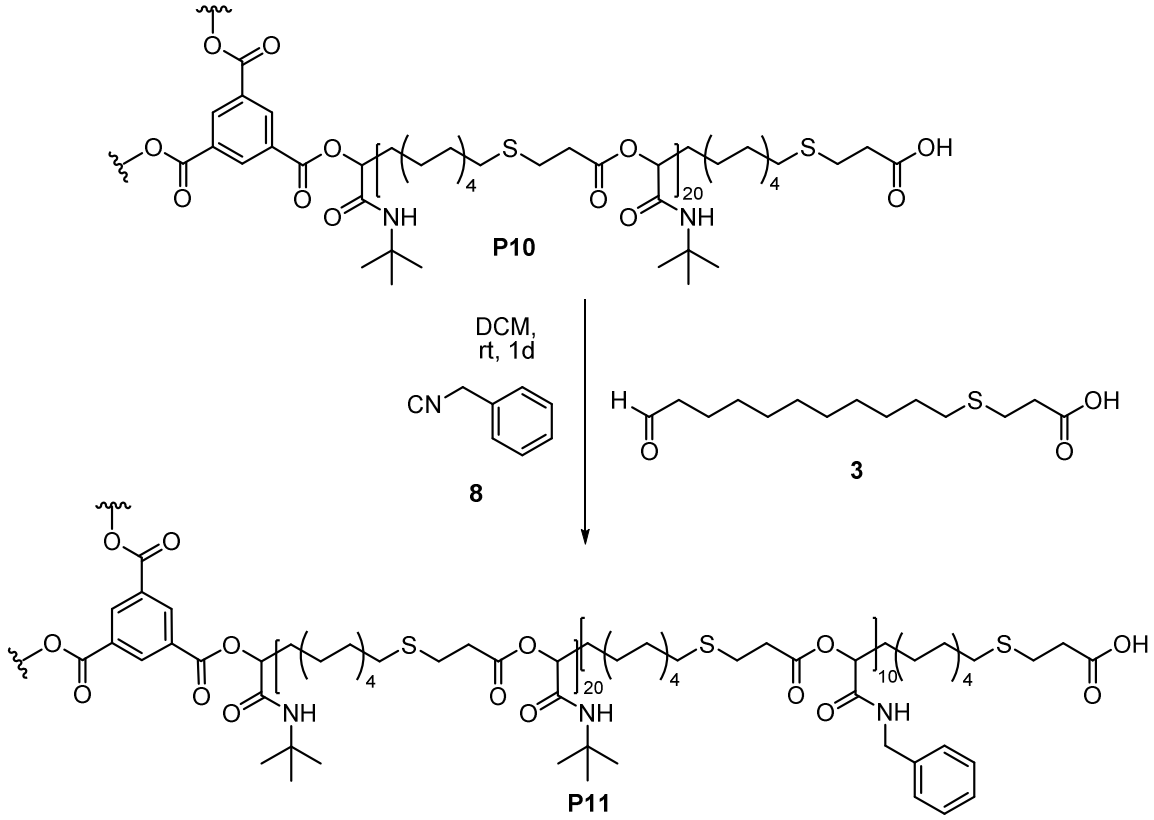

Scheme 28: Passerini-3CR to obtain star-shaped block copolymer **P11** using benzyl isocyanide **8**.

While the first block still exhibits 20 monomer units, the second block was synthesized with a ratio of 10:1 (AB-type monomer **3** : homopolymer **P10**). This leads to an overall ratio of the two blocks of 20:10, which was confirmed by the integrated signal of protons **b-c** and **d-g** (see associated sections in the Experimental Part). The growth of the second block can be seen again in the SEC results of star-shaped homopolymer

P10 and star-shaped block copolymer **P11** by a shift of the curves to lower retention times as well as the presence of a unique star-shaped block copolymer and full monomer conversion (Figure 10).

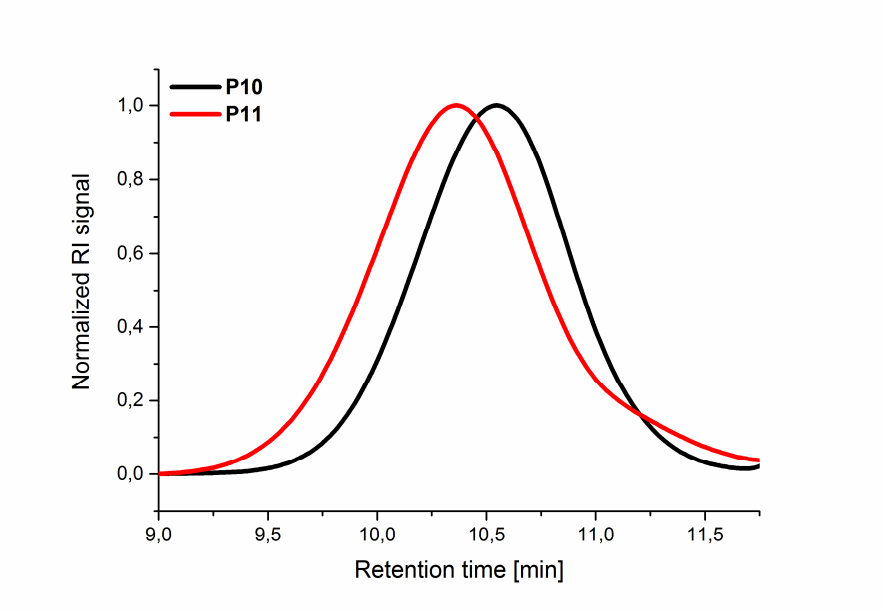

Figure 10: SEC results of star-shaped homopolymer **P10** and star-shaped copolymer **P11**.

In order to investigate the reactivity and end-group fidelity of the carboxylic acid end groups, **P10** was activated with carbonyldiimidazole **10** (CDI).[173] The reaction was carried out in DCM at room temperature for one day to obtain **P12** (Scheme 29).
The modification of the end group with CDI **10** was verified by 1H NMR analysis (see associated sections in the Experimental Part). The ratio of the protons e, d and f to protons a of the core unit indicate full conversion of the end groups. This proves that the carboxylic acid chain ends are still reactive and further modifications can be carried out.

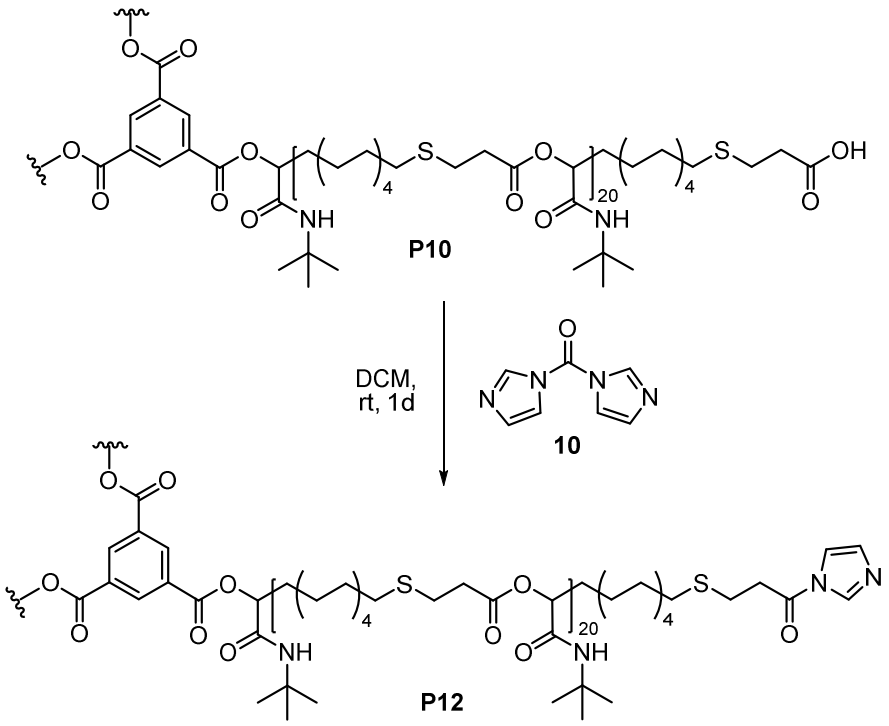

Scheme 29: Activation of the end group of star-shaped homopolymer **P10** with CDI **10**.

Conclusion

In summary, a new approach for the synthesis of polymers with a defined macromolecular architecture by a non-classic step-growth polymerization technique was demonstrated. An AB-type monomer containing an aldehyde and a carboxylic acid moiety was synthesized and polymerized in a Passerini reaction with four different isocyanides and an ICTA. With this simple polyaddition process, *α*-amide substituted polyesters with controlled molecular weights were synthesized. Furthermore, diblock copolymers, star-shaped homo- and copolymers could be synthesized in this way. By modifying the carboxylic acid end group, further reactions can be performed on the polymer to tune the properties of these materials. The described strategy offers a variety of straightforward new possibilities for the design of defined polymer architectures.

4.2. Synthesis and investigation of unimolecular micelles *via* the Passerini-3CR

This chapter and the associated sections in the Experimental Part were published previously:

S. Oelmann, M. A. R. Meier, *RSC Adv.*, **2017**, *7*, 45195. Copyright © 2017, permission from the Royal Society of Chemistry.

Abstract

A series of new amphiphilic star-shaped block copolymers with hydrophobic cores and hydrophilic shells was synthesized, using the Passerini three-component step-growth polymerization (Passerini-3CP). The degree of polymerization of the Passerini hydrophobic cores (20, 10 and 5 repeating units) was controlled and the chain ends were quantitatively functionalized with different sized PEG-aldehydes and/or PEG-isocyanides *via* another Passerini reaction. The encapsulation and phase transfer properties of the star-shaped block copolymers were followed visually and by UV/VIS-spectroscopy, using Orange II and Para Red dyes as guest molecules. The investigated polymers showed a unimolecular micellar behavior, as confirmed by dynamic light scattering (DLS) and the already mentioned encapsulation experiments.

Introduction

Unimolecular micelles show interesting properties for a wide range of applications, including catalysis or the encapsulation of low molecular weight organic guest molecules.[174, 175] The first in literature described systems behaving like unimolecular micelles were based on dendrimers.[176-178] However, dendrimers often require difficult multi-step organic syntheses. Polymer-based systems with core-shell architecture often show similar properties but are easier to synthesize and thus constitute suitable alternatives. For example, amphiphilic star-shaped polymers having a defined number of arms and, accordingly, end groups, can be used in different applications, due to their behavior as unimolecular micelles.[179-183] Most commonly, these amphiphilic star-shaped polymers are synthesized by ATRP or other controlled/living polymerization techniques (e.g. nitroxide-mediated radical polymerization (NMP), RAFT or anionic polymerization).[184 - 186] Additionally, ring-opening polymerization of lactides and lactones is often used to synthesize star-shaped polymers.[187] In the previous chapter, it was demonstrated that star-shaped block copolymers can be synthesized *via* the-Passerini-3CR in a step-growth process.[188, 189]

4.2.1 Synthesis of three-armed star-shaped homopolymers

Following the work of the previous study, this chapter describes the synthesis of well-defined amphiphilic star-shaped block copolymers using the Passerini-3CR and the subsequent encapsulation of two different dyes. This approach is based on the use of a trifunctional carboxylic acid as an ICTA in combination with the AB-type monomer **3**. It was recently shown, that by using an ICTA, an AB-type monomer (combination of aldehyde and carboxylic acid), and an excess of isocyanide, the molecular weights obtained in a Passerini-3CR are determined by the ratio of monomer : ICTA (in analogy to the monomer : initiator ratio in living/controlled polymerizations). To investigate potential applications of these star-shaped homopolymers, it was focused on their functionalization with PEG chains, to produce amphiphilic polymers and to study their encapsulation behavior. The synthesis of AB-type monomer **3** and star-shaped homopolymer **P10** has been described in a previous publication and in the previous section.[188] Additionally, two star-shaped homopolymers with shorter arm lengths (**P13**

and **P14**, 10 and 5 repeating units) were synthesized using ratios of 30:1 and 15:1 of [**3**]:[**9**] (10:1 and 5:1 per arm respectively) (Scheme 30).

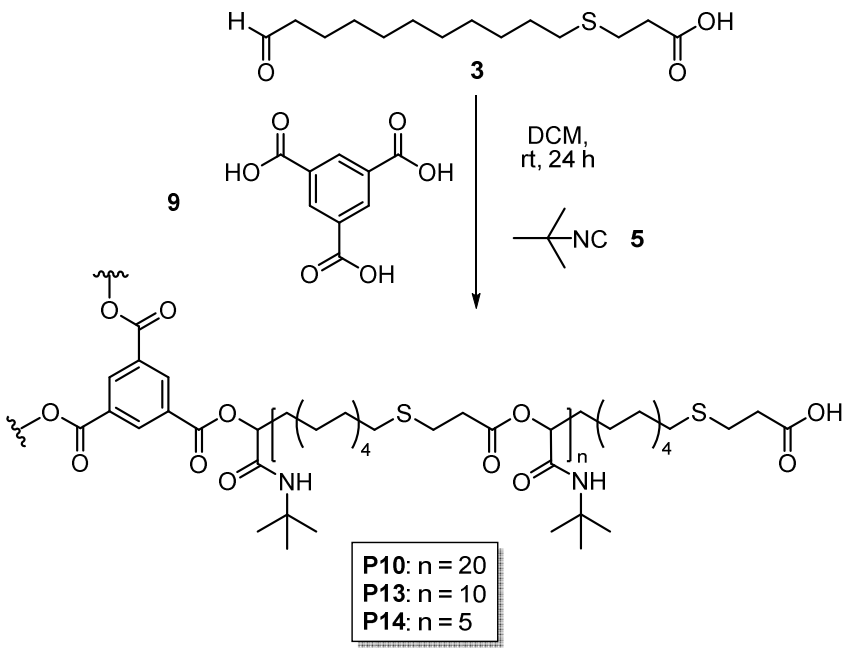

Scheme 30: Passerini-3CR to obtain star-shaped homopolymers **P10**, **P13** and **P14** with different number of repeating units.[188]

The molecular weights (M_n) of the star-shaped polymers, determined by ^{1}H NMR end group integration, were consistent with the expected molecular weights (see associated sections in the Experimental Part) and confirmed a degree of polymerization of 10 and 5, respectively (Table 4).

Table 4: Molecular weights of polyesters **P10**, **P13** and **P14** synthesized with different ratios of AB-type monomer **3** and trimesic acid **9**.

polymer	ratio [**3**]:[**9**] per arm	M_n calc. [g/mol]	M_n NMR [g/mol]	M_n SEC [g/mol]	Đ M_w/M_n
P10	20:1	21,663	22,031	13,500	1.40
P13	10:1	10,937	10,829	10,200	1.23
P14	5:1	5,573	5,859	6,500	1.40

The observed molecular weight distribution (Figure 11) was symmetric and confirmed full monomer conversion. The obtained dispersities (1.23-1.40) are lower than for a classic step-growth polymerization, indicating the presence of both step-growth and chain-growth mechanisms in this system, as expected.

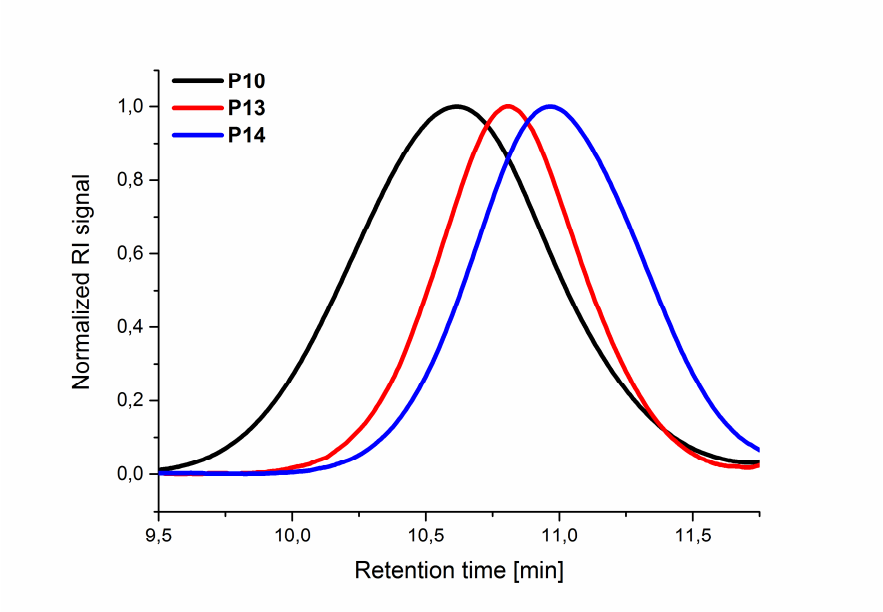

Figure 11: SEC results of star-shaped homopolymers **P10**, **P13** and **P14** with varying ratio of AB-type monomer **3** and trimesic acid **9** (**P10** = 20:1, **P13** = 10:1, **P14** = 5:1; per arm).

4.2.2 Functionalization with PEG-isocyanides and PEG-aldehydes

The star-shaped homopolymers **P13** and **P14** were subsequently functionalized with a water-soluble PEG-based shell to obtain water-soluble star-shaped block copolymers with the goal to achieve unimolecular micellar behavior. Two strategies based on the Passerini-3CR were used to produce linear or branched star-shaped block copolymers. For this purpose, the COOH end groups of the star-shaped polymers were reacted with a PEG aldehyde and an isocyanide or with a PEG aldehyde and a PEG isocyanide in a Passerini-3CR to form a water-soluble shell with either one or two PEG chains per arm. In first tests, **P13** was converted with a commercially available PEG-aldehyde **12** (2,000 g/mol) in a ratio of 1:1 (per arm) and an excess of *tert*-butyl isocyanide **5**, benzyl isocyanide **8** or *tert*-butyl-2-isocyanoacetate **11** (Scheme 31). After precipitation in diethyl ether, the functionalized polymers **P15**, **P16** and **P17** were obtained in good yields.

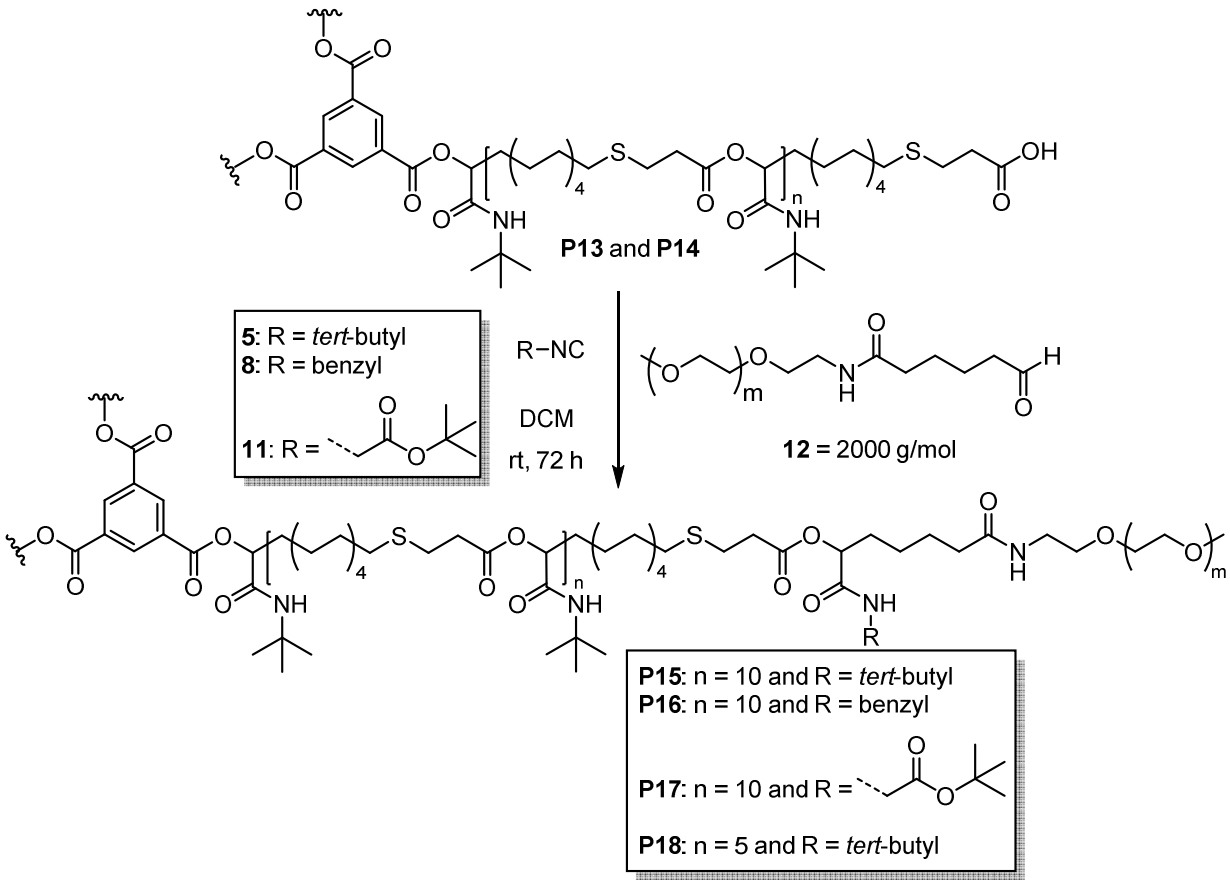

Scheme 31: Functionalization of **P13** and **P14** with different isocyanides **5**, **8**, **11** and PEG aldehyde **12** (2,000 g/mol) to obtain block copolymers **P15**, **P16**, **P17** and **P18**.

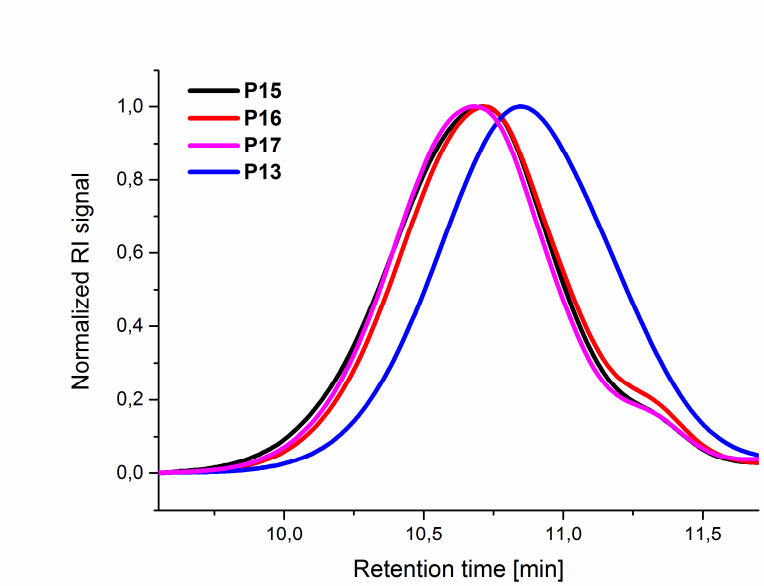

Figure 12: SEC results of the functionalization of **P13** using a PEG aldehyde (2,000 g/mol) and different isocyanides.

Complete conversion of the end groups was confirmed by ^{1}H NMR (see associated sections in the Experimental Part) and SEC measurements (Figure 12).

Although the polymer end groups were fully functionalized, the water solubility of the polymers **P15**, **P16** and **P17** were rather poor and insufficient to obtain unimolecular micelles soluble in water. Thus, the smaller cores were used (**P13** and **P14**) and it was not continued with the investigations of **P10**. Therefore, **P18** was synthesized using the smaller hydrophobic core **P14** with *tert*-butyl isocyanide **5** and PEG aldehyde **12** to increase the hydrophilic fraction of the copolymers (Scheme 31).

Moreover, in order to investigate the influence of the molecular weight of the PEG chains as well as the effect of branching at the core-shell connection on the aggregation and encapsulation behavior of the star-shaped block copolymers in water, lower molecular weight functionalized PEGs were used. For the preparation of PEG isocyanide **21**, an end-group modification of methoxy PEG **20** *via* a transesterification with isocyanide **19** was used. The three-step synthesis of isocyanide **19** starting from amine **13** is known in literature.[190] First, methyl ester **15** is obtained and afterwards formamide **17** is formed, which is finally converted to isocyanide **19** (Scheme 32).

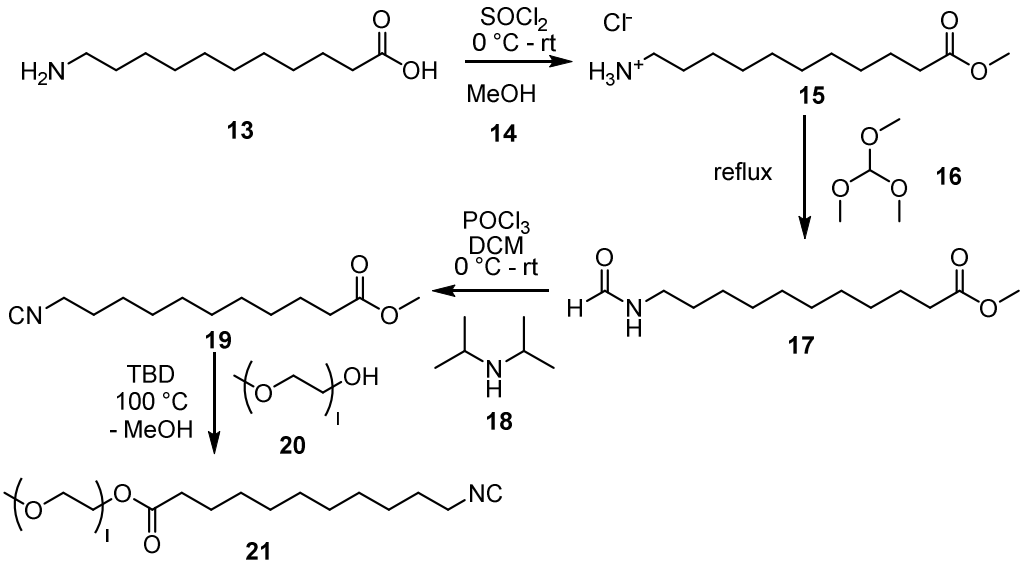

Scheme 32: Synthesis route of PEG isocyanide **21**.[190]

PEG aldehyde **23** (950 g/mol) was synthesized by end group modification of commercially available PEG thiol **22** *via* a thiol-ene reaction with 10-undecenal **1** (Scheme 33).

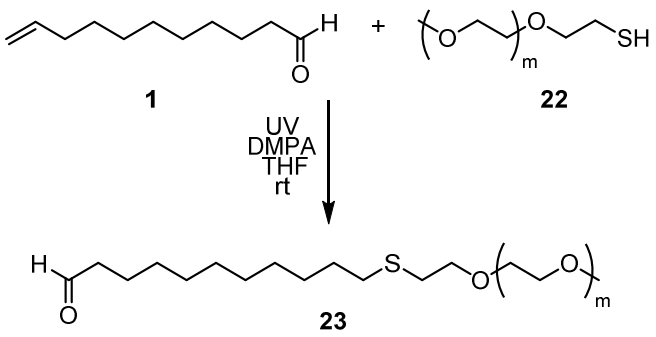

Scheme 33: Synthesis of PEG aldehyde **23** *via* thiol-ene reaction.

Having the functionalized PEGs in hand, the star-shaped block copolymers **P19**, **P20** and **P21** were synthesized *via* the Passerini-3CR, using *tert*-butyl isocyanide **5** and PEG aldehyde **23**, or PEG isocyanide **21** and PEG aldehyde **23** to obtain polymers with either one or two PEGs (950 g/mol) and either 5 or 10 repeating units of the core (Scheme 34).

Thus, a small library of four different amphiphilic star-shaped block copolymers was produced and further investigated, allowing the correlation of the different polymer architecture to the performance as unimolecular micelles. The full conversion of the end groups was determined by ^{1}H NMR measurements (see associated sections in the Experimental Part). Due to an increased hydrophilic ratio, polymers **P18**, **P19**, **P20** and **P21** showed improved water solubility. All following evaluations were performed only on these four water soluble polymers.

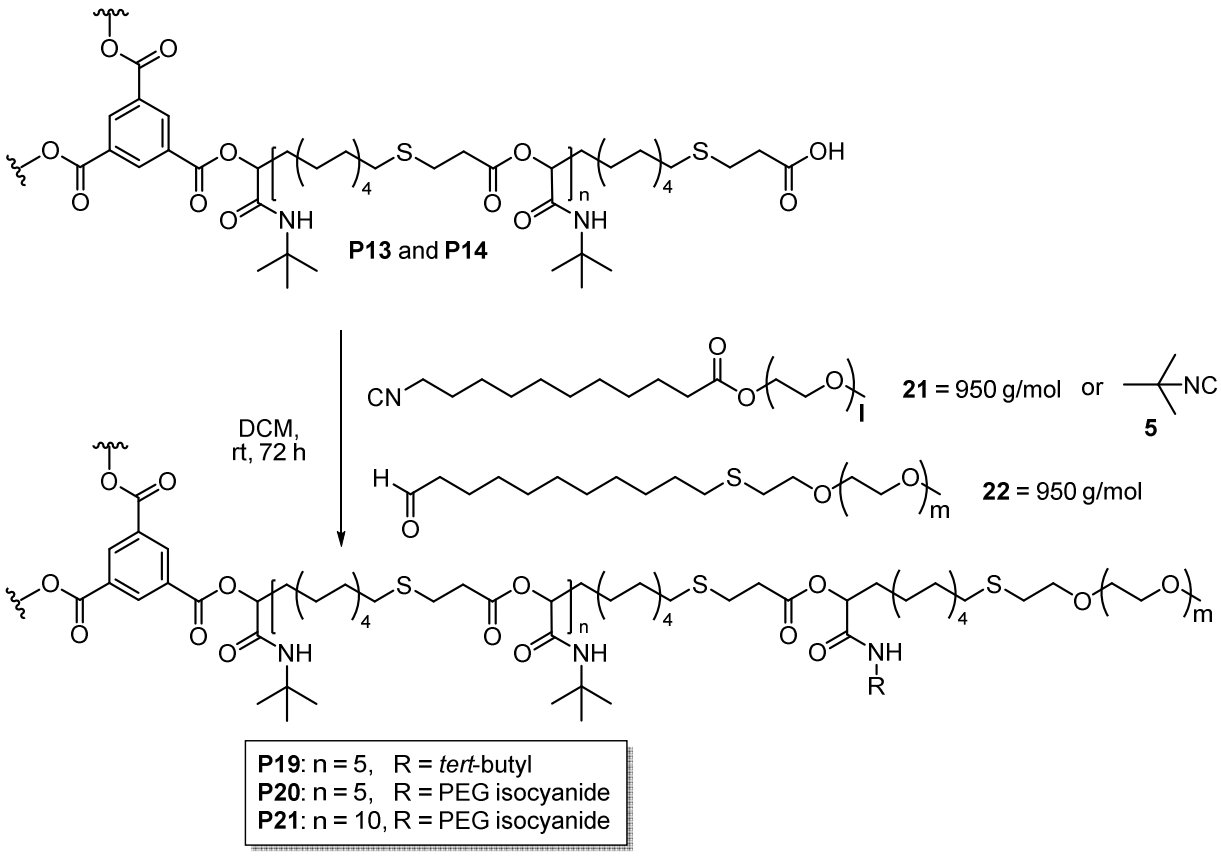

Scheme 34: Functionalization of **P14** with *tert*-butyl isocyanides **5** and PEG aldehyde **22** (950 g/mol) to obtain star-shaped block copolymer **P19** and additional functionalization of **P13** and **P14** with PEG isocyanide **21** and PEG aldehyde **22** (950 g/mol) to obtain star-shaped block copolymers **P20** and **P21**.

Due to the differences in solubility of the two blocks in water, the formation of aggregates might be expected, contradicting a unimolecular micellar behavior. Nevertheless, dynamic light scattering (DLS) measurements confirmed unimolecularity for the four star-shaped block copolymers in a concentration range from 0.1 mg/mL and 1.0 mg/mL (see associated sections in the Experimental Part). The measurements were carried out in water and dichloromethane (DCM). Two different preparation protocols, typical for the preparation of micellar solutions, were used for the analysis in water.[191] On the one hand, the sample was directly dissolved in water (without acetone: woA) and on the other hand, the sample was dissolved in 2-3 drops of acetone and then water was added dropwise (with acetone: wA). The values of all four polymers measured woA were slightly higher (13.5-21.0 nm) compared to the values wA (8.7-15.7 nm), which may indicate some aggregation in water. To confirm this and possibly break these aggregates, **P18** wA and woA was ultrasonicated for 5 minutes each (**P18** showed the largest size difference for the two preparation modes).

Afterwards, all samples showed the same value (value of the sample wA: Figure 13), indeed indicating that small aggregates were present for the woA samples and also indicating that the wA samples indeed represent unimers that cannot be further dissociated. The values measured in DCM were slightly lower (4.2-6.5 nm), which can be attributed to a different swelling behavior of these macromolecules in an aqueous solution.

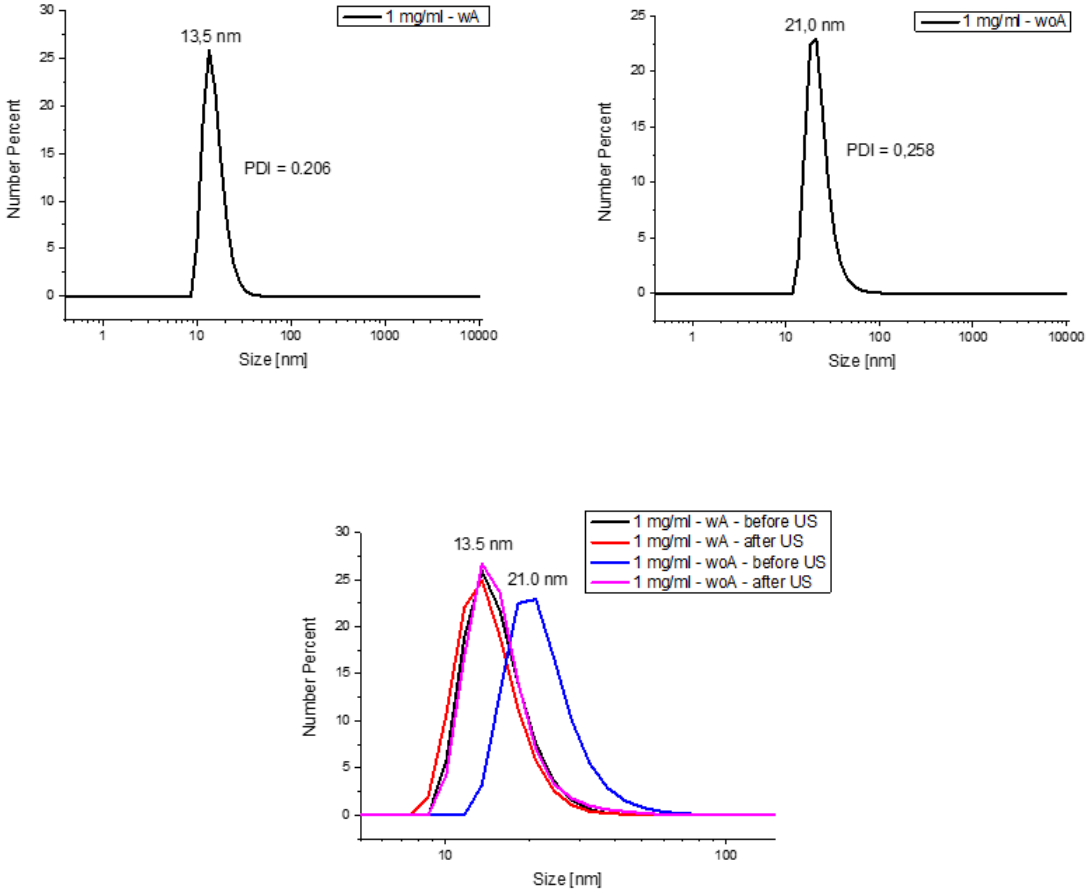

Figure 13: DLS results of functionalized star-shaped polymer **P18**: comparison of 1 mg/mL **P18** with and without acetone after and before ultrasonication (US).

4.2.3 Encapsulation and phase transfer studies of various dyes

Most interestingly, the guest encapsulation of the star-shaped block copolymers and a phase transfer phenomenon was observed and could be visualized in the following tests, also unambiguously confirming unimolecularity. Encapsulation behavior was obtained for all four tested star-shaped block copolymers **P18**, **P19**, **P20** and **P21** (see

associated sections in the Experimental Part), but the best results were received for polymer **P20** (Figure 14). First, amphiphilic star-shaped block copolymers were added to the water insoluble dye Para Red, rendering it water-soluble due to encapsulation. Polymers with shorter hydrophobic cores and higher hydrophilic parts were better soluble in water and exhibited the best encapsulation behavior of the dye (Figure 14, left).

In a second test, the water-soluble dye Orange II was added to a two-phase water/DCM system (Figure 14, right). After addition of the amphiphilic star-shaped block copolymer and shaking for a few seconds, most of the dye was transferred to the DCM phase. The color change from orange to yellow of Orange II is due to a change of the microenvironment of the dye and confirms that the polymers can encapsulate and phase transfer the investigated guest molecule. This result is a clear proof of the unimolecular behavior of the polymer, since a self-assembled micelle would dissociate in DCM, not being able to phase transfer the dye.

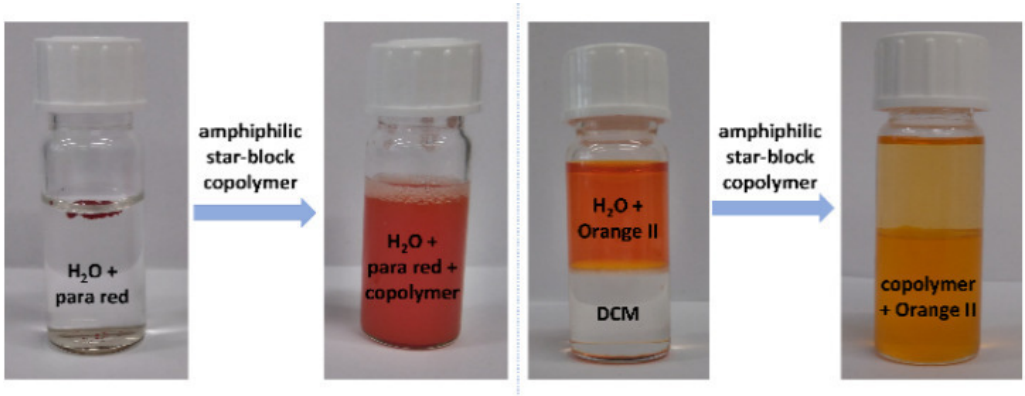

Figure 14: Visualization of the encapsulation of water-insoluble Para Red in water by block copolymer **P20** (left) and visualization of the encapsulation and phase transfer of Orange II from the water to the DCM phase by **P20** (right).

Like already mentioned, using these initial visual inspections, the best results for both tests were obtained for polymer **P20**, which shows the highest ratio of hydrophilic : hydrophobic parts. Therefore, the phase transfer behavior (water/DCM) of **P20** was investigated by a UV/VIS titration experiment (**P20** was titrated to the biphasic mixture of dye and the solvents, Figure 15). The absorption of the dye in both phases was separately measured and the concentration of **P20** was increased after each

measurement by addition of further aliquots. While the absorption of the dye in water decreased with increasing concentration **P20**, the absorption in DCM increased.

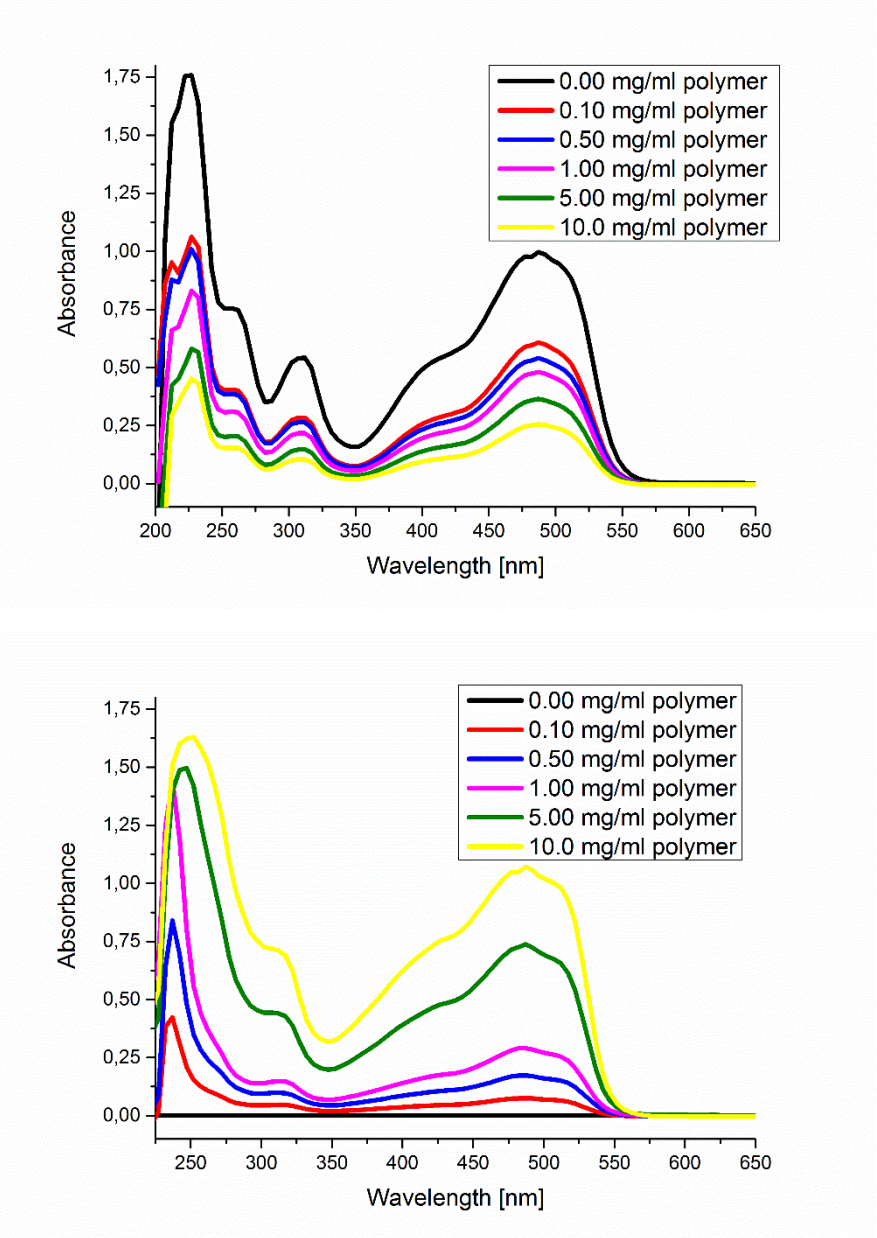

Figure 15: UV/VIS spectra of the encapsulation and phase transfer of Orange II from the water phase to the DCM phase by block copolymer **P20** (above: absorbance of Orange II in water with increasing concentration of **P20**, below: absorbance of Orange II in DCM with increasing concentration of **P20**).

This behavior can be explained by an encapsulation and phase transfer of Orange II from the water to the organic phase by the amphiphilic star-shaped block copolymer **P20**. After recording a calibration curve for Orange II in water (Figure 16), the concentrations in water could be determined as well as the number of encapsulated dye molecules per polymer (Table 5). An average up to 2.50 dye molecules per

polymer were encapsulated when 0.10 mg/mL of **P20** were added, starting with 0.0225 mg/mL of dye in water. However, at this concentration, less than half of the introduced dye phase transfers to the DCM phase. A concentration of **P20** of 10 mg/mL was required to encapsulate around 75% of the dye.

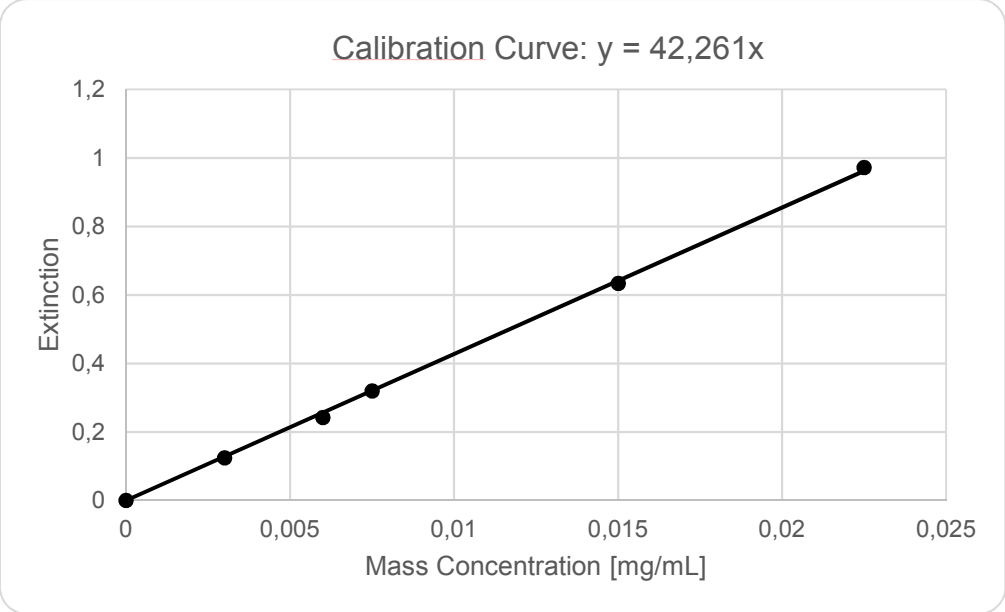

Figure 16: UV/VIS calibration curve of Orange II in water.

Table 5: Concentration of Orange II in water and DCM with increasing concentrations of **P20** and the ratio of encapsulated dye per polymer in DCM measured *via* UV/VIS.

conc. polymer [mg/mL]	conc. dye in water [mg/mL]	conc. dye in DCM [mg/mL]	ratio polymer : dye in DCM
0.00	0.0225	0.00	-
0.10	0.0144	0.0081	1 : 2.50
0.50	0.0128	0.0097	1 : 0.75
1.00	0.0114	0.0111	1 : 0.38
5.00	0.0086	0.0139	1 : 0.10
10.00	0.0061	0.0164	1 : 0.06

Finally, the hydrodynamic diameter of polymer **P20** with and without guest molecule was compared *via* DLS (Figure 17). The slight increase of around 25 % and the

absence of larger aggregates also indicate that the guest molecules are encapsulated in the polymers.

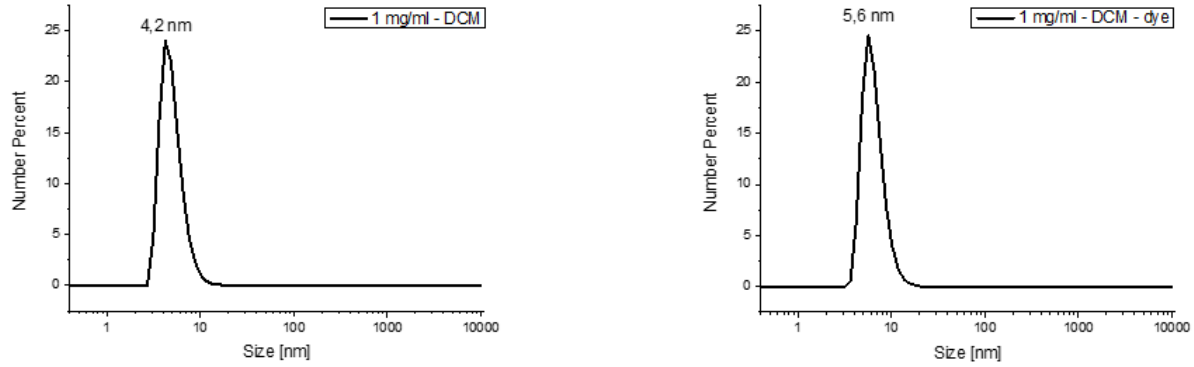

Figure 17: DLS results of functionalized star-shaped polymer **P20** (five repeating units and two PEG arms (950 g/mol)): comparison of 1 mg/mL **P20** in DCM without encapsulated dye (left) and with encapsulated dye (right).

Conclusion

In conclusion for this chapter, new unimolecular core-shell architectures were successfully synthesized *via* Passerini-3CR. Controlling the polymerization conditions, amphiphilic three-arm star-shaped block copolymers with Passerini derived cores and different PEG shells were obtained. The unimolecular behavior, the encapsulation of water-soluble and water-insoluble guest molecules as well as the transport abilities from water to an organic phase were demonstrated by UV/VIS spectroscopy and DLS measurements. Thus, these star-shaped block copolymers are multifunctional materials with a potential for applications in drug delivery systems or as phase-transfer catalysts.

4.3 Biocompatible unimolecular micelles *via* the Passerini-3CR for potential medical applications

This chapter and the associated sections in the Experimental Part were submitted to *Biomacromolecules*.

Parts of this project were performed at the University of Nottingham together with Alessandra Travanut in the working group of Prof. Dr. Alexander Cameron.

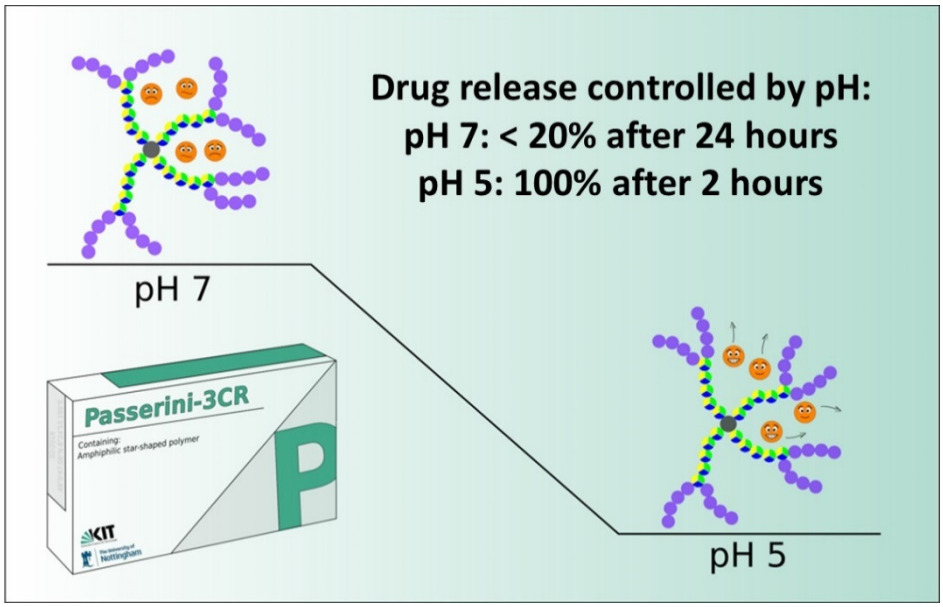

Abstract

A Passerini-3CP was performed for the synthesis of amphiphilic star-shaped block copolymers with hydrophobic cores and hydrophilic coronae. The degree of polymerization of the hydrophobic core was varied across 5-10 repeating units and the side chain ends were conjugated by performing a Passerini-3CR with PEG-isocyanide and/or PEG-aldehyde (950 g/mol). The resultant amphiphilic star-shaped block copolymers contained thioether groups which could be oxidized to sulfones in order to tune the polarity of the polymer chains. The ability of the amphiphilic copolymers to act as unimolecular micellar encapsulant was tested with the water-insoluble dye Orange II, the water-soluble dye Para Red and the macrolide antibiotic, Azithromycin. The results showed that the new copolymers were able to retain drug cargo at pH levels

corresponding to circulating blood and selectively release therapeutically effective doses of antibiotic as measured by bacterial cell kill. The polymers were also well-tolerated by differentiated THP-1 macrophages in the absence of encapsulated drugs.

Introduction

Within this chapter, the above described encapsulation study[192] was extended by varying the polarity of the core of the star-shaped block copolymers as well as the number of arms of these unimolecular micelles and utilize the resultant materials to encapsulate and release an antimicrobial agent, Azithromycin. Polymer syntheses were performed *via* the Passerini-3CR and by using different isocyanides and core molecules within the Passerini-3CR, as well as oxidizing the sulfides to sulfones in the backbone of the polymers. Thus, the polarity as well as the architecture of the resulting star-shaped polymers were adjusted.

As exemplars for the ability of these polymers to encapsulate a variety of active molecules, both hydrophobic dyes and Azithromycin were incorporated as guest molecules in formulations with the Passerini-3CR polymers. The data from encapsulation and release experiments clearly suggested the investigated unimolecular micelles showed promise as potential drug delivery systems, due to their good drug loading capacities and controlled release properties. In addition, as Passerini-3CR polymers are biodegradable polyesters, these results imply that developed materials of this class may find widespread future use as active carrier and release agents in a range of biomedical applications.

4.3.1 Synthesis of amphiphilic three-armed star-shaped block copolymers

The synthesis of star-shaped homopolymers with controlled molar masses is based on the introduction of a trifunctional carboxylic acid as an irreversible chain transfer agent **9** (ICTA) in a polymerization process of an AB-type monomer **3** (combination of carboxylic acid and aldehyde) and an excess of isocyanide (Scheme 35).[188, 192] The ratio of ICTA **9** to AB-type monomer **3** enables the prediction of the molar masses of the obtained polymers comparable with the initiator to monomer ratio in living controlled polymerization techniques. In order to investigate the encapsulation behavior of the

polymers, two star-shaped homopolymers **P13** and **P14** with different numbers of repeating units were synthesized as previously described (10 and 5 repeating units per arm), using ratios of 15:1 and 30:1 of monomer **3** and ICTA **9**.

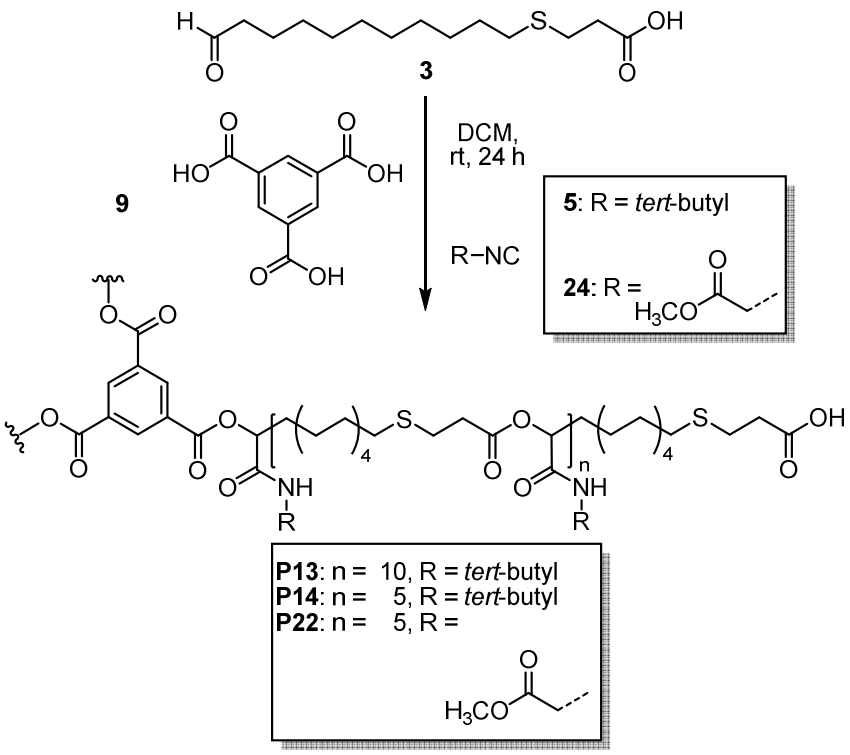

Scheme 35: Passerini-3CR using different ratios of AB-type monomer **3** and trifunctional ICTA **9** and different isocyanides **5** and **24** to obtain star-shaped homopolymers **P13**, **P14** and **P22**.

The symmetric molecular weight distributions (Figure 11) and the molecular weights obtained by ^{1}H NMR end group integration, which were comparable to the calculated molecular weights (see associated sections in the Experimental Part and Table 4), confirmed complete monomer conversion and the expected degrees of polymerization. In order to change the polarity of the star-shaped polymers in a straightforward fashion, methyl isocyanoacetate **24** was used as isocyanide component with the same degree of polymerization as **P14**, which leads to star-shaped polymer **P22**, providing more polar side chains.

In order to obtain amphiphilic star-shaped block copolymers showing unimolecular micellar behavior, **P13**, **P14** and **P22** were post modified applying the conditions examined in previous studies[192] (section 4.2.2) using a water-soluble PEG-based (polyethylene glycol) shell (Scheme 36). Therefore, the carboxylic acid end groups of the star-shaped homopolymers were reacted with the previously synthesized PEG

aldehyde **23** (950 g/mol) and PEG isocyanide **21** (950 g/mol), to form a water-soluble shell owing two PEG chains attached to the arms, leading to amphiphilic star-shaped block copolymers. ^{1}H NMR end group integration again confirmed full conversion to the desired products (see associated sections in the Experimental Part).

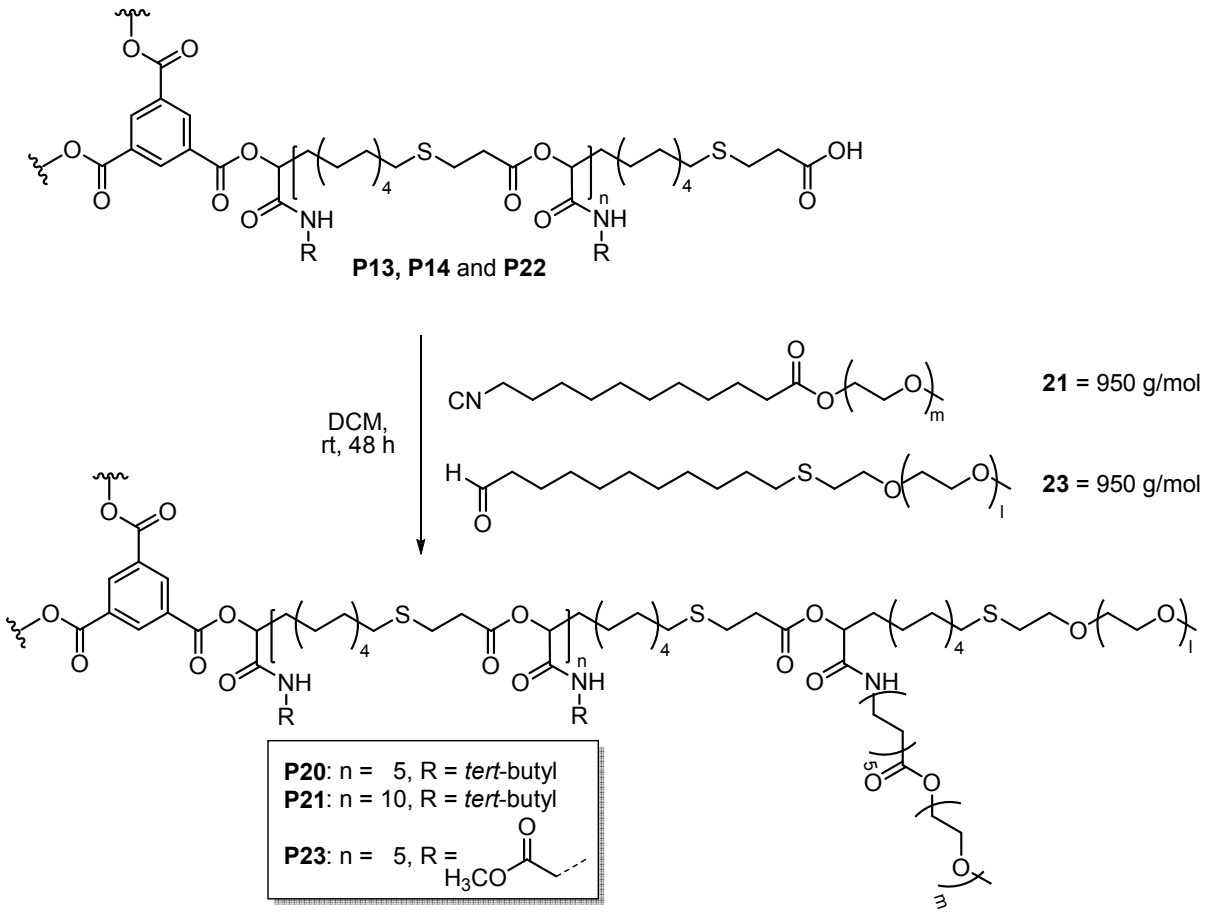

Scheme 36: Functionalization of **P13**, **P14** and **P22** with PEG isocyanide **21** (950 g/mol) and PEG aldehyde **23** (950 g/mol) to obtain amphiphilic star-shaped block copolymers **P20**, **P21** and **P23**.

In comparison to common less polar thioethers, sulfones in general show a higher polarity. Interestingly, in this case, the synthesized star-shaped block copolymers have a sulfur containing backbone and it is known that thioethers can be easily oxidized to sulfones using oxidation reagents such as 3-chloroperbenzoic acid (*m*CPBA) or hydrogen peroxide.[168, 193] Consequently, besides the choice of the isocyanide, the polarity could be adjusted according to the desired application by simply oxidizing the polymers. Therefore, the sulfur containing backbones of the star-shaped block copolymers **P20** and **P23** were oxidized using two different procedures to obtain star-shaped polymers **P24** and **P25** with a higher polarity. In the first procedure, *m*CPBA

was used as oxidizing agent at room temperature. In a more sustainable way, hydrogen peroxide was used at a higher temperature of 60 °C. The oxidation of **P20** and **P23** proceeded readily leading to star-shaped block copolymers **P24** and **P25** with an increased polarity (Scheme 37). Subsequent ^{1}H NMR analysis of the obtained polymers confirmed a successful oxidation of each sulfur atom. The neighboring protons to the sulfur showed a shift towards higher ppm values, while all the other signals remained unchanged (see associated sections in the Experimental Part).

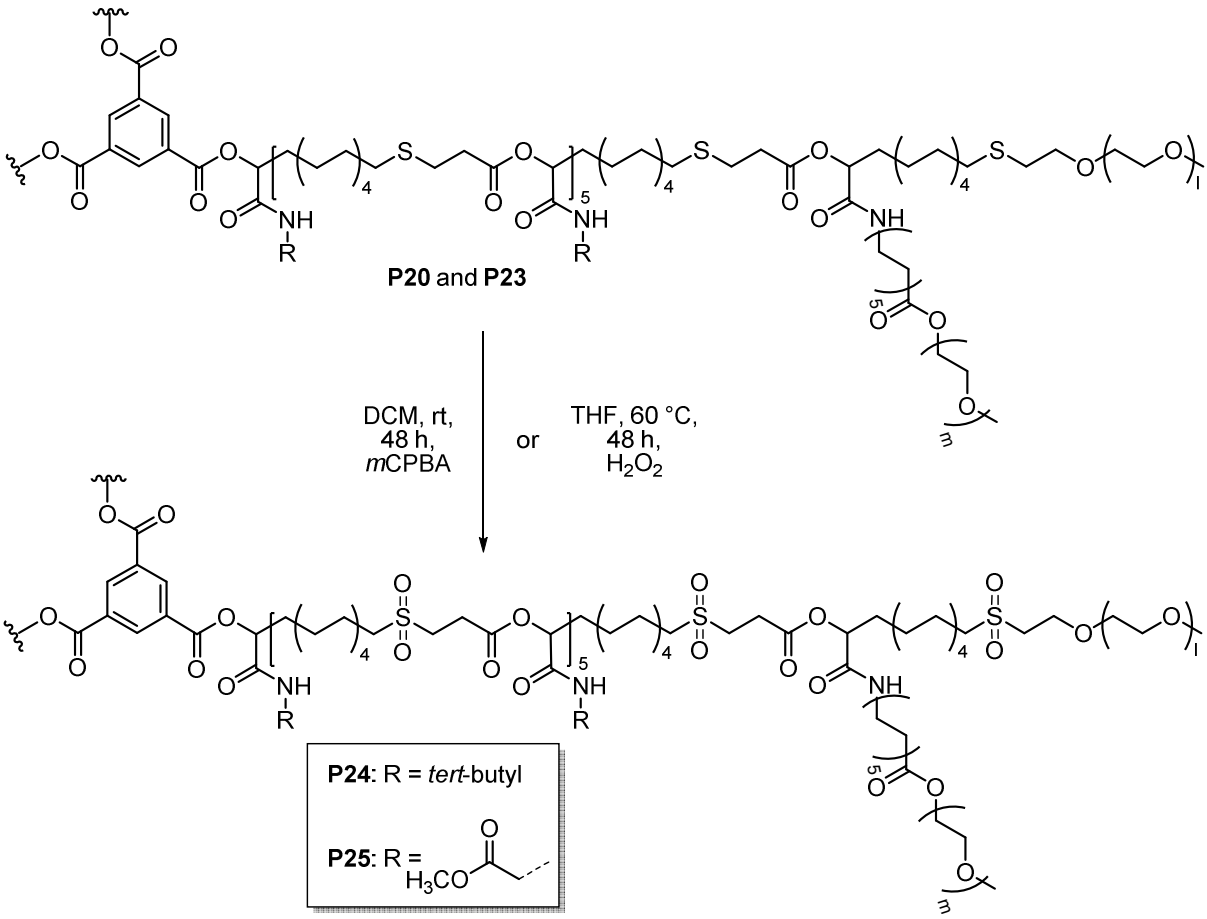

Scheme 37: Oxidation procedure of star-shaped block copolymers **P20** and **P23** with *m*CPBA or hydrogen peroxide to sulfone analogues **P24** and **P25**.

Furthermore, IR spectra of the reduced and oxidized star-shaped block copolymers **P20** and **P24** were recorded and compared, confirming the oxidation and sulfone formation (Figure 18). In principle, sulfoxides absorb at a region of 1030–1060 cm^{-1}, while sulfones show characteristic absorptions at 1120–1260 cm^{-1} and 1300–1350 cm^{-1}. For polymer **P24** a strong absorption at 1120 cm^{-1} and a broad intensive band between 1270 and 1330 cm^{-1} were detected, in contrast with the

absorptions of the starting polymer **P20**. Since in the region of sulfoxide absorption no bands were detected, a full conversion to the corresponding sulfone was confirmed.

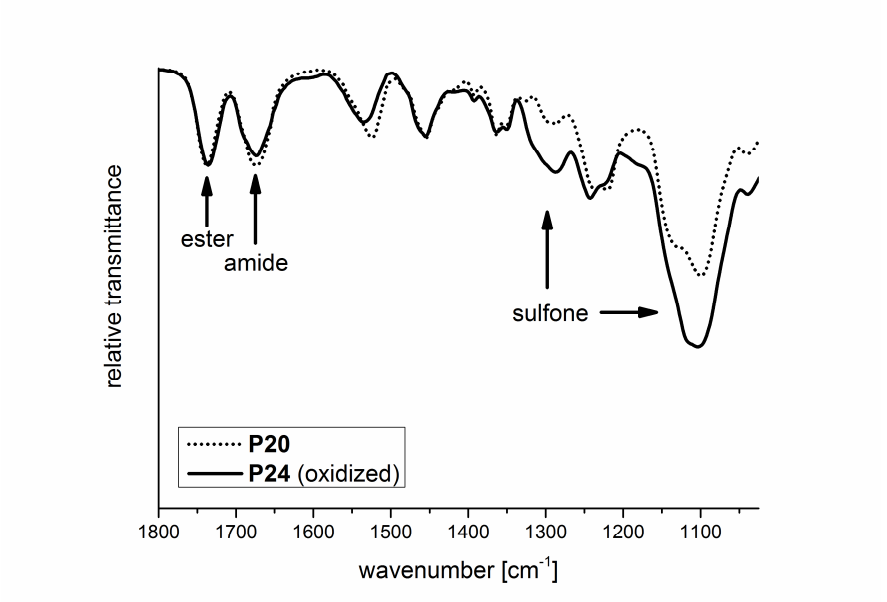

Figure 18: IR spectra (ATR) of the relevant region of reduced and oxidized 3-armed star-shaped block copolymers **P20** and **P24**.

4.3.2 Synthesis of amphiphilic four-armed star-shaped block copolymers

This chapter and the associated sections in the Experimental Part were developed in a “Vertieferarbeit” by Dennis Barther under supervision of Stefan Oelmann.

Furthermore, it was shown that, in addition to the variation of the polarity for the desired unimolecular micellar behavior, the number of arms of the star-shaped polymers is highly relevant. Therefore, a star-shaped polymer with four arms was synthesized. In this case, a suitable ICTA should contain four carboxylic acid end groups to form the four-armed stars. In order to determine their length by ^{1}H NMR spectroscopy, it was advantageous, that the ICTA compound used in the synthesis contained aromatic protons. These protons did not overlap with those of the backbone, due to their high ppm values, whereby the ratio of the protons between the core and repeating unit could be determined exactly. Furthermore, it was of high importance, that the corresponding ICTA had a good solubility in the corresponding solvent. Therefore, 3,3'5,5'-tetracarboxydiphenylmethane **25** was chosen as the most suitable ICTA. Due to the good solubility, the reaction with the four-armed ICTA **25** was carried out in THF. The

reaction time had to be increased to 72 h (Scheme 38). Again, by performing this reaction, it was shown that the number of repeating units can be varied selectively and easily by varying the ratio of ICTA **25** to AB-type monomer **3**. Different four-armed star-shaped homopolymers with 5 repeating units per arm ([**3**]:[**25**], 5:1 per arm **P26**) and with 10, 20 and 30 repeat units per arm ([**3**]:[**25**], 10:1 **P27**, 20:1 **P28**, 30:1 **P29** per arm) could be synthesized.

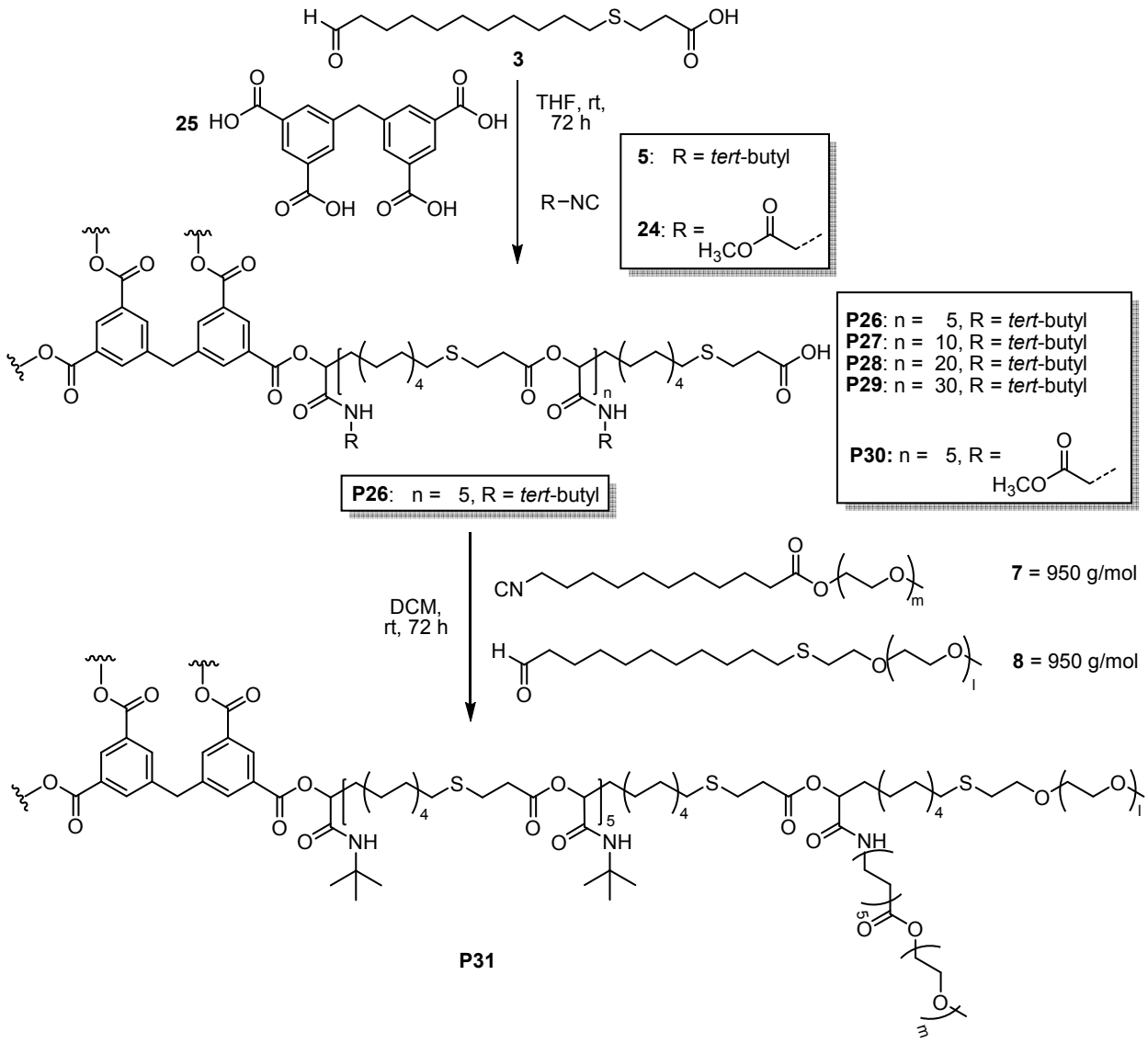

Scheme 38: Synthesis of different four-armed star-shaped homopolymers and the following functionalization to obtain amphiphilic four-armed star-shaped copolymer **P31**.

It was also shown, that the symmetric molecular weight distribution shifts towards smaller retention times with increasing arm length or with increasing hydrodynamic radius (Figure 19). ^{1}H NMR analysis of the resulting polymers **P26**–**P29** showed an

excellent correlation of the aromatic proton signals of the ICTA and the signals of the repeating units (see associated sections in the Experimental Part and Table 6).

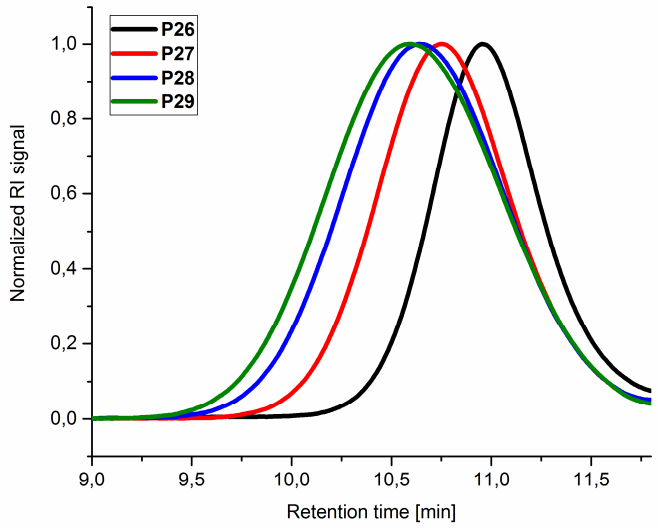

Figure 19: SEC results of four-armed star-shaped homopolymers **P26**, **P27**, **P28** and **P29** with varying ratio of AB-type monomer **3** and four-armed ICTA **25** (**P26** = 5:1, **P27** = 10:1, **P28** = 20:1, **P29** = 30:1 per arm).

Table 6: Molecular weights of four-armed star-shaped homopolymers **P26**, **P27**, **P28** and **P29** synthesized with different ratios of AB-type monomer **3** and four-armed ICTA **25**.

polymer	ratio [**3**]:[**25**]	M_n calc. [g/mol]	M_n NMR [g/mol]	M_n SEC [g/mol]	Đ M_w/M_n
P26	5:1	7,495	7,538	7,900	1.33
P27	10:1	14,646	14,149	14,400	1.30
P28	20:1	28,948	28,927	15,100	1.47
P29	30:1	43,250	43,379	16,100	1.49

Additionally, it was shown, that it is also possible to obtain four-armed star-shaped polymers with different side groups, dependent on the choice of isocyanide. This was performed in order to vary the polarity of the polymer as well. Therefore, the reaction was tested with methyl isocyanoacetate **24** and 5 repeating units per arm to finally obtain star-shaped homopolymer **P30**. The functionalization with PEG isocyanide **21** and PEG aldehyde **23** resulted in a hydrophilic shell around the hydrophobic core,

leading to amphiphilic four-armed star-shaped block copolymer **P31** (Scheme 38). The previously synthesized star-shaped homopolymer **P26** was used as four-armed acid component within the Passerini-3CR.

4.3.3 Polarity characterization and dye encapsulation studies of amphiphilic star-shaped block copolymers

Thereafter, the octanol-water partition coefficients (P) of the reduced and oxidized three-armed star-shaped copolymers **P20**, **P23**, **P24** and **P25** and two dyes (Orange II and Para Red) were determined. The octanol-water partition coefficient (P) directly correlates with the polarity of the chemical substrates. An easy and fast method to obtain the polarity of a substance is the indirect determination of partition coefficients from chromatographic retention data, using the reverse phase HPLC (RP-HPLC) method.[161] Therefore, octanol was displaced by a mixture of methanol and water (70:30) as eluent.[194] The HPLC system was calibrated with different substances of known P.[195] To determine the dead time of the column, which is defined as the time needed for a compound not interacting with the stationary phase while passing the column (t_0), thiourea was chosen. By using t_0 and t (retention time of the polymers), the capacity factor k, which is described as the retention of a substance, can be calculated and is defined as followed:

$$k = \frac{t - t_0}{t_0}$$

The linear relation between k and the octanol-water partition coefficient, enabled the experimental value of P to be easily determined.

Figure 20 shows the obtained results for **P20**, **P23**, **P24** and **P25** compared to the two dyes Orange II and Para Red. Oxidation of the star-shaped polymers increased their polarity, as indicated by a negative value of log k of **P24** and **P25**. Using methyl isocyanoacetate **22** instead of *tert*-butyl isocyanide **5** also increased the polarity. Interestingly, Para Red was of a similar polarity as the starting polymers, and Orange II showed a comparable polarity to the oxidized polymers.

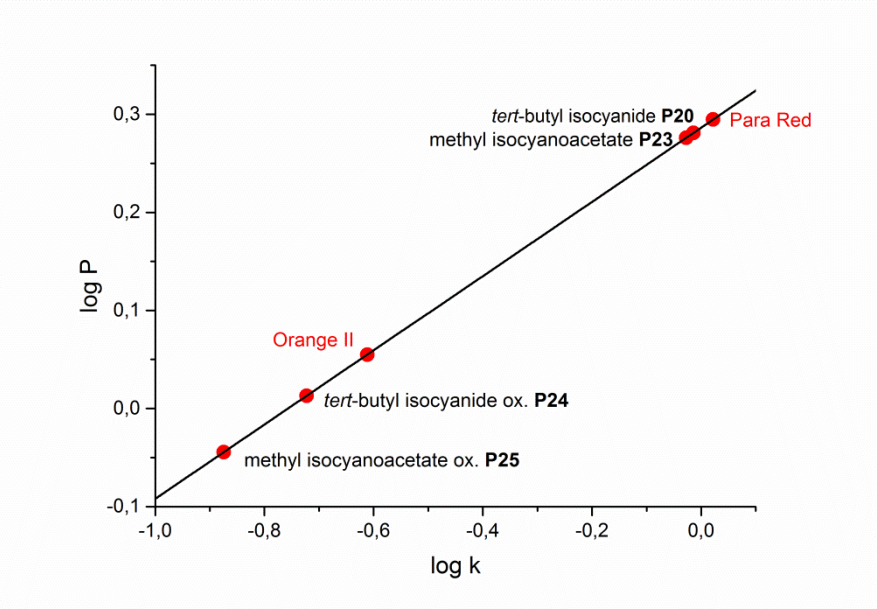

Figure 20: RP-HPLC determination of octanol water partition coefficients of reduced and oxidized three-armed star-shaped block copolymers **P20**, **P23**, **P24** and **P25** compared with Orange II and Para Red.

In a further test, the encapsulation ability of the star-shaped block copolymers **P20**, **P23**, **P24** and **P25**, possessing different polarities, was investigated by UV/VIS measurements (Figure 21) using water insoluble Para Red in water and Orange II (insoluble in DCM) in DCM. An excess of 10 molecules Orange II per star-shaped polymer molecule (5.00 mg) was added to 5.00 mL DCM, in which it is not soluble. After addition of the star-shaped polymer, the dye was encapsulated and dissolved in DCM (i.e. within the core of the star-shaped block copolymer). Afterwards, the non-encapsulated dye molecules were filtered off and the UV/VIS absorption of the resultant orange solution was carried out. The test was performed with the reduced and oxidized star-shaped block copolymers **P20**, **P23**, **P24** and **P25**. The same preparation and measurement was repeated using water-insoluble Para Red as dye in water. The encapsulation was expected to be more efficient, if the polarity of polymers and dye were similar. It could thus be shown, that the encapsulation of the more polar Orange II was more efficient using oxidized star-shaped block copolymers **P24** and **P25**. On the other hand, the encapsulation of Para Red was better with the reduced star-shaped block copolymers **P20** and **P23**. Due to the insolubility of Orange II in DCM, it was not possible to record a calibration curve, which is why these results are relative to each other. Summarizing, this is a clear proof that the polarity of the star-shaped polymers can be tuned by using different polar isocyanides and by oxidizing

the polymer backbone. Furthermore, it could be shown, that the polarity significantly affected the encapsulation behavior.

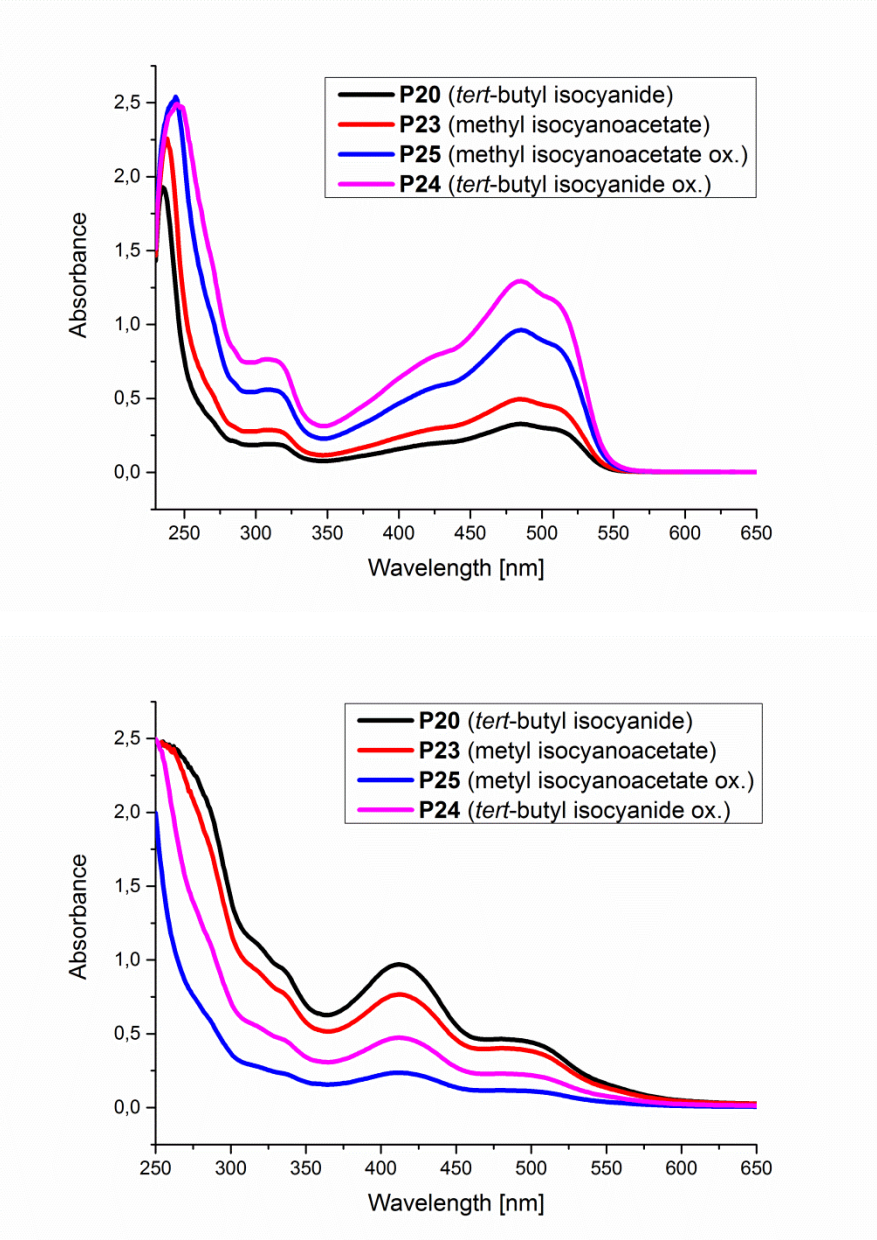

Figure 21: UV/VIS spectra of the encapsulation of Orange II in DCM by reduced and oxidized star-shaped block copolymers **P20**, **P23**, **P24** and **P25** (above), water insoluble Para Red in water by reduced and oxidized star-shaped block copolymers **P20**, **P23**, **P24** and **P25** (below).

The same set of polymers were used again to visualize the polarity within a solvatochromism experiment.[196] The effect of solvatochromism describes the ability of a chemical substrate to change its color depending on the polarity of the solvent in which it is dissolved.[197] The Reichardt's dye shows one of the largest solvachromic effects with a color change over the whole visible spectrum.[198] The star-shaped block

copolymers **P20**, **P23**, **P24** and **P25** were able to encapsulate this dye and, due to the different microenvironment within their core, the different colors were made visible through the solvatochromism effect of the dye (Figure 22, above).

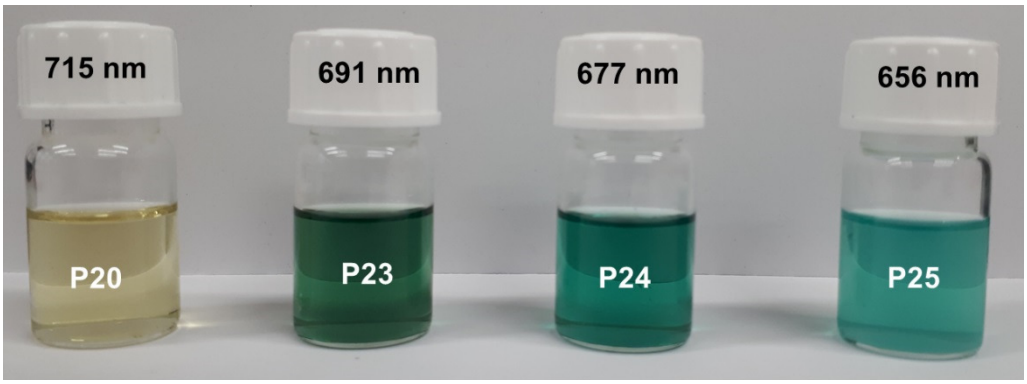

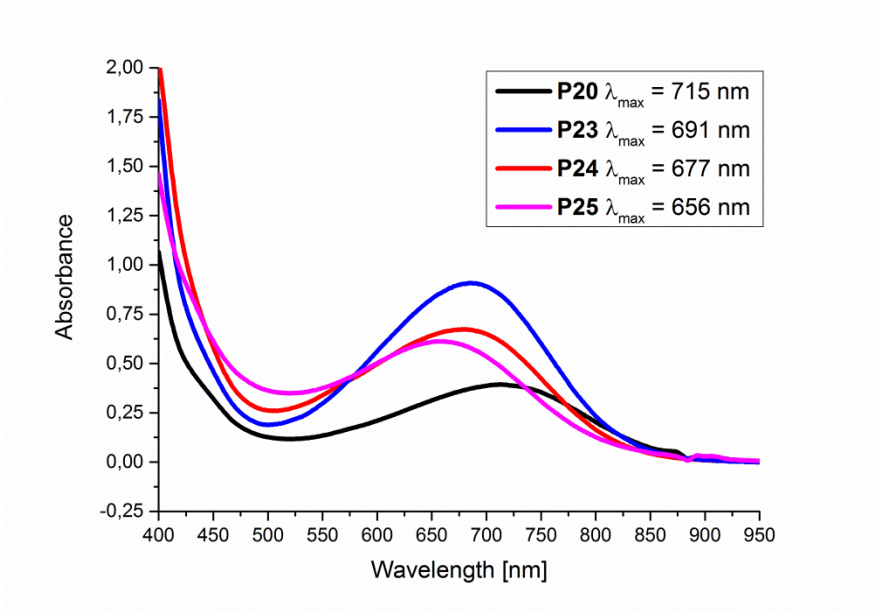

Figure 22: Pictures (above) and UV/VIS spectra (below) of the encapsulation of Reichardt's Dye in DCM by reduced and oxidized star-shaped block copolymers **P20**, **P23**, **P24** and **P25** showing different wavelength maxima, due to their different polarity and due to the solvatochromism effect of the encapsulated dye.

These visual results, confirmed by UV/VIS absorption experiments, showed different wavelength maxima, due to the different polarity of the star-shaped block copolymers (Figure 22, below). The higher the polarity, the lower was the wavelength maximum. Therefore, the Reichardt's dye was encapsulated (one molecule per star-shaped polymer) in 5.00 mL DCM and the UV/VIS absorption measured, using 5.00 mg of the reduced and oxidized three-armed star-shaped block copolymers **P20**, **P23**, **P24** and **P25**.

4.3.4 Comparison of the encapsulation behavior of four-armed and three-armed star-shaped polymers

Furthermore, it was shown that not only the polarity has an influence on the encapsulation behavior, but also the number of arms. Therefore, Orange II was added to 10.0 mL of a water/DCM biphasic system. Orange II was soluble in the water phase, but not in the DCM phase. After addition of four-armed star-shaped block copolymer **P31** and shaking, the dye was encapsulated and phase-transferred to the DCM phase (Figure 23). These results were compared to previous results of amphiphilic three-armed star-shaped block copolymer **P20** in former studies (section 4.3.2). The phase transfer behavior was additionally investigated by a UV/VIS experiment (Figure 24). In both solvent phases, the absorption was measured separately, and it could be shown that **P31** could encapsulate more dye, due to the higher number of arms. The absorption of the dye, using **P31**, was higher in DCM, whereas it was lower in the water phase as compared to the results for **P20**.

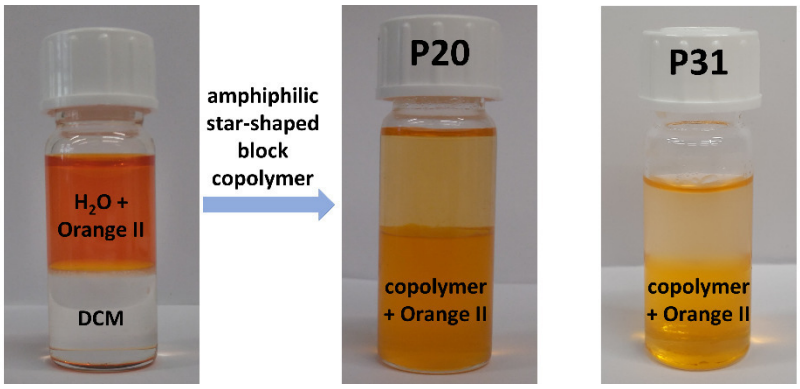

Figure 23: Picture of the encapsulation and phase transfer of Orange II from the water phase to the DCM phase by three-armed star-shaped block copolymer **P20** and four-armed star-shaped block copolymer **P31**.

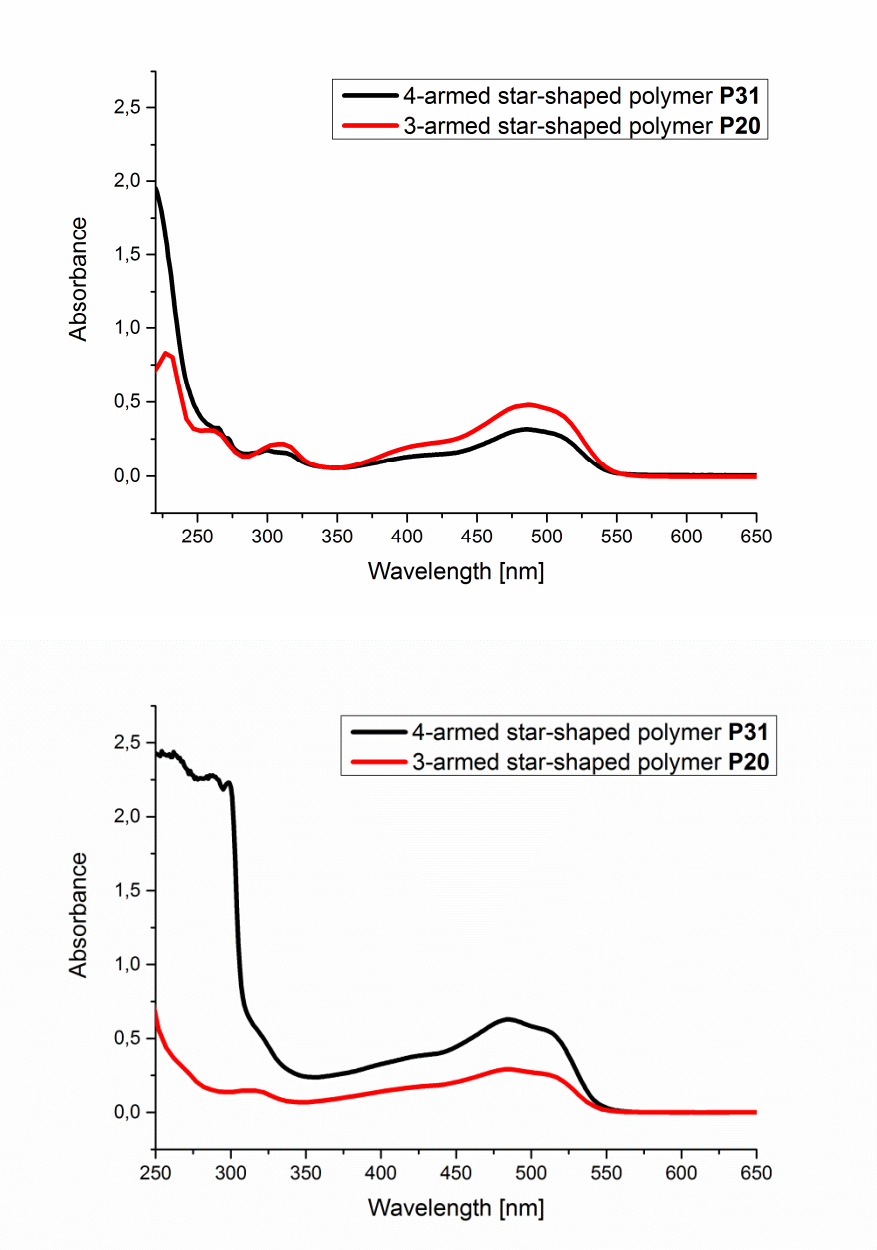

Figure 24: UV/VIS spectra of the encapsulation and phase transfer of Orange II from the water phase to the DCM phase by three-armed star-shaped block copolymer **P20** and four-armed star-shaped block copolymer **P31** (above: absorbance of Orange II in water, below: absorbance of Orange II in DCM).

4.3.5 In vitro drug loading and release efficiency studies of amphiphilic star-shaped block copolymers

The preparation methods of the following studies can be seen in the associated sections of the Experimental Part. All results described in this subchapter are a result of a collaboration with the group of Prof. Alexander Cameron at the University of Nottingham, UK.

Azithromycin is a semi-synthetic macrolide antibiotic, which is extensively used in the treatment of respiratory tract and skin infections (Figure 25). This drug is slightly water-soluble, with a similar solubility profile to many approved active pharmaceutical ingredients, and has good bioavailability in both oral and injectable formulations.[199] However, for pediatric settings, where dosing is more critical and the gap between toxic and minimum therapeutic levels is much lower, a sustained release formulation of Azithromycin is highly desirable.[200] Owing to the widespread existing use of polyester materials in controlled release formulations,[201] we therefore were interested in the ability of the Passerini-3CR star-shaped block copolymers to encapsulate the Azithromycin molecule in a unimolecular micelle formulation, and to release it under physiologically relevant conditions. Azithromycin was here tested as a hydrophobic drug model.

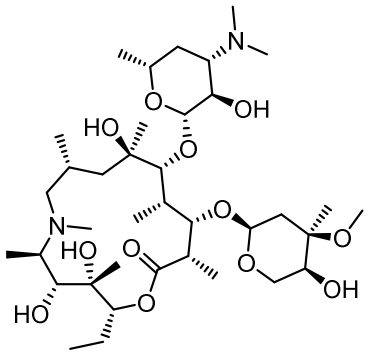

Azithromycin

Figure 25: Structure of Azithromycin

The Azithromycin loading, encapsulation efficiency and polymer to drug molar ratio were calculated using the following equations:

$$Drug\ loading\ (\%) = \frac{Weight\ of\ loaded\ drug}{Total\ weight\ of\ micelles} X\ 100$$

$$Drug\ encapsulation\ \%\ (w/w) = \frac{Total\ amount\ of\ drug - Unloaded\ drug}{Total\ amount\ of\ drug}\ X\ 100$$

The results for the star-shaped block copolymers **P20**, **P21**, **P23**, **P24**, **P25**, and **P31** were summarized in Table 7. The highest drug loading was observed for **P31**. This confirmed, that the encapsulation ability was affected by the number of arms of the star-shaped block copolymer. The results of **P21** further confirmed how the drug encapsulation could be improved by increasing the number of homopolymer repeating units. **P20, P23, P24** and **P25** data showed, how the drug loading could be driven, not only by the hydrophobic but also by the hydrogen-bonding interactions. The high drug encapsulation observed for **P24** and **P25** (compared to **P20** and **P23** respectively) suggested, that the sulfone groups were interacting as hydrogen bond acceptors with the seven hydrogen bond donors of Azithromycin (Figure 25). In contrast, **P20** and **P23** showed low drug encapsulation.

Table 7: Drug loading and encapsulation efficiency data of **P20**, **P21**, **P23**, **P24**, **P25** and **P31** (SD = standard deviation, pol:Az = polymer:Azithromycin).

polymer	drug loading (wt%) ± SD	encapsulation efficiency (%) ± SD	molar ratio pol:Az
P20	8.00 ± 1.24	8.09 ± 2.14	1 : 1.35
P21	25.3 ± 1.06	30.37 ± 3.24	1 : 5.00
P23	8.90 ± 0.4	11.74 ± 1.78	1 : 1.32
P24	17.7 ± 0.8	44.13 ± 2.03	1 : 2.68
P25	21.9 ± 1.3	38.00 ± 2.95	1 : 3.36
P31	35.0 ± 0.6	42.06 ± 1.20	1 : 6.00

The drug release profile of **P31** (Figure 26) was studied at pH 7.4 (blood pH) and pH 5 (lysosomal pH). It was found that at pH 7.4 only 20 % of the loaded Azithromycin was released in 5 hours and the remaining content was retained over three days. It was observed that at pH 5 the drug was completely released within 2 hours. These results suggested that Azithromycin, as a weakly dibasic antibiotic,[202] was protonated at acidic pH and thus released faster than at pH 7.4. These studies impressively showed how **P31** could potentially retain the loaded drug during circulation in the bloodstream (blood, pH 7.4), but selectively and completely release it inside acidified intracellular compartments (lysosomes, pH ~ 5) or in regions of enhanced acidity at infection sites.

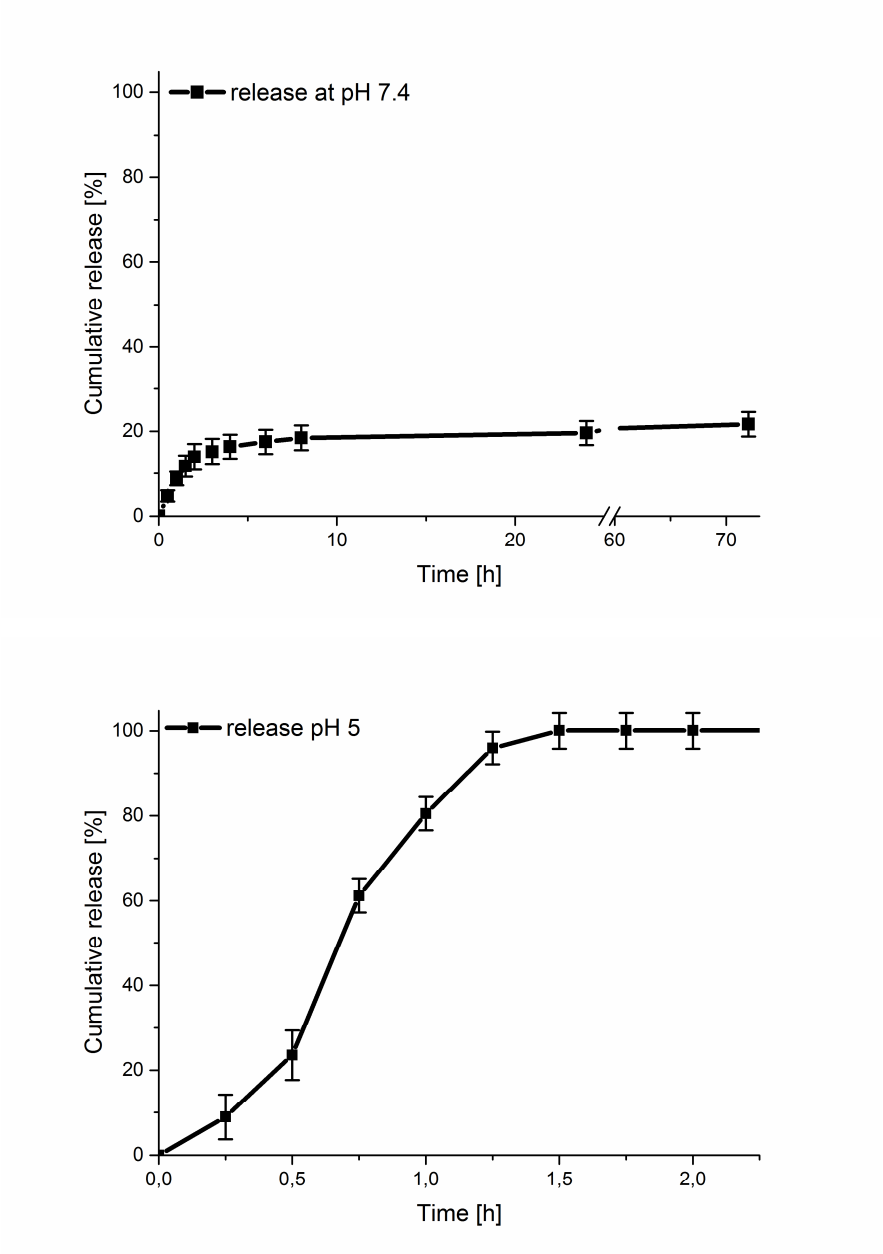

Figure 26: Analysis of Azithromycin release from star-shaped block copolymer **P31** at above: pH 7.4 (blood mimicking, above) and below: pH 5 (lysosome mimicking, below).

4.3.6 Viability, bacterial susceptibility and cellular uptake studies of amphiphilic star-shaped block copolymers

All experiments and results described in this subchapter were performed and described by Alessandra Travanut from Nottingham and shown here to demonstrate a possible application of the novel unimolecular micelles.

The preparation methods of the following studies can be seen in the associated sections of the Experimental Part.

Afterwards a CellTiter-Fluor™ cell viability assay was performed to assess the effects of star-shaped block copolymer **P31** in THP-1 macrophage differentiated cells over an incubation period of 72 hours. Untreated cells, cells exposed to highly lytic surfactants and polymer solutions were tested as controls. It was found that **P31** did not have any cytotoxic effect as measured by the CellTiter-Fluor™ assay, thus suggesting this polymer was well-tolerated by THP-1 differentiated macrophages (Figure 27).

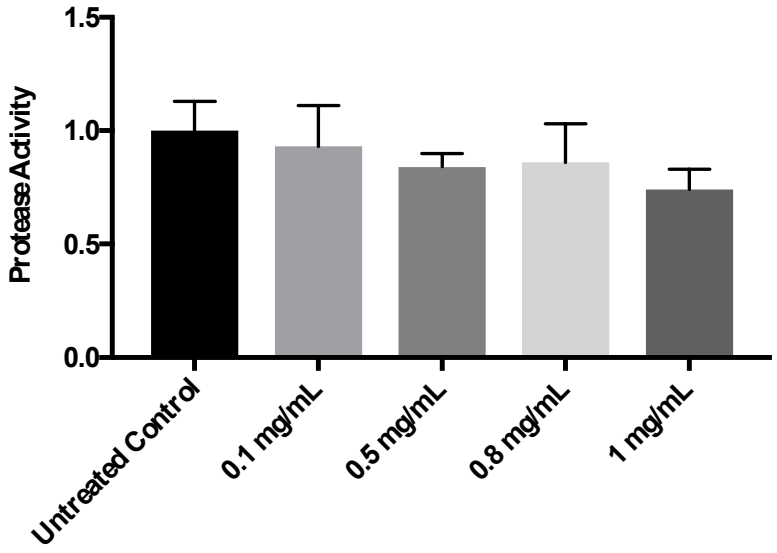

Figure 27: Viability Assay showing the protease activity of differentiated THP-1 cells treated with different concentrations of **P31**. Untreated Control: cells untreated with **P31**.

The antibiotic activity of the free and encapsulated Azithromycin in **P31** was assessed by performing a susceptibility assay with the common opportunistic pathogen *Staphyloccocus aureus* (Figure 28). It was observed that the bacteriostatic activity of the encapsulated drug was the same of the free drug, suggesting that the encapsulation did not affect the Azithromycin antibiotic activity. This assay was repeated three times with reproducible results; untreated wells and wells supplemented with solvent or polymer were set as controls.

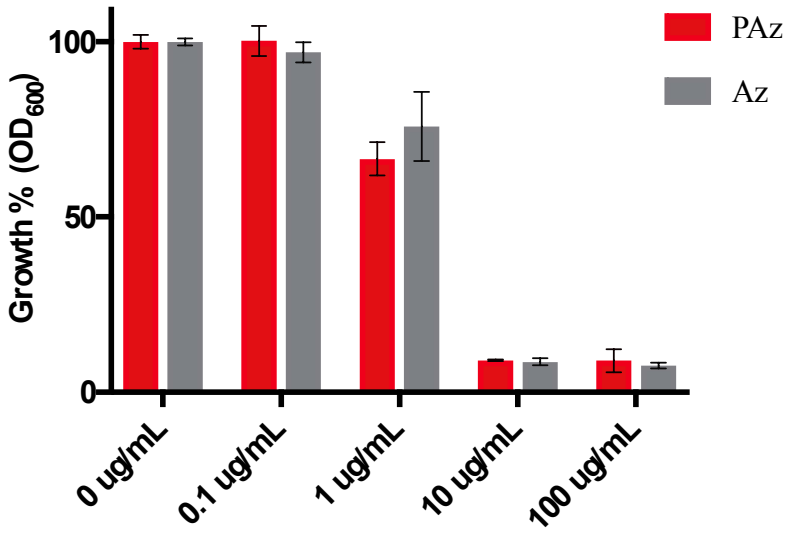

Figure 28: Effect of encapsulated Azithromycin on *Staphyloccocus aureus* growth. Bacteriostatic activity of serial concentrations (100-0.1 µg/mL) of free Azithromycin (Az) or **P31**-encapsulated Azithromycin (PAz) were assessed in TSB cultures. Values given are averages from three different cultures ± standard deviation and correspond to the area under the curve derived from plotting single OD_{600} measurements over time (24 h), and as percentage of the corresponding growth obtained in the untreated controls (set at 100 %). Controls wells Az 0 µg/mL and Paz 0 µg/mL were supplemented with solvent or only **P31** respectively.

Confocal laser scanning microscopy was performed in order to assess the intracellular localization of the cargo carried by star-shaped copolymer **P31**. Differentiated THP-1 macrophages were incubated for 1 hour with **P31**, loaded with Oregon-green (100 µg/mL; Synthesis see associated sections in the Experimental Part)[208] (Figure 29). It was observed that the green fluorescence (Oregon-green) is localized in the cytoplasm (Figure 29C), thus the star-shaped copolymer **P31** was able to deliver its cargo inside the cells.

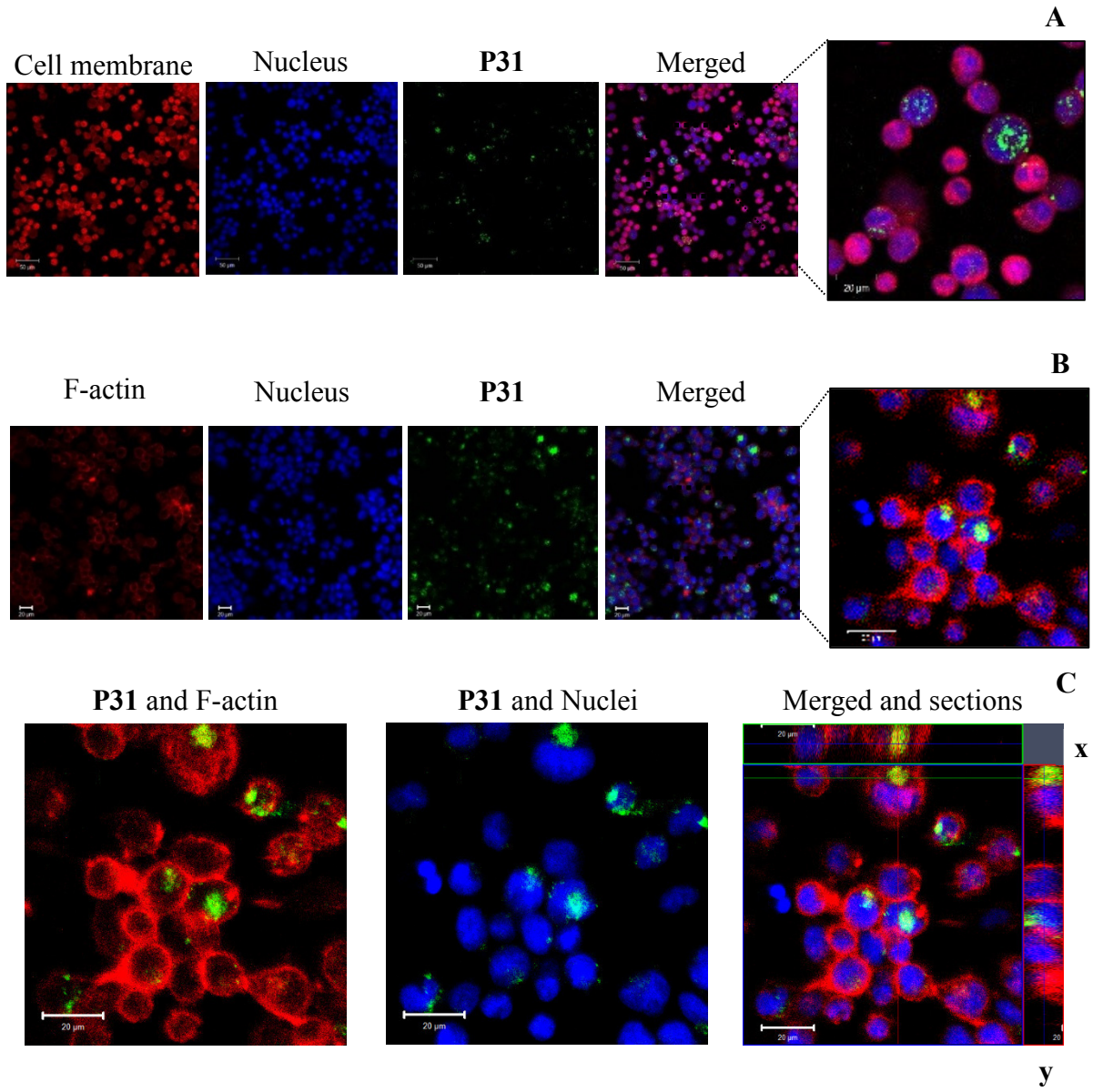

Figure 29: Confocal laser scanning microscopic images of cellular uptake in macrophage differentiated THP-1 cells cultured with Oregon-green loaded **P31** unimolecular micelles. (A) Staining protocol I (see associated sections in the Experimental Part) and (B) Staining protocol II (see associated sections in the Experimental Part). (C) Figure B section and zoom. Nuclei of cells were stained with Hoechst (blue fluorescence), cells membranes were stained with CellMaskTM deep red plasma membrane stain (red fluorescence) and F-actin was stained with Alexa FluorTM 647 Phalloidin (red fluorescence).

Conclusion

In conclusion, a library of amphiphilic star-shaped block copolymers *via* Passerini-3CR reactions was prepared. The polarity of the hydrophobic block was increased by oxidizing the sulfide groups to sulfones leading to the encapsulation of hydrophobic and hydrophilic molecules respectively. It was found that the encapsulation ability was

not only related to the polarity, but also to the number of arms of the hydrophobic core of the star-shaped copolymers. For the antimicrobial drug Azithromycin, the drug loading was found to be 35 mol%, which, considering the physical properties of Azithromycin are analogous to many other active pharmaceutical ingredients, suggests a potential biomedical application for the amphiphilic star-shaped block copolymers presented in this study. The polymers were found to be well tolerated by macrophages, which are the first cells to internalize most injected formulations and the sanctuary sites for many bacterial pathogens. Furthermore, the Passerini polymers were able to retain Azithromycin within their unimolecular micellar structure at pH levels found in the bloodstream but release the drug under acidic pH values similar to those in intracellular digestive compartments. Finally, the activity of the drug, when delivered from the unimolecular micelle formulations, was fully retained in terms of bacterial cell kill, as susceptibility assays using the common pathogen *Staphylococcus aureus* showed. In summary, these results clearly suggest the investigated unimolecular micelles have potential as easy-to-synthesize, cytocompatible drug delivery systems, with good drug loading and release properties.

5. CONCLUSION AND OUTLOOK

In summary, a new and versatile approach for the synthesis of three- and four-armed star-shaped polymers with defined molecular weights and adjustable polarity by a non-classic step-growth polymerization technique was developed. These polymers, synthesized *via* the Passerini-3CR, were used as unimolecular micelles and the encapsulation and phase transfer behavior of different dyes were tested. Furthermore, the drug loading capacities, the controlled release properties and the biocompatibility of the Passerini-polymers were investigated, using a macrolide antibiotic (Azithromycin) to show the potential as drug delivery system.

Therefore, an AB-type monomer containing an aldehyde and carboxylic acid end group was synthesized and polymerized *via* a Passerini-3CR with different isocyanides and a linear ICTA. With this simple polyaddition process, *α*-amide substituted polyesters with controlled molecular weights were synthesized. Due to the still active carboxylic acid end groups, diblock copolymers could be synthesized in a further Passerini reaction. Using a trifunctional ICTA, three-armed star-shaped homopolymers could be obtained in the same way. To obtain unimolecular core-shell architectures with an amphiphilic behavior, these star-shaped polymers were functionalized *via* a Passerini-3CR with different PEG-based shells. The unimolecular behavior, the encapsulation of water-soluble and water-insoluble guest molecules as well as the transport abilities from water to an organic phase were successfully tested. Afterwards, the polarity of the hydrophobic core block was increased by oxidizing the sulfide groups of the polymer backbone to sulfones and by using isocyanides of different polarity to tune the properties of these multifunctional materials. It could be shown that the encapsulation and transport properties of different polar guest molecules could be influenced by the polarity of the polymers. It was also demonstrated that the encapsulation ability was not only related to the polarity but also to the number of arms of the star-shaped copolymers. Therefore, four-armed star-shaped polymers were synthesized, examined and compared to three-armed analogous. Thus, a library of defined amphiphilic star-shaped block copolymers was synthesized *via* Passerini-3CR reactions in a straightforward fashion. To evaluate the potential of these easy-to-synthesize polymers for applications as drug delivery system, the drug loading capacity was tested with the antimicrobial drug Azithromycin. Depending on the polymer, up to six drug molecules

per polymer could be encapsulated. Furthermore, the Passerini polymers were able to retain Azithromycin within their unimolecular micellar structure at a pH found in the bloodstream but release the drug under acidic pH similar to those found in macrophages. The biocompatibility of these star-shaped polymers was successfully tested, revealing that these polymers were well tolerated by macrophages. Finally, it could be demonstrated that the activity of the drug was fully retained while delivered from the amphiphilic Passerini star-shaped block copolymers.

For the future, the herein presented novel non-classic step-growth polymerization technique offers diverse opportunities to synthesize new well defined macromolecular architectures for a wide variety of applications. The number of arms and the size of the core and shell of these star-shaped polymers could be increased to encapsulate more and/or larger guest molecules. Thereby, these systems could be tested with anticancer drugs or in the field of phase transfer catalysis. In addition to the Passerini-3CR, other multicomponent reactions, like the Ugi or the Biginelli reaction could be tested in an analogous procedure to obtain unimolecular micelles with different architectures and new properties. Furthermore, the synthesis of monodisperse star-shaped polymers using the Passerini-3CR in a sequence defined way could provide more accurate information about the encapsulation and release behavior. Another attractive possibility would be the introduction of chirality by using chiral core molecules or by synthesizing chiral arms, due to the very interesting properties of chiral materials, which can be used in stereoselective catalysis.

6. EXPERIMENTAL PART

6.1 Materials

The following chemicals were used as received: 10-undecenal (≥90%, Aldrich), 3-mercaptopropionic acid (≥99%, Aldrich), 2,2-dimethoxy-2-phenylacetophenone (DMPA, 99%, Aldrich), 10-undecenoic acid (98%, Aldrich), cyclohexyl isocyanide (98%, Aldrich), *tert*-butyl isocyanide (98%, Aldrich), benzyl isocyanide (98%, Aldrich), pentyl isocyanide (98%, Aldrich), *tert*-butyl 2-isocyanoacetate (98%, Aldrich), trimesic acid (95%, Aldrich), O-Methyl-O′-[2-(6-oxocaproylamino)ethyl]polyethylene glycol 2000, (PEG aldehyde 2000, Aldrich), 11-aminoundecanoic acid (97%, Aldrich), methanol (99%, Aldrich), thionyl chloride (97%, Aldrich), trimethyl orthoformate (99%, Aldrich), diisopropyl amine (99%, Aldrich), phosphorus(V) oxychloride (99%, Aldrich), 1,5,7-triazabicyclo[4.4.0]dec-5-ene (TBD, 98%, Aldrich), poly(ethylene glycol) methyl ether 750 (Methoxy PEG 750, Aldrich), poly(ethylene glycol) methyl ether thiol 800 (PEG thiol 800, Aldrich), Orange II sodium salt (85% dye content, Aldrich), Para Red (95% dye content, Aldrich), Reichardt's dye (90%, Aldrich), 3-chloroperbenzoic acid (*m*CPBA, 77%, Aldrich), hydrogen peroxide solution (30% in water, Aldrich), methyl isocyanoacetate (95%, Aldrich), 3,3,5,5-tetracarboxydiphenylmethane (95%, Aldrich), silica gel 60 (0.035–0.070, Aldrich), chloroform-*d* ($CDCl_3$, 99.8 atom-% D, euriso-top), methanol-d_4 (99.8 atom-% D, euriso-top), CellTiter-Fluor™ Cell Viability Assay (Promega, Madison WI), Azithromycin (PHR1088, Aldrich), Tween® 20 (P1379, Aldrich), Dulbecco's Phosphate Buffered Saline - PBS (Aldrich), Citric Acid (C-3674, Aldrich), Slide-A-Lyzer® MINI Dialysis Units (Thermo SCIENTIFIC), Phorbol 12-myristate 13-acetate (PMA) (99%, Aldrich), Penicillin/Streptomycin (Aldrich), L-Glutamine (Aldrich), THP-1 human cells were purchased from ATCC in frozen from (Manassas, VI, USA), RPMI-1640 media and fetal bovine serum were obtained from Life Technologies (Carlsbad, CA, USA). All solvents used were of technical grade.

6.2 Instrumentation

Thin-layer chromatography (TLC) identification of reactants and products was performed on silica-gel-coated aluminum foil (Aldrich, silica gel 60, F 254 with fluorescence indicator). Compounds were visualized by Seebach reagent (mixture of phosphomolybdic acid, cerium(IV) sulfate, water and sulfuric acid).

NMR spectra were recorded on a Bruker AVANCE DPX spectrometer (measuring frequency: ^{1}H NMR = 300 MHz, ^{13}C NMR = 75 MHz) or a Bruker AMX R 500 spectrometer (measuring frequency: ^{1}H NMR = 500 MHz, ^{13}C NMR = 126 MHz). NMR spectra were obtained using $CDCl_3$. All ^{1}H NMR spectra are reported in ppm relative to the solvent signal for $CDCl_3$ at 7.26 ppm, ^{13}C NMR spectra are reported relative to the solvent signal for $CDCl_3$ at 77.16 ppm.

Polymers were characterized on a SEC System LC-20A (Shimadzu) equipped with a SIL-20A autosampler and a RID-10A refractive index detector using THF (flow rate 1 mL/min) at 50 °C. The analysis was performed on the following column system: analytical main-column PSS SDV (5 µm, 300 mm × 8.0 mm, 10,000 Å) with a PSS SDV analytical precolumn (5 µm, 50 mm × 8.0 mm). For the calibration narrow linear poly(methyl methacrylate) standards (Polymer Standards Service PPS, Germany) ranging from 1.1 to 981 kDa were used.

FAB (fast atom bombardment) mass spectra were recorded on a MAT95 (Finnigan) instrument.

Infrared (IR) spectra were recorded on a Bruker alpha-p instrument applying KBr- as well as ATR-technology.

The thermal properties of the prepared polymers were studied via DSC (differential scanning calorimetry) with a Mettler Toledo DSC star system, operating under nitrogen atmosphere and using about 5 mg of the respective polymer for the analysis. The glass transition temperature (T_g) was recorded on the second heating scan by using the following method: heating from −70 to 150 °C at 10 °C min^{-1}, cooling from 150 to −70 °C at 10 °C min^{-1}, and heating from −70 to 150 °C at 10 °C min^{-1}.

Size exclusion chromatography–electrospray ionization–mass spectra (SEC–ESI–MS) were recorded on a Q Exactive (Orbitrap) mass spectrometer (Thermo Fisher Scientific, San José, CA, USA) equipped with an HESI II probe. The instrument was calibrated in the *m/z* range 74–1822 using premixed calibration solutions (Thermo

Scientific). A constant spray voltage of 4.6 kV, a dimensionless sheath gas of 8, and a dimensionless auxiliary gas flow rate of 2 were applied. The capillary temperature and the S-lens RF level were set to 320 °C and 62.0 °C, respectively. The Q Exactive was coupled to an UltiMate 3000 UHPLC System (Dionex, Sunnyvale, CA, USA) consisting of a pump (LPG 3400SD), autosampler (WPS 3000TSL), and a thermostated column department (TCC 3000SD). Separation was performed on two mixed bed size exclusion chromatography columns (Polymer Laboratories, Mesopore 250 × 4.6 mm, particle diameter 3 µm) with precolumn (Mesopore 50 × 4.6 mm) operating at 30 °C. THF at a flow rate of 0.30 mL min^{-1} was used as eluent. The mass spectrometer was coupled to the column in parallel to a RI-detector (RefractoMax520, ERC, Japan). 0.27 mL min^{-1} of the eluent were directed through the RI-detector and 30 µL min^{-1} infused into the electrospray source after post column addition of a 100 µM solution of sodium iodide in methanol at 20 µL min^{-1} by a micro-flow HPLC syringe pump (Teledyne ISCO, Model 100DM). A 20 µL aliquot of a polymer solution with a concentration of 2 mg mL^{-1} was injected onto the HPLC system.

Dynamic light scattering (DLS) was performed on a Zeta Sizer Nano S (Malvern Instruments) with a scattering angle of 176.1°. The reported diameter (d_{DLS}) is an intensity-weighted average size (*z*-average), comprised of five to nine measurements analyzed in 10 to 20 runs. The reported polydispersity index values (PD_{DLS}) are those given by the instrument and are referred to as Malvern polydispersity.

A UV/VIS spectrometer of the type Cary 60 from Agilent Technologies was used to record UV/VIS spectra. It scanned the entire wavelength range (190 to 1100 nm) in under three seconds and collect data from single or multiple wavelengths at 80 data points per second. The measurements were performed in water and DCM. Therefore, a 10 mm Semi-Micro Quartz Cuvette was used.

HPLC measurements were performed using an Agilent HPLC 1200 system equipped with a MZ Refill PerfectSil Target ODS-3 5 mm column (4.0 x 250 mm) and a DAD detector. A mixture of methanol and water (70:30) was used as eluent with a flow rate of maximum 5.0 mL/min and an injection volume of maximum 100 µL.

The cellular uptake of unimolecular micelles was observed using a Carl Zeiss LSM 700 BW microscope. A 488 nm wavelength laser was used to excite the Oregon-green (excitation/emission maxima = 495/521 nm). AlexaFluor 647 far red F-actin stain (excitation/emission maxima = 650/665 nm) and CellMask™ deep red plasma

membrane stain (excitation/emission maxima = 649/666 nm) were excited with a laser of 633 nm wavelength. The Hoechst 33342 stain (excitation/emission maxima = 350/462 nm) was illuminated with a 100-Watt high-pressure mercury plasma arc-discharge lamp (HBO 100). Oregon-green polymer-free (100 µg/mL) treated cells were used as control.

6.3 Experimental procedures – chapter 4.1

Synthesis of AB-type monomer 3 *via* thiol-ene reaction

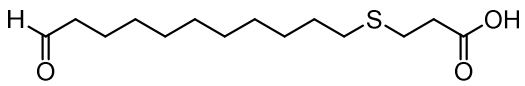

10-undecenal **1** (1.68 g, 10.0 mmol) and DMPA (130 mg, 0.50 mmol) were dissolved in 4.0 mL THF. After purging with argon for 10 minutes, the solution was exposed to UV light (365 nm) for 30 s. Subsequently, 3-mercaptopropionic acid **2** (1.17 g, 959 µL, 11.0 mmol) was slowly added and the reaction mixture was stirred for 2 h under UV irradiation. After evaporating the solvent under reduced pressure, the crude product was purified by silica gel column chromatography (*n*-hexane/ethyl acetate = 3:1 – 1:1) to yield a white solid (2.10 g, 77 %). R_f = 0.30 (dichloromethane/methanol = 20:1); ^{1}H NMR ($CDCl_3$, 300 MHz): δ (ppm) = 1.21–1.41 (m, 12 H, 6 CH_2), 1.51–1.69 (m, 4 H, 2 CH_2), 2.42 (td, *J* = 7.3, 1.7 Hz, 2 H, C*H*$_2$CHO), 2.53 (t, *J* = 7.3 Hz, 2 H, CH_2S), 2.61–2.70 (m, 2 H, C*H*$_2$COOH), 2.73–2.82 (m, 2 H, SCH_2), 9.76 (t, *J* = 1.8 Hz, 1 H, CHO); ^{13}C NMR ($CDCl_3$, 75 MHz): δ (ppm) = 22.13, 26.67, 28.88, 29.20, 29.22, 29.37, 29.39, 29.47, 29.56, 32.25, 34.78, 178.12, 203.31; FAB of $C_{14}H_{26}O_3S$ $[M+H]^+$ = 275.1; HRMS (FAB) of $C_{14}H_{26}O_3S$ $[M+H]^+$ calc. 275.1681, found 275.1680; IR (KBr) ν = 2914.7, 2847.2, 2742.6, 1708.0, 1684.7, 1466.7, 1407.2, 1338.2, 1263.9, 1197.5, 1064.0, 915.4, 894.3, 761.7, 737.7, 721.1, 696.0, 660.8, 490.5 cm^{-1}; T_m = 70 °C.

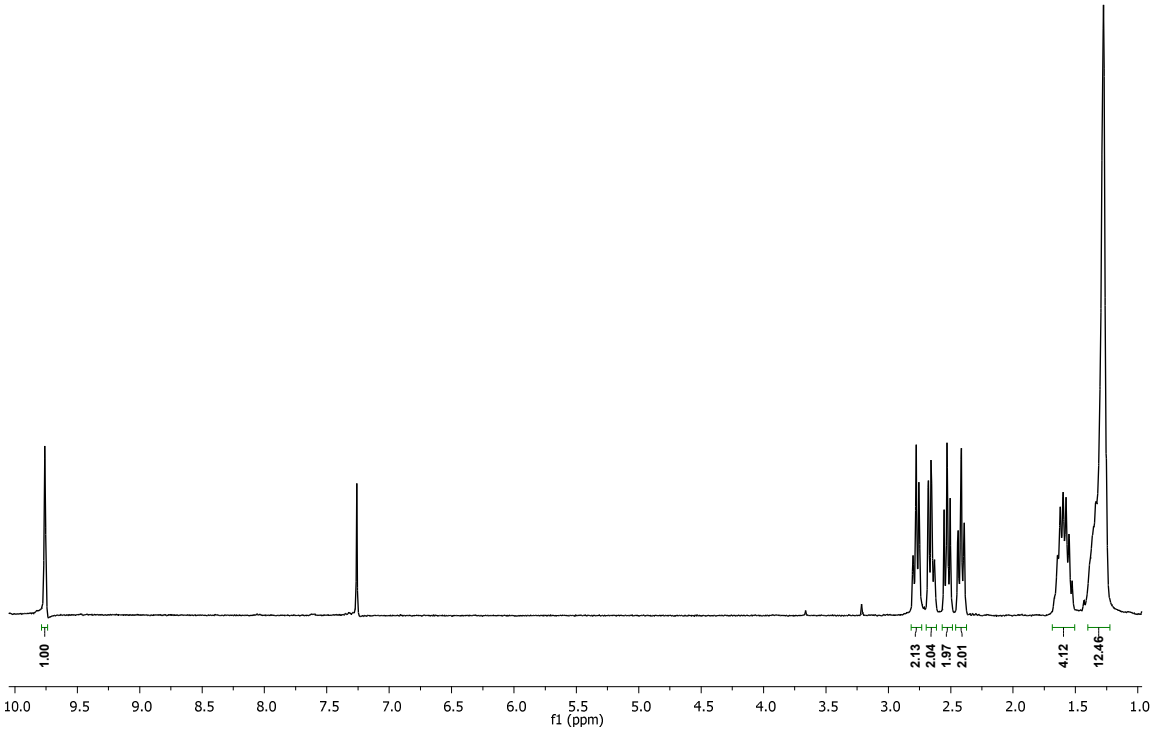

Synthesis of homopolymers P1-P4 *via* Passerini-reaction

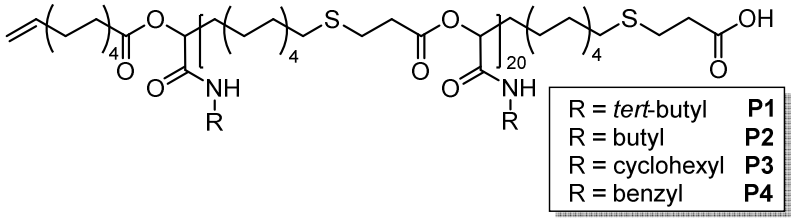

General procedure: To a vigorously stirred solution of 10-undecenoic acid **4** (13.3 mg, 0.0722 mmol) and the corresponding isocyanide **5-8** (7.20 mmol), the AB-type monomer **3** (400 mg, 0.36 mmol) in 1.0 mL dichloromethane (DCM) was added slowly. After stirring for 24 hours at room temperature, the polymer was precipitated from diethyl ether.

Homopolymer P1

Following the aforementioned procedure, **P1** was obtained as a white solid (96 %). ^{1}H NMR ($CDCl_3$, 300 MHz): δ (ppm) = 1.20–1.32 (m, 280 H, 140 CH_2), 1.35–1.42 (m, 196 H, 180 *t*-Bu, 8 CH_2 end group), 1.52–1.62 (m, 40 H, 20 C*H*$_2$CH$_2$S), 1.75–1.88 (m, 40 H, 20 CHC*H*$_2$), 2.53 (t, *J* = 7.4 Hz, 40 H, 20 CH_2S), 2.69 (t, *J* = 6.5 Hz, 40 H, 20

SCH_2), 2.81 (t, *J* = 6.2 Hz, 40 H, 20 CH_2COO), 4.87–5.00 (m, 2 H, CH_2 double bond), 5.07 (t, *J* = 6.2 Hz, 20 H, OCH(CO)), 5.93–6.03 (m, 1 H, CH double bond), 6.09 (s, 20 H, NH); T_g = 5 °C.

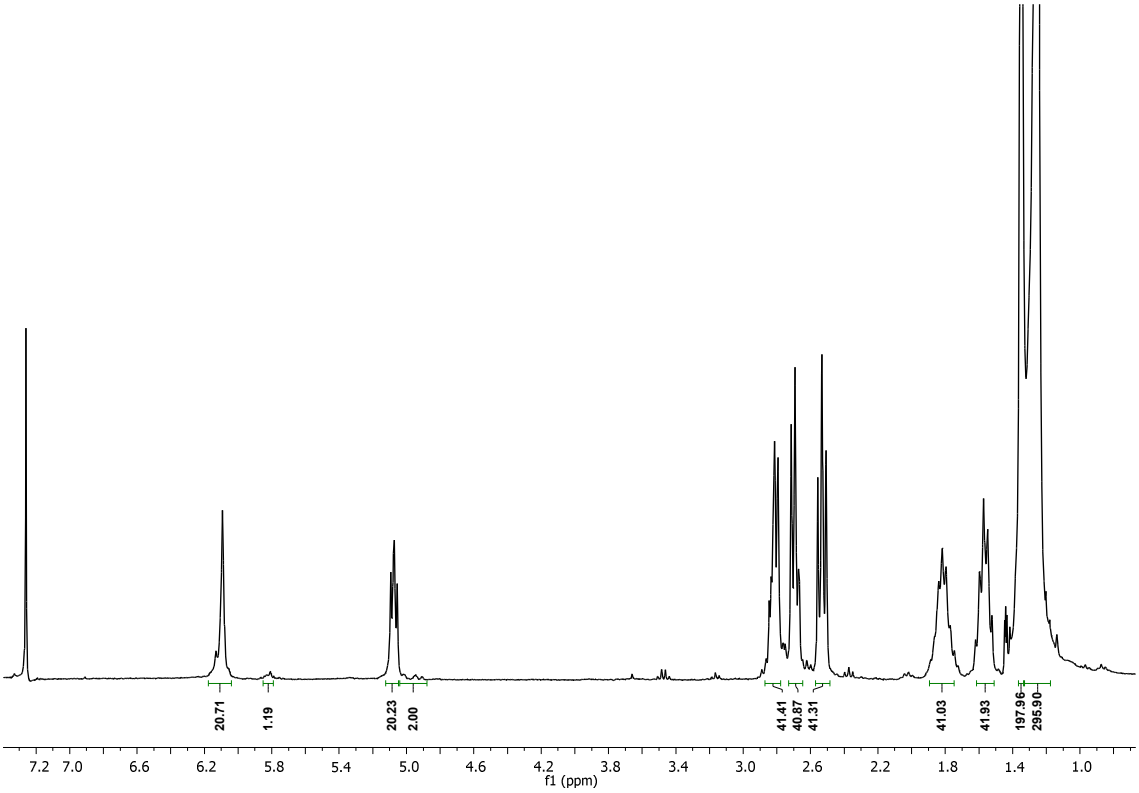

Homopolymer P2

Following the aforementioned procedure, **P2** was obtained as sticky yellow solid (81 %). ^{1}H NMR ($CDCl_3$, 300 MHz): δ (ppm) = 0.84–0.92 (m, 60 H, 20 CH_3), 1.23–1.38 (m, 376 H, 180 CH_2, 8 CH_2 end group), 1.45–1.61 (m, 80 H, 20 C*H*$_2$$CH_2S$, 20 $NHCH_2CH_2$), 1.75–1.91 (m, 40 H, 20 CHC*H*$_2$), 2.53 (t, *J* = 7.4 Hz, 40 H, 20 CH_2S), 2.67–2.75 (m 40 H, 20 SCH_2), 2.79–2.91 (m, 40 H, 20 CH_2COO), 3.18–3.29 (m, 40 H, 20 CHC*H*$_2$), 4.92–4.97 (m, 2 H, CH_2 double bond), 5.16–5.23 (m 20 H, OCH(CO)), 5.98–6.07 (m, 1 H, CH double bond), 6.57 (t, J = 6.2 Hz, 20 H, NH); T_g = –11 °C.

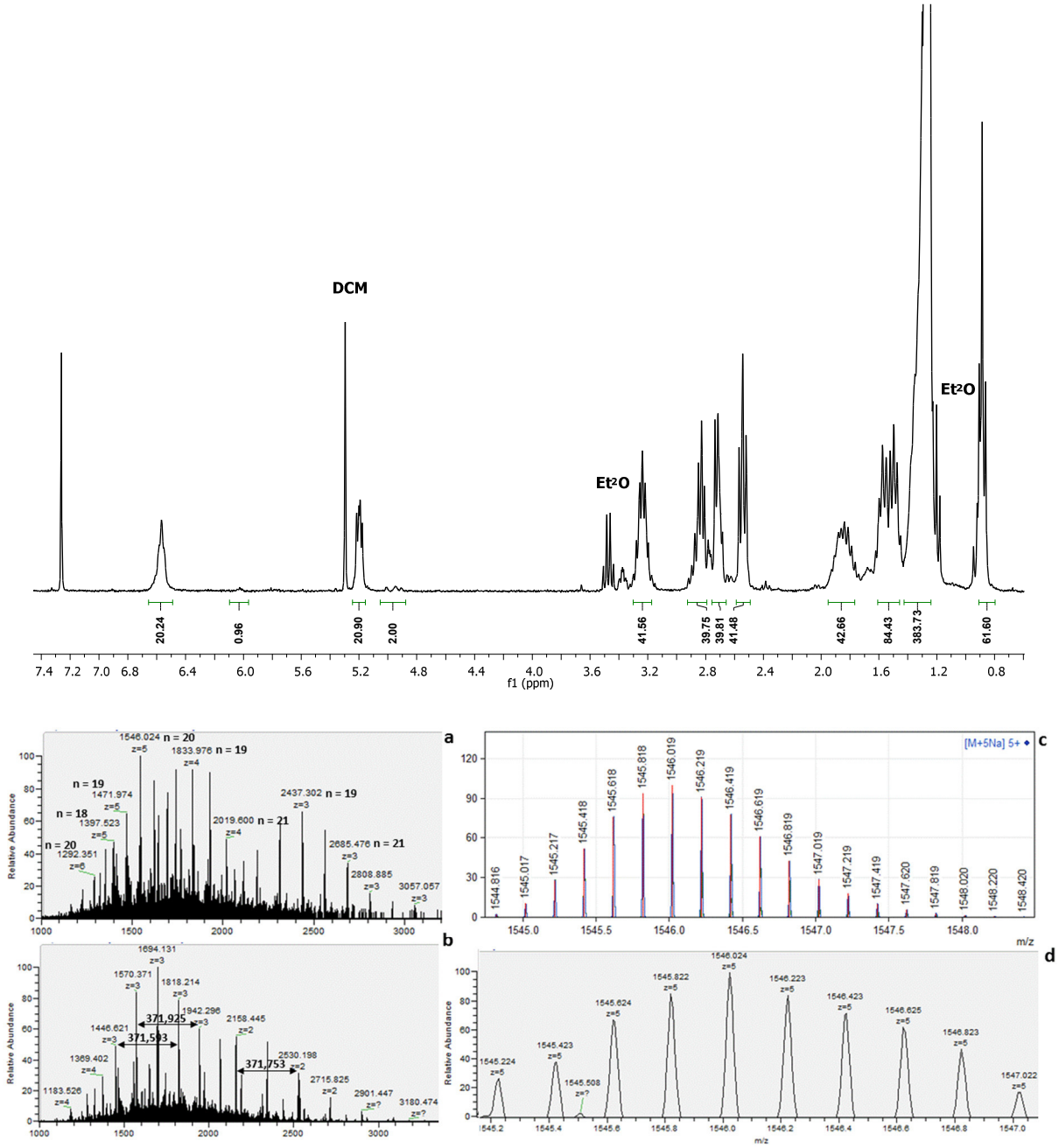

Figure 30: Mass spectra of homopolymer **P2** with n repeating units and a calculated mass of 371.580 g/mol per repeating unit (a = retention time of 13.17 min, b = retention time of 11.94-13.93 min, c = calculated isotope pattern, d = experimental isotope pattern at a retention time of 13.17 min).

Homopolymer P3

Following the aforementioned procedure, **P3** was obtained as sticky colorless solid (81 %). ^{1}H NMR ($CDCl_3$, 300 MHz): δ (ppm) = 1.20–1.43 (m, 412 H, 198 CH_2, 8 CH_2 end group), 1.56–1.75 (m, 132 H,66 CH_2), 1.80–1.89 (m, 88 H, 22 C*H*$_2$CH$_2$S, 22 CHC*H*$_2$), 2.54 (t, *J* = 7.4 Hz, 44 H, 22 CH_2S), 2.65–2.74 (m, 44 H, 22 SCH_2), 2.77–

2.88–2.99 (m, 44 H, 22 CH_2COO), 3.69–3.82 (m, 22 H, NCH) 4.89–4.94 (m, 2 H, CH_2 double bond), 5.11–5.20 (m, 22 H, OCH(CO)), 5.29–5.34 (m, 1 H, CH double bond), 6.35 (d, J = 8.2 Hz, 22 H, NH); T_g = 3 °C.

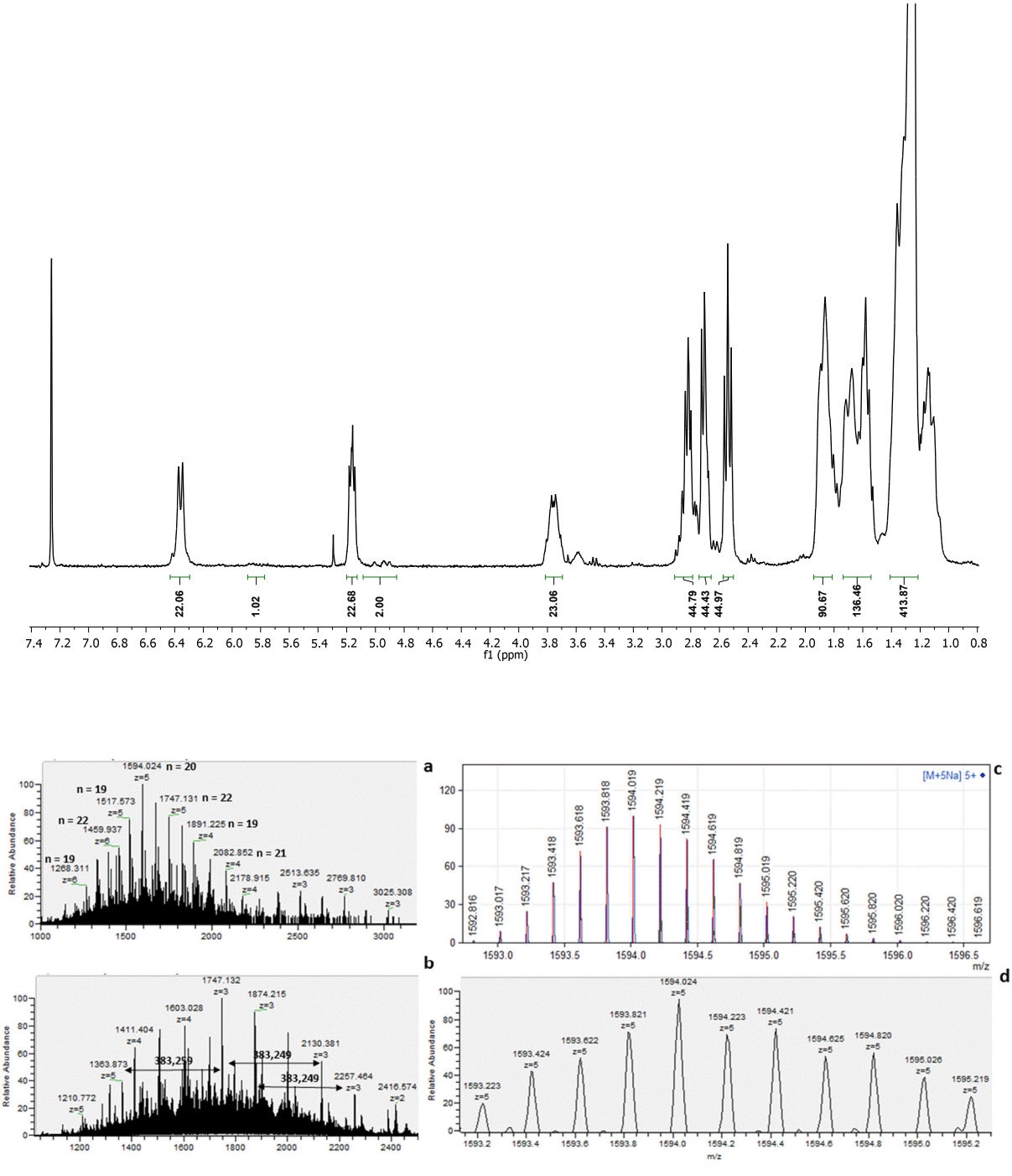

Figure 31: Mass spectra of homopolymer **P3** with n repeating units and a calculated mass of 383.249 g/mol per repeating unit (a = retention time of 13.16 min, b = retention time of 11.74-13.83 min, c = calculated isotope pattern, d = experimental isotope pattern at a retention time of 13.16 min).

Homopolymer P4

Following the aforementioned procedure, **P4** was obtained as sticky brown solid (92 %). ^{1}H NMR ($CDCl_3$, 300 MHz): δ (ppm) = 1.15–1.46 (m, 304 H, 144 CH_2, 8 CH_2 end group), 1.81–1.95 (m, 36 H, 18 CHC*H*$_2$), 2.34 (t, *J* = 7.3 Hz, 36 H, 18 CH_2S), 2.63–2.72 (m, 36 H, 18 SCH_2), 2.74–2.84 (m, 36 H, 18 CH_2COO), 4.41–4.49 (m, 36 H, 18 NCH_2) 4.95–4.99 (m, 2 H, CH_2 double bond), 5.23–5.31 (m, 18 H, OCH(CO)), 5.73–5.84 (m, 1 H, CH double bond), 6.96–7.04 (m, 18 H, NH), 7.11–7.24 (m, 36 H, 36 Ar-H), 7.28–7.39 (m, 54 H, 54 Ar-H); T_g = 1 °C.

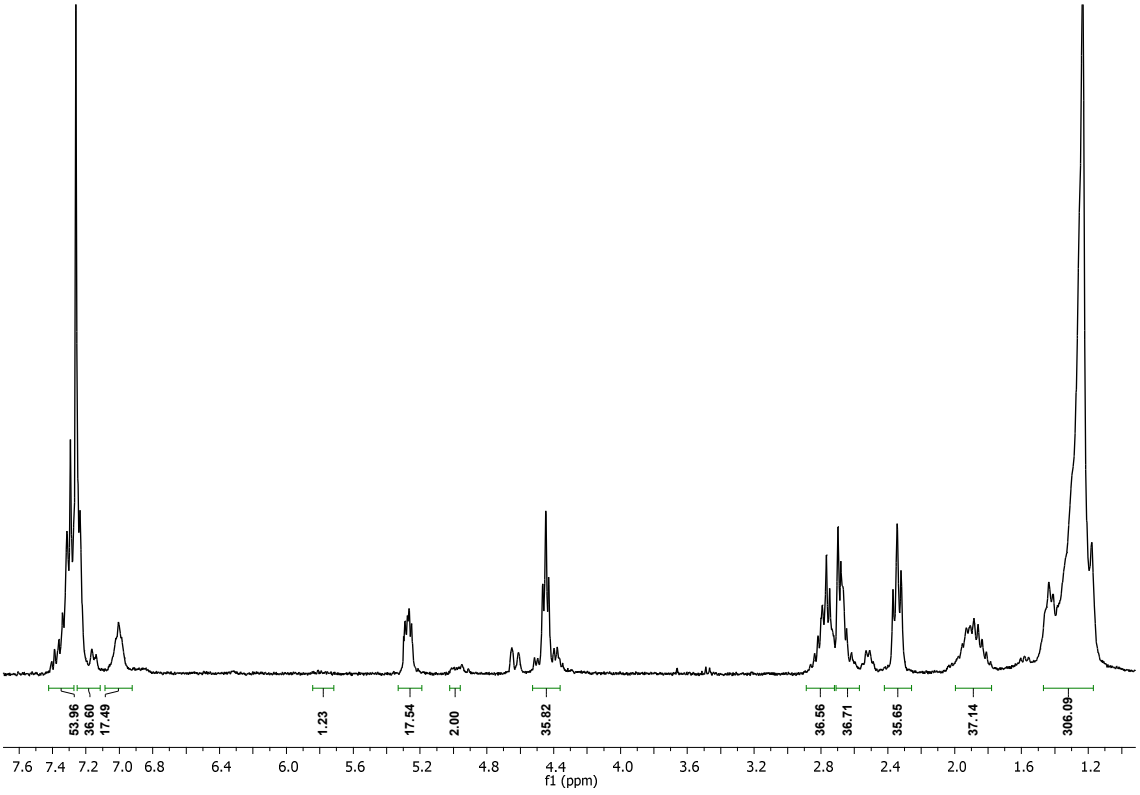

Synthesis of homopolymers P5-P7 *via* Passerini-reaction

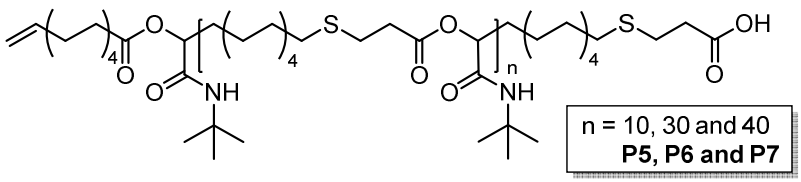

General procedure: To a vigorously stirred solution of 10-undecenoic acid **4** (1.00 equiv.) and isocyanide **5** (50, 150, 200 equiv.), the AB-type monomer **3** (10, 30, 40 equiv.) in 1.50 mol/L dichloromethane (DCM) was added slowly. After stirring for 24 hours at room temperature, the polymer was precipitated from diethyl ether.

Homopolymer P5

Following the aforementioned procedure, **P5** was obtained as a white solid (93 %). ^{1}H NMR ($CDCl_3$, 300 MHz): δ (ppm) = 1.20–1.32 (m, 140 H, 70 CH_2), 1.35–1.45 (m, 106 H, 90 *t*-Bu, 8 CH_2 end group), 1.52–1.62 (m, 20 H, 10 C*H*$_2$$CH_2S$), 1.75–1.88 (m, 20 H, 10 CHC*H*$_2$), 2.53 (t, *J* = 7.3 Hz, 20 H, 10 CH_2S), 2.69–2.77 (m, 20 H, 10 SCH_2), 2.81–2.92 (m, 20 H, 10 CH_2COO), 4.87–5.00 (m, 2 H, CH_2 double bond), 5.07–5.18 (m, 10 H, OCH(CO)), 5.93–6.03 (m, 1 H, CH double bond), 6.09 (s, 10 H, NH).

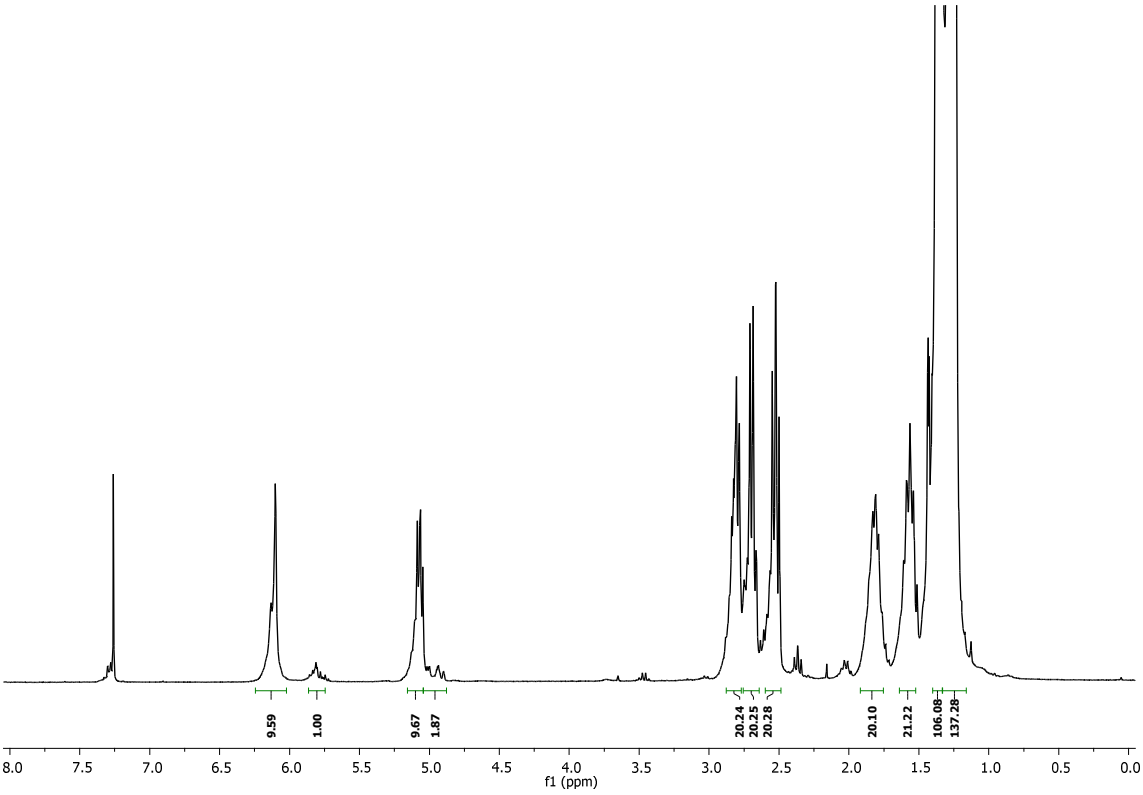

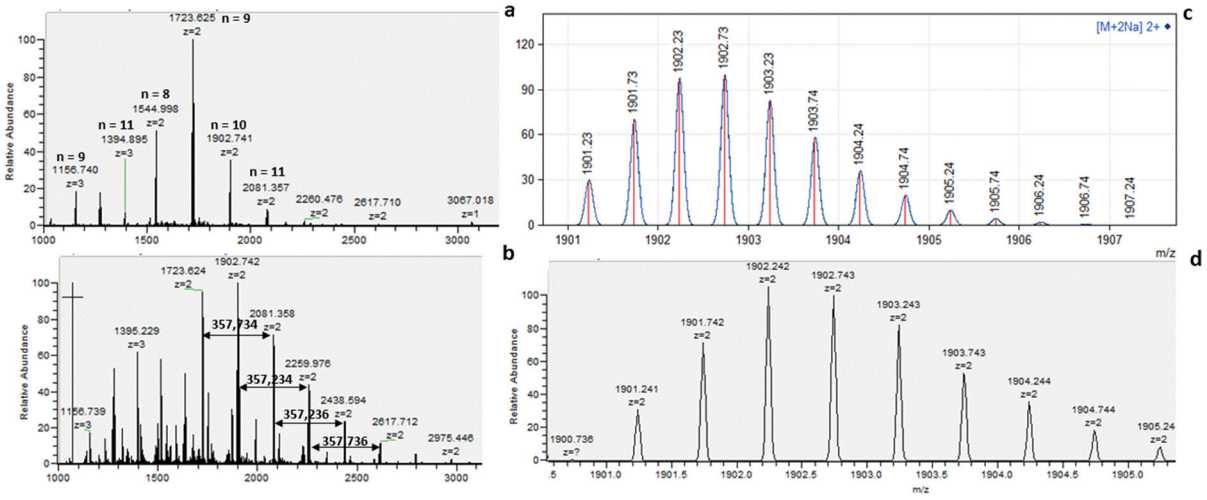

Figure 32: Mass spectra of homopolymer **P5** with n repeating units and a calculated mass of 357.234 g/mol per repeating unit (a = retention time of 14.27 min, b = retention time of 12.76-14.28 min, c = calculated isotope pattern, d = experimental isotope pattern at a retention time of 14.27 min).

Homopolymer P6

Following the aforementioned procedure, **P6** was obtained as a white solid (95 %). ^{1}H NMR ($CDCl_3$, 300 MHz): δ (ppm) = 1.19–1.31 (m, 420 H, 210 CH_2), 1.32–1.41 (m, 286 H, 270 *t*-Bu, 8 CH_2 end group), 1.51–1.64 (m, 60 H, 30 C*H*$_2$$CH_2S$), 1.72–1.88 (m, 60 H, 30 CHC*H*$_2$), 2.54 (t, *J* = 7.5 Hz, 60 H, 30 CH_2S), 2.67–2.78 (m, 60 H, 30 SCH_2), 2.83–2.90 (m, 60 H, 30 CH_2COO), 4.88–5.00 (m, 2 H, CH_2 double bond), 5.05–5.22 (m, 30 H, OCH(CO)), 5.90–6.01 (m, 1 H, CH double bond), 6.07 (s, 30 H, NH).

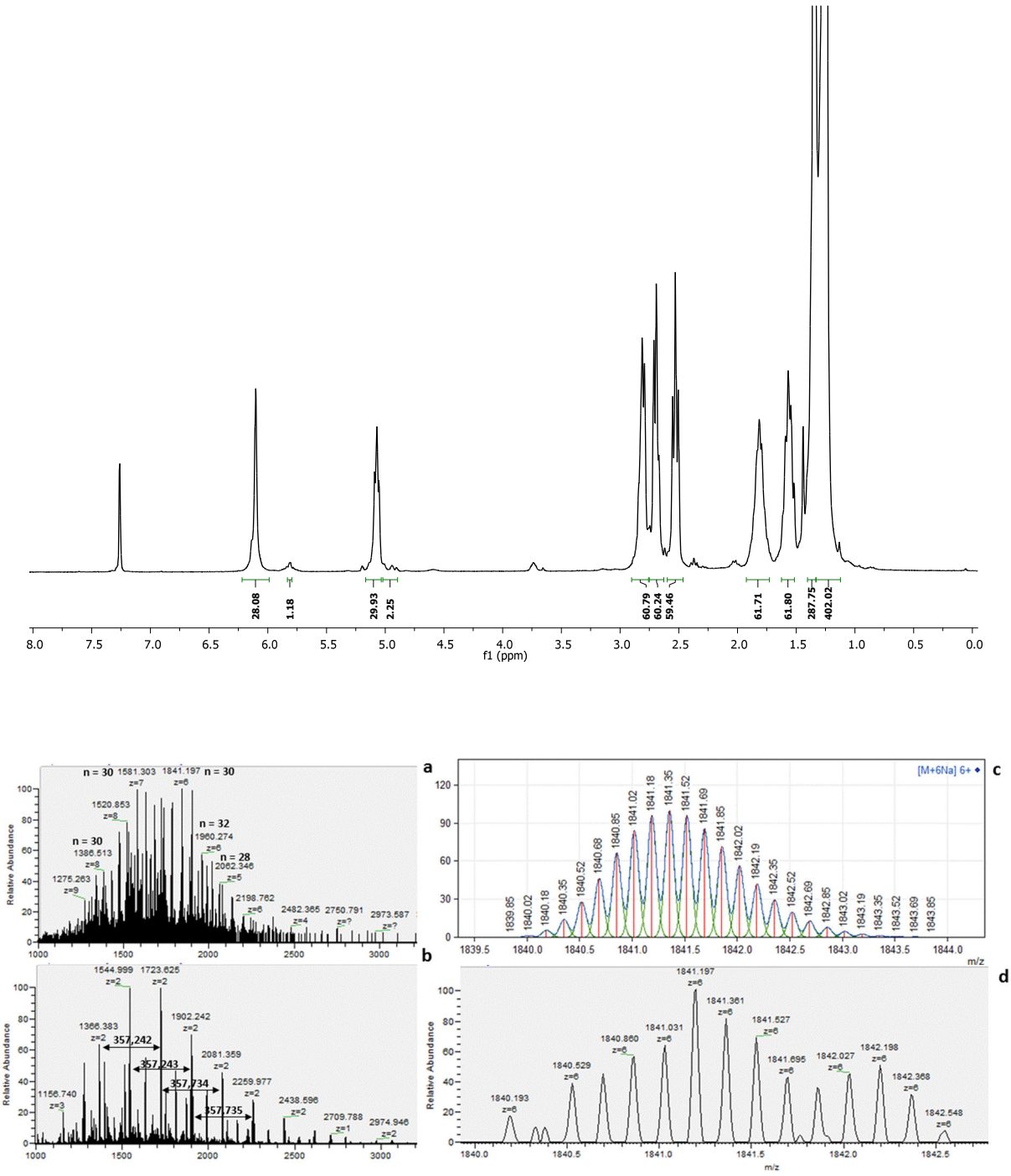

Figure 33: Mass spectra of homopolymer **P6** with n repeating units and a calculated mass of 357.234 g/mol per repeating unit (a = retention time of 12.61 min, b = retention time of 11.79-14.73 min, c = calculated isotope pattern, d = experimental isotope pattern at a retention time of 12.61 min).

Homopolymer P7

Following the aforementioned procedure, **P7** was obtained as a white solid (91 %). ^{1}H NMR ($CDCl_3$, 300 MHz): δ (ppm) = 1.17–1.27 (m, 560 H, 280 CH_2), 1.31–1.44 (m, 376 H, 360 *t*-Bu, 8 CH_2 end group), 1.50–1.62 (m, 80 H, 40 C*H*$_2$CH$_2$S), 1.76–1.89 (m,

80 H, 40 CHC*H*$_2$), 2.55 (t, *J* = 7.4 Hz, 80 H, 40 CH_2S), 2.66–2.76 (m, 80 H, 40 SCH_2), 2.83–2.95 (m, 80 H, 40 CH_2COO), 4.88–5.01 (m, 2 H, CH_2 double bond), 5.06–5.17 (m, 40 H, OCH(CO)), 5.92–6.01 (m, 1 H, CH double bond), 6.11 (s, 40 H, NH).

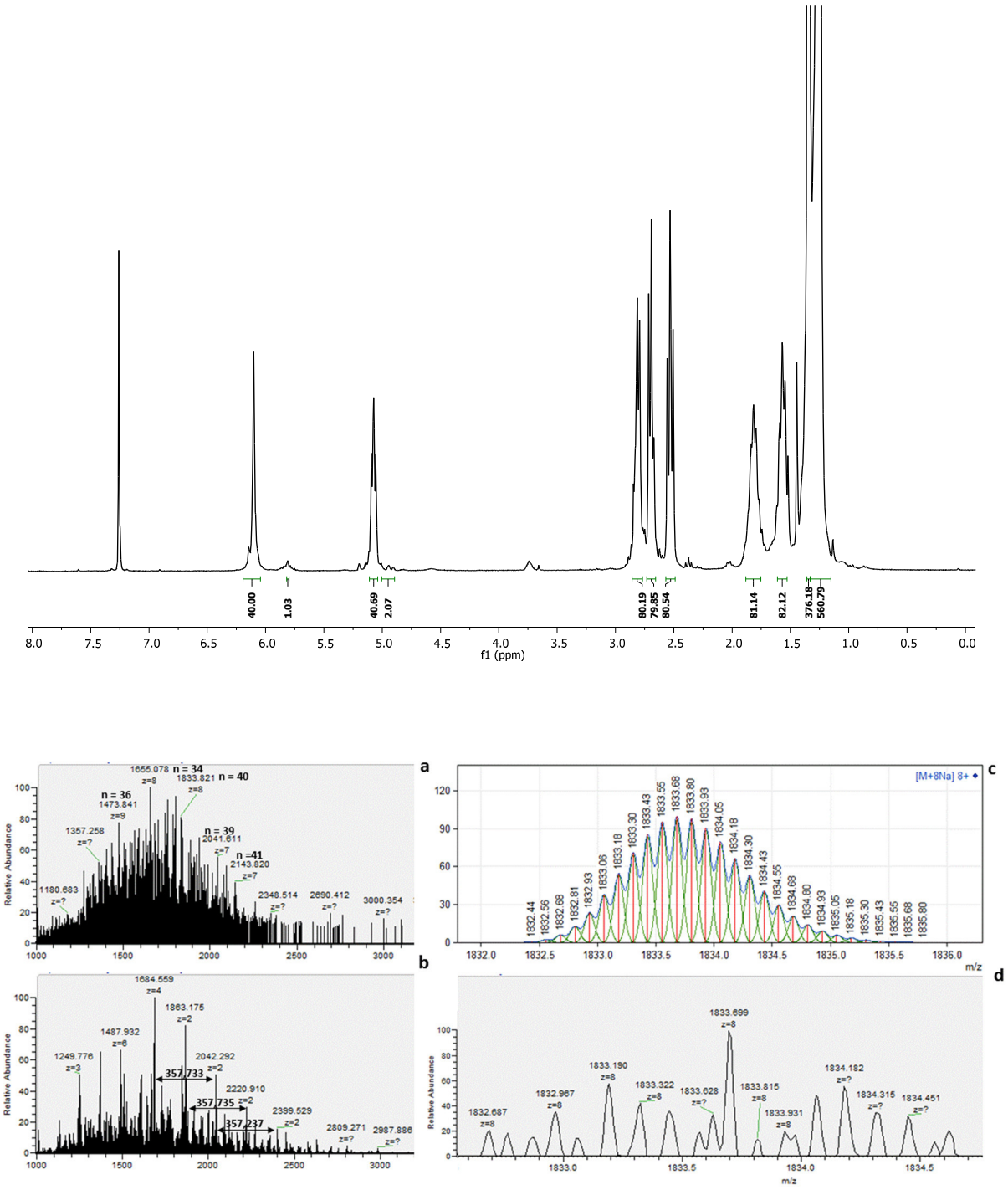

Figure 34: Mass spectra of homopolymer **P7** with n repeating units and a calculated mass of 357.234 g/mol per repeating unit (a = retention time of 12.37 min, b = retention time of 11.76-14.39 min, c = calculated isotope pattern, d = experimental isotope pattern at a retention time of 12.37 min).

Synthesis of copolymers P8 and P9 *via* Passerini reaction

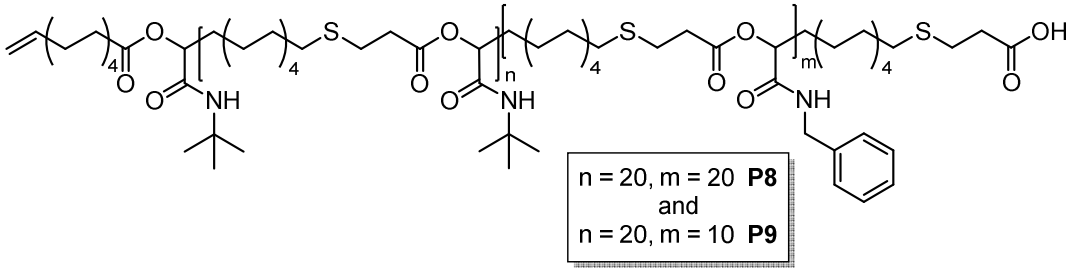

General procedure: To a vigorously stirred solution of homopolymer **P1** (100 mg, 0.0137 mmol) and benzyl isocyanide **8** (1.37 mmol, 0.685 mmol,) in 1.50 mL DCM, the AB-type monomer **3** (0.274 mmol, 0.137 mmol,) in 1.50 mol/L DCM was added slowly. After stirring for 24 hours at room temperature, the polymer was precipitated from diethyl ether.

Copolymer P8

Following the aforementioned procedure, **P8** was obtained as sticky brown solid (87 %). ^{1}H NMR ($CDCl_3$, 300 MHz): δ (ppm) = 1.14–1.29 (m, 560 H, 280 CH_2), 1.31–1.40 (m, 196 H, 180 *t*-Bu, 8 CH_2 end group), 1.50–1.64 (m, 80 H, 40 C*H*$_2$$CH_2$S), 1.75–1.93 (m, 80 H, 40 CHC*H*$_2$), 2.28–2.34 (m, 40 H, 20 CH_2S), 2.53 (t, *J* = 7.3 Hz, 40 H, 20 CH_2S), 2.63–2.65 (m, 80 H, 40 SCH_2), 2.77–2.89 (m, 80 H, 40 CH_2COO), 4.32–4.52 (m, 40 H, 20 NCH_2), 4.91–4.97 (m, 2 H, CH_2 double bond), 5.03–5.11 (m, 20 H, OCH(CO)) 5.16–5.36 (m, 20 H, OCH(CO)), 5.78–5.85 (m, 1 H, CH double bond), 6.10 (s, 20 H, NH), 6.95–7.07 (m, 20 H, NH), 7.11–7.23 (m, 40 H, 40 Ar-H), 7.29–7.41 (m, 60 H, 60 Ar-H); T_g = 5 °C.

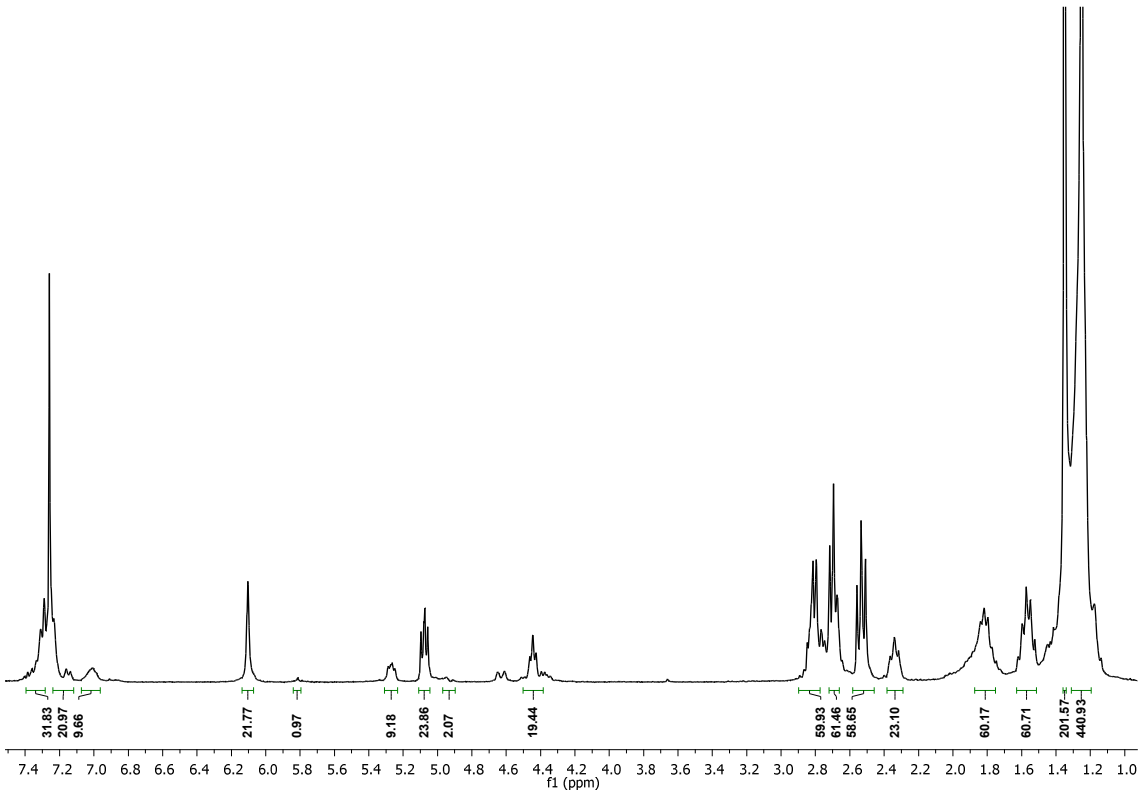

Copolymer P9

Following the aforementioned procedure, **P9** was obtained as sticky brown solid (88 %). ^{1}H NMR ($CDCl_3$, 300 MHz): δ (ppm) = 1.14–1.29 (m, 420 H, 210 CH_2), 1.31–1.40 (m, 196 H, 180 *t*-Bu, 8 CH_2 end group), 1.50–1.64 (m, 60 H, 30 C*H*$_2$$CH_2S$), 1.75–1.93 (m, 60 H, 30 CHC*H*$_2$), 2.28–2.34 (m, 20 H, 10 CH_2S), 2.53 (t, *J* = 7.3 Hz, 40 H, 20 CH_2S), 2.63–2.65 (m, 60 H, 30 SCH_2), 2.77–2.89 (m, 60 H, 30 CH_2COO), 4.32–4.52 (m, 20 H, 10 NCH_2), 4.91–4.97 (m, 2 H, CH_2 double bond), 5.03–5.11 (m, 20 H, OCH(CO)) 5.16–5.36 (m, 10 H, OCH(CO)), 5.78–5.85 (m, 1 H, CH double bond), 6.10 (s, 20 H, NH), 6.95–7.07 (m, 10 H, NH), 7.11–7.23 (m, 20 H, 20 Ar-H), 7.29–7.41 (m, 30 H, 30 Ar-H); T_g = 5 °C.

Synthesis of star-shaped homopolymer P10 *via* Passerini reaction

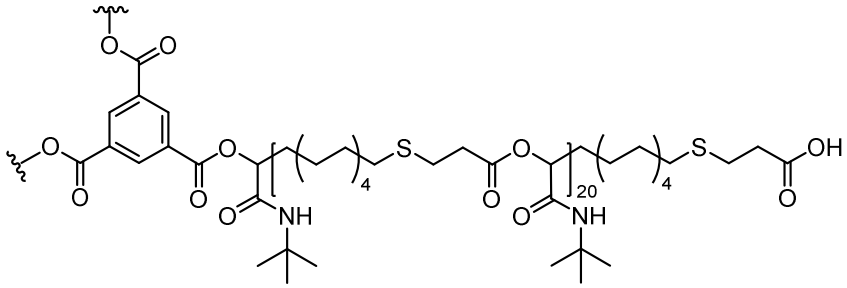

To a vigorously stirred solution of trimesic acid **9** (5.12 mg, 0.024 mmol) and *tert*-butyl isocyanide **5** (606 mg, 7.30 mmol) in 0.5 mL THF, the AB-type monomer **3** (400 mg, 1.46 mmol) in 0.5 mL DCM was added slowly. After stirring for 24 hours at room temperature, the polymer was precipitated from diethyl ether.

Following the aforementioned procedure, **P10** was obtained as white solid (93 %). ^{1}H NMR ($CDCl_3$, 300 MHz): δ (ppm) = 1.22–1.30 (m, 840 H, 420 CH_2), 1.32–1.36 (m, 540 H, *t*-Bu), 1.53–1.61 (m, 120 H, 60 C*H*$_2$CH$_2$S), 1.75–1.87 (m, 120 H, 60 CHC*H*$_2$), 2.53 (t, *J* = 7.5 Hz, 120 H, 60 CH_2S), 2.66–2.72 (m, 120 H, 60 SCH_2), 2.77–2.85 (m, 120 H, 60 CH_2COO), 5.04–5.11 (m, 60 H, OCH(CO)), 6.06–6.16 (m, 60 H, NH), 8.89–8.91 (m, 3 H, Ar-H); T_g = 6 °C.

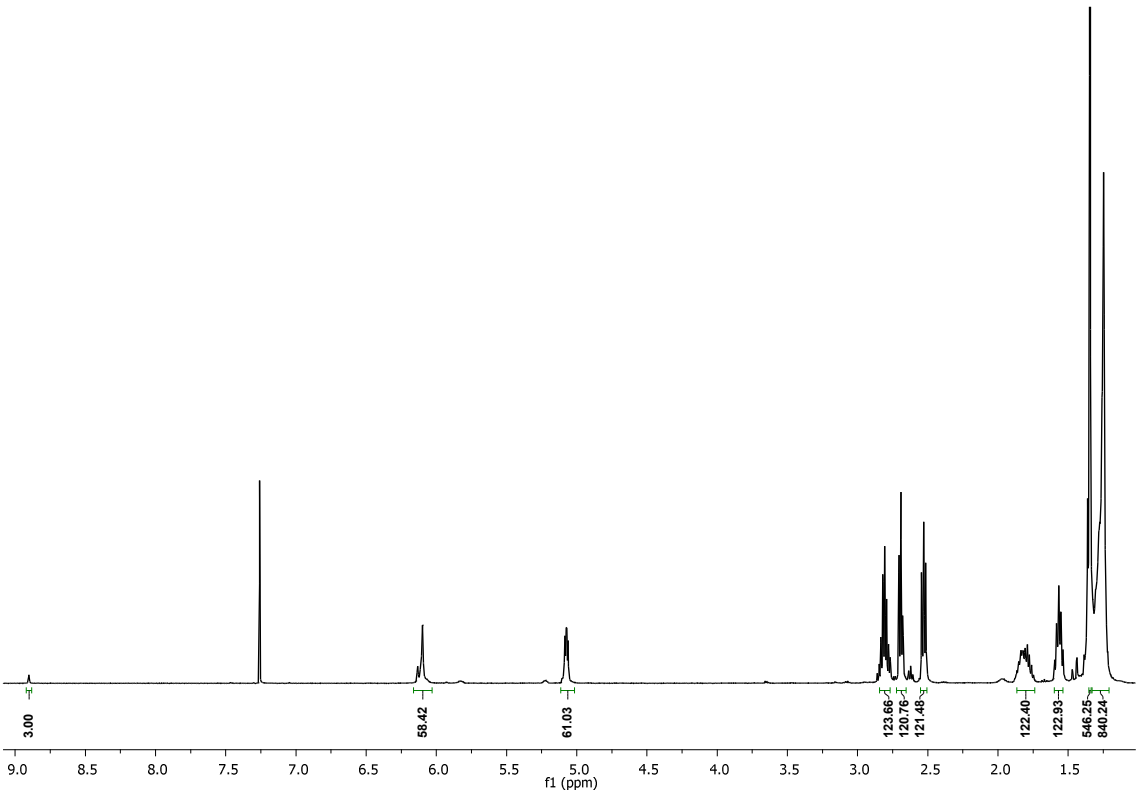

Synthesis of star-shaped copolymer P11 *via* Passerini reaction

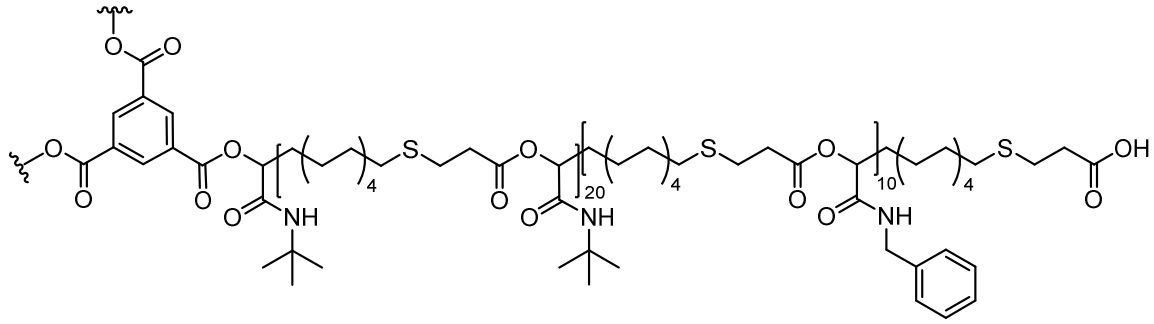

To a vigorously stirred solution of star-shaped homopolymer **P10** (100 mg, 0.0046 mmol) and benzyl isocyanide **8** (162 mg, 1.38 mmol) in 0.1 mL DCM, the AB-type monomer **3** (76 mg, 0.276 mmol) in 0.1 mL DCM was added slowly. After stirring for 24 hours at room temperature, the polymer was precipitated from diethyl ether.

Following the aforementioned procedure, **P11** was obtained as sticky brown solid (82 %). ^{1}H NMR ($CDCl_3$, 300 MHz): δ (ppm) = 1.06–1.28 (m, 1320 H, 660 CH_2), 1.32–1.39 (m, 540 H, *t*-Bu), 1.48–1.64 (m, 180 H, 90 C*H*$_2$$CH_2S$), 1.72–1.91 (m, 180 H, 90 CHC*H*$_2$), 2.26–2.35 (m, 60 H, 30 CH_2S), 2.52 (t, *J* = 7.4 Hz, 120 H, 60 CH_2S), 2.63–2.74 (m, 180 H, 60 SCH_2), 2.76–2.85 (m, 180 H, 60 CH_2COO), 4.31–4.50 (m, 60 H, 30 NCH_2), 5.01–5.09 (m, 60 H, OCH(CO)) 5.18–5.31 (m, 30 H, OCH(CO)), 6.11 (s, 60 H, NH), 6.98–7.09 (m, 30 H, NH), 7.17–7.25 (m, 60 H, 60 Ar-H), 7.27–7.35 (m, 90 H, 90 Ar-H), 8.87–8.92 (m, 3 H, Ar-H); T_g = 8 °C.

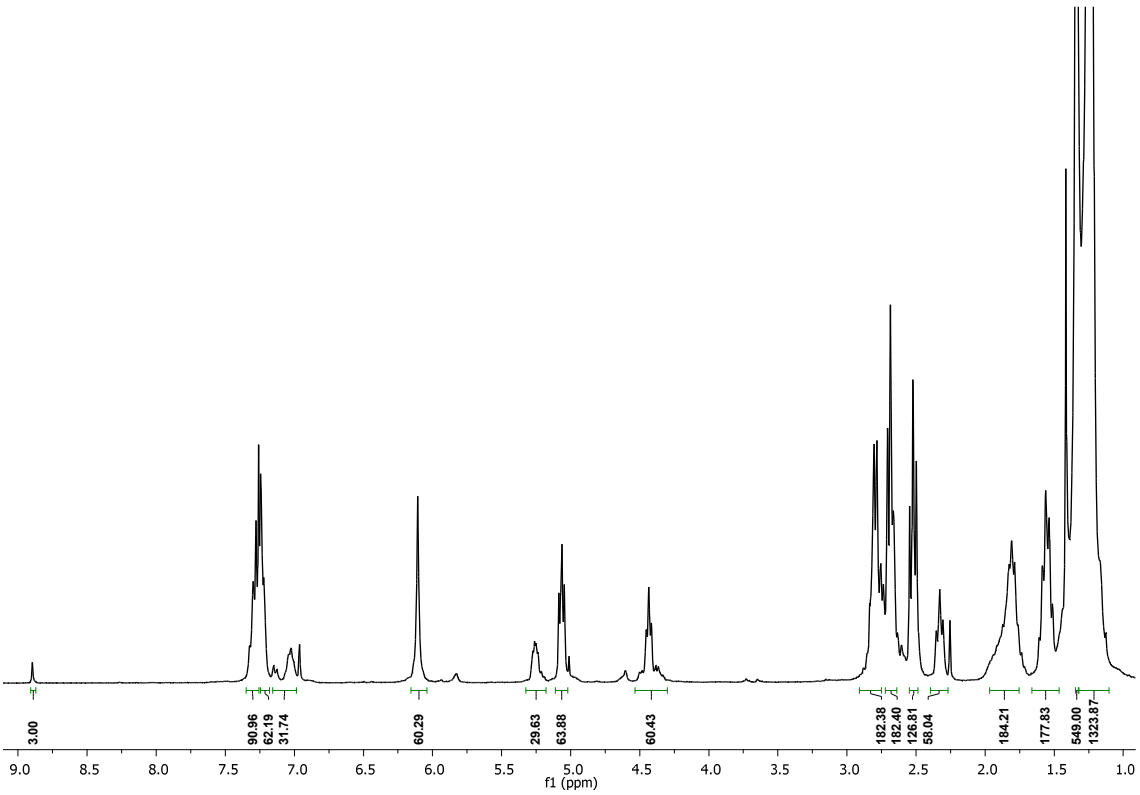

Esterification with CDI to obtain star-shaped homopolymer P12[173]

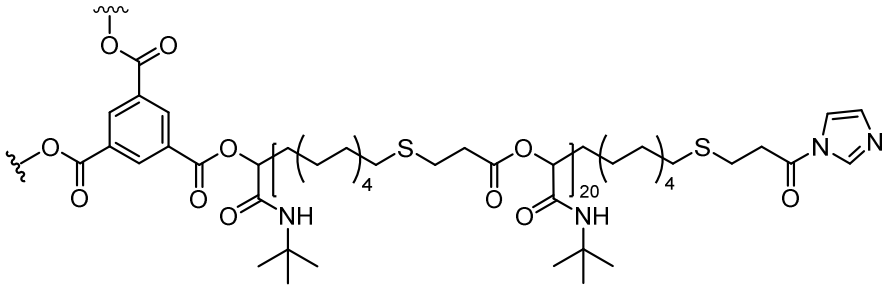

To a vigorously stirred solution of CDI **10** (32.4 mg, 0.20 mmol) in dry CH_2Cl_2 (0.60 mL), the star polymer **P10** (average MW 21.8 kDa) (200 mg, 0.01 mmol) in dry CH_2Cl_2 (0.90 mL) was added slowly under nitrogen. After stirring for 24 h at room temperature, the solution was precipitated in diethyl ether.

Following the aforementioned procedure, **P12** was obtained as white solid (90 %). ^{1}H NMR ($CDCl_3$, 300 MHz): δ (ppm) = 1.16–1.29 (m, 840 H, 420 CH_2), 1.31–1.36 (m, 540 H, *t*-Bu), 1.53–1.59 (m, 120 H, 60 C*H*$_2$CH$_2$S), 1.74–1.86 (m, 120 H, 60 CHC*H*$_2$), 2.52 (t, *J* = 7.4 Hz, 120 H, 60 CH_2S), 2.67–2.70 (m, 120 H, 60 SCH_2), 2.76–2.84 (m, 120 H, 60 CH_2COO), 5.03–5.10 (m, 60 H, OCH(CO)), 6.06–6.13 (m, 60 H, NH), 7.09–7.12 (m, 3 H, OCNCHC*H*), 7.46–7.49 (m, 3 H, OCNCH), 8.16–8.19 (m, 3 H, NCHN), 8.88–8.91 (m, 3 H, Ar-H); T_g = 6 °C.

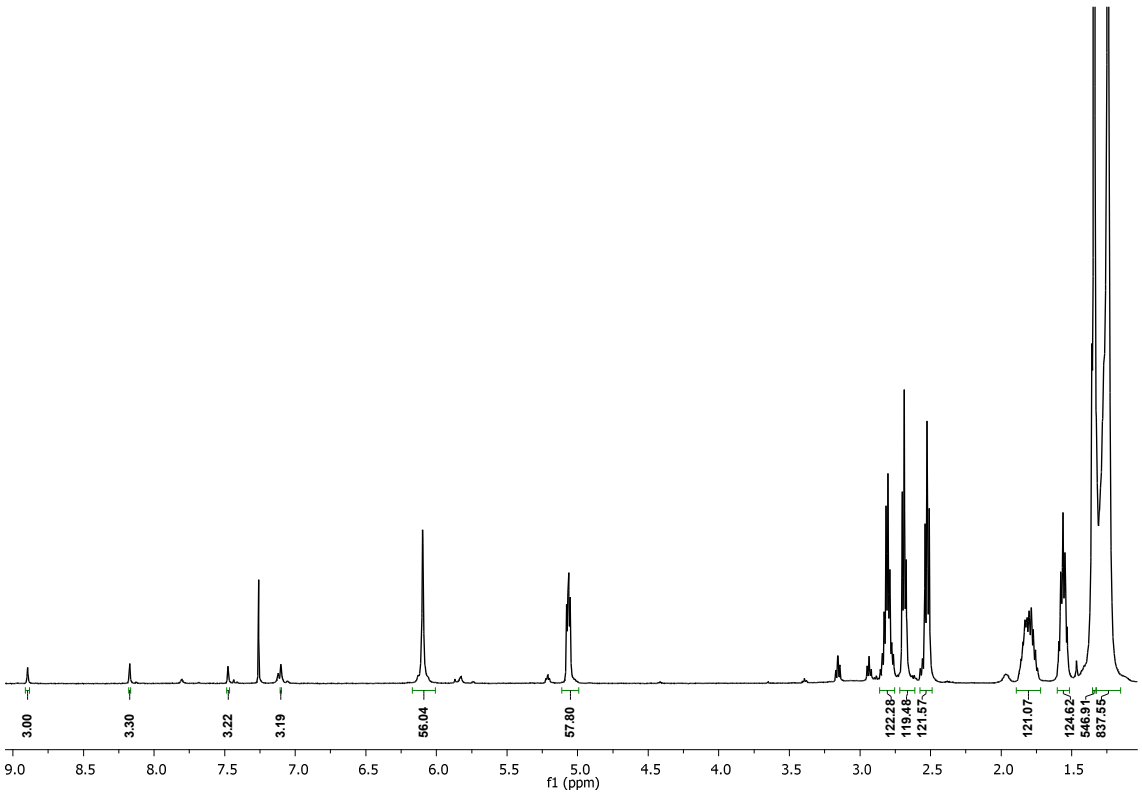
3.00
3.30
3.22
3.19
56.04
57.80
122.28
119.48
121.57
121.07
124.62
546.91
837.55
9.0
8.5
8.0
7.5
7.0
6.5
6.0
5.5
5.0
4.5
4.0
3.5
3.0
2.5
2.0
1.5
f1 (ppm)

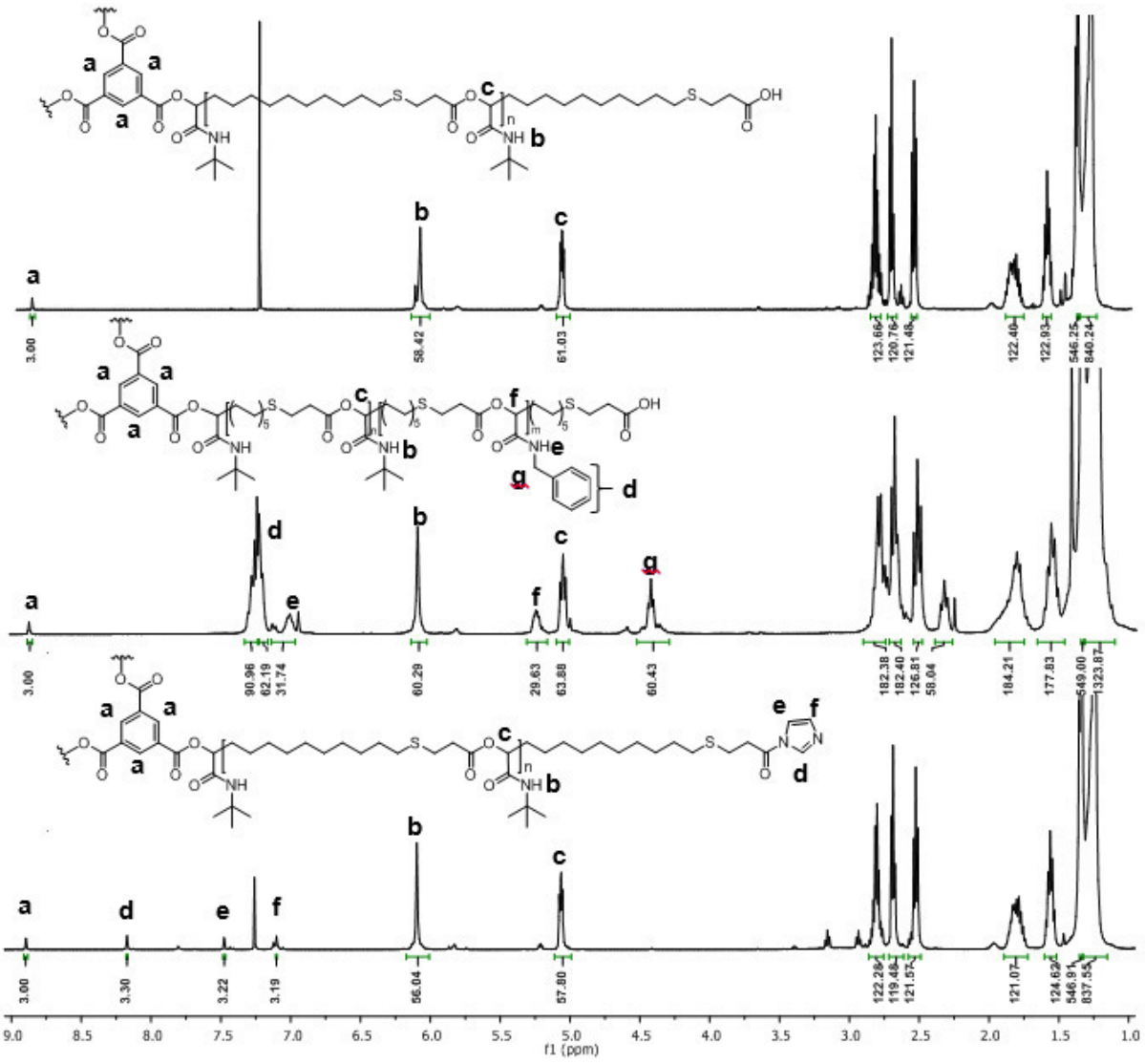

Figure 35: ^{1}H NMR spectra of star-shaped homopolymer **P10**, star-shaped copolymer **P11** and esterified star-shaped homopolymer **P12**.

6.4 Experimental procedures – chapter 4.2

Synthesis of star-shaped homopolymers P13 and P14 *via* Passerini reaction

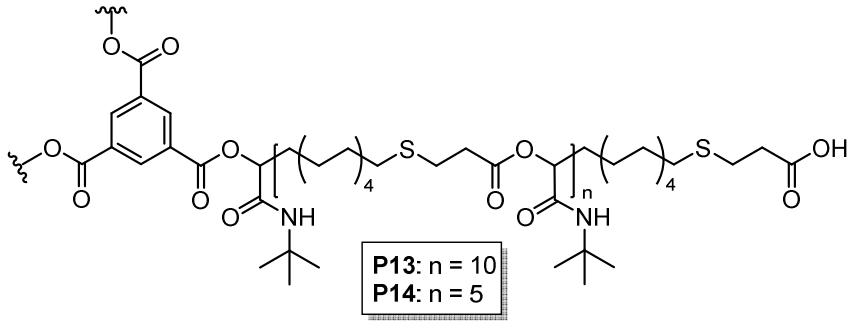

General procedure: To a vigorously stirred solution of trimesic acid **9** (1.00 equiv.) and *tert*-butyl isocyanide **5** (75.0 equiv., 150 equiv.) in 1.50 mol/L THF, AB-type monomer **3** (15.0 equiv., 30.0 equiv.) in 0.50 mL DCM was added slowly. After stirring for 24 hours at room temperature, the polymer was precipitated from ice-cold diethyl ether.

Homopolymer P13

Following the aforementioned procedure, **P13** was obtained as white solid (93 %). ^{1}H NMR ($CDCl_3$, 300 MHz): δ (ppm) = 1.22–1.30 (m, 420 H, 210 CH_2), 1.32–1.36 (m, 270 H, *t*-Bu), 1.53–1.61 (m, 60 H, 30 C*H*$_2$CH$_2$S), 1.75–1.87 (m, 60 H, 30 CHC*H*$_2$), 2.53 (t, *J* = 7.5 Hz, 60 H, 30 CH_2S), 2.66–2.72 (m, 60 H, 30 SCH_2), 2.77–2.85 (m, 60 H, 30 C*H*$_2$COO), 5.04–5.11 (m, 30 H, OCH(CO)), 6.06–6.16 (m, 30 H, NH), 8.89–8.91 (m, 3 H, Ar-H).

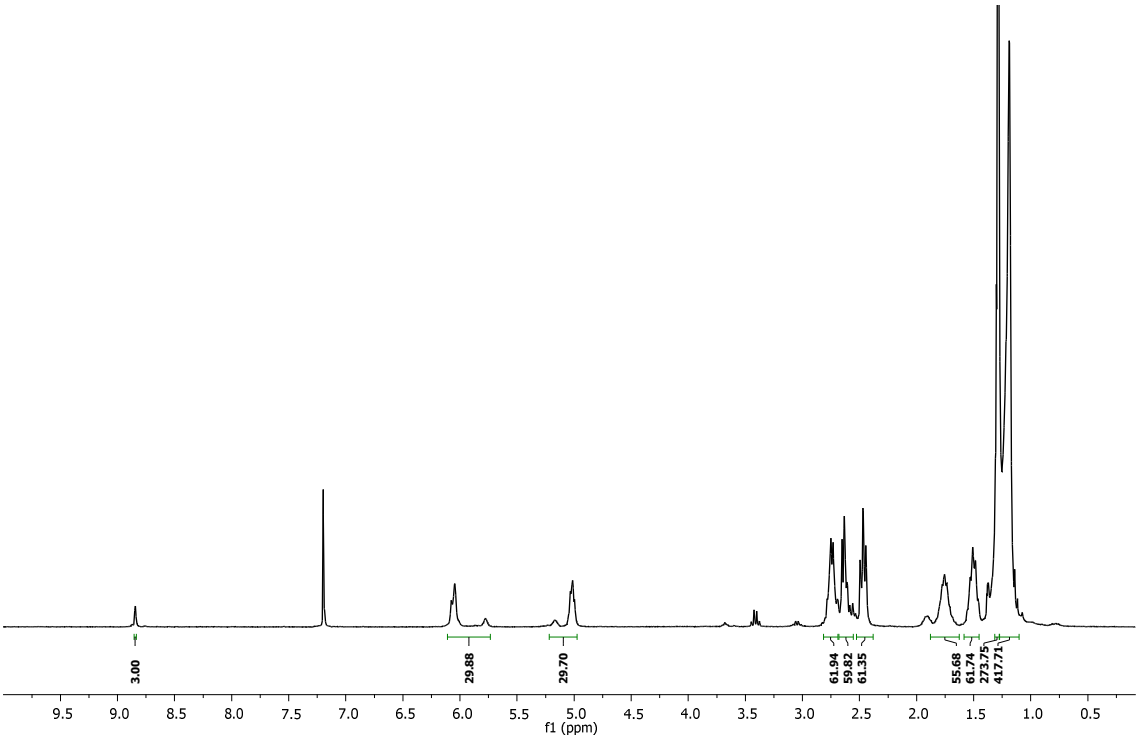

Homopolymer P14

Following the aforementioned procedure, **P14** was obtained as white solid (95 %). ^{1}H NMR ($CDCl_3$, 300 MHz): δ (ppm) = 1.20–1.33 (m, 210 H, 105 CH_2), 1.31–1.36 (m, 135 H, *t*-Bu), 1.55–1.64 (m, 30 H, 15 C*H*$_2$CH$_2$S), 1.71–1.83 (m, 30 H, 15 CHC*H*$_2$), 2.53 (t, *J* = 7.4 Hz, 30 H, 15 CH_2S), 2.65–2.72 (m, 30 H, 15 SCH_2), 2.77–2.86 (m, 30 H, 15 C*H*$_2$COO), 5.00–5.09 (m, 15 H, OCH(CO)), 6.05–6.16 (m, 15 H, NH), 8.88–8.91 (m, 3 H, Ar-H).

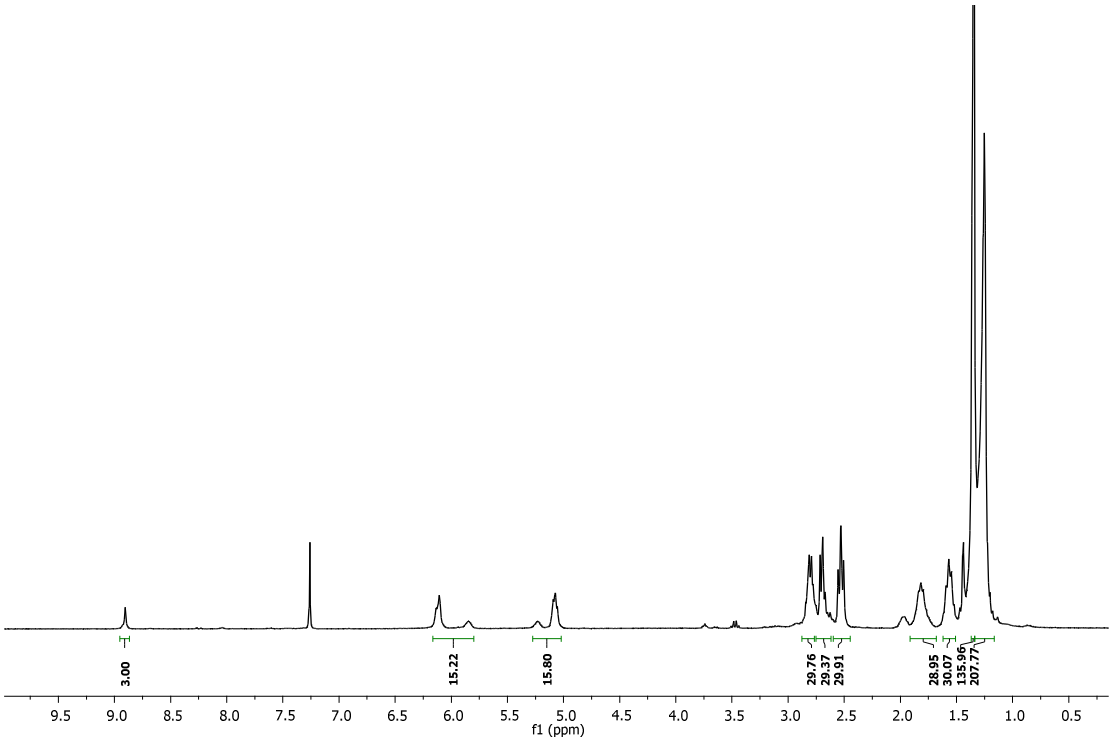

Synthesis of PEG isocyanide 21

11-Methoxy-11-oxoundecan-1-aminium chloride 15

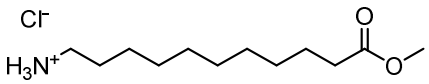

10.0 g 11-aminoundecanoic acid **13** (50.0 mmol, 1.00 equiv.) were suspended in 75.0 mL methanol **14** (1.875 mol, 37.5 equiv.), which works as solvent and reactant. The suspension was cooled in an ice bath and subsequently 11.2 mL thionyl chloride (18.4 g, 0.155 mol, 3.10 equiv.) were added dropwise at 0 °C. After addition of thionyl chloride, the solution was warmed to room temperature and stirred overnight. The yellow solution was then poured into 350 mL diethyl ether and stored in the freezer overnight. The product was filtered off and dried under high vacuum. 11-(Methoxy)-11-oxoundecan-1-aminium chloride **15** was obtained as a white solid (10.0 g, 80 %). ^{1}H NMR (CD_3OD, 300 MHz) δ (ppm) = 1.21–1.45 (m, 12 H, 6 CH_2), 1.47–1.71 (m, 4 H, 2 CH_2), 2.30 (t, J = 7.4 Hz, 2 H, CH_2), 2.90 (t, J = 7.5 Hz, 2 H, CH_2), 3.56–3.63 (m, 3 H, CH_3); ^{13}C NMR (CD_3OD, 75 MHz) δ (ppm): 26.0, 27.4, 28.5, 30.1, 30.2, 30.3, 30.4, 30.4, 34.8, 40.8, 52.0, 176.0; FAB of $[C_{12}H_{26}NO_2]^+$ = 216.2; HRMS (FAB) of $[C_{12}H_{26}NO_2]^+$ calc. 216.1958, found 216.1956; IR (KBr) ν = 2918.6, 2848.1, 1722.4,

1561.0, 1510.4, 1467.9, 1443.6, 1375.6, 1334.0, 1306.1, 1276.8, 1245.0, 1210.6, 1174.5, 1097.3, 1001.1, 970.7, 938.2, 885.7, 723.3, 425.6 cm^{-1}.

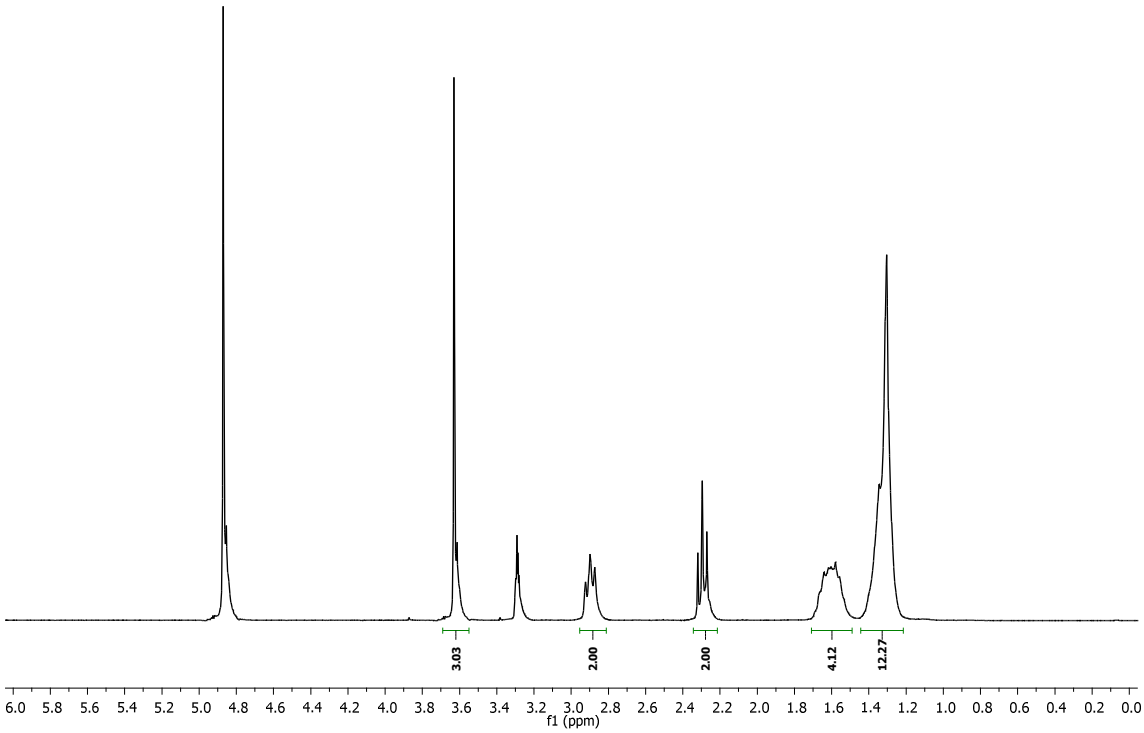

Methyl 11-formamidoundecanoate 17

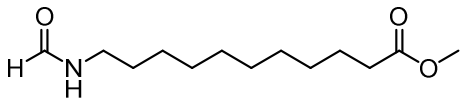

9.80 g 11-(methoxy)-11-oxoundecan-1-aminium chloride **15** (0.039 mol, 1.00 equiv.), were dissolved in 43.0 mL trimethyl orthoformate **16** (41.4 g, 0.39 mol, 10.0 eq.), which is used as solvent and reactant and heated to 100 °C for 12 hours. Trimethyl orthoformate was removed under reduced pressure and the product was used without further purification. Methyl 11-formamidoundecanoate **17** was obtained as a white solid (9.55 g, quant.). ^{1}H NMR ($CDCl_3$, 300 MHz) δ (ppm) = 1.16–1.40 (m, 12 H, 6 CH_2), 1.42–1.70 (m, 4 H, 2 CH_2), 2.28 (t, J = 7.5 Hz, 2 H, CH_2), 3.16–3.35 (m, 2 H, CH_2), 3.66 (s, 3 H, CH_3), 5.71 (s, 1 H, NH), 8.01–8.28 (m, 1 H, OCH); ^{13}C NMR ($CDCl_3$, 75 MHz) δ (ppm): 25.0, 26.5, 26.9, 29.2, 29.3, 29.4, 29.5, 29.6, 34.2, 38.3, 51.6, 161.3, 174.5; FAB of $[C_{13}H_{26}NO_3]^+$ = 244.2; HRMS (FAB) of $[C_{13}H_{26}NO_3]^+$ calc. 244.1907, found 244.1906; IR (KBr) ν = 3255.9, 2914.8, 2848.0, 1734.9, 1682.5, 1637.3, 1534.4,

1462.8, 1435.5, 1378.3, 1334.1, 1300.6, 1268.2, 1226.0, 1203.7, 1168.0, 1113.0, 1070.0, 1002.0, 980.5, 883.3, 720.7, 518.7, 449.4, 380.1 cm^{-1}.

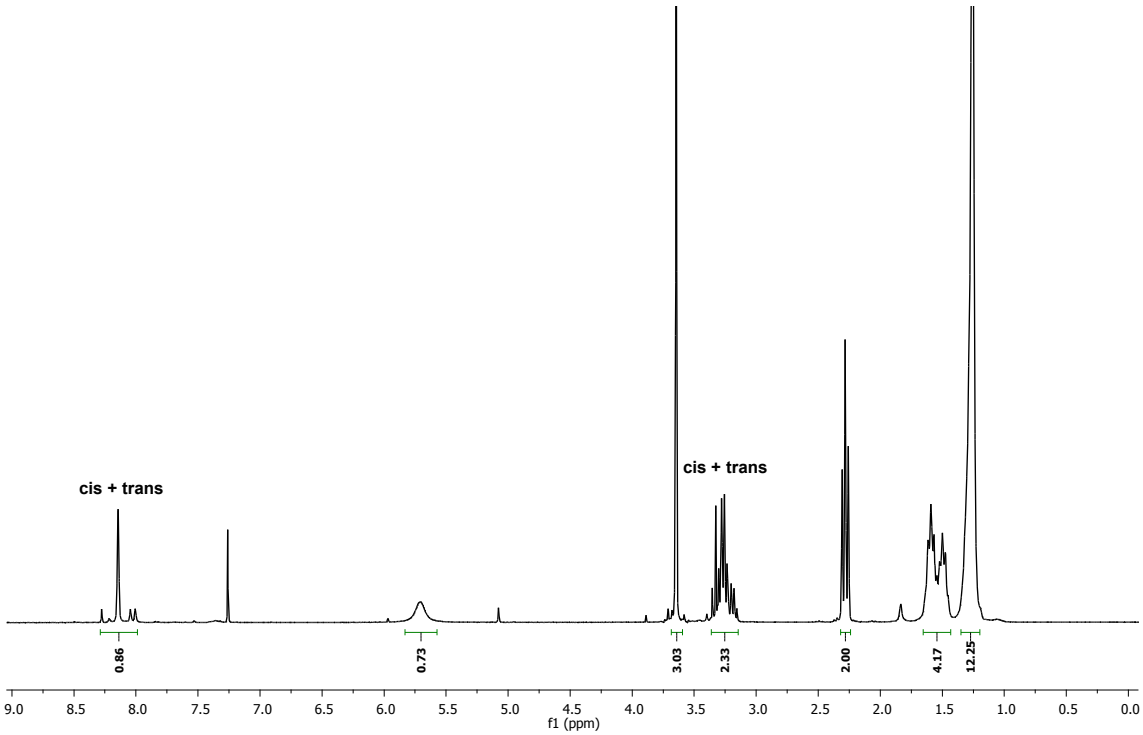

Methyl 11-isocyanoundecanoate 19

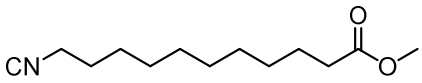

9.55 g methyl 11-formamidoundecanoate **17** (0.039 mol, 1.00 equiv.) were dissolved in 120 mL dichloromethane (0.33 M), 17.2 mL diisopropylamine **18** (12.4 g, 0.122 mol, 3.10 equiv.) were added and the reaction mixture was cooled to 0 °C. Subsequently, 4.77 mL phosphorous oxy chloride (7.82 g, 0.051 mmol, 1.30 equiv.) were added dropwise and the reaction mixture was stirred at room temperature for two hours. The reaction was quenched by adding sodium carbonate solution (20 %, 75.0 mL) at 0 °C. After stirring this mixture for 30 minutes, 50.0 mL water and 50.0 mL dichloromethane were added. The aqueous phase was separated and the organic layer was washed with brine (4 x 80.0 mL). The combined organic layers were dried over sodium sulfate and the solvent was evaporated under reduced pressure. The crude product was then purified by column chromatography (*n*-hexane / ethyl acetate 19:1 – 8:1). Methyl 11-isocyanoundecanoate **19** was obtained as slightly yellow oil (4.30 g, 52 %). R_f = 0.49 (*n*-hexane/ethyl acetate = 5:1); ^{1}H NMR ($CDCl_3$, 300 MHz) δ (ppm) = 1.18–1.50 (m, 12

H, 6 CH_2), 1.52–1.75 (m, 4 H, 2 CH_2), 2.29 (t, J = 7.5 Hz, 2 H, CH_2), 3.30–3.43 (m, 2 H, CH_2), 3.66 (s, 3 H, CH_3); ^{13}C NMR ($CDCl_3$, 75 MHz) δ (ppm): 24.9, 26.3, 28.6, 29.1, 29.1, 29.2, 34.0, 41.4, 41.5, 41.5, 51.4, 155.7, 174.2; FAB of $[C_{13}H_{22}NO_2]^-$ = 224.2; HRMS (FAB) of $[C_{13}H_{22}NO_2]^-$ calc. 224.1645, found 224.1644; IR (KBr) ν = 2925.0, 2854.2, 2146.0 (isocyanide), 1735.0, 1435.6, 1352.7, 1194.4, 1169.1, 1103.9, 1010.8, 850.2, 722.1 cm^{-1}.

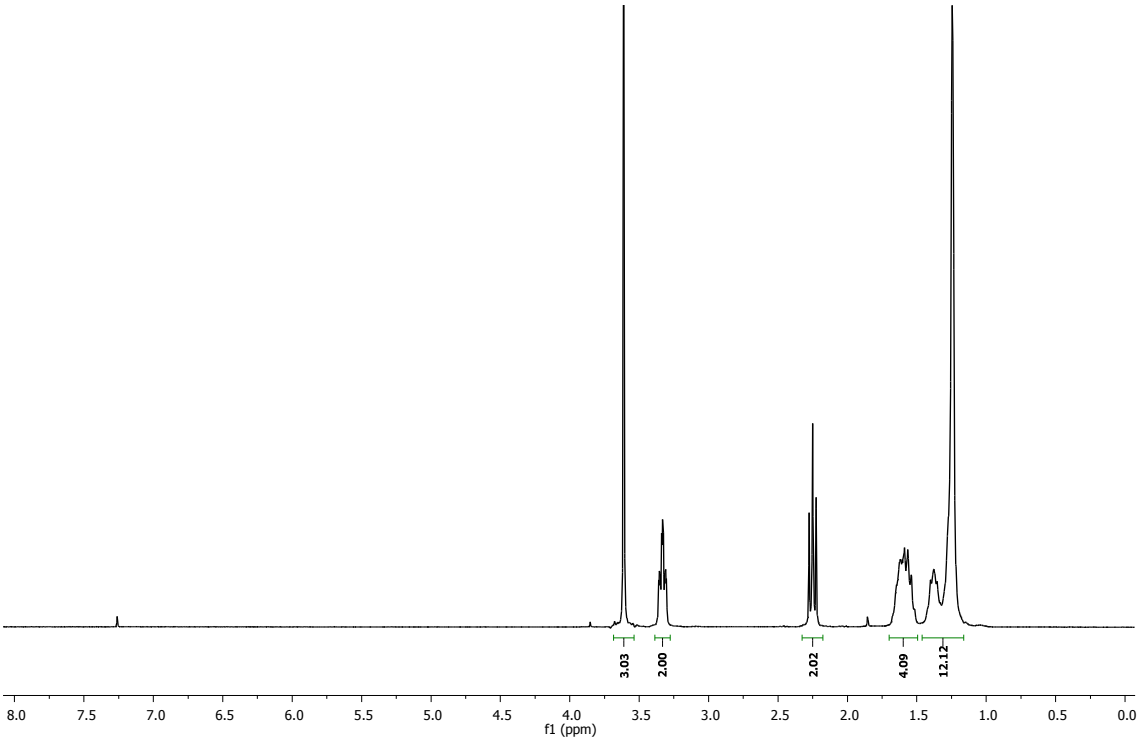

PEG isocyanide 21

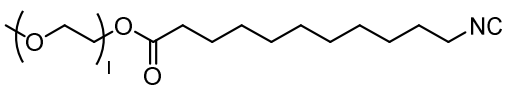

3.00 g poly(ethylene glycol) methyl ether **20** (4.00 mmol, 1.00 equiv., 750 g/mol) and 4.50 g methyl 11-isocyanoundecanoate **21** (20.0 mmol, 5.00 equiv.) were placed and 28.0 mg TBD (0.20 mmol, 5.00 mol%) were added and the reaction mixture was distilled at 100 °C for 3 days (a continuous air flow was bubbled through the solution to remove the resulting methanol from the reaction mixture). Afterwards, the polymer was precipitated from ice-cold diethyl ether to obtain a yellow solid (1.85 g, 50 %). ^1H NMR ($CDCl_3$, 300 MHz) δ (ppm) = 1.19–1.47 (m, 12 H, 6 CH_2), 1.49–1.71 (m, 4 H, 2 CH_2), 2.29 (t, J = 7,5 Hz, 2 H, CH_2), 3.27–3.41 (m, 5 H, CH_2, CH_3), 3.49–3.67 (m, 66 H, 33 PEG-CH_2), 4.18 (t, J = 4,8 Hz, 2 H, $OCOCH_2$).

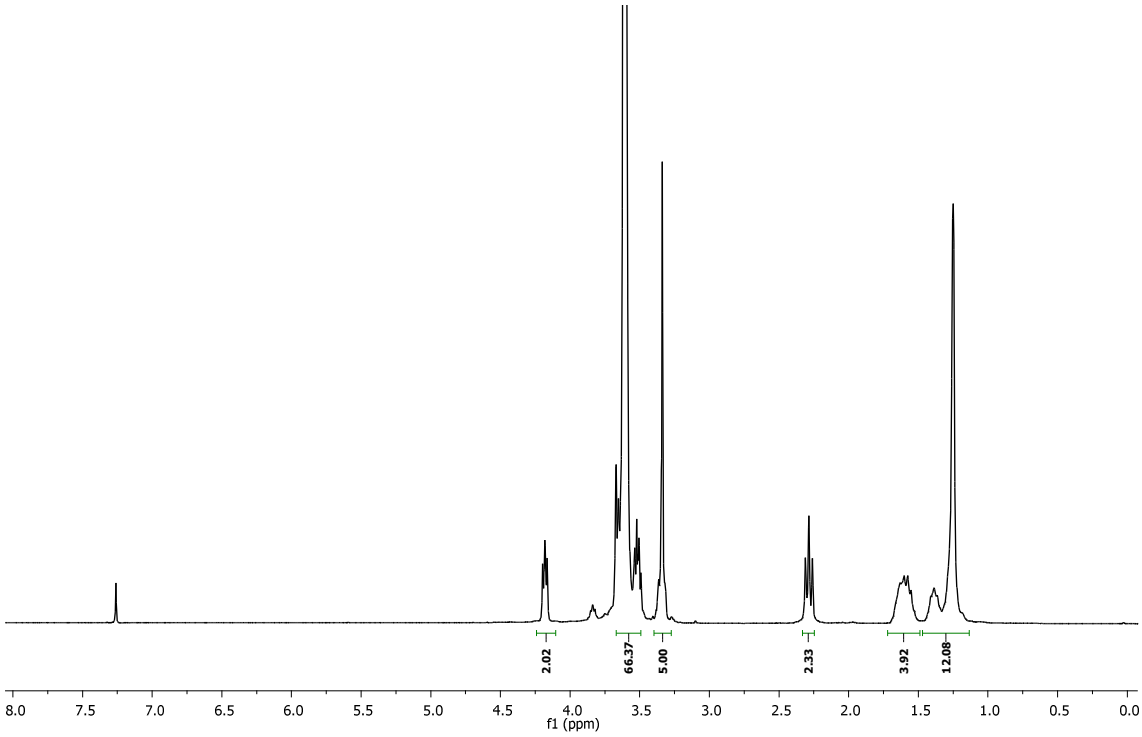

Synthesis of PEG aldehyde 23

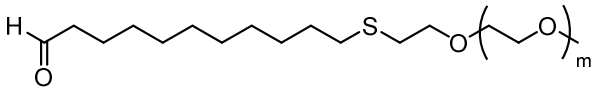

316 mg 10-undecenal **1** (1.875 mmol, 2.00 equiv.) and 12.0 mg DMPA (0.047 mmol, 5.00 mol%) were placed in a quartz tube and dissolved in 0.50 mL THF. Then, the tube was purged with argon for 10 min and afterwards the solution was exposed to UV light (365 nm) for 30 s. Subsequently, 750 mg PEG thiol **22** (0.9375 mmol, 1.00 equiv., 800 g/mol) dissolved in 0.40 mL THF were added. The reaction mixture was stirred for 24 h under UV irradiation. Afterwards, the product was precipitated from ice-cold diethyl ether to obtain a white solid (610 mg, 70 %). ^{1}H NMR ($CDCl_3$, 300 MHz) δ (ppm) = 1.17–1.41 (m, 12 H, 6 CH_2), 1.47–1.68 (m, 4 H, 2 CH_2), 2.34–2.46 (m, 2 H, CH_2), 2.47–2.58 (m, 2 H, CH_2), 2.63–2.78 (m, 2 H, CH_2), 3.37 (s, 3 H, CH_3), 3.48–3.57 (m, 2 H, CH_2), 3.58–3.71 (m, 60 H, 30 PEG-CH_2), 9.75 (s, 1 H, OCH).

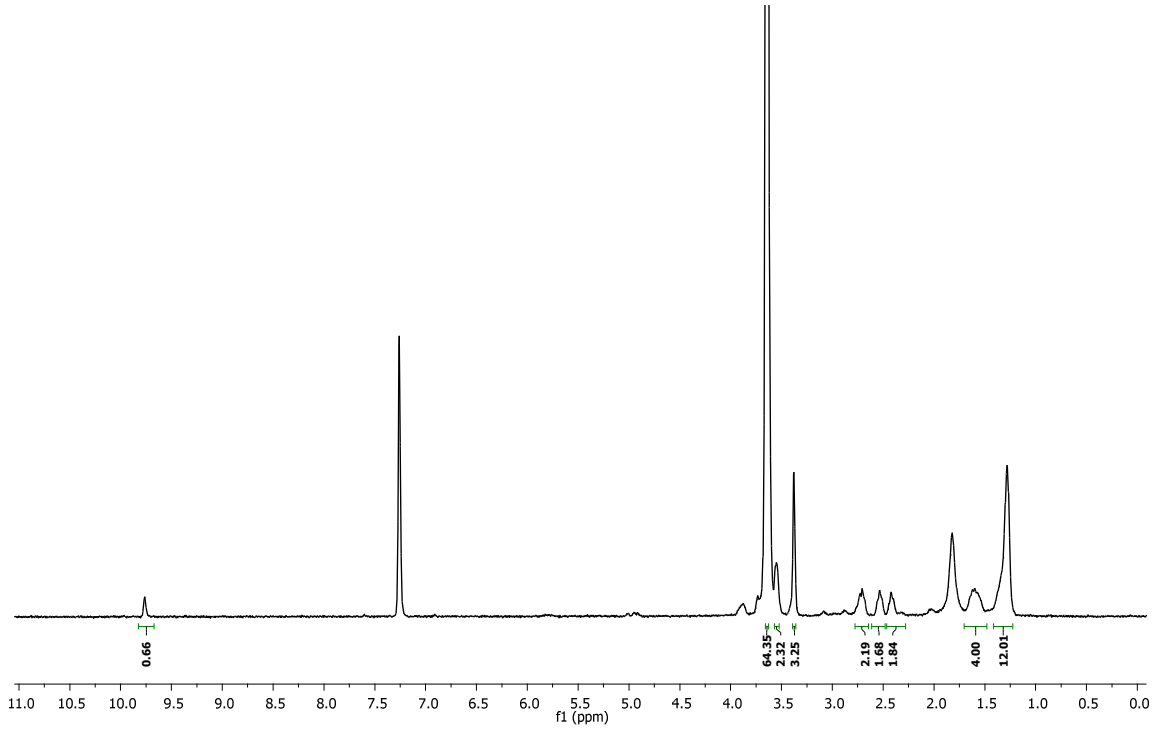

Synthesis of functionalized star-shaped polymers

Star-shaped polymer P15, P16 and P17 (10 repeating units, 1 PEG 2000 g/mol) using different isocyanides

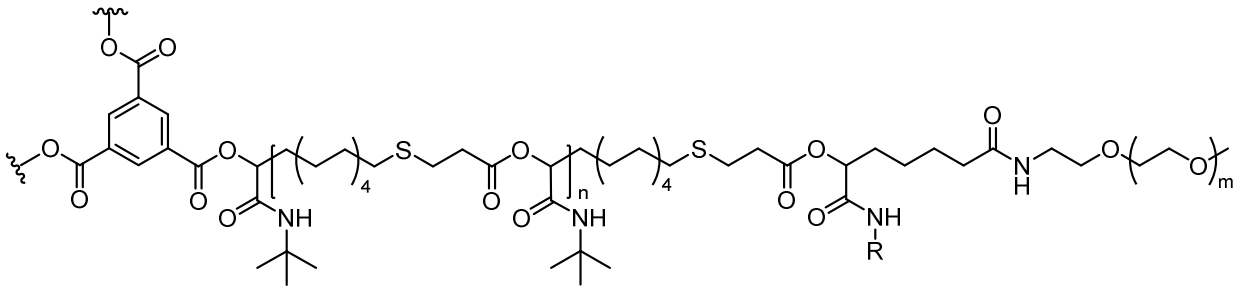

P15: n = 10 and R = *tert*-butyl
P16: n = 10 and R = benzyl
P17: n = 10 and R =

General procedure: To a vigorously stirred solution of star-shaped polymer **P13** (1.00 equiv.) and PEG aldehyde (2000 g/mol) **12** (3.00 equiv.) in 0.05 mol/L DCM, *tert*-butyl isocyanide **5**, benzyl isocyanide **8** or *tert*-butyl 2-isocyanoacetate **11** (15.0 equiv.) were added slowly. After stirring for 72 hours at room temperature, the polymer was precipitated from diethyl ether.

Following the aforementioned procedure, **P15** was obtained as white solid (94 %). ^{1}H NMR ($CDCl_3$, 300 MHz): δ (ppm) = 1.12–1.31 (m, 420 H, 210 CH_2), 1.32–1.41 (m, 297 H, *t*-Bu), 1.46–1.66 (m, 72 H, 30 C*H*$_2$CH$_2$S, 3 C*H*$_2$CH$_2$CONH, 3 C*H*$_2$CH$_2$CHO), 1.72–1.90 (m, 60 H, 30 CHC*H*$_2$), 1.93–2.01 (m, 6 H, 3 C*H*$_2$CONH), 2.13–2.21 (m, 6 H, 3 C*H*$_2$COO), 2.53 (t, *J* = 7.4 Hz, 60 H, 30 CH_2S), 2.65–2.75 (m, 60 H, 30 SCH$_2$), 2.77–2.86 (m, 60 H, 30 C*H*$_2$COO), 3.36 (s, 3 H, CH_3), 3.46–3.50 (m, 12 H, 3 OC*H*$_2$, 3 NHC*H*$_2$), 3.59–3.69 (m, 492 H, 246 PEG-CH_2), 5.03–5.25 (m, 33 H, OCH(CO)), 5.81–6.10 (m, 33 H, NH), 8.88–8.92 (m, 3 H, Ar-H).

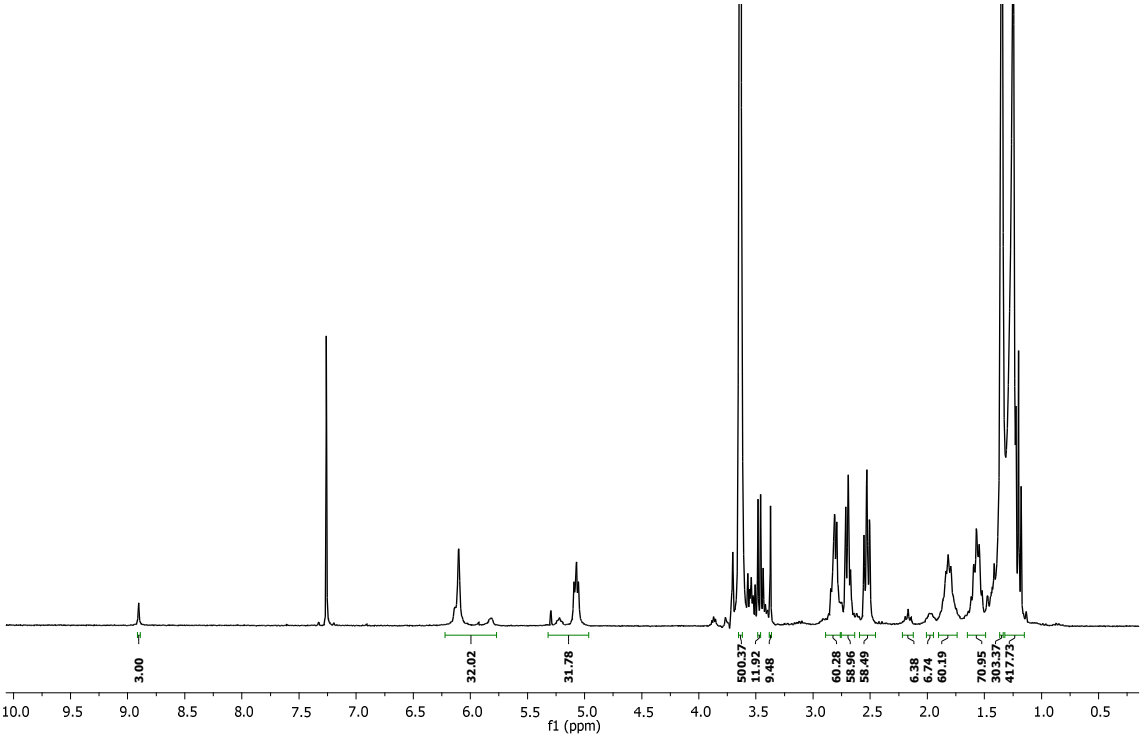

Following the aforementioned procedure, **P16** was obtained as yellow solid (89 %). ^{1}H NMR ($CDCl_3$, 300 MHz): δ (ppm) = 1.17–1.30 (m, 420 H, 210 CH_2), 1.31–1.36 (m, 270 H, *t*-Bu), 1.47–1.67 (m, 72 H, 30 C*H*$_2$CH$_2$S, 3 C*H*$_2$CH$_2$CONH, 3 C*H*$_2$CH$_2$CHO), 1.68–1.90 (m, 60 H, 30 CHC*H*$_2$), 1.92–2.01 (m, 6 H, 3 C*H*$_2$CONH), 2.10–2.23 (m, 6 H, 3 C*H*$_2$COO), 2.53 (t, *J* = 7.4 Hz, 60 H, 30 CH_2S), 2.65–2.75 (m, 60 H, 30 SCH$_2$), 2.76–2.88 (m, 60 H, 30 C*H*$_2$COO), 3.37 (s, 3 H, CH_3), 3.45–3.49 (m, 12 H, 3 OC*H*$_2$, 3 NHC*H*$_2$), 3.58–2.68 (m, 492 H, 246 PEG-CH_2), 5.03–5.26 (m, 33 H, OCH(CO)), 5.80–6.13 (m, 33 H, NH), 7.21–7.43 (m, 15 H, Ar$_{benzyl}$-H), 8.88–8.92 (m, 3 H, Ar-H).

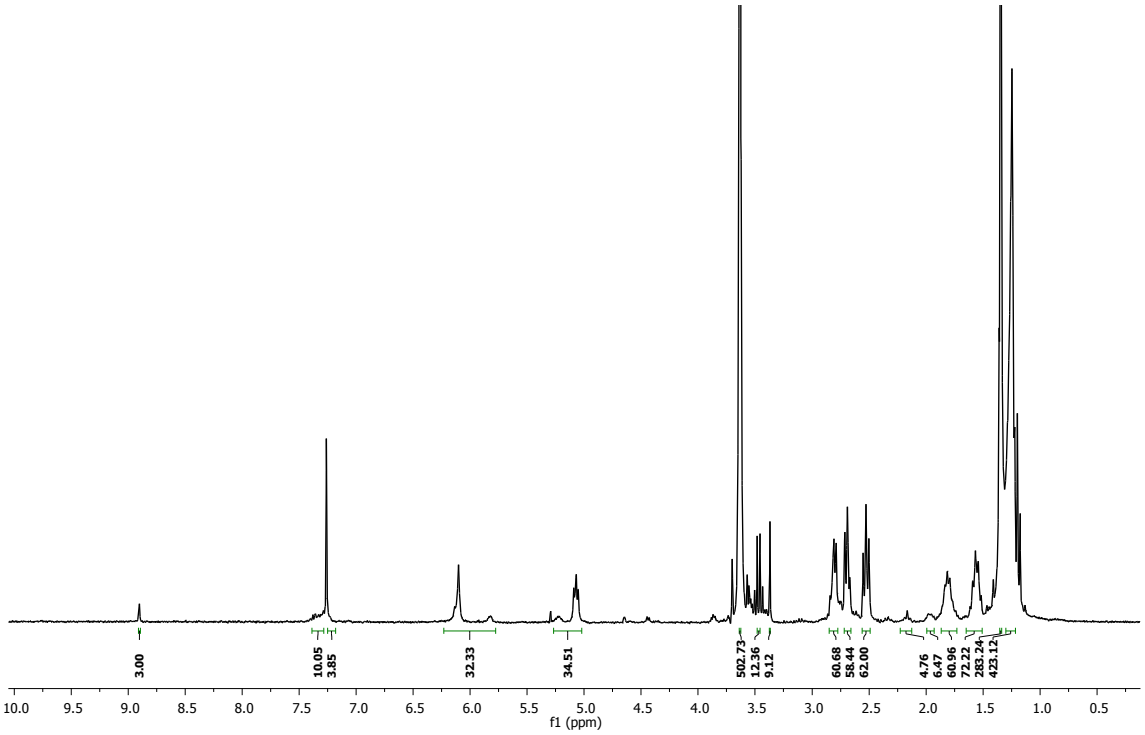

Following the aforementioned procedure, **P17** was obtained as yellow solid (91 %). ^{1}H NMR ($CDCl_3$, 300 MHz): δ (ppm) = 1.17–1.31 (m, 420 H, 210 CH_2), 1.32–1.37 (m, 297 H, *t*-Bu), 1.53–1.64 (m, 72 H, 30 C*H*$_2$CH$_2$S, 3 C*H*$_2$CH$_2$CONH, 3 C*H*$_2$CH$_2$CHO), 1.74–1.90 (m, 60 H, 30 CHC*H*$_2$), 1.92–2.04 (m, 12 H, 3 C*H*$_2$CONH, 3 NHC*H*$_2$CO), 2.14–2.22 (m, 6 H, 3 C*H*$_2$COO), 2.54 (t, *J* = 7.4 Hz, 60 H, 30 CH_2S), 2.66–2.74 (m, 60 H, 30 SCH_2), 2.78–2.87 (m, 60 H, 30 C*H*$_2$COO), 3.38 (s, 3 H, CH_3), 3.45–3.51 (m, 12 H, 3 OC*H*$_2$, 3 NHC*H*$_2$), 3.56–3.73 (m, 492 H, 246 PEG-CH_2), 5.04–5.23 (m, 33 H, OCH(CO)), 5.82–6.14 (m, 33 H, NH), 8.89–8.92 (m, 3 H, Ar-H).

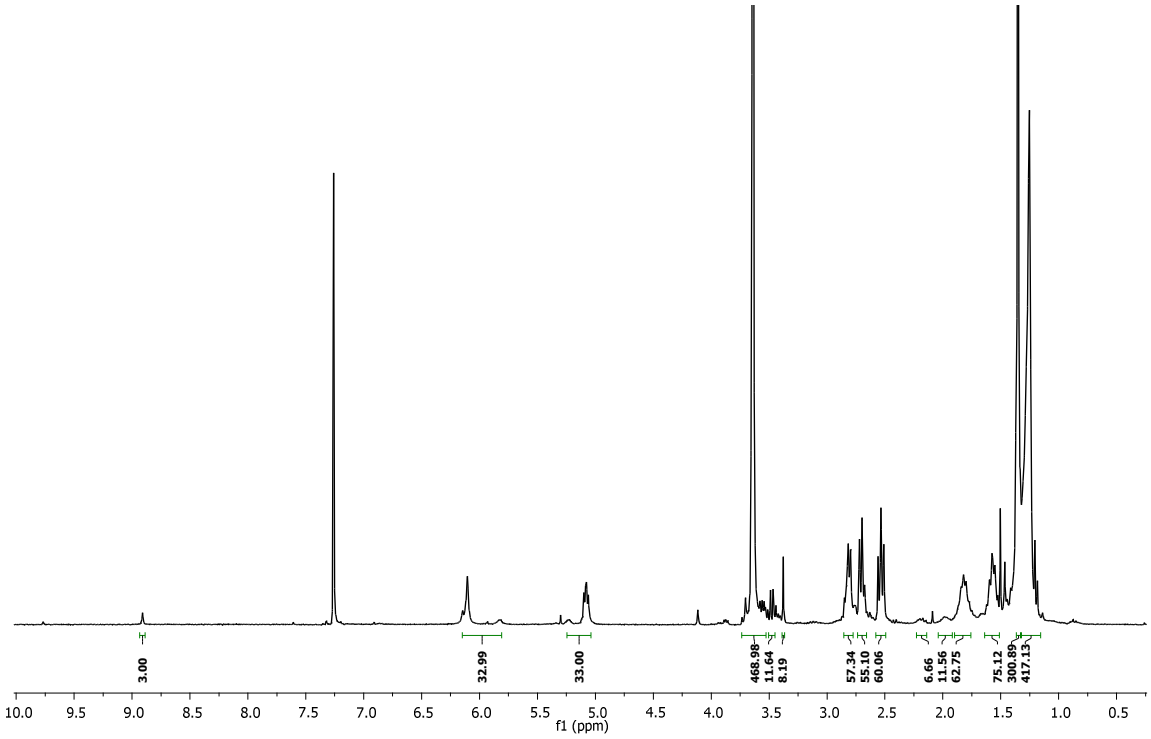

Star-shaped polymer P18 (5 repeating units, 1 PEG 2000 g/mol)

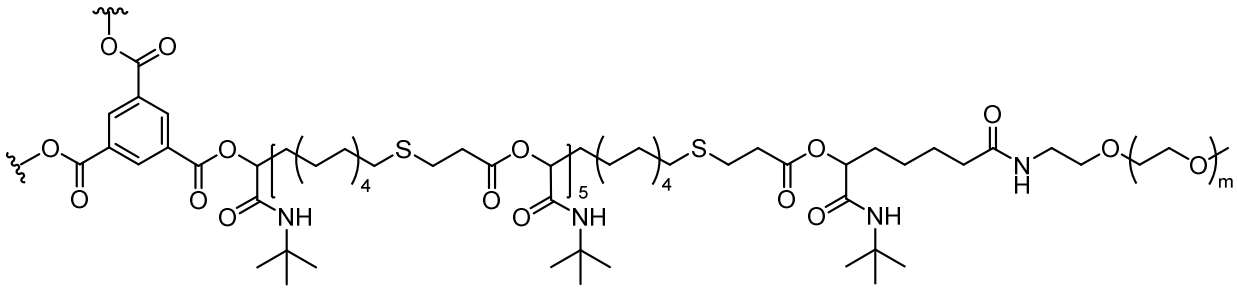

General procedure: To a vigorously stirred solution of star-shaped polymer **P14** (1.00 equiv.) and PEG aldehyde (2000 g/mol) **12** (3.00 equiv.) in 0.05 mol/l DCM, *tert*-butyl isocyanide **5** (15.0 equiv.) was added slowly. After stirring for 72 hours at room temperature, the polymer was precipitated from diethyl ether.

Following the aforementioned procedure, **P14** was obtained as white solid (85 %). ^{1}H NMR ($CDCl_3$, 300 MHz): δ (ppm) = 1.17–1.31 (m, 210 H, 105 CH_2), 1.32–1.41 (m, 162 H, *t*-Bu), 1.49–1.66 (m, 42 H, 15 C$H_2$$CH_2$S, 3 C$H_2$$CH_2$CONH, 3 C$H_2$$CH_2$CHO), 1.72–1.88 (m, 30 H, 15 CHCH_2), 1.93–2.00 (m, 6 H, 3 CH_2CONH), 2.12–2.21 (m, 6 H, 3 CH_2COO), 2.52 (t, *J* = 7.4 Hz, 30 H, 15 CH_2S), 2.63–2.74 (m, 30 H, 15 SCH_2), 2.76–2.85 (m, 30 H, 15 CH_2COO), 3.37 (s, 3 H, CH_3), 3.50–3.56 (m, 12 H, 3 OCH_2, 3

NHC*H*$_2$), 3.58–3.68 (m, 492 H, 246 PEG-CH_2), 5.02–5.23 (m, 18 H, OCH(CO)), 5.78–6.13 (m, 18 H, NH), 8.87–8.92 (m, 3 H, Ar-H).

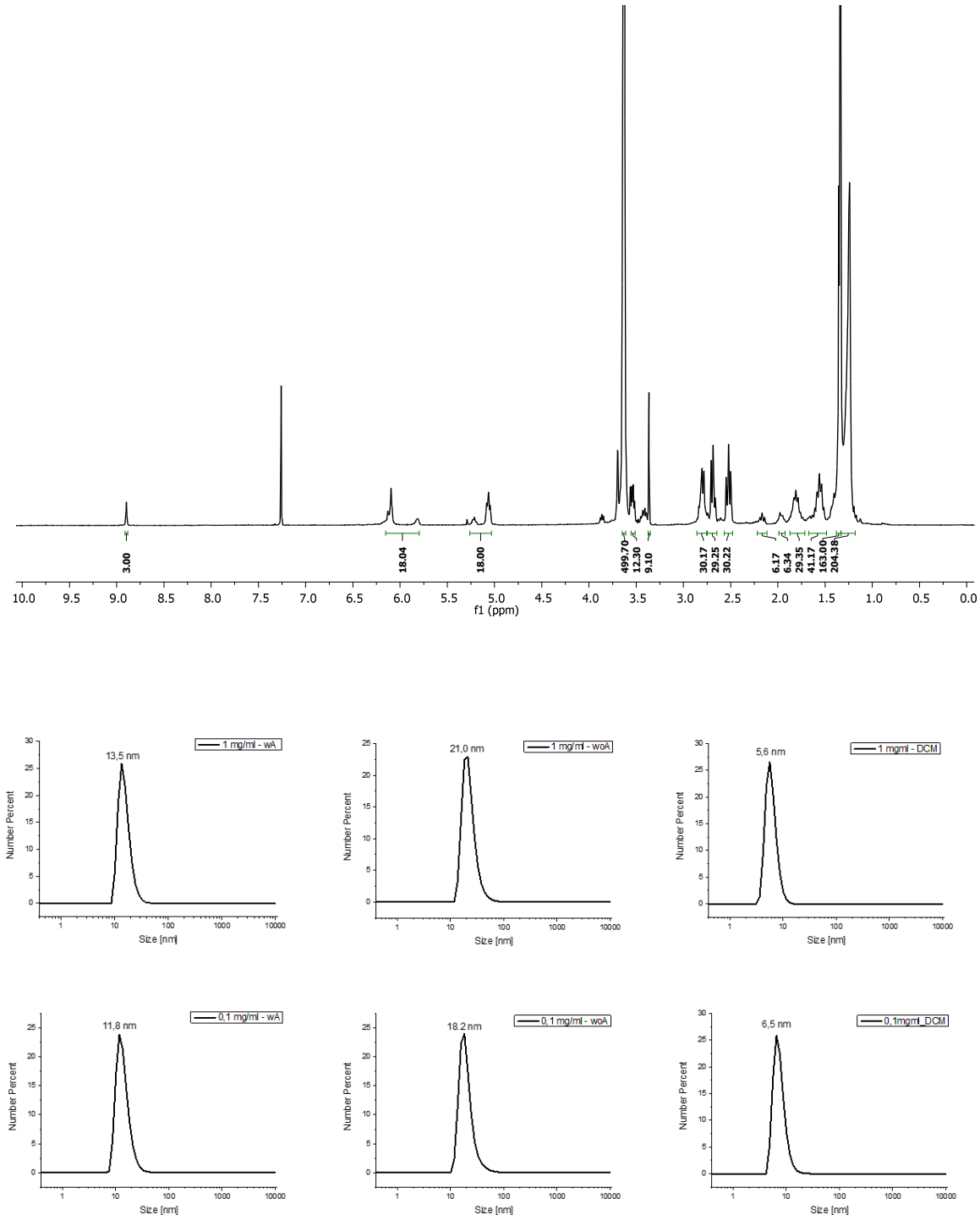

Figure 36: DLS results of functionalized star-shaped polymer **P18** (5 repeating units and 1 PEG (2000 g/mol)): first row 1 mg/mL of **P18**, second row 0.1 mg/mL of **P18**, left in water with acetone (wA), middle in water without acetone (woA), right in dichloromethane (DCM).

Star-shaped polymer P19 (5 repeating units, 1 PEG 950 g/mol)

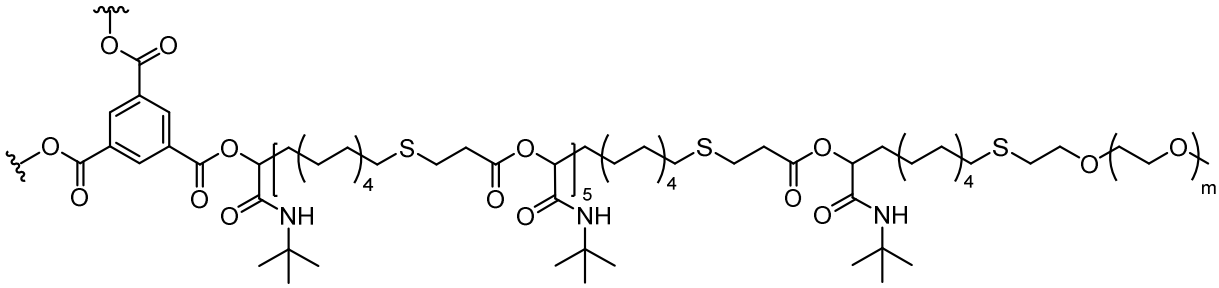

General procedure: To a vigorously stirred solution of star-shaped polymer **P14** (1.00 equiv.) and PEG aldehyde (950 g/mol) **23** (3.00 equiv.) in 0.05 mol/l DCM, *tert*-butyl isocyanide **5** (15.0 equiv.) was added slowly. After stirring for 72 hours at room temperature, the polymer was precipitated from diethyl ether.

Following the aforementioned procedure, **P19** was obtained as white solid (74 %). ^{1}H NMR ($CDCl_3$, 300 MHz): δ (ppm) = 1.14–1.31 (m, 252 H, 126 CH_2), 1.32–1.40 (m, 162 H, *t*-Bu), 1.48–1.61 (m, 36 H, 18 C*H*$_2$CH$_2$S), 1.68–1.90 (m, 36 H, 18 CHC*H*$_2$), 2.52 (t, *J* = 7.4 Hz, 36 H, 18 CH_2S), 2.63–2.74 (m, 36 H, 18 SCH_2), 2.76–2.88 (m, 36 H, 15 C*H*$_2$COO, 3 CH_2O), 3.37 (s, 3 H, CH_3), 3.59–3.70 (m, 180 H, 90 PEG-CH_2), 5.02–5.23 (m, 18 H, OCH(CO)), 5.78–6.13 (m, 18 H, NH), 8.88–8.91 (m, 3 H, Ar-H).

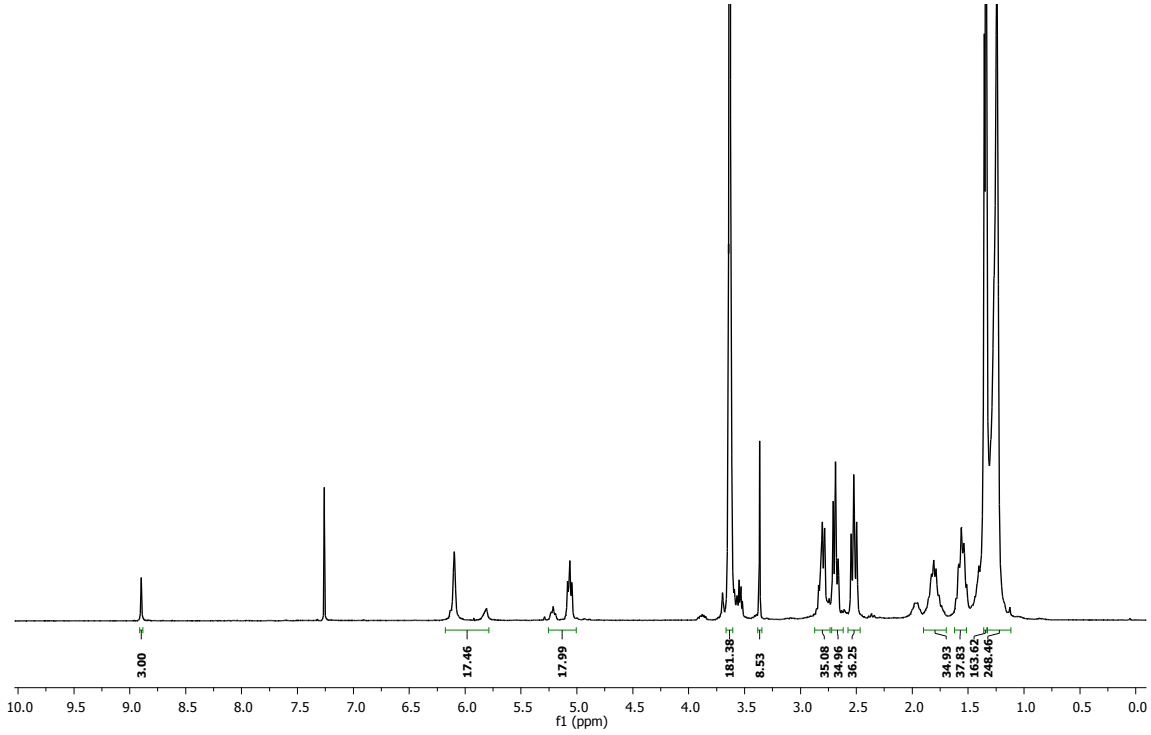

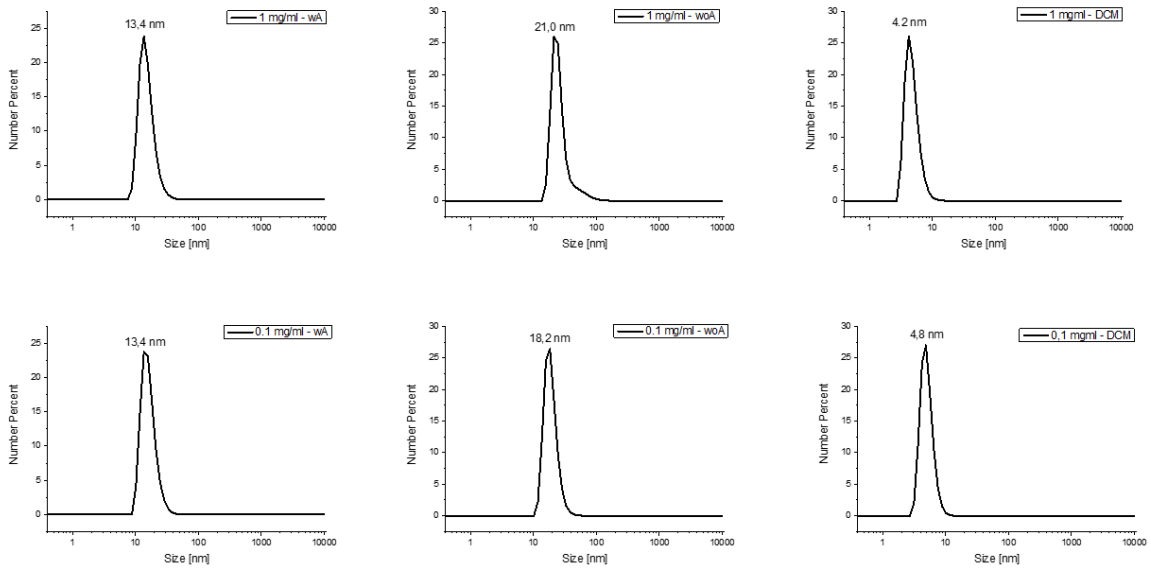

Figure 37: DLS results of functionalized star-shaped polymer **P19** (5 repeating units and 1 PEG (950 g/mol)): first row 1 mg/mL of **P19**, second row 0.1 mg/mL of **P19**, left in water with acetone (wA), middle in water without acetone (woA), right in dichloromethane (DCM).

Star-shaped polymer P20 (5 repeating units, 2 PEG a 950 g/mol)

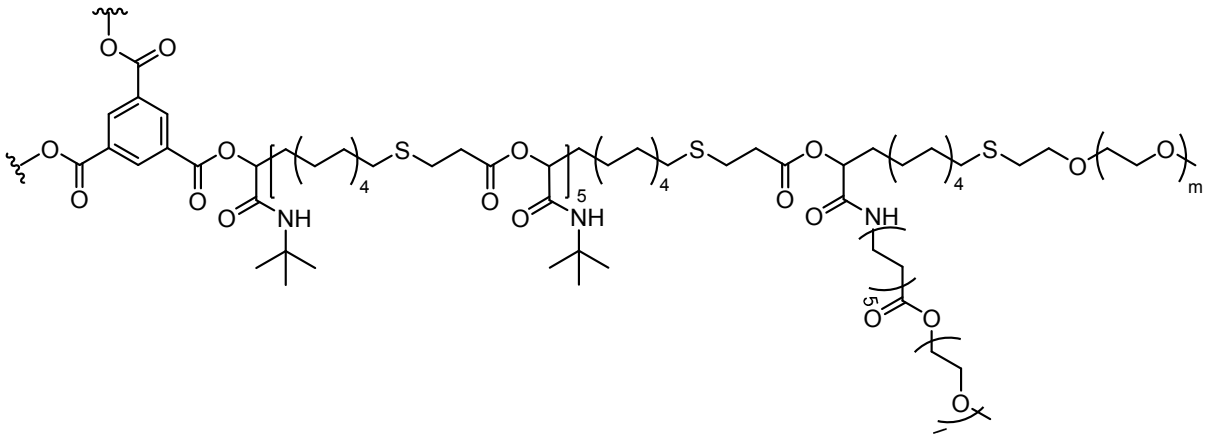

General procedure: Star-shaped polymer **P14** (1.00 equiv.), PEG aldehyde (950 g/mol) **23** (3.00 equiv.) and PEG isocyanide (950 g/mol) **21** (3.00 equiv.) were dissolved in 0.05 mol/l DCM. After 24 hours at room temperature PEG aldehyde (950 g/mol) **23** (3.00 equiv.) and PEG isocyanide (950 g/mol) **21** (3.00 equiv.) were added again and precipitated from diethyl ether after 72 hours.

Following the aforementioned procedure, **P20** was obtained as slightly yellow solid (78 %). ^{1}H NMR ($CDCl_3$, 300 MHz): δ (ppm) = 1.16–1.29 (m, 300 H, 150 CH_2), 1.30–1.42 (m, 135 H, *t*-Bu), 1.46–1.66 (m, 36 H, 18 C*H*$_2$CH$_2$S), 1.67–1.90 (m, 36 H, 18 CHC*H*$_2$), 2.27–2.32 (m, 6 H, 3 C*H*$_2$COO), 2.51 (t, *J* = 7.4 Hz, 36 H, 18 CH_2S), 2.60–2.73 (m, 36 H, 18 SCH_2), 2.74–2.86 (m, 36 H, 15 C*H*$_2$COO, 3 CH_2O), 3.35 (s, 3 H, CH_3), 3.54–3.77 (m, 378 H, 189 PEG-CH_2), 4.13–4.24 (m, 6 H, 3 NHC*H*$_2$), 4.97–5.26 (m, 18 H, OCH(CO)), 5.75–6.16 (m, 18 H, NH), 8.83–8.92 (m, 3 H, Ar-H).

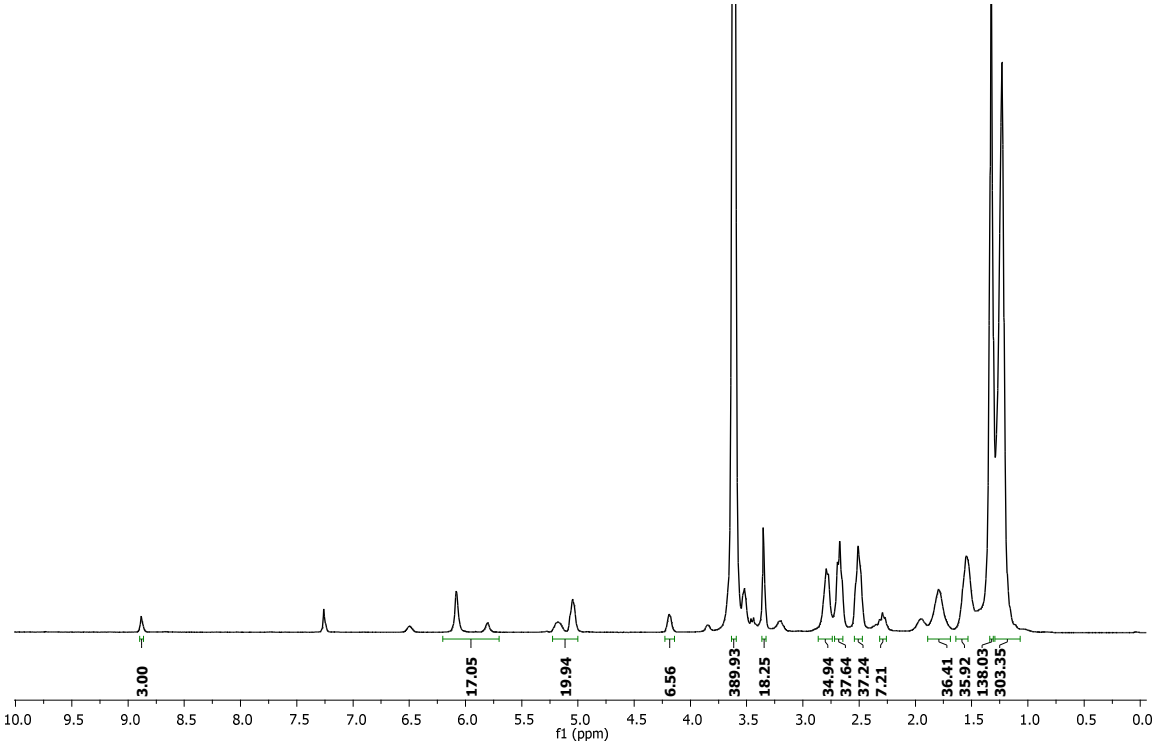

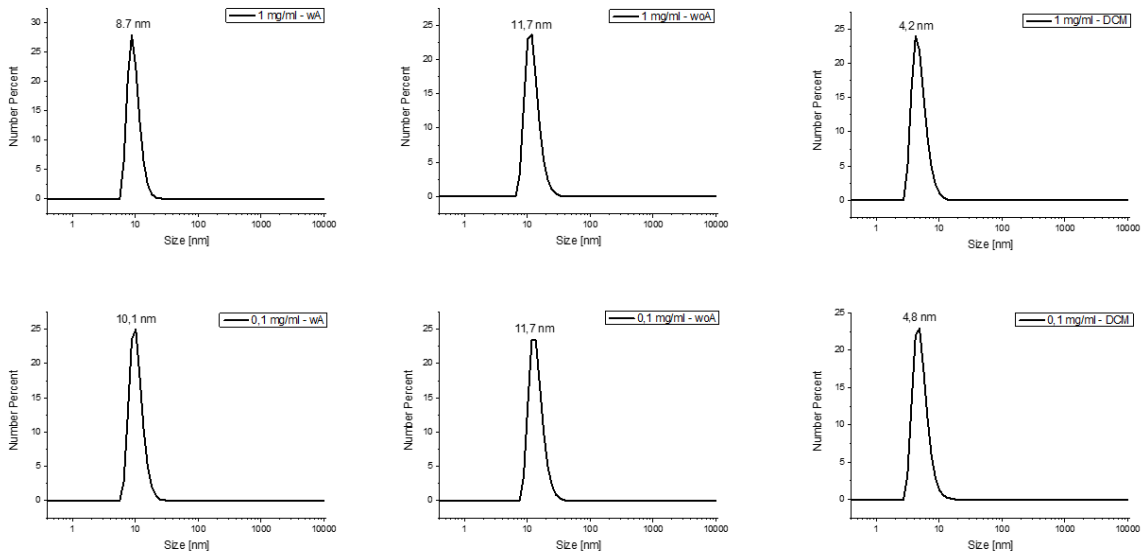

Figure 38: DLS results of functionalized star-shaped polymer **P20** (5 repeating units and 2 PEG (950 g/mol)): first row 1 mg/mL of **P20**, second row 0.1 mg/mL of **P20**, left in water with acetone (wA), middle in water without acetone (woA), right in dichloromethane (DCM).

Star-shaped polymer P21 (10 repeating units, 2 PEG a 950 g/mol)

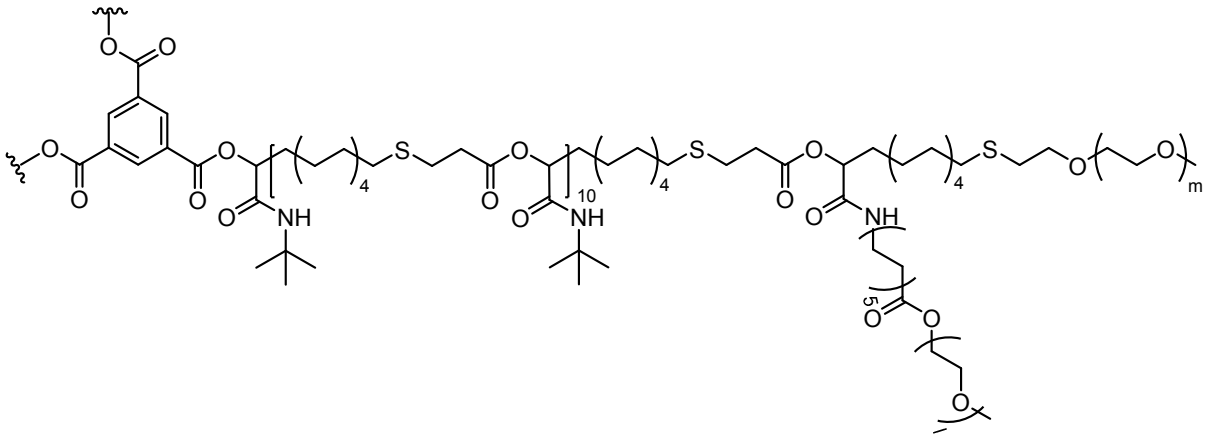

General procedure: Star-shaped polymer **P13** (1.00 equiv.), PEG aldehyde (950 g/mol) **23** (3.00 equiv.) and PEG isocyanide (950 g/mol) **21** (3.00 equiv.) were dissolved in 0.05 mol/l DCM. After 24 hours at room temperature PEG aldehyde (950 g/mol) **23** (3.00 equiv.) and PEG isocyanide (950 g/mol) **21** (3.00 equiv.) were added again and precipitated from diethyl ether after 72 hours.

Following the aforementioned procedure, **P21** was obtained as slightly yellow solid (80 %). ^{1}H NMR ($CDCl_3$, 300 MHz): δ (ppm) = 1.17–1.30 (m, 510 H, 255 CH_2), 1.31–1.41 (m, 270 H, *t*-Bu), 1.47–1.66 (m, 66 H, 33 C*H*$_2$CH$_2$S), 1.74–1.93 (m, 66 H, 33 CHC*H*$_2$), 2.24–2.36 (m, 6 H, 3 C*H*$_2$COO), 2.52 (t, *J* = 7.4 Hz, 66 H, 33 CH_2S), 2.63–2.73 (m, 66 H, 33 SCH_2), 2.74–2.85 (m, 66 H, 30 C*H*$_2$COO, 3 CH_2O), 3.36 (s, 3 H, CH_3), 3.58–3.66 (m, 378 H, 189 PEG-CH_2), 4.14–4.24 (m, 6 H, 3 NHC*H*$_2$), 5.01–5.26 (m, 18 H, OCH(CO)), 5.78–6.16 (m, 18 H, NH), 8.88–8.92 (m, 3 H, Ar-H).

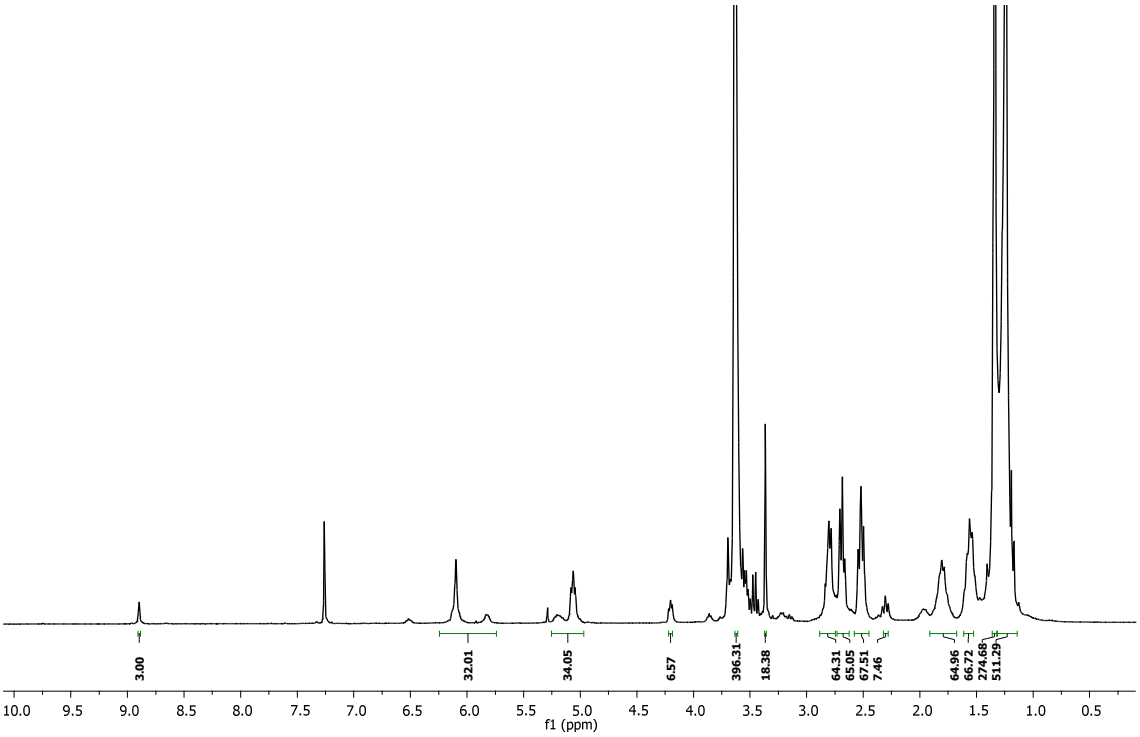

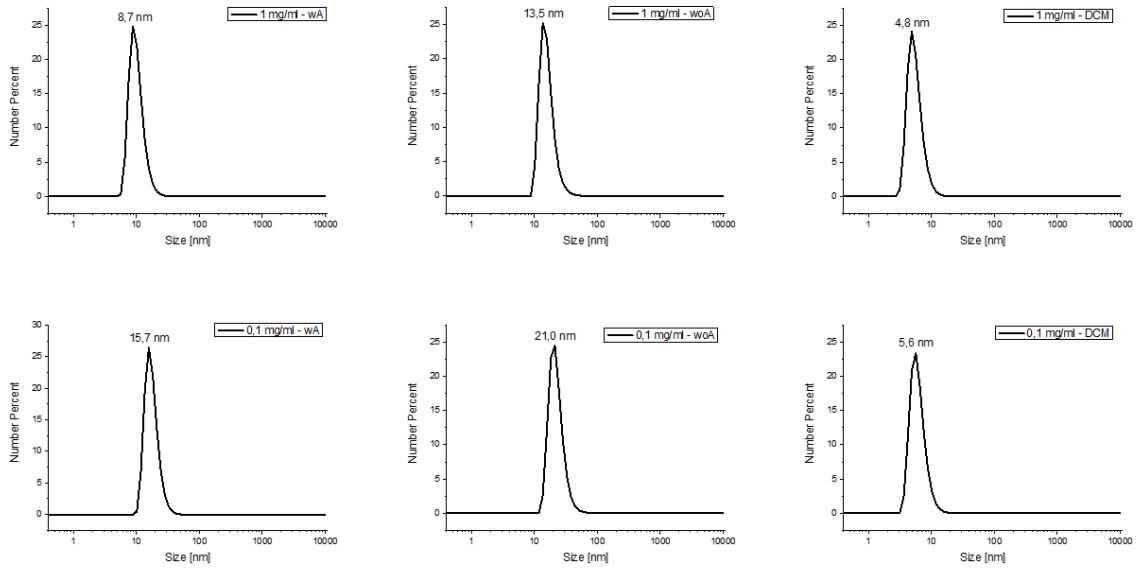

Figure 39: DLS results of functionalized star-shaped polymer **P21** (10 repeating units and 2 PEG (950 g/mol)): first row 1 mg/mL of **P21**, second row 0.1 mg/mL of **P21**, left in water with acetone (wA), middle in water without acetone (woA), right in dichloromethane (DCM).

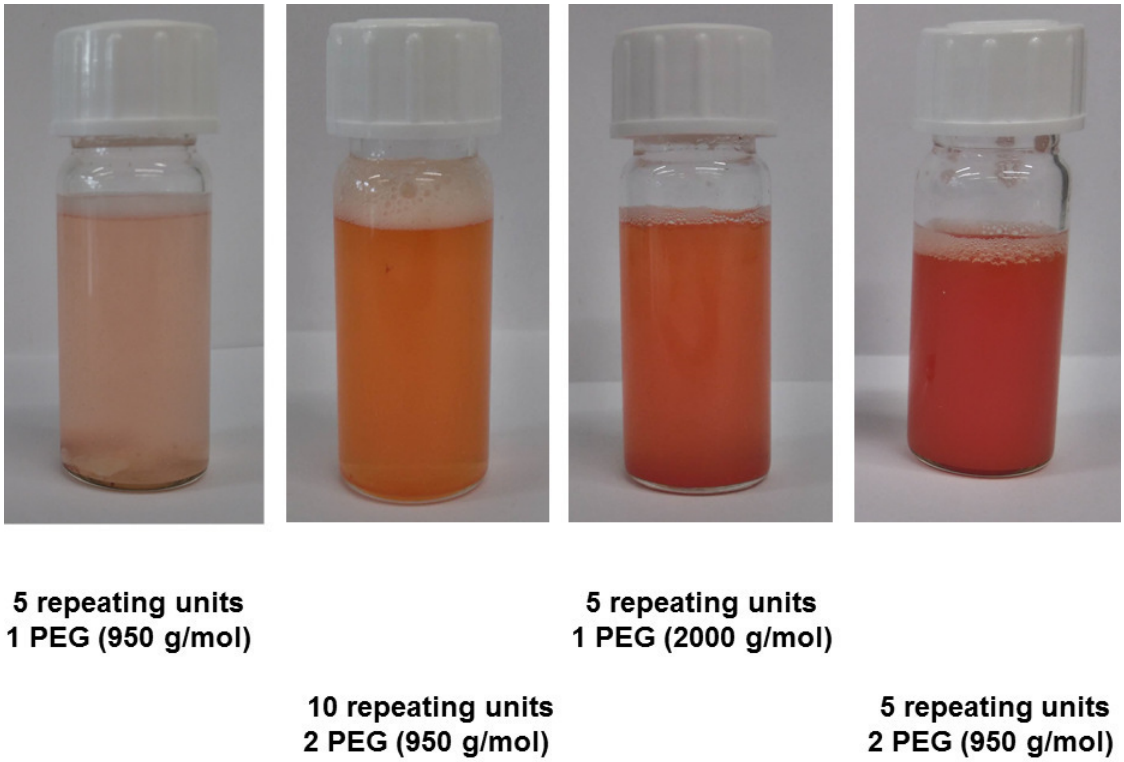

Figure 40: Pictures of the encapsulation of water-insoluble para red in water of four different polymers (from the left side to the right side: **P19**, **P21**, **P18** and **P20**).

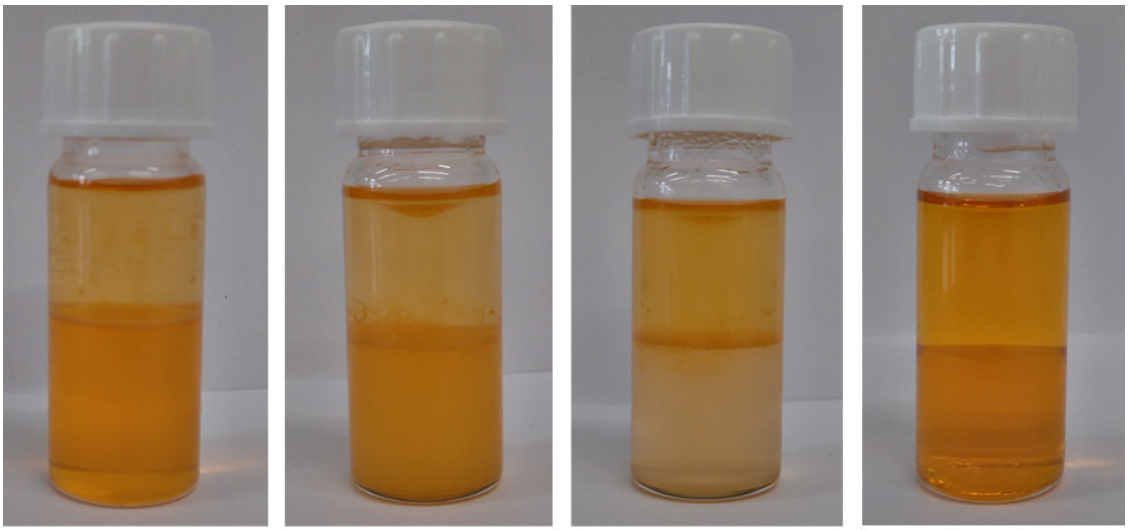

Figure 41: Pictures of the encapsulation and the phase transfer of Orange II from water (top phase) to dichloromethane (bottom phase) of four different polymers (from the left side to the right side: **P20**, **P19**, **P18** and **P21**).

6.5 Experimental procedures – chapter 4.3

Star-shaped homopolymer P22

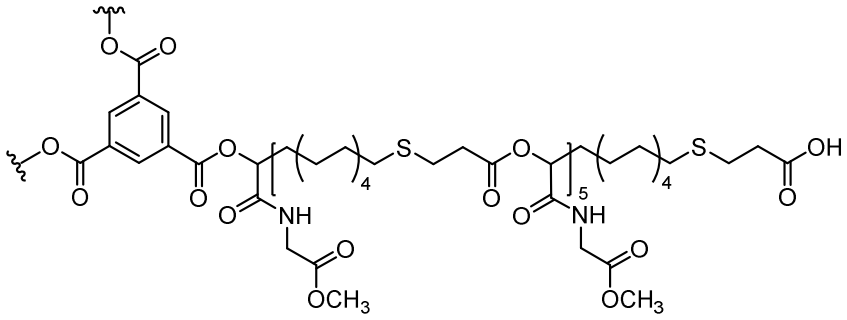

General procedure: To a vigorously stirred solution of trimesic acid **9** (1.00 equiv.) and methyl isocyanoacetate **24** (75.0 equiv.) in 1.50 mol/L THF, AB-type monomer **3** (15.0 equiv.) in 0.50 mL DCM was added slowly. After stirring for 24 hours at room temperature, the polymer was precipitated from ice-cold diethyl ether.

Following the aforementioned procedure, **P22** was obtained as yellow solid (89 %). ^{1}H NMR ($CDCl_3$, 300 MHz): δ (ppm) = 1.20–1.41 (m, 210 H, 105 CH_2), 1.52–1.64 (m, 30 H, 15 C*H*$_2$CH$_2$S), 1.81–2.07 (m, 30 H, 15 CHC*H*$_2$), 2.46–2.58 (m, 30 H, 15 CH_2S), 2.67–2.77 (m, 30 H, 15 SCH_2), 2.79–2.89 (m, 30 H, 15 C*H*$_2$COO), 3.75 (s, 45 H, 15 OCH_3), 3.90–4.17 (m, 30 H, 15 NHC*H*$_2$), 5.24–5.46 (m, 15 H, OCH(CO)), 6.79–7.06 (m, 15 H, NH), 8.87–9.01 (m, 3 H, Ar-H).

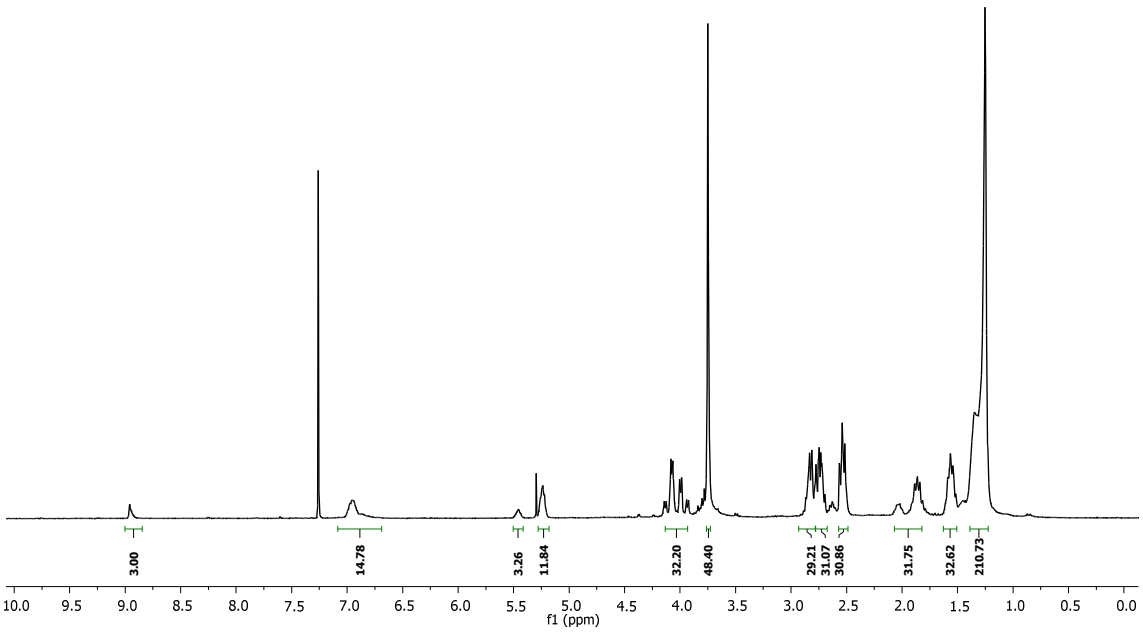

Star-shaped copolymer P23

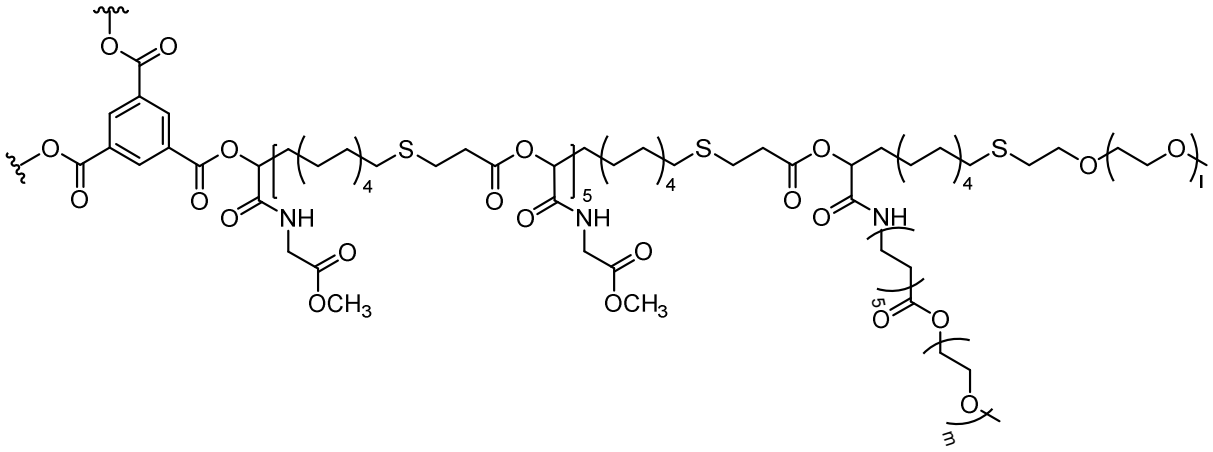

General procedure: Star-shaped polymer **P22** (1.00 equiv.), PEG aldehyde (950 g/mol) **23** (3.00 equiv.) and PEG isocyanide (950 g/mol) **21** (3.00 equiv.) were dissolved in 0.05 mol/l DCM. After 24 hours at room temperature PEG aldehyde (950 g/mol) **23** (3.00 equiv.) and PEG isocyanide (950 g/mol) **21** (3.00 equiv.) were added again and precipitated from diethyl ether after 72 hours.

Following the aforementioned procedure, **P22** was obtained as yellow solid (72 %). ^{1}H NMR ($CDCl_3$, 300 MHz): δ (ppm) = 1.17–1.41 (m, 300 H, 150 CH_2), 1.50–1.57 (m, 36 H, 18 C*H*$_2$CH$_2$S), 1.76–1.92 (m, 36 H, 18 CHC*H*$_2$), 2.26–2.35 (m, 6 H, 3 C*H*$_2$COO), 2.47–2.58 (m, 36 H, 18 CH_2S), 2.66–2.76 (m, 36 H, 18 SCH_2), 2.78–2.88 (m, 36 H, 15 C*H*$_2$COO, 3 CH_2O), 3.36 (s, 18 H, CH_3), 3.59–3.67 (m, 378 H, 189 PEG-CH_2), 3.74 (s, 45 H, OCH_3), 3.95–4.24 (m, 36 H, 15 NHC*H*$_2$, 3 NHC*H*$_2$), 5.15–5.44 (m, 18 H, OCH(CO)), 6.53–6.93 (m, 18 H, NH), 8.92–8.96 (m, 3 H, Ar-H).

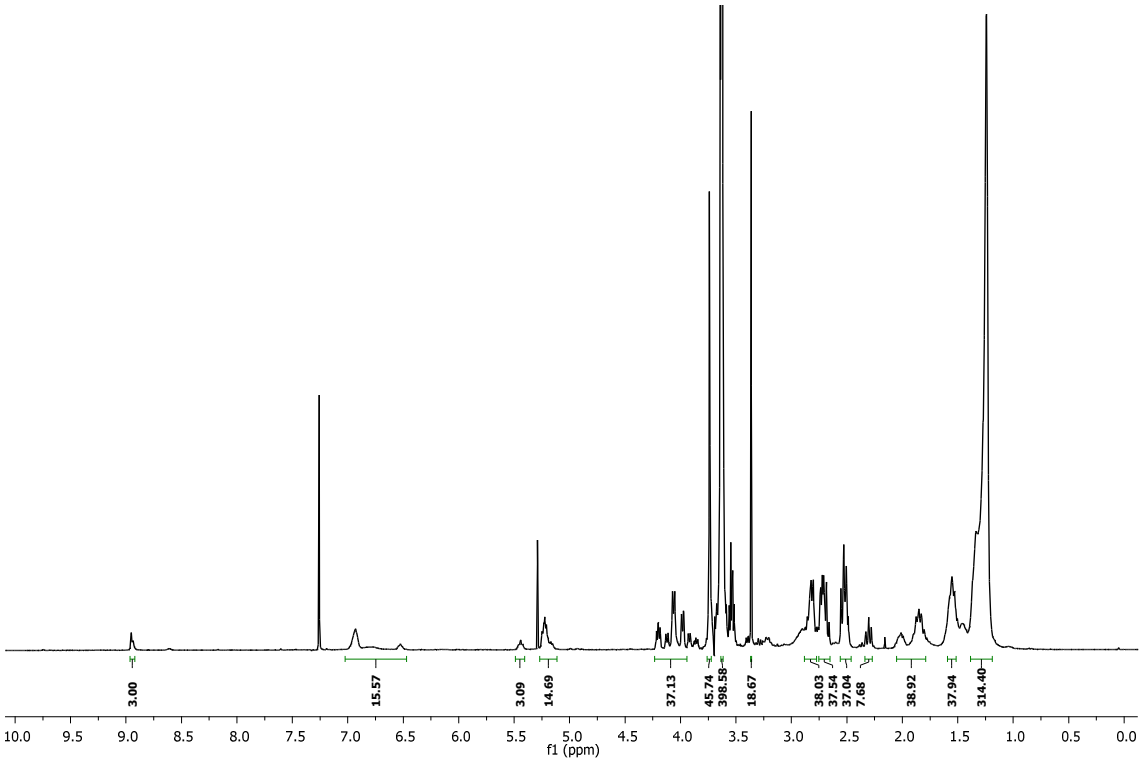

Oxidized star-shaped copolymers P24 and P25

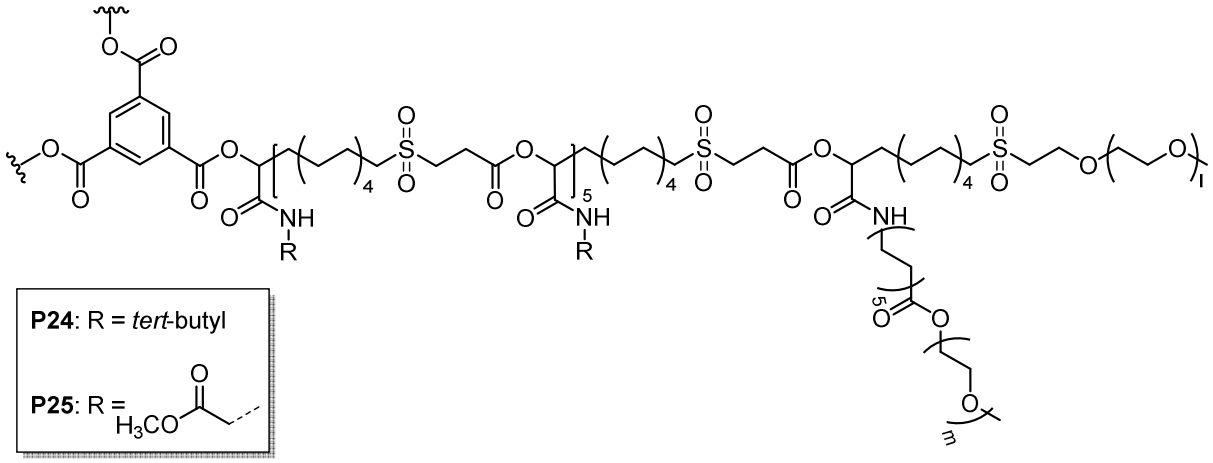

General procedure: Star-shaped copolymer **P20** or **P23** (1.00 equiv.) was dissolved in 35 mL dichloromethane and afterwards 3-chloroperbenzoic acid (6.0 eq. with respect to the sulfur atom) was added. The reaction mixture was stirred at room temperature for 2 days. By the addition of saturated sodium sulfite solution, remaining oxidizing agent was quenched. Subsequently, the organic layer was separated and the aqueous layer was extracted with DCM (two times). To obtain the oxidized star-shaped copolymer **P24** or **P25**, the combined organic layers were washed with 1 M sodium

hydroxide solution, dried over sodium sulfate and the solvent was evaporated under reduced pressure.

Alternative procedure: Star-shaped copolymer **P20** or **P23** (100 mg, 1.00 equiv.) was dissolved in THF (5.0 mL) and hydrogen peroxide (30%, 2.0 mL) was added. After stirring the mixture for 1 day at 60 °C, additional hydrogen peroxide (30%, 2.0 mL) was added and the mixture was stirred for one more day. Afterwards, the reaction mixture was cooled down to room temperature and the oxidized polymer was precipitated into cold diethyl ether. The crude polymer was dissolved in DCM and washed with water. Subsequently, the organic layers were dried over sodium sulfate, filtered and evaporated under reduced pressure to obtain the oxidized star-shaped copolymer **P24** or **P25**.

Following the general procedure, **P24** was obtained as slightly yellow solid (89 %). ^{1}H NMR ($CDCl_3$, 300 MHz): δ (ppm) = 1.18–1.33 (m, 300 H, 150 CH_2), 1.35–1.40 (m, 135 H, *t*-Bu), 1.52–1.67 (m, 36 H, 18 C*H*$_2$CH$_2$S), 1.74–1.88 (m, 36 H, 18 CHC*H*$_2$), 2.27–2.36 (m, 6 H, 3 C*H*$_2$COO), 2.81–3.35 (m, 108 H, 18 CH_2S, 18 SCH_2, 15 C*H*$_2$COO, 3 CH_2O), 3.37 (s, 18 H, CH_3), 3.58–3.68 (m, 378 H, 189 PEG-CH_2), 4.18–4.25 (m, 6 H, 3 NHC*H*$_2$), 4.99–5.25 (m, 18 H, OCH(CO)), 5.80–6.11 (m, 18 H, NH), 8.88–8.93 (m, 3 H, Ar-H).

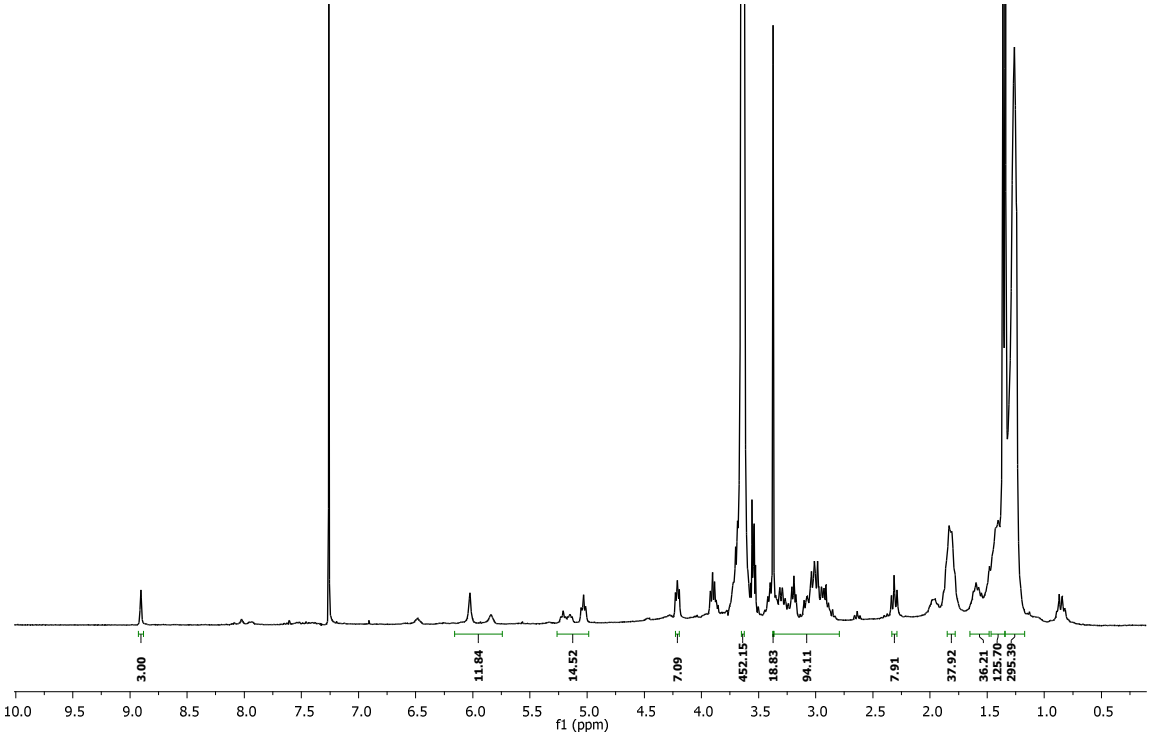

Following the general procedure, **P25** was obtained as yellow solid (81 %). ^{1}H NMR ($CDCl_3$, 300 MHz): δ (ppm) = 1.20–1.38 (m, 300 H, 150 CH_2), 1.40–1.53 (m, 36 H, 18 C*H*$_2$CH$_2$S), 1.77–1.87 (m, 36 H, 18 CHC*H*$_2$), 2.26–2.34 (m, 6 H, 3 C*H*$_2$COO), 2.75–3.35 (m, 108 H, 18 CH_2S, 18 SCH_2, 15 C*H*$_2$COO, 3 CH_2O), 3.37 (s, 18 H, CH_3), 3.57–3.70 (m, 378 H, 189 PEG-CH_2), 3.73 (s, 45 H, OCH_3), 3.88–4.22 (m, 36 H, 15 NHC*H*$_2$, 3 NHC*H*$_2$), 5.11–5.48 (m, 18 H, OCH(CO)), 6.46–7.11 (m, 18 H, NH), 8.90–8.97 (m, 3 H, Ar-H).

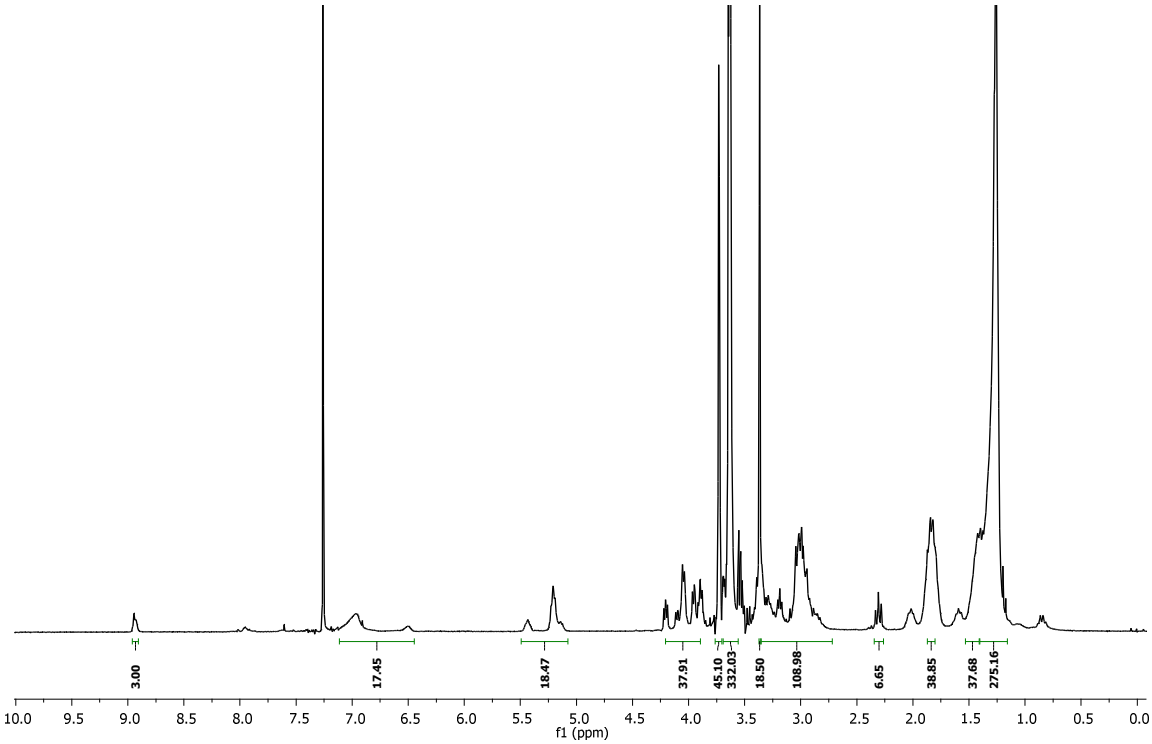

Synthesis of four-armed star-shaped polymers *via* Passerini reaction

Four-armed star-shaped homopolymers P26, P27, P28 and P29

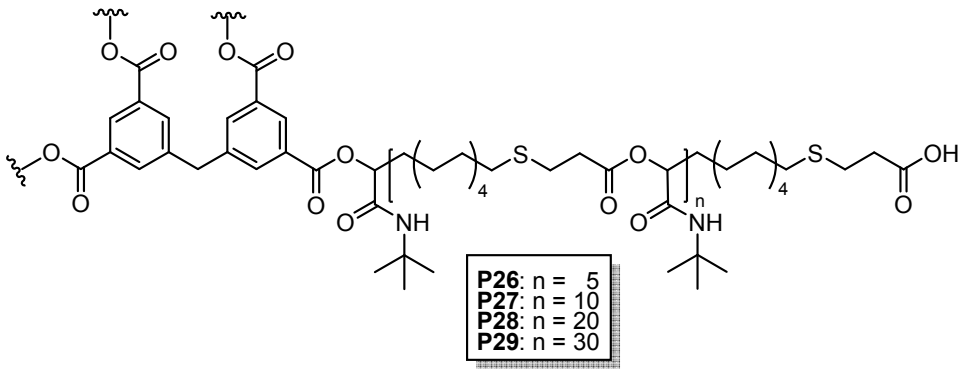

General procedure: To a vigorously stirred solution of 3,3,5,5-tetracarboxydiphenylmethane **25** (1.00 equiv.) and *tert*-butyl isocyanide **5** (20.0 equiv.,

40 equiv., 80.0 equiv., 120 equiv.) in 1.50 mol/L THF, AB-type monomer **3** (100 equiv., 200 equiv., 400 equiv., 600 equiv.) was added slowly. After stirring for 48 hours at room temperature, the polymers were precipitated from ice-cold diethyl ether to obtain four-armed star-shaped homopolymers **P26**, **P27**, **P28**, and **P29**.

Following the aforementioned procedure, **P26** (5 repeating units) was obtained as yellow solid (60 %). ^{1}H NMR ($CDCl_3$, 300 MHz): δ (ppm) = 1.22–1.28 (m, 280 H, 140 CH_2), 1.32–1.36 (m, 180 H, *t*-Bu), 1.49–1.68 (m, 40 H, 20 C*H*$_2$CH$_2$S), 1.69–1.99 (m, 40 H, 20 CHC*H*$_2$), 2.53 (t, *J* = 7.4 Hz, 40 H, 20 CH_2S), 2.58–2.73 (m, 40 H, 20 SCH_2), 2.74–2.89 (m, 40 H, 20 C*H*$_2$COO), 4,20–4,26 (m, 2 H, CH_2-Ar), 5.03–5.26 (m, 20 H, OCH(CO)), 5.80–6.20 (m, 20 H, NH), 8.03–8.14 (m, 4 H, Ar-H), 8.54–8.60 (m, 2 H, Ar-H).

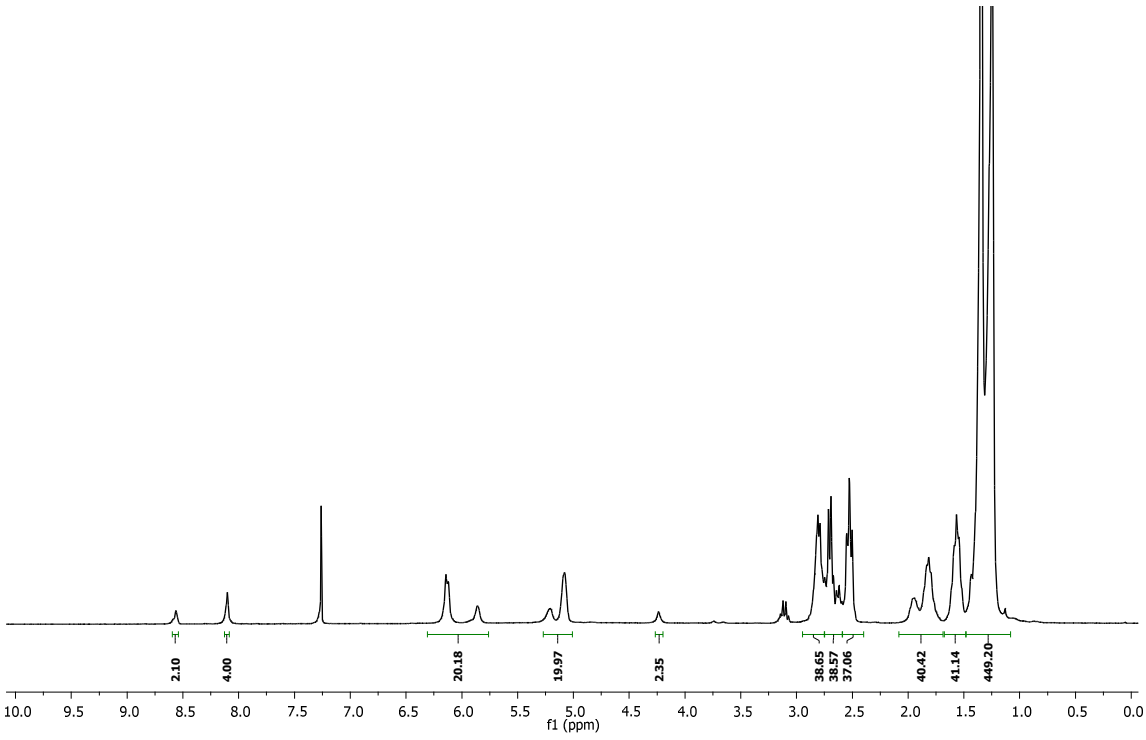

Following the aforementioned procedure, **P27** (10 repeating units) was obtained as yellow solid (31 %). ^{1}H NMR ($CDCl_3$, 300 MHz): δ (ppm) = 1.16–1.31 (m, 560 H, 280 CH_2), 1.32–1.46 (m, 360 H, *t*-Bu), 1.49–1.69 (m, 80 H, 40 C*H*$_2$CH$_2$S), 1.70–2.00 (m, 80 H, 40 CHC*H*$_2$), 2.53 (t, *J* = 7.4 Hz, 80 H, 40 CH_2S), 2.58–2.72 (m, 80 H, 40 SCH_2), 2.73–2.89 (m, 80 H, 40 C*H*$_2$COO), 4,21–4,25 (m, 2 H, CH_2-Ar), 5.01–5.26 (m, 40 H,

OCH(CO)), 5.79–6.26 (m, 40 H, NH), 8.03–8.12 (m, 4 H, Ar-H), 8.54–8.61 (m, 2 H, Ar-H).

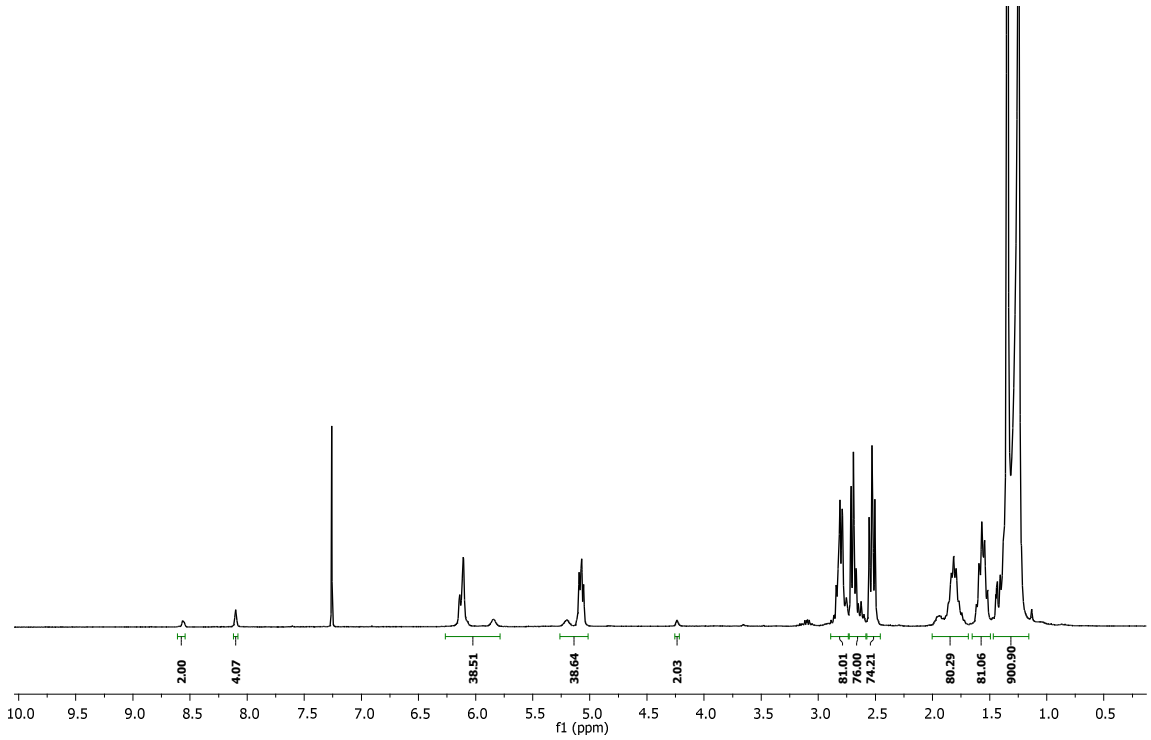

Following the aforementioned procedure, **P28** (20 repeating units) was obtained as yellow solid (50 %). ^{1}H NMR ($CDCl_3$, 300 MHz): δ (ppm) = 1.16–1.31 (m, 1120 H, 560 CH_2), 1.32–1.49 (m, 720 H, *t*-Bu), 1.50–1.68 (m, 160 H, 80 C*H*$_2$CH$_2$S), 1.69–2.00 (m, 160 H, 80 CHC*H*$_2$), 2.53 (t, *J* = 7.4 Hz, 160 H, 80 CH_2S), 2.58–2.73 (m, 160 H, 80 SCH$_2$), 2.74–2.89 (m, 160 H, 80 C*H*$_2$COO), 4.22–4.26 (m, 2 H, CH_2-Ar), 5.00–5.25 (m, 80 H, OCH(CO)), 5.80–6.25 (m, 80 H, NH), 8.08–8.13 (m, 4 H, Ar-H), 8.53–8.62 (m, 2 H, Ar-H).

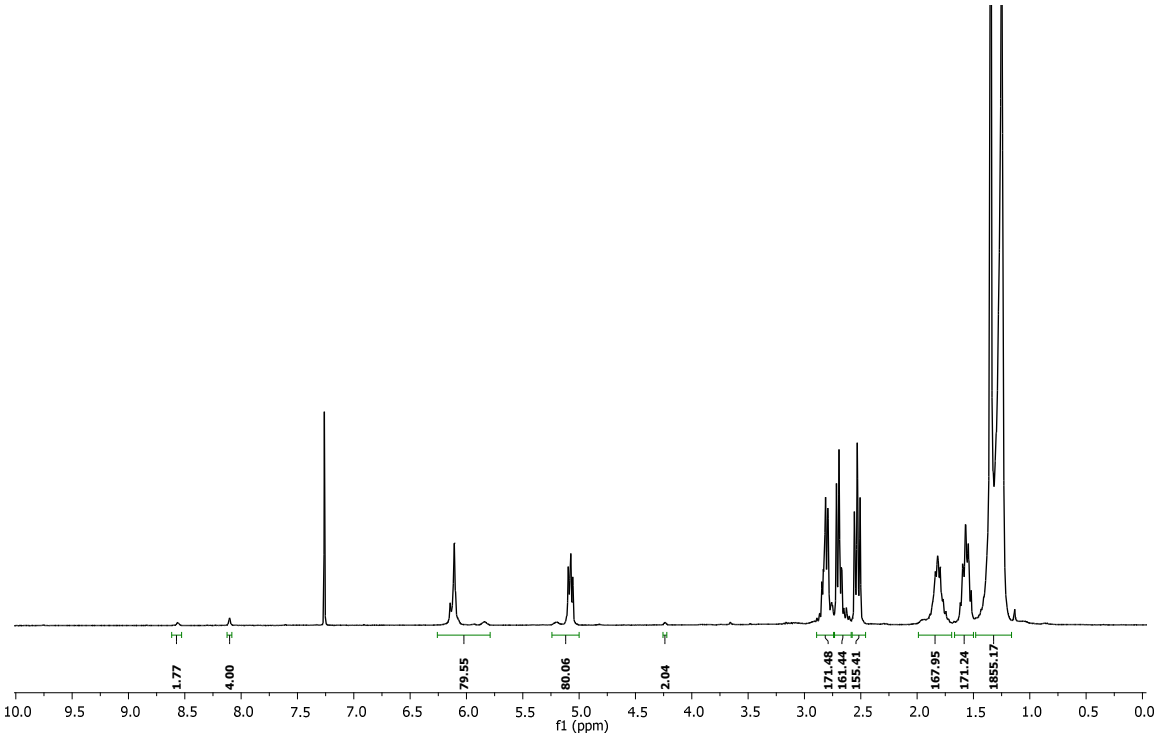

Following the aforementioned procedure, **P29** (30 repeating units) was obtained as yellow solid (33 %). ^{1}H NMR ($CDCl_3$, 300 MHz): δ (ppm) = 1.15–1.31 (m, 1680 H, 840 CH_2), 1.32–1.46 (m, 1080 H, *t*-Bu), 1.49–1.67 (m, 240 H, 120 C*H*$_2$CH$_2$S), 1.68–1.92 (m, 240 H, 120 CHC*H*$_2$), 2.53 (t, *J* = 7.4 Hz, 240 H, 120 CH_2S), 2.58–2.73 (m, 240 H, 120 SCH_2), 2.74–2.89 (m, 240 H, 120 C*H*$_2$COO), 4,21–4,26 (m, 2 H, CH_2-Ar), 5.04–5.22 (m, 120 H, OCH(CO)), 5.80–6.18 (m, 120 H, NH), 8.07–8.12 (m, 4 H, Ar-H), 8.53–8.58 (m, 2 H, Ar-H).

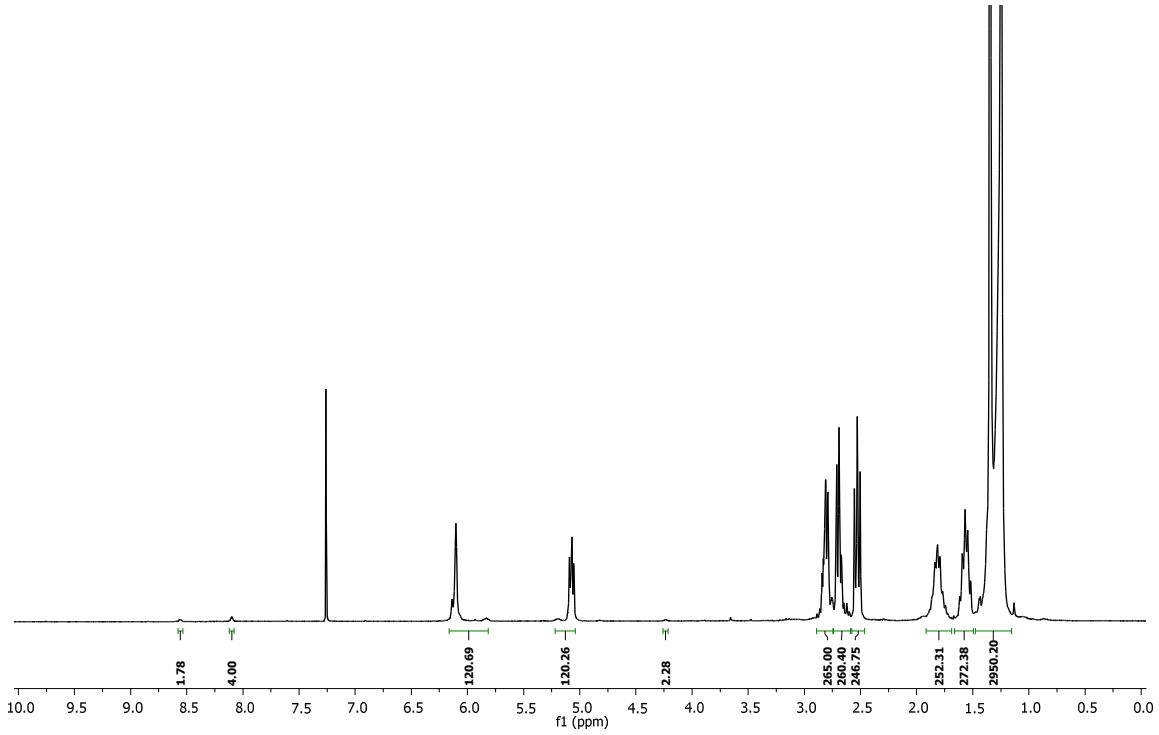

Four-armed star-shaped homopolymer P30

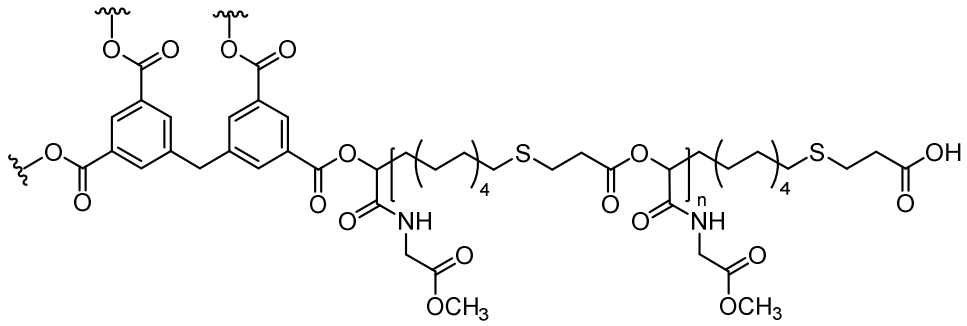

General procedure: To a vigorously stirred solution of 3,3,5,5-tetracarboxydiphenylmethane **25** (1.00 equiv.) and methyl isocyanoacetate **24** (50.0 equiv.) in 1.50 mol/L THF, AB-type monomer **3** (20.0 equiv.) was added slowly. After stirring for 48 hours at room temperature, the polymer was precipitated from ice-cold diethyl ether.

Following the aforementioned procedure, **P30** was obtained as yellow solid (58 %). ^{1}H NMR ($CDCl_3$, 300 MHz): δ (ppm) = 1.10–1.47 (m, 280 H, 140 CH_2), 1.49–1.67 (m, 40 H, 20 C*H*$_2$CH$_2$S), 1.75–2.06 (m, 40 H, 20 CHC*H*$_2$), 2.45–2.58 (m, 40 H, 20 CH_2S), 2.59–2.76 (m, 40 H, 20 SCH_2), 2.77–2.95 (m, 30 H, 15 C*H*$_2$COO), 3.72–3.80 (m, 60 H, 15 OCH_3), 3.91–4.16 (m, 40 H, 20 NHC*H*$_2$), 4.24–4.28 (m, 2 H, CH_2-Ar), 5.18–5.49 (m,

20 H, OCH(CO)), 6.65–7.16 (m, 20 H, NH), 8.11–8.27 (m, 4 H, Ar-H), 8.57–8.68 (m, 2 H, Ar-H).

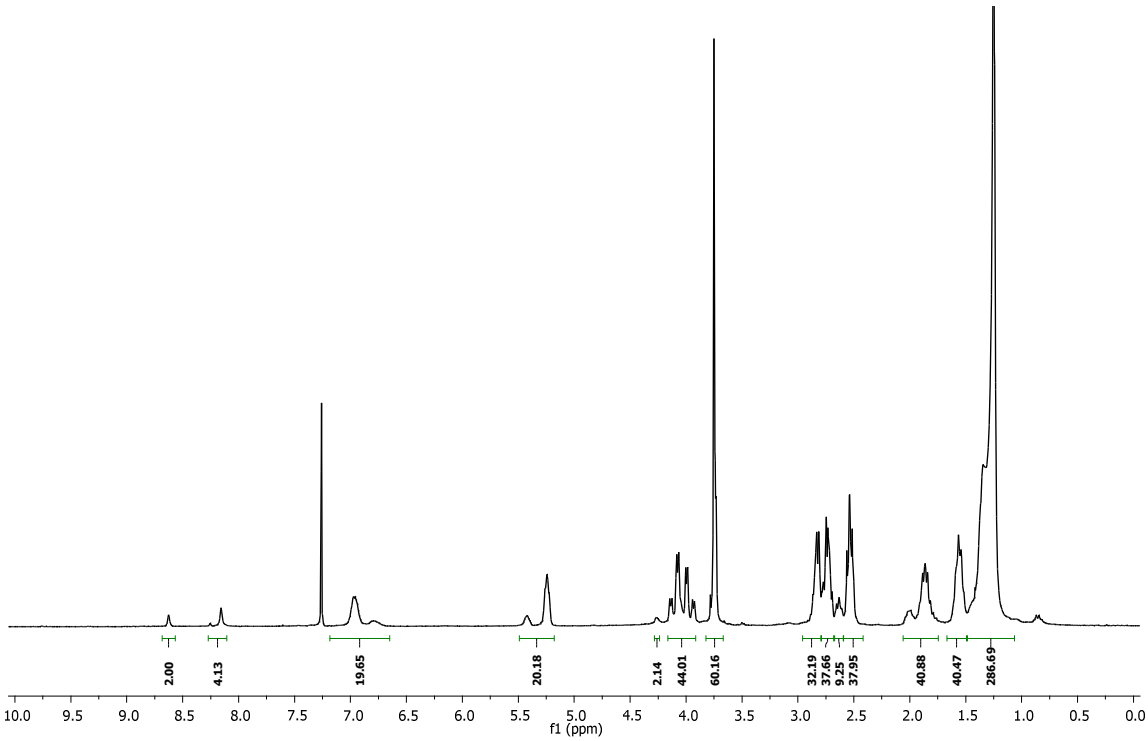

Four-armed star-shaped copolymer P31

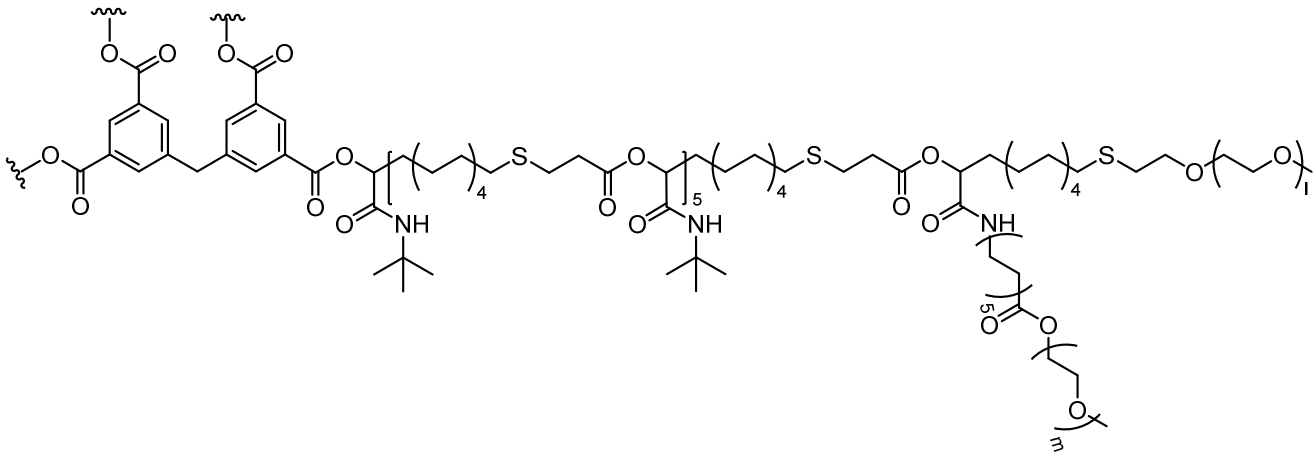

General procedure: Star-shaped polymer **P26** (1.00 equiv.), PEG aldehyde (950 g/mol) **23** (4.00 equiv.) and PEG isocyanide (950 g/mol) **21** (4.00 equiv.) were dissolved in 0.05 mol/l DCM. After 24 hours at room temperature PEG aldehyde (950 g/mol) **23** (4.00 equiv.) and PEG isocyanide (950 g/mol) **21** (4.00 equiv.) were added again and precipitated from diethyl ether after 72 hours.

Following the aforementioned procedure, **P31** was obtained as slightly yellow solid (82 %). ^{1}H NMR ($CDCl_3$, 300 MHz): δ (ppm) = 1.16–1.30 (m, 408 H, 204 CH_2), 1.31–1.42 (m, 180 H, *t*-Bu), 1.47–1.66 (m, 48 H, 24 C*H*$_2$CH$_2$S), 1.70–1.95 (m, 48 H, 24 CHC*H*$_2$), 2.28–2.35 (m, 8 H, 4 C*H*$_2$COO), 2.49–2.57 (m, 48 H, 24 CH_2S), 2.65–2.75 (m, 48 H, 24 SCH$_2$), 2.76–2.86 (m, 48 H, 24 C*H*$_2$COO), 3.37 (s, 24 H, CH_3), 3.61–3.67 (m, 504 H, 252 PEG-CH_2), 4.18–4.26 (m, 10 H, 4 NHC*H*$_2$, ArCH_2), 5.03–5.23 (m, 24 H, OCH(CO)), 5.76–6.17 (m, 24 H, NH), 8.08–8.12 (m, 4 H, Ar-H), 8.54–8.58 (m, 2 H, Ar-H).

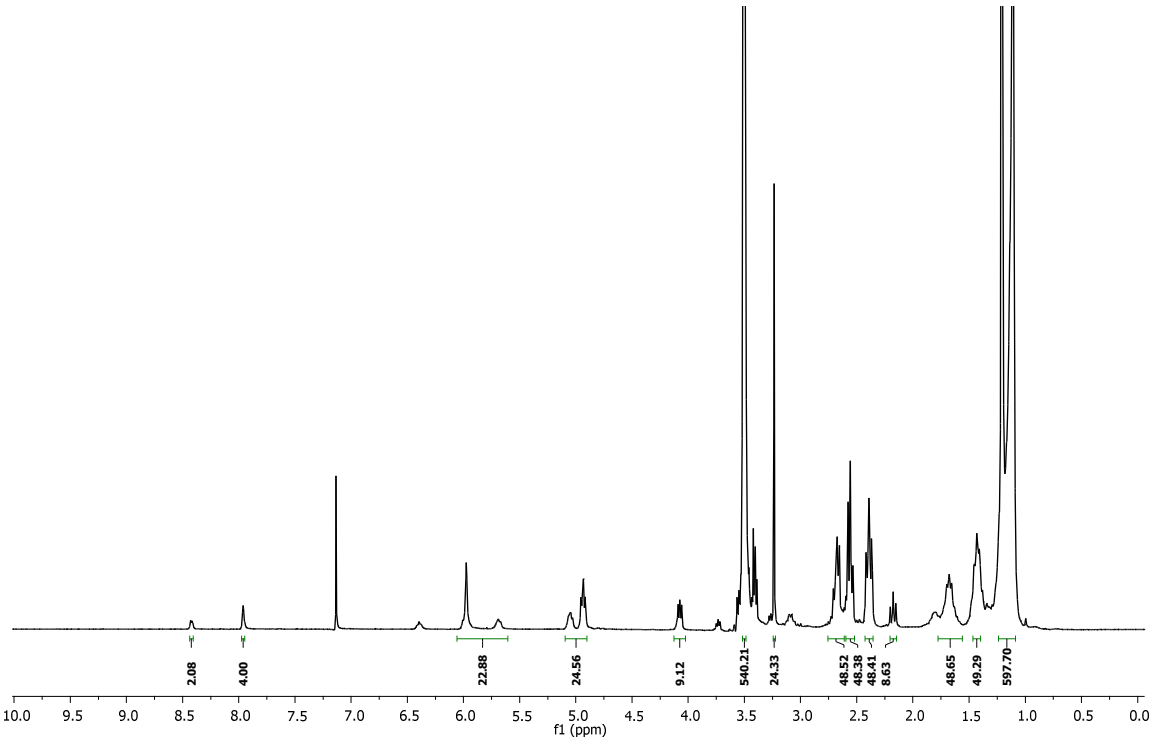

Drug loading and Encapsulation Efficiency

A 100 mg/mL solution of star-shaped block copolymers in THF was mixed with a 100 mg/mL solution of Azithromycin in THF - molecular ratio of 1:10 - and introduced into 10 volumes of deionized water under vigorous stirring. The organic solvent was removed using a rotary evaporator and the solution was centrifuged for 5 min at 14000 rpm. The supernatant containing the Azithromycin loaded star-shaped block copolymers micelles was removed and freeze dried, whereas the unloaded water-insoluble Azithromycin was collected, solubilized in a ACN/water solution (1:1) and quantified by UV/VIS spectrophotometry at 210 nm referring to a standard calibration curve (Figure 42). Therefore, a 5.00 mg/mL Azithromycin solution in ACN/water (1:1)

was prepared and diluted with ACN/water (1:1) solution. The absorbance was measured in triplicate at 210 nm by UV/VIS spectrophotometry.

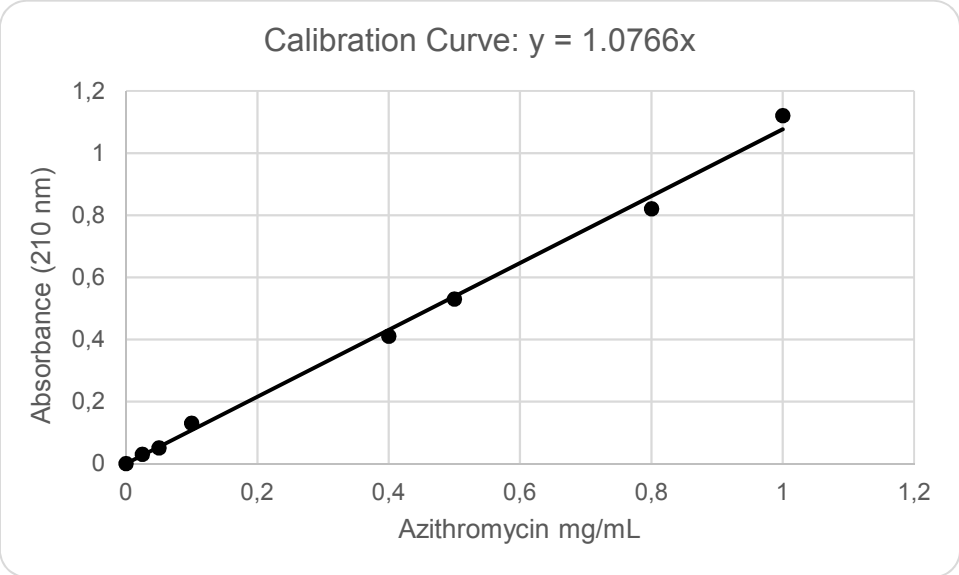

Figure 42: Azithromycin standard calibration curve.

The total amount of drug was determined by simultaneously preparing a polymer-free sample with an equal content of Azithromycin. The amount of loaded drug was calculated by taking the difference between both samples.

In Vitro Drug Release Study

Drug release studies were performed in phosphate-buffered saline (PBS with 0.10 % Tween 20) at pH 7.4 (blood pH)[203] and citrate phosphate buffer (0.10 M citric acid, 0.20 M Na_2HPO_4 and 0.10 % Tween 20)[204] at pH 5.0 (lysosome pH). A sample (5.00 mg) of Azithromycin-loaded and freeze-dried **P31** micelles were dispersed in 0.50 mL of release media and the solution was placed in a dialysis device (Slide-A-Lyzer™ mini dialysis device, 3.5 K MWCO, Thermo Scientific). The micellar solution was dialyzed against 1.50 mL of release media at 37 °C and samples (0.20 mL) were taken at appropriate time points and replaced with 0.20 mL fresh medium.[205] The collected samples were diluted with the same volume of ACN and the released Azithromycin was quantified by UV-Vis spectrophotometry at 210 nm referring to a standard calibration curve (Figure 42). The cumulative release (%) was defined based

on the concentration of Azithromycin calculated in the samples collected at different time points and considering the initial amount of encapsulated drug into the micelles.

The following parts of this section were performed from Alessandra Travanut at the University of Nottingham in the working group of Alexander Cameron.

Cell Culture

The THP-1 (a human monocytic cell line) were cultured in RPMI 1640 media supplemented with 10 % fetal bovine serum, 5 % penicillin/streptomycin and 5 % L-glutamine. To differentiate the monocytes to macrophages, cells were treated with 50 ng/mL of PMA, which is dissolved in the medium, for 24 h at 37 °C, 5 % CO_2.[206] Cells were differentiated at 0.1, 0.3, 0.5, 0.75, and 1 × 10^6 THP-1 cells/mL/ well in 96-well tissue cultured-treated polystyrene plates (Corning Life Sciences). After 24 h, cells were washed with fresh media and incubated for 72 h at 37 °C, 5 % CO_2 with 0.09 mL of media and 0.01 mL of PBS. Then, cells were washed with fresh media and 0.1 mL of fresh media and 0.10 mL of CellTiter-Fluor Cell Viability Assay solution were added. After 90 min of incubation at 37 °C, 5 % CO_2, the fluorescence was measured with Tecan Spark 10M (400nm_{Em}/505nm_{Ex}). The background fluorescence was determined by setting up triplicate wells without cells. The positive control was set up in triplicate wells containing cells 0.75 × 10^6 THP-1 cells/mL/well treated with 0.10 mL of 4 % paraformaldehyde in PBS.

Viability Assay

CellTiter-Fluor™ cell viability Assay was performed to determine the cytotoxicity[207] of **P31** against macrophage differentiated cells following the protocol provided by the vendor (Promega, Madison WI). Cells were treated for 72 h with different concentrations of **P31**.

The THP-1 cells were cultured and differentiated (0.75 × 10^6 THP-1 cells/mL/well in 96-well plate) as previously mentioned. After 24 h, cells were washed with fresh media and incubated for 72 h at 37 °C, 5 % CO_2 with 0.09 mL of media and 0.01 mL of different concentrations of **P31** in PBS (1.00, 5.00, 8.00 and 10.0 mg/mL - sterilized under 254 nm UV light for 30 minutes). Then, cells were washed with fresh media and

0.10 mL of fresh media and 0.10 mL of CellTiter-Fluor Cell Viability Assay solution were added. After 90 min of incubation at 37 °C, 5 % CO_2, the fluorescence was measured with Tecan Spark 10M ($400nm_{Em}/505nm_{Ex}$). The background fluorescence was determined by setting up triplicate wells without cells. The untreated control was set up in triplicate with untreated cells and 10 % of PBS. The positive control was set up in triplicate wells containing cells 0.75 $x10^6$ THP-1 cells/mL/well treated with 0.10 mL of 4 % paraformaldehyde in PBS. 1.00 mg/mL solution of **P31** in media was tested in triplicate wells without cells to test for possible interference with the assay chemistry. The protease activity was obtained using the following equation:

$$Protease\ Activity = \frac{RFUsample - RFUbackground}{RFUuntreated\ control - RFUbackground}$$

Bacterial susceptibility assay

To evaluate the bacteriostatic activity of Azithromycin-loaded unimolecular micelles **P31**, free or encapsulated Azithromycin was tested at drug concentrations of 0.10, 1.00, 10.0 and 100 µg/mL against *Staphyloccocus aureus* SH1000 cultures. Bacteria were grown overnight in tryptic soy broth (TSB Difco). The next day, the optical density (OD_{600}) of the culture was adjusted to 0.01 in fresh TSB and 200 µL aliquots of the culture supplemented with antibiotic were loaded in wells of a microtiter plate. As controls, untreated wells, and wells supplemented with solvent or polymer, were set. Bacterial growth was monitored for 24 hours at 37°C using a 96-well plate TECAN Genios Pro spectrophotometer (Tecan, UK). The minimum inhibitory concentration (MIC) was defined as the antibiotic concentration where no visible bacterial growth was observed or the OD600 was <10 % compared to the untreated control after 24 h of antibiotic exposure.

Cellular Uptake Study

Oregon-green loaded **P31** unimolecular micelles were prepared by mixing 0.10 mL of a 100 mg/mL **P31** solution in THF with 0.03 mL of a 28 mg/mL solution of Oregon-green in DMSO - molecular ratio of 1:3 - and introduced into 10 volumes of deionized water under vigorous stirring. The solution was purified by dialysis for three days

against 5.00 L of deionized water using a cellulose dialysis membrane (Thermofisher, cut-off 3500) to remove the organic solvents and the free Oregon-green. The solution was then sterilized by filtration (0.22 µm, Millipore filters).

Protocol I:

THP-1 cells (3 × 10^5 cells per well) were differentiated in an 8-well glass bottom µ-slide (ibidi, Germany) for 24 h at 37 °C, 5 % CO_2. Cell medium was removed and cells were then treated with fresh medium containing Oregon-green (100 µg/mL) loaded **P31** unimolecular micelles and incubated for 1 hour.[208] Cell culture medium was removed; cells were washed with PBS (twice) and incubated with CellMask™ deep red plasma membrane stain (1.00 µg/mL, life technologies) for 15 minutes at 37 °C, 5 % CO_2. After removing the solution, cells were washed with PBS (twice) and fixed with 4 % paraformaldehyde for 20 min at room temperature. After removing the solution, cells were washed with PBS (twice) and incubated with Hoechst 33342 dye (1.00 µg/mL, ThermoFisher) for 10 minutes to label the cells nuclei. After removing the solution, cells were washed with PBS (twice), covered with PBS and examined using examined using a Carl Zeiss LSM 700 BW microscope.

Protocol II:

THP-1 cells (3 × 10^5 cells per well) were differentiated in an 8-well glass bottom µ-slide (ibidi, Germany) for 24 h at 37 °C, 5 % CO_2. Cell medium was removed and cells were then treated with fresh medium containing Oregon-green (100 µg/mL) loaded **P31** unimolecular micelles and incubated for 1 hour.[208] Cell culture medium was removed; cells were washed with PBS (twice) and fixed with 4 % paraformaldehyde for 20 min at room temperature. After removing the solution, cells were washed with PBS (twice) and incubated with Hoechst 33342 dye (1.00 µg/mL, ThermoFisher) for 10 minutes to label the cells nuclei. After removing the solution, cells were washed with PBS (twice) and incubated with Alexa Fluor™ 647 Phalloidin (1.00 µg/mL, ThermoFisher) for 30 minutes to label the cells F-actin. Cells were washed with PBS (twice), covered with PBS and examined using a Carl Zeiss LSM 700 BW microscope.

Synthesis of Oregon-green 28[209]

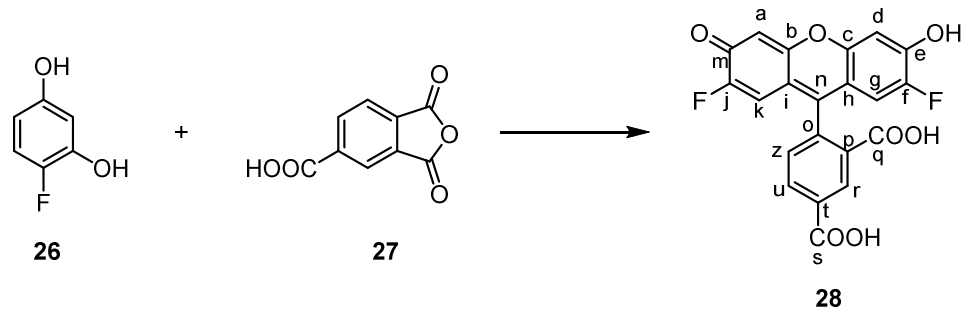

Scheme 39: Synthesis of Oregon green **28**.[209]

4-Fluororesorcinol **26** (254.5 mg, 1.98 mmol) was dissolved in concentrated methanesulfonic acid (2.00 mL) and deoxygenated using nitrogen gas for 30 minutes before adding 1,2,4-benzenetricarboxylic anhydride **27** (254.5 mg, 1.32 mmol). The reaction mixture was heated at 80°C under nitrogen for 48 h. The mixture was then cooled down to room temperature and dropped into 7 volumes of ice water. The precipitate was recovered by filtration and dissolved in a small amount of methanol and precipitated again from cold water. The solid was subsequently freeze-dried and then purified by silica column chromatography (n-hexane/ethyl acetate = 1:1 – 0:1) to yield Oregon-green **28** as an orange solid (370.5 mg, 68 %). R_f = 0.33 (ethyl acetate).

^{1}H NMR ($CDCl_3$, 400 MHz) δ (ppm) = 6.50 (s, 2H, CH^{ad}), 6.87 (s, 2H, CH^{kg}), 7.78 (d, *J* = 8.0 Hz, 1H, CH^{z}), 8.11 (d, *J* = 8.0 Hz, 1H, CH^{u}), 8.39 (s, 1H, CH^{r}), 8.64 (s, 1H, OH); ^{13}C NMR ($CDCl_3$, 101 MHz,) δ (ppm) = 106.12 C^{a}, 114.12 C^{d}, 114.34 C^{k}, 114.40 C^{g}, 126.27 C^{z}, 127.18 C^{i}, 127.97 C^{r}, 128.35 C^{p}, 129.51 C^{t}, 131.00 C^{u}, 132.38 C^{n}, 133.14 C^{o}, 136.34 C^{e}, 136.92 C^{bc}, 150.63 C^{jf}, 170.05 C^{sq}, 187.99 C^{m}; MS (ESI-TOF): *m*/*z* $[C_{21}H_{10}F_2O_7H]^+$ calc. 413.04, found 413.04; $[C_{21}H_{10}F_2O_7]^-$ calc. 411.04 found 411.03.

7. ABBREVIATIONS AND SYMBOLS

°C	degrees Celsius
ACN	acetonitrile
ADMET	acyclic diene metathesis
AFM	atomic force microscopy
ATRP	atom transfer radical polymerization
Az	Azithromycin
calc.	calculated
cat.	catalyst
CDI	carbonyldiimidazole
cm	centimeter
d	deuterated, days
Đ	dispersity
DCM	dichloromethane
dd	doublet of doublets
DLS	dynamic light scattering
DMPA	2,2-dimethoxy-2-phenylacetophenone
DMSO	dimethyl sulfoxide
DP_n	number-averaged degree of polymerization
DSC	differential scanning calorimetry
e.g.	for example
eq.	equivalent
ESI-MS	electrospray ionization mass spectrometry
et al.	and others
EVAc	ethylene-vinyl acetate
EWG	electron-withdrawing groups
FAB	fast atom bombardment
g	gram

GC	gas chromatography
GPC	gel permeation chromatography
h	hours
Hz	hertz
HPLC	high-performance liquid chromatography
HRMS	high resolution mass spectrometry
ICTA	irreversible chain transfer agent
IBX	2-iodoxybenzoic acid
i.e.	id est (that is)
IMCR	isocyanide-based multicomponent reaction
IR	infrared
k	capacity factor
K	Kelvin
kDa	kilo dalton
m	meter, multiplet
max	maximum
*m*CPBA	3-chloroperbenzoic acid
MCR	multicomponent reaction
mg	milligram
MIC	minimum inhibitory concentration
min	minute
mL	milliliter
mm	millimeter
mmol	millimole
M_n	number average molecular weight
MPS	mononuclear phagocyte system
M_w	weight average molecular weight
n	normal
nm	nanometer
NMP	nitroxide-mediated polymerization, N-methyl-2-pyrrolidone
NMR	nuclear magnetic resonance

ox.	oxidized
Passerini-3CR	Passerini three-component reaction
Passerini-3CP	Passerini three-component polymerization
Passerini-3KR	Passerini-Dreikomponentenreaktion
PBS	phosphate-buffered saline
PEG	polyethylene glycol
PDI	polydispersity index
pol	polymer
ppm	parts per million
q	quartet
R	variable functional group
rad	radiation
RAFT	reversible addition-fragmentation chain transfer
R_f	retarding-front
ROMP	ring-opening metathesis polymerization
ROP	ring-opening polymerization
RP-HPLC	reverse phase high-performance liquid chromatography
rt	room temperature
s	second, singlet
SEC	size exclusion chromatography
T	temperature
t	triplet, retention time
TEM	transmission electron microscopy
T_g	glass transition temperature
THF	tetrahydrofuran
TLC	thin layer chromatography
T_m	melting transition
Ugi-4CR	Ugi four-component reaction
Ugi-5CR	Ugi-five component reaction
UCST	upper critical solution temperature

UV	ultraviolet
VIS	visible
wt%	percentage by weight
X_n	degree of polymerization
δ	phase shift, chemical shift
µg	microgram
µm	micrometer

8. REFERENCES

[1] https://www.pharmazeutische-zeitung.de/index.php?id=28898 (last access 13.04.2018).

[2] J. Kreuter, *Pharm. Acta Helv.*, **1983**, *58*, 196.

[3] K. Langer, S. Balthasar, V. Vogel, N. Dinauer, H. von Briesen and D. Schubert, *Int. J. Pharm.*, **2003**, *257*, 169.

[4] V. Schäfer, H. von Briesen, H. Rübsamen-Waigmann, A. M. Steffan, C. Royer and J. Kreuter, *J. Microencapsul.*, **2009**, *11*, 261.

[5] M. K. Basu and S. Lala, *Curr. Mol. Med.,* **2004**, *4*, 681.

[6] V. Schäfer, J. Kreuter, H. Rübsamen-Waigmann, S. Gerte and H. von Briesen, *Clin. Diagn. Virol.*, 1994, 1, 279.

[7] G. R. Newkome, C. N. Moorefield. G. R. Baker, M. J. Saunders and S. H. Grossman, *Angew. Chem.,* **1991**, *103*, 1207.

[8] A. Dömling*, Curr. Opin. Chem. Biol.*, **2002**, *6*, 306.

[9] J. G. Rudick, *J. Polym. Sci., Part A: Polym. Chem.*, **2013**, *51*, 3985.

[10] I. Ugi, A. Dömling and W. Hörl, *Endeavour,* **1994**, *18*, 115.

[11] A. Dömling and I. Ugi, *Angew. Chem. Int. Ed.*, **2000**, *39*, 3168.

[12] A. Dömling, *Chem. Rev.*, **2006**, *106*, 17.

[13] P. A. Wender, S. T. Handy, D. L. Wright, *ChemInform.,* **1998**, *29*, 1.

[14] J. Zhu and H. Bienaymé, Multicomponent reactions, *John Wiley & Sons,* **2006**.

[15] J. Zhu, Q Wang and M. Wang, Multicomponent reactions in organic synthesis, *John Wiley & Sons,* **2014**.

[16] R. Kakuchi, Multi-Component and Sequential Reactions in Polymer Synthesis, *Springer International Publishing*, **2015**, 1.

[17] A. Strecker, *Justus Liebigs Ann. Chem.*, **1850**, *75*, 27.

[18] S. J. Zuend, M. P. Coughlin, M. P. Lalonde and E. N. Jacobsen, *Nature*, **2009**, *461*, 968.

[19] J. Wang, X. Liu and X. Feng, *Chem. Rev.* **2011**, *111*, 6947.

[20] A. Hantzsch, *Justus Liebigs Ann., Chem.* **1882**, *215*, 1.

[21] A. Hantzsch, Ber. *Dtsch. Chem. Ges.*, **1890**, *23*, 1474.

[22] P. Biginelli, *Ber. Dtsch. Chem. Ges.*, **1891**, *24*, 1317.

[23] C. Mannich and W. Krösche, *Arch. Pharm.*, **1912**, *250*, 647.

[24] H. T. Bucherer and H. T. Fischbeck, *J. Prakt. Chem.,* **1934**, *140*, 69.

[25] H. Bergs, Ger. pat., 566,094, **1929**.

[26] E. K. Fields, *J. Am. Chem. Soc.,* **1952**, *74*, 1528.

[27] F. Asinger, *Angew. Chem.,* **1956**, *68*, 376.

[28] B. Cornils, W. A. Herrmann and M. Rasch, *Angew. Chem.*, **1994**, *106*, 2219.

[29] W. Reppe, Neue Entwicklungen auf dem Gebiete der Chemie des Acetylens und Kohlenoxyds, *Springer Berlin*, **1949**, 93.

[30] I. U. Khand, G. R. Knox, P. L. Pauson and W. E. Watts, *J. Chem. Soc.*, **1971**, 36a.

[31] P. L. Pauson and I. U. Khand, *Ann. N.Y. Acad. Sci.,* **1977**, *295*, 2.

[32] P. L. Pauson, *Tetrahedron*, **1985**, *41*, 5855-5860.

[33] A. Gautier, *Liebigs Ann. Chem.*, **1869**, *146*, 119.

[34] S. Marcaccini and T. Torroba, *Org. Prep. Proced. Int.,* **1993**, *25*, 141.

[35] R. Schröder, U. Schöllkopf, E. Blume and I. Hoppe, *Justus Liebigs Ann. Chem.,* **1975**, *1975*, 533.

[36] A. M. Van Leusen, J. Wildeman and O. H. Oldenziel, *J. Org. Chem.,* **1977**, *42*, 1153.

[37] M. S. Edenborough and R. B. Herbert, *Nat. Prod.*, **1988**, *5*, 229.

[38] P. J. Scheuer, *Acc. Chem. Res.,* **1992**, *25*, 433.

[39] W. Lieke, *Justus Liebigs Ann. Chem.,* **1859**, *112*, 316.

[40] A. Gautier, *Justus Liebigs Ann. Chem.* **1868**, *146*, 119.

[41] A. W. Hofmann, *Liebigs Ann. Chem.*, **1867**, *144*, 114.

[42] W. P. Weber, G. W. Gokel and I. K. Ugi, *Angew. Chem,.* **1972**, *84*, 587.

[43] I. Ugi, R. Meyr, *Angew. Chem.,* **1958**, *70*, 702.

[44] I. Ugi, U. Fetzer, U. Eholzer, H. Knupfer and K. Offermann, *Angew. Chem.*, **1965**, *77*, 492.

[45] H. Eckert and B. Forster, *Angew. Chem.,* **1987**, *99*, 922.

[46] G. Skorna and I. Ugi, *Angew. Chem. Int. Ed.*, **1977**, *16*, 259.

[47] C. G. Neochoritis, T. Zarganes-Tzitzikas, S. Stotani, A. Dömling, E. Herdtweck, K. Khoury and A. Dömling, *ACS Comb. Sci.,* **2015**, *17*, 493.

[48] C. G. Neochoritis, S. Stotani, B. Mishra, A. Dömling and *Org. Lett.,* **2015**, *17*, 2002.

[49] M. Passerini, and L. Simone, *Gazz Chem. Ital.*, **1921**, *51*, 126.

[50] R. H. Baker and D. Stanonis, *J. Am. Chem. Soc.,* **1951**, *73*, 699.

[51] I. Ugi and R. Meyr, *Chem. Ber.,* **1961**, *94*, 2229.

[52] I. Hagedorn and U. Eholzer, *Chem. Ber.,* **1965**, *98*, 936.

[53] S. Maeda, S. Komagawa, M. Uchiyama and K. Morokuma, *Angew. Chem. Int. Ed.,* **2011**, *50*, 644.

[54] R. Ramozzi, K. Morokuma, *J. Org. Chem.,* **2015**, *80*, 5652.

[55] T. Nixey and C. Hulme, *Tetrahedron Lett.,* **2002**, *43*, 6833.

[56] T. Yue, M.-X. Wang, D.-X. Wang and J. Zhu, *Angew. Chem. Int. Ed.,* **2008**, *47*, 9454.

[57] X.-H. Cai, H. Guo and B. Xie, *Int. J. Chem.,* **2011**, *3*, 216.

[58] H. Yanai, T. Oguchi and T. Taguchi, *J. Org. Chem.,* **2009**, *74*, 3927.

[59] L. Lyu, H. Xie, H. Mu, Q. He, Z. Bian and J. Wang, *Organic Chemistry Frontiers,* **2015**, *2*, 815.

[60] L. El Kaim, M. Gizolme and L. Grimaud, *Org. Lett.,* **2006**, *8*, 5021.

[61] E. Martinand-Lurin, A. Dos Santos, L. El Kaim, L. Grimaud and P. Retailleau, *Chem. Commun.,* **2014**, *50*, 2214.

[62] T. Ngouansavanh, andJ. Zhu, *Angew. Chem. Int. Ed.,* **2006**, *45*, 3495-3497.

[63] I. Ugi and K. Rosendahl, *Chem. Ber.,* **1961**, *94*, 2233.

[64] R. Neidlein, *Z. Naturforsch.,* **1964**, *19*, 1159.

[65] O. Kreye, T. Tóth and M. A. R. Meier, *J. Am. Chem. Soc.* **2011**, *133*, 1790.

[66] O. Kreye, C. Trefzger, A. Sehlinger and M. A. R. Meier, *Macromol. Chem. Phys.* **2014**, *215*, 2207.

[67] A. Sehlinger, L. Monteiro de Espinosa and M. A. R. Meier, *Macromol. Chem. Phys.,* **2013**, *214*, 2821.

[68] A. Sehlinger, O. Kreye and M. A. R. Meier, *Macromolecules,* **2013**, *46*, 6031.

[69] L. Li, X.-W. Kan, X.-X. Deng, C.-C. Song, F.-S. Du and Z.-C. Li, *J. Polym. Sci. A: Polym. Chem.*, **2013**, *51*, 865.

[70] F. Leon, D. G. Rivera and L. A. Wessjohann, *J. Org. Chem.,* **2008**, *73*, 1762.

[71] X.-X. Deng, L. Li, Z.-L. Li, A. Lv, F.-S. Du and Z.-C. Li, *ACS Macro Lett.,* **2012**, *1*, 1300.

[72] X.-W. Kan, X.-X. Deng, F.-S. Du and Z.-C. Li, *Macromol. Chem. Phys.,* **2014**, *215*, 2221.

[73] T. Ngouansavanh and J. Zhu, *Angew. Chem. Int. Ed.,* **2006**, *45*, 3495.

[74] A. Sehlinger, R. Schneider, M. A. R. Meier, *Eur. Polym. J.* **2014**, 50, 150.

[75] L.-J. Zhang, X.-X. Deng, F.-S. Du and Z.-C. Li, *Macromolecules* **2013**, *46*, 9554.

[76] J. Zhang, M. Zhang, F.-S. Du and Z.-C. Li, *Macromolecules*, **2016**, *49*, 2592.

[77] W. Lin, X. Guan, T Sun, Y. Huang, X. Jing and Z. Xie, *Colloids and Surfaces B: Biointerfaces*, **2015**, *126*, 217.

[78] X.-X. Deng, Y. Cui, F.-S. Du and Z.-C. Li, *Polym. Chem.,* **2014**, *5*, 3316.

[79] A. E. J. de Nooy, D. Capitani, G. Masci and V. Crescenzi, *Biomacromolecules,* **2000**, *1*, 259.

[80] L. Li, A. Lv, X.-X. Deng, F.-S. Du and Z.-C. Li, *Chem. Commun.,* **2013**, *49*, 8549.

[81] J.-A. Jee, L.A. Spagnuolo and J. G. Rudick, *Org. Lett.* **2012**, *14*, 3292.

[82] S. C. Solleder and M. A. R. Meier, *Angew. Chem. Int. Ed.,* **2014**, *53*, 711.

[83] I. Ugi and C. Steinbrückner, *Angew. Chem.*, **1960**, *72*, 267.

[84] O. Mumm O, *Berichte der deutschen chemischen Gesellschaft*, **1910**, *43*, 886.

[85] N. Chéron, R. Ramozzi, L. E. Kaïm, L. Grimaud and P. Fleurat-Lessard, *J. Org. Chem.,* **2012**, *77*, 1361.

[86] I. Ugi and C. Steinbrückner, *Angew. Chem.,* **1960**, *72*, 267.

[87] I. Ugi and C. Steinbrückner, *Chem. Ber.,* **1961**, *94*, 734.

[88] I. Ugi, F. K. Rosendahl and F. Bodesheim, *Justus Liebigs Ann. Chem.,* **1963**, *666*, 54.

[89] I. Ugi and C. Steinbrückner, *Chem. Ber.,* **1961**, *94*, 2802.

[90] T. A. Keating and R. W. Armstrong, *J. Org. Chem.,* **1998**, *63*, 867.

[91] [101] L. El Kaïm and L. Grimaud, J. Oble, *Angew. Chem. Int. Ed.,* **2005**, *44*, 7961.

[92] L. El Kaïm, M. Gizolme, L. Grimaud and J. Oble, *J. Org. Chem.,* **2007**, *72*, 4169.

[93] A. A. Levy, H. C. Rains and S. Smiles, *J. Chem. Soc.,* **1931**, 3264.

[94] A. Sehlinger, P.-K. Dannecker, O. Kreye and M. A. R. Meier, *Macromolecules*, **2014**, *47*, 2774.

[95] A. Sehlinger, R. Schneider and M. A. R. Meier, *Macromol. Rapid Commun.*, **2014**, *35*, 1866.

[96] N. Gangloff, D. Nahm, L. Döring, D. Kuckling and R. Luxenhofer, *J. Polym. Sci. A.*, **2015**, *53*, 1680.

[97] M. Hartweg and C. R. Becer, *Green Chem.*, **2016**, *18*, 3272.

[98] X. Zhang, S. Wang, J. Liu, Z. Xie, S. Luan, C. Xiao, Y. Tao and X. Wang, *ACS Macro Lett.*, **2016**, *5*, 1049.

[99] A. Sehlinger and M. A. R. Meier, *Adv. Polym. Sci.,* **2015**, *269*, 61.

[100] L. A. Wessjohann, M. Henze, O. Kreye and D. G. Rivera, (2011) MCR dendrimers. Patent WO 2011/134607.

[101] L. A. Wessjohann, M. Henze, O. Kreye and D. G. Rivera, (2013) MCR dendrimers. European Patent EP 2563847.

[102] O. Kreye, D. Kugele, L. Faust and M. A. R. Meier, *Macromol. Rapid. Commun.*, **2014**, *35*, 317.

[103] X.-X Deng, F.-S. Du and Z.-C. Li, *ACS Macro. Lett*., **2014**, *3*, 667.

[104] J.-A. Jee, L. A. Spagnuolo and J. G. Rudick, *Reaction. Org. Lett.*, **2012**, 14, 3292.

[105] J.-A. Jee, S. Song and J. G. Rudick, *Chem. Commun*., **2015**, *51*, 5456.

[106] X.-X. Deng, Y. Cui, Y.-Z. Wang, F.-S. Du and Z.-C. Li, *Aust. J. Chem.*, **2014**, *67*, 555.

[107] L. Li, X.-W. Kan, X.-X. Deng, C.-C. Song, F.-S. Du and Z.-C. Li, *J. Polym. Sci. A.*, **2013**, *51*, 865.

[108] B. Yang, Y. Zhao, C. Fu, C. Zhu, Y. Zhang, S. Wang, Y. Wei and L. Tao, *Polym. Chem.*, **2014**, *5*, 2704.

[109] L. Tao, J. Xu, D. Gell and T. P. Davis, *Macromolecules*, **2010**, *43*, 3721.

[110] S. Jevsevar, M. Kunstelj and V. G. Porekar. *Biotechnol. J.*, **2010**, *5*, 113.

[111] B. Yang, Y. Zhao, S. Wang, Y. Zhang, C. Fu, Y. Wei and L. Tao, *Macromolecules*, **2014**, *47*, 5607.

[112] X. Li, Y. Qian, T. Liu, X. Hu, G. Zhang, Y. You and S. Liu, *Biomaterials,* **2011**, *32*, 6595.

[113] D. Poree, M. D. Giles, L. B. Lawson, J. He and S. M. Grayson, *Biomacromolecules,* **2011**, *12*, 898.

[114] F. Wang, T. K. Bronich, A. V. Kabanov, R. D. Rauh and J. Roovers, *Bioconjugate Chem*., **2005**, *16*, 397.

[115] J. Zhu, Z. Zhou, C. Yang, D. Kong, Y. Wan and Z. Wang, *J. Biomed. Mat. Res. A,* **2011**, *97A*, 498.

[116] A. Heise, J. L. Hedrick, C. W. Frank and R. D. Miller, *J. Am. Chem. Soc.,* **1999**, *121*, 8647.

[117] G. Chen and Z. Guan, *J. Am. Chem. Soc.,* **2004**, *126*, 2662.

[118] Y. Ma, Q. Mou, D. Wang, X. Zhu and D. Yan, *Theranostics*, **2016**, *6*, 930.

[119] E. F. Connor, L. K. Sundberg, H.-C. Kim, J. J. Cornelissen, T. Magbitang, P. M. Rice, V. Y. Lee, C. J. Hawker, W. Volksen, J. L. Hedrick and R. D. Miller, *Angew. Chem.*, **2003**, *115*, 3915.

[120] C. Nguyen, C. J. Hawker, R. D. Miller, E. Huang and J. L. Hedrick, *Macromolecules,* **2000**, *33*, 4281.

[121] C. J. Hawker, F. Chu, P. J. Pomery and D. J. T. Hill, *Macromolecules,* **1996**, *77*, 71.

[122] K.-Y. Baek, M. Kamigaito and M. Sawamoto, *Macromolecules*, **2001**, *34*, 7629.

[123] M. Gauthier, J. Li and J. Dockendorff, *Macromolecules*, **2003**, *36*, 2642.

[124] J. L. Hedrick, T. Magbitang, E. F. Connor, T. Glauser, W. Volksen, C. J. Hawker, V. Y. Lee and R. D. Miller, *Chem. Eur. J.*, **2002**, *8*, 3308.

[125] J. L. Hedrick, M. Trollsas, C. J. Hawker, B. Atthoff, H. Claesson, A. Heise, R. D. Miller, D. Mecerreyes, R. Jérôme and P. Dubois, *Macromolecules*, **1998**, *31*, 8691.

[126] S. Hecht and J. M. J. Fréchet, *Angew. Chem. Int. Ed.*, **2001**, *40*, 74.

[127] S. M. Grayson and J. M. J. Fréchet, *Chem. Rev.,* **2001**, *101*, 3819.

[128] D. Boris and M. Rubinstein*, Macromolecules*, **1996**, *29*, 7251.

[129] I. O. Gotze and C. N. Likos, *Macromolecules,* **2003**, *36*, 8189.

[130] M. Ballauff and C. N. Likos, *Angew. Chem.*, **2004**, *116*, 3060.

[131] A. Heise, C. Nguyen, R. Malek, J. L. Hedrick, C. W. Frank and R. D. Miller, *Macromolecules,* **2000**, *33*, 2346.

[132] H. Liu, A. Jiang, J. Guo and K. E. Uhrich, *J. Polym. Sci. Polym. Chem.*, **1999**, *37*, 703.

[133] C. J. Hawker, A. W. Bosman and E. Harth, Chem. Rev., **2001**, *101*, 3661.

[134] N. Hadjichristidis, S. Pispas and G. Floudas, *Block Copolymers: Synthetic Strategies, Physical Properties, and Applications,* 1 ed.; Wiley VCH: Weinheim, **2003**; Vol. 1.

[135] J. Huang, H. Liang, D. Cheng and J. Lu, *Polym. Chem.,* **2016**, *7*, 1792.

[136] T. Higashihara, S. Ito, S. Fukuta, T. Koganezawa, M. Ueda, T. Ishizone and A. Hirao, *Macromolecules,* **2015**, *48*, 245-255.

[137] C. Boyer, A. Derveaux, P. B. Zetterlund and M. R. Whittaker, *Polym. Chem.,* **2012**, *3*, 117.

[138] X. Pang, L. Zhao, M. Akinc, J. K. Kim and Z. Lin, *Macromolecules,* **2011**, *44*, 3746.

[139] R. Buckles, *J. Biomed. Mater. Res.*, **1983**, 17, 109.

[140] E. Wintermantel and S.-W. Ha, Medizintechnik – Life Science Engineering, *Springer Verlag*, **2009**, 1297.

[141] S. Dumitriu and D. Dumitriu, Biocompatibility of polymers, *Marcel Dekker Inc. New York*, **1994**, 99.

[142] K. Heilmann, Therapeutische Systeme, *Ferdinand Enke Verlag*, **1982**.

[143] M. R. Brundstedt and J. M. Anderson, Materials for drug delivery in Materials Science and Technology, *VCH Publishers*, **1992**, 413.

[144] H. Planck, Kunststoffe und Elastomere in der Medizin, *Verlag W. Kohlhammer*, **1993**.

[145] S. Dumitriu and M. Dumitriu, Polymeric drug carriers, in Biocompatibility of polymers, *Marcel Dekker Inc. New York*, **1994**.

[146] R. S. Langer and N. A. Peppas, *Biomaterials*, **1982**, *2*, 201.

[147] R. Duncan, *Anti-Cancer Drugs*, **1992**, *3*, 175.

[148] H. Ringsdorf, *J. Polym. Sci. Polym. Symp*., **1975**, *51*, 135.

[149] N. K. Jain, A. C. Rana and S. K. Jain, *Drug. Dev. Ind. Pharm.*, **1998**, *24*, 671.

[150] G. Tiwari, R. Tiwari, B. Sriwastawa, L. Bhati, S. Pandey, P. Pandey and S. K. Bannerjee, *Int. J. Pharm. Investig.*, **2012**, *2*, 2.

[151] A. K. Uppadhyay and V. K. Dixit, *Pharmazie*, **1998**, *53*, 421.

[152] M. L. Immordino, F. Dosio and L. Cattel, *Int. J. Nanomedicine*, **2006**, *1*, 297.

[153] A. Sharma, E. Mayhew, L. Bolcsak, C. Cavanaugh, P. Harmon, A. Janoff and R. J. Bernacki, *Int. J. Cancer*, **1997**, *71*, 103.

[154] J. M. J. Fréchet, *Scienc*e, **1994**, *263*, 1710.

[155] W. A. Braunecker and K. Matyjaszewski, *Prog. Polym. Sci.*, **2007**, *32*, 93.

[156] T. Yokozawa and A. Yokoyama, *Prog Polym. Sci.,* **2007**, *32*, 147.

[157] T. Yokozawa and A. Yokoyama, *Chem Rec.*, **2005**, *5*, 547.

[158] A. Sandeaua, S. Mazieres and M. Destarac, *Polymer*, **2012**, *53*, 5601.

[159] L. Montero de Espinosa and M. A. R. Meier, *Chem. Commun.,* **2011**, *47*, 1908.

[160] A. Sehlinger, L. Montero de Espinosa and M. A. R. Meier, *Macromol. Chem. Phys.,* **2013**, *214*, 2821.

[161] M. Unverferth and M. A. R. Meier, *Polymer*, **2014**, *55*, 5571.

[162] O. Kreye, T. Tóth and M. A. R. Meier, *J. Am. Chem. Soc.,* **2011**, *133*, 1790.

[163] J. G. Rudick, *J. Polym. Sci. A Polym. Chem.*, **2013**, *51*, 3985.

[164] M. Passerini, *Gazz*, and L. Simone, *Chem. Ital.*, **1921**, *51*, 126.

[165] A. Sehlinger and M. A. R. Meier, *Adv. Polym. Sci.* **2015**, *269*, 61.

[166] X.-X. Deng, L. Li, Z.-L. Li, A. Lv, F.-S. Du and Z.-C. Li, *ACS Macro. Lett.*, **2012**, *1*, 1300.

[167] Y.-Z. Wang, X.-X. Deng, L. Li, Z.-L. Li, F.-S. Du and Z.-C. Li, *Polym. Chem.*, **2013**, *3*, 444.

[168] A. Sehlinger, R. Schneider and M. A. R. Meier, *Eur. Polym. J.*, **2014**, *50*, 150.

[169] L.-J. Zhang, X.-X. Deng, F.-S. Du, and Z.-C. Li, *Macromolecules* **2013**, *46*, 9554.

[170] A. Lv, X.-X. Deng, L. Li, Z.-L. Li, Y.-Z. Wang, F.-S. Du and Z.-C. Li, *Polym. Chem.*, **2013**, *13*, 3659.

[171] C. Y. K. Chan, N.-W. Tseng, J. W. Y. Lam, J. Liu, R. T. K. Kwok and B. Z. Tang, *Macromolecules*, **2013**, *9*, 3246.

[172] R. Kakuchi and P. Theato, *ACS Macro. Lett*., **2013**, *5*, 419.

[173] H. A. Staab, *Angew. Chem. Int. Ed.,* **1962**, *1*, 351.

[174] A. Heise, J. L. Hedrick, C. W. Frank and R. D. Miller, *J. Am. Chem. Soc.,* **1999**, *121*, 8647.

[175] G. Chen and Z. Guan, *J. Am. Chem. Soc.,* **2004**, *126*, 2662.

[176] M. E. Piotti, F. Rivera, R. Bond, C. J. Hawker and J. M. J. Fréchet, *J. Am. Chem. Soc.,* **1999**, *121*, 9471.

[177] S. Stevelmans, J. C. M. van Hest, J. F. G. A. Jansen, D. A. F. J. van Boxtel, E. M. M. de Brabander-van den Berg and E. W. Meijer, *J. Am. Chem. Soc.,* **1996**, *118*, 7398.

[178] J. F. G. Jansen, E. M. M. de Brabander-van den Berg and E. W. Meijer, *Science,* **1994**, *266*, 1226.

[179] O. G. Schramm, G. M. Pavlov, H. P. van Erp, M. A. R. Meier, R. Hoogenboom and U. S. Schubert, *Macromolecules,* **2009**, *42*, 1808.

[180] M. A. R. Meier and U. S. Schubert, *J. Comb. Chem.,* **2005**, *7*, 356.

[181] M. A. R. Meier, J.-F. Gohy, C.-A. Fustin and U. S. Schubert, *J. Am. Chem. Soc.,* **2004**, *126*, 11517.

[182] D. Kul, L. M. van Rentergheim, M. A. R. Meier, S. Strandmann, H. Tenhu, S. S. Yilmaz, U. S. Schubert and F. E. Du Prez, *J. Polym. Sci. A Polym. Chem.*, **2007**, *46*, 650.

[183] M. A. R. Meier and U. S. Schubert, *Chem. Commun.,* **2005**, *36*, 4610.

[184] W. Yuan, J. Zhang, J. Wei, C. Zhang and J. Ren, *Eur. Polym. J.,* **2011**, *47*, 949.

[185] J.-L. Zhu, K. L. Liu, Z. Zhang, X.-Z. Zhang and J. Li, *Chem. Commun.,* **2011**, *47*, 12849.

[186] A. Vazaios, D. J. Lohse and N. Hadjichristidis, *Macromolecules,* **2005**, *38*, 5468.

[187] W.-P. Zhu, A. Nese and K. Matyjaszewski, *J. Polym. Sci., Part A: Polym. Chem.,* **2011**, *49*, 1942.

[188] S. Oelmann, S. C. Solleder and M. A. R. Meier, *Polym. Chem.,* **2016**, *7*, 1857.

[189] A. Llevot, A. C. Boukis, S. Oelmann, K. Wetzel and M. A. R. Meier, *Top Curr Chem*, **2017**, *375*, 66.

[190] S. C. Solleder, D. Zengel, K. S. Wetzel and M. A. R. Meier, *Angew. Chem. Int. Ed.*, **2016**, *55*, 1204.

[191] H. M. Aliabadi, S. Elhasi, A. Mahmud, R. Gulamhusein, P. Mahdipoor and A. Lavasanifar, *International Journal of Pharmaceutics*, **2017**, *329*, 158.

[192] S. Oelmann and M. A. R. Meier, *RSC Adv.*, 2017, **7**, 45195.

[193] O. Kreye, S. Oelmann and M. A. R. Meier, *Macromolecular Chemistry and Physics,* **2013,** 214, 1452.

[194] J. T. Andersson and W. A. Schräder, *Analytical Chemistry* **1999,** *71*, 3610.

[195] OECD, *Test No. 117: Partition Coefficient (n-octanol/water), HPLC Method*. OECD Publishing.

[196] K. Dimroth, C. Reichardt, T. Siepmann and F. Bohlmann, *Justus Liebigs Annalen der Chemie*, **1963**, *661*, 1.

[197] V. G. Machado and C. Machado, *J. Chem. Educ.*, **2001**, *78*, 649.

[198] C. Reichardt, *Chem. Rev.*, **1994**, *94*, 2319.

[199] P. Matzneller, S. Krasniqi, M. Kinzig, F. Sorgel, S. Huttner, E. Lackner, M. Muller and M. Zeitlinger, *Antimicrob Agents Chemother,* **2013,** *57*, 1736.

[200] T. Kauss, K. Gaudin, A. Gaubert, B. Ba, S. Tagliaferri, F. Fawaz, J.-L. Fabre, J.-M. Boiron, X. Lafarge, N. J. White, P. L. Olliaro and P. Millet, *International Journal of Pharmaceutics,* **2012,** *436*, 624.

[201] F. Danhier, E. Ansorena, J. M. Silva, R. Coco, A. Le Breton, and V. Préat, *Journal of Controlled Release,* **2012,** *161*, 505.

[202] W. L. Hand and D. L. Hand, *Int J Antimicrob Agents,* **2001,** *18*, 419.

[203] J. A. Anderson, S. Lamichhane, T. Remund, P. Kelly and G. Mani, *Acta Biomaterialia,* **2016,** *29*, 333.

[204] A. C. Carreira, R. F. M. Almeida and L. C. Silva, *Scientific Reports,* **2017**, *7*, 3949.

[205] M. Gulfam, T. Matini, P. F. Monteiro, R. Riva, H. Collins, K. Spriggs, S. M. Howdle, C. Jérôme and C. Alexander, *Biomater. Sci.*, **2017**,*5*, 532.

[206] C. Dollinger, S. Ciftci, H. Knopf-Marques, R. Guner, A. M. Ghaemmaghami, C. Debry, J. Barthes and N. E. Vrana, *J Tissue Eng Regen Med,* **2018,** *12*, 330.

[207] T. L. Riss, R. A. Moravec, A. L. Niles, S. Duellman, H. A. Benink, T. J. Worzella and L. Minor, *Cell Viability Assays.*, **2016**.

[208] I. H. Hall, U. E. Schwab, E. S. Ward, J. C. Rublein, J. D. Butts, andT. J. Ives, *J Infect Chemother,* **2004,** *10*, 11.

[209] E. P. Magennis, N. Francini, F. Mastrotto, R. Catania, M. Redhead, F. Fernandez-Trillo, D. Bradshaw, D. Churchley, K. Winzer, C. Alexander and G. Mantovani, *PLOS one,* **2017**, *12*, 1.

List of Scientific Publications

- Bachelorthesis: Polyphenol- und fettsäurehaltige nachwachsende Polymere.
- Masterthesis: Synthese modifizierter Polycaprolactame auf Basis nachwachsender Rohstoffe.

- O. Kreye, S. Oelmann, M. A. R. Meier, Renewable Aromatic-Aliphatic Copolyesters Derived from Rapeseed, *Macromol. Chem. Phys.* **2013**, *214*, 1452.
- W. Maaßen, S. Oelmann, D. Peter, W. Oswald, N. Willenbacher, M. A. R. Meier, Novel insights into pressure sensitive adhesives based on plant oils, *Macromol. Chem. Phys.* **2015**, *216*, 1609. **(COVER)**
- S. Oelmann, M. A. R. Meier, Synthesis of Modified Polycaprolactams Obtained from Renewable Resources, *Macromol. Chem. Phys.* **2015**, *216*, 1972.
- S. Oelmann, S. C. Solleder, M. A. R. Meier, Controlling molecular weight and polymer architecture during the Passerini three component step-growth polymerization, *Polym. Chem.* **2016**, *7*, 1857. **(COVER)**
- A. Llevot, A. C. Boukis, S. Oelmann, K. Wetzel, M. A. R. Meier, An Update on Isocyanide-Based Multicomponent Reactions in Polymer Science, *Top. Curr. Chem.* **2017**, *375*, 66.
- S. Oelmann, M. A. R. Meier, Synthesis and unimolecular micellar behavior of amphiphilic star-shaped block copolymers obtained *via* the Passerini three component reaction, *RSC Adv.* **2017**, *7*, 45195.
- S. Oelmann, A. Travanut, D. Barther, M. Romero, S. M. Howdle, C. Alexander, M. A. R. Meier, Biocompatible unimolecular micelles obtained *via* the Passerini reaction as versatile nanocarriers for potential medical applications, *Biomacromolecules*, accepted.